Author/s:
Morrish, Emma Louise

Title:
Smac-mimetic combination therapies for the treatment of cancer and infectious disease

Date:
2020

Persistent Link:
https://hdl.handle.net/11343/237538

Smac-mimetic Combination Therapies for the Treatment of Cancer and Infectious Disease

Emma Louise Morrish

ORCID: 0000-0002-4909-2589

Doctor of Philosophy
January 2020

The Walter and Eliza Hall Institute of Medical Research
Department of Medical Biology
The University of Melbourne

Thesis submitted to the University of Melbourne in total fulfillment of the requirements for the degree of Doctor of Philosophy

Abstract

Acute myeloid leukaemia (AML) is an aggressive disease with a current 5-year survival rate of only ~30%, therefore development of more effective treatments is urgently needed. Overexpression of inhibitor of apoptosis (IAP) proteins, responsible for the regulation of tumour necrosis factor (TNF)-mediated apoptosis, have been correlated with cancer progression and treatment resistance. Natural IAP antagonists exist, termed second mitochondria-derived activator of caspases or Smac, leading to the pharmaceutical development of Smac-mimetics. Smac-mimetics, such as the drug birinapant, are currently in clinical trials for a range of cancers, including AML. Although, birinapant has shown promising anti-cancer effects, its efficacy as a single-agent and in combination with numerous anti-cancer therapies, has been variable and limited. Therefore, overcoming patient resistance to Smac-mimetic therapy and potentiating treatment are still major challenges.

Using a library of more than 5,700 bioactive compounds, we examined the emergence of resistance to birinapant in AML. Here I present the identification of multidrug resistance protein 1 (MDR1/ABCB1) inhibitors as a class of clinical drugs that can overcome Smac-mimetic resistance in cancer. Inhibition of MDR1 with 3rd generation specific inhibitors increased intracellular levels of birinapant and sensitised AML and ovarian cancer patient cells to birinapant killing. Using the clustered regularly interspaced short palindromic repeats (CRISPR)/Cas9 system, I show that MDR1 is a predictor of response to birinapant-based

therapies in cancer cells. Moreover, the combined therapy of MDR1 inhibitors and birinapant effectively killed leukaemic stem cells (LSCs) and prolonged survival of AML burdened mice *in vivo* (Chapter 3).

The findings observed in Chapter 3 in AML and ovarian cancer cells, were extended to a chronic hepatitis B virus (HBV) infection model (Chapter 4). Birinapant has previously shown efficacy at eradicating HBV infection, however due to toxicity concerns, in-human clinical trials have ceased. In Chapter 4, I demonstrate that a lower concentration of birinapant can be combined with the MDR1 inhibitor zosuquidar, to potentiate birinapant-mediated HBV infected liver cell death and HBV-DNA clearance *in vivo.*

An investigation into the remaining high throughput screen hit compounds, revealed half were psychotropic and inhibited MDR1 to synergise with birinapant. In Chapter 5, I focus on the serotonin receptor 7 (5-HT_7) agonists, LP-44 and LP-12, as well as the psychoactive compounds Fluphenazine dihydrochloride, SDZ 21009, GR-127935 and CGP-71683. My identification that these compounds inhibit MDR1 to synergise with birinapant underlines the dependence cancer cells have on MDR1 to evade Smac-mimetic therapy.

This thesis presents a comprehensive analysis of birinapant as a substrate for MDR1 and identifies MDR1 as a biomarker of Smac-mimetic therapy. Furthermore, this study provides evidence towards a novel combination regimen combining birinapant with 3rd generation MDR1 inhibitors to potentiate Smac-

mimetic therapy for the treatment of AML, ovarian cancer and HBV. Altogether these findings suggest a therapeutic opportunity for Smac-mimetic plus MDR1 inhibitor combination therapy in cancer and infectious disease.

Declaration

This is to certify that:

i) this thesis comprises only my original work towards the degree of Doctor of Philosophy, except where indicated in the preface,

ii) due acknowledgement has been made in the text to all other material used,

iii) the thesis is less than 100,000 words in length, exclusive of tables, maps, bibliographies and appendices.

Emma Louise Morrish

31/01/2020

Preface

The work presented in this thesis would not have been possible without the continuous guidance of my supervisors Dr. Gabriela Brumatti and Prof. John Silke. Furthermore, collaboration with a diverse range of people, whom are experts in their field, has greatly enriched the content and story of the work presented in this thesis. I am incredibly grateful and appreciative of their support and acknowledge their contributions in detail below.

Chapter 1: Introduction

The basis of this introduction is from an invited Review, ***"Future therapeutic directions targeting Smac-mimetic resistance"***, that was submitted for publication to the peer-reviewed journal *Cells* on the 21/01/2020 and is currently under revision. Please see the relevant Declaration Thesis with Publication and Co-author Authorisation documents that stipulate I am responsible for more than fifty percent of the work, drafting the initial manuscript and for all subsequent revisions and edits.

Co-authors of this manuscript are:

Emma L. Morrish[1,2], Gabriela Brumatti[1,2] and John Silke[1,2]

[1]Inflammation Division, Walter and Eliza Hall Institute of Medical Research, Melbourne, VIC 3052, Australia
[2]Department of Medical Biology, University of Melbourne, VIC 3010, Australia

Below is a detailed description of each authors contribution:

- E.L.M. wrote the manuscript.
- G.B. and J.S. provided expert opinion and edited the manuscript.

Chapter 3: Clinical MDR1 Inhibitors and Smac-mimetics Combine to Kill Leukaemic Stem Cells and Overcome Resistance in Acute Myeloid Leukaemia

In its entirety, contains the manuscript, ***"Clinical MDR1 inhibitors and Smac-mimetics combine to kill leukaemic stem cells and overcome resistance in acute myeloid leukaemia",*** which was submitted for publication to the peer-reviewed journal, *Leukemia* on the 29/11/2019 and is currently under review. Additional material that is no longer included in the scope of the submitted manuscript, but is relevant to Chapter 3, is included as supplemental material. Please see the relevant Declaration Thesis with Publication and Co-author Authorisation documents that stipulate I am responsible for more than fifty percent of the work, drafting the initial manuscript and for all subsequent revisions and edits.

Co-authors of this manuscript are:

Emma L. Morrish,[1,2] Anthony Copeland,[1,2] Donia M. Moujalled,[3,4] Jason A. Powell,[5,6] Natasha Silke,[1] Kate E. Jarman,[1,2] Jarrod J. Sandow,[1,2] Gregor Ebert,[1,2] Liana Mackiewicz,[1] Jessica A. Beach,[7,8] Elizabeth L. Christie,[7,8] Alexander C. Lewis,[5] Giovanna Pomilio,[3,4] Karla C. Fischer,[1,2] Laura MacPherson,[7,8] David D.L. Bowtell,[7,8] Andrew I. Webb,[1,2] Marc Pellegrini,[1,2] Mark A. Dawson,[7,8] Stuart M. Pitson,[5,6] Andrew H. Wei,[3,4] John Silke[1,2,*] and Gabriela Brumatti[1,2,*]

[1]Inflammation Division, Walter and Eliza Hall Institute of Medical Research, Melbourne, VIC 3052, Australia

[2]Department of Medical Biology, University of Melbourne, Melbourne, VIC 3010, Australia

[3]Australian Centre for Blood Diseases, Monash University, Melbourne, VIC 3004, Australia
[4]Department of Clinical Haematology, The Alfred Hospital, Melbourne, VIC 3181, Australia
[5]Molecular Signalling Laboratory, Centre for Cancer Biology, University of South Australia and SA Pathology, Adelaide, SA 5001, Australia
[6]Adelaide Medical School, University of Adelaide, Adelaide SA, 5000, Australia
[7]Peter MacCallum Cancer Centre, Melbourne, VIC 3000, Australia
[8]Sir Peter MacCallum Department of Oncology, University of Melbourne, Melbourne, VIC 3010, Australia
*These authors contributed equally to this work

Below is a detailed description of each authors contribution:

- E.L.M. performed the majority of the experiments.
- G.B., A.C., N.S., G.E., L.M., G.P., K.C.F. performed the remaining experiments.
- J.A.B. and E.L.C completed AOCS experiments.
- J.J.S. provided expertise and performed the mass spectrometry analyses.
- K.E.J. performed initial drug screen.
- D.M.M., A.H.W., J.A.P., A.C.L. and S.M.P, provided expertise, processing and analysis of primary patient leukaemia samples.
- L.M. and M.A.D. provided MLL-AF9 leukaemic blasts and stem cells.
- E.L.M., J.S. and G.B. planned the project, designed the experiments, analysed the data and wrote the manuscript.
- All authors contributed to discussion of the results and review of the manuscript.

Chapter 4: Investigating the Efficacy of MDR1 Inhibitors to Potentiate Smac-mimetic Treatment in a Chronic Hepatitis B Virus (HBV) Model

This chapter contains unpublished material not submitted for publication, but that is in preparation for publication. I am responsible for more than fifty percent of the work and am currently drafting the manuscript where I will be first author.

Co-authors of this manuscript are:

Emma L. Morrish,[1,2] Gregor Ebert,[1,2] Liana Mackiewicz,[1] Marc Pellegrini,[1,2] John Silke,[1,2*] and Gabriela Brumatti[1,2*]

[1]Walter and Eliza Hall Institute of Medical Research, Melbourne, VIC 3052, Australia
[2]Department of Medical Biology, University of Melbourne, Melbourne, VIC 3010, Australia
[*]These authors contributed equally to this work

Below is a detailed description of each authors contribution:

- E.L.M. performed the majority of the experiments and analysed the data.
- G.E. analysed the ALT and HBV-DNA PCR data and provided technical expertise.
- L.M. provided technical animal expertise, assisted in all *in vivo* procedures and performed the HBV-DNA PCR.
- E.M., M.P., G.B., G.E. and J.S. planned the project, designed the experiments and wrote the manuscript.

Chapter 5: Understanding the Molecular Mechanisms by which Psychoactive Drugs Potentiate Smac-mimetic Mediated Killing in Acute Myeloid Leukaemia

This chapter contains unpublished material not submitted for publication. I am responsible for all experiments and data presented in this chapter, with technical assistance from Natasha Silke.

Editorial Assistance

I was responsible for planning, writing and drafting the first version of all chapters, including figures and tables, of this thesis. My supervisors Prof. John Silke and Dr. Gabriela Brumatti have provided their expert opinion and suggestions regarding content and editorial assistance to all chapters. Prof. Andreas Strasser and A/Prof. Paul Ekert provided editorial assistance in the preparation of the manuscript which forms Chapter 3. Prof. Andreas Strasser and A/Prof. Paul Ekert are experts in the field and are not listed as authors on the manuscript.

Funding Sources

My PhD candidature stipend was generously provided by an Australian Postgraduate Award (2016), an Australian Government Research Training Program Scholarship (2017-2019), an Edith Moffatt Stipend (2019) and a Walter and Eliza Hall Institute PhD Student Top-up Scholarship (2017-2018). This work was supported by a Leukemia & Lymphoma Society [SCOR (Specialized Centre of Research, grant #7015-18 to J.S.), the National Health and Medical Research

Council (NHMRC; grants 1025594, 1046010, and 1081376), Cancer Australia and Leukaemia Foundation Australia priority grant (PdCCRS 1162023 to G.B.), NHMRC fellowship (1058190 to J.S.) and a Victoria Cancer Agency (VCA) mid-career fellowship (MCRF 15027 to G.B.). This work was made possible through the Australian Cancer Research Foundation and Victorian State Government Operational Infrastructure Support and Australian Government NHMRC IRIISS (9000433). Additional funding from ECDO 2019, ISEH 2019, Edith Moffatt Travel Scholarship 2019, MATS 2019 and EMBL 2018 has enabled me to attend National and International conferences to present the work described here.

Acknowledgments

First and foremost, I would like to thank my supervisors Prof. John Silke and Dr. Gabriela Brumatti for giving me the opportunity to complete my PhD within the Silke Lab at WEHI. Their encouragement, supervision, advise and unwavering support has enabled me to have both a successful and enjoyable PhD experience. I would also like to thank whole heartedly Natasha Silke, my lab partner and friend. From the first weeks of my PhD until the end, Natasha has held my hand through many experiments and has been a continuous source of comfort, support and laughs. To the other students of the Cell Signalling and Cell Death (CSCD) and Inflammation Division, I would like to say a big thank you for all of their support, to the long nights and numerous hours in the lab on the weekend, the PhD journey would not have been as fun if it weren't for them; Holly Anderton, Valentine Heim, Zikou Liu, Annette Jacobson, Lin Liu, Denise Heckman, Daniel Frank and previous members, Maria Tanzer, Che Stafford, Jonathon Bernardini and Mark Li. I would also like to thank all other members of the Division and Level 5 West for their input during lab meetings, divisional seminars and in the lab. My mentor Dr. James Dromey, whom I connected with through IMNIS, has been an incredible support and has truly enabled me to understand and articulate my passion for science and how I can achieve my dreams. I would also like to thank and acknowledge the support and advice my PhD Committee members Prof. Louise Purton and Dr. Gemma Kelly have given me over these 4 years. I have always looked forwards to sharing my achievements with them each progress review.

I have thoroughly enjoyed my time at WEHI and that would not have been possible without the friendship from WESA 2018 and the Curry Group, in particular Simona Seizova, Catia Pierotti, Anna Quaglieri, Roberto Bonelli, Lizzie Lieschke, Katharina Stracke, Robyn Schenk, Marie Parsons, Alexis Lucattini, Melanie Heinlein and Tan Nguyen. My Kensington house mates Helen and Christina and my West Brunswick house mates Bel and Vanessa have always been incredibly understanding and supportive, even taking the time to decode my science cooking metaphors.

I would like to express my love and appreciation towards my family; Ros, Tony, Chris, Szu-Ting, Baby Mary and my partner Ben. It has been a haven to spend time with them throughout my PhD, to share my worries and successes. I would also like to thank my grandmother Mary and close family friend Jen, whom have showered me with their endearing support and pride throughout my life. To my partner Ben, thank you for always listening and comforting me, for staying tuned in to the never-ending roller coaster of disappointments and triumphs involving manuscripts, experiments and lastly, this thesis.

Table of Contents

List of Figures

CHAPTER 1

CHAPTER 3

CHAPTER 4

CHAPTER 5

List of Tables

Abbreviations

5-HT	5-hydroxytrptamine
5-HT$_7$R	5-hydroxytrptamine receptor 7
AAVP-TNF	Adeno-associated virus bacteriophage-TNF
ABC	ATP-binding cassette
AC	Adenylyl cyclase
ADS	Ascending dose schedule
Akt	Protein kinase B
ALL	Acute lymphoblastic leukaemia
ALT	Alanine Aminotransferase
AML	Acute myeloid leukaemia
AMP	5’ adenosine monophosphate-activated protein kinase
anti-CTLA-4	anti-Cytotoxic T-Lymphocyte-Associated protein 4
Ara-C	Cytarabine
ATP	Adenosine-triphosphate
Bcl-2	B-cell lymphoma 2
BCRP	Breast cancer resistance protein
BIR	Baculoviral IAP repeats
Bir	Birinapant
BM	Bone marrow
Bruce	BIR-containing ubiquitin-conjugating enzyme
BSS	Bliss synergy score
cAMP	Cyclic 5’ adenosine monophosphate-activated protein kinase
Cas9	CRISPR-associated protein 9
cIAP	Cellular inhibitor of apoptosis protein
Cl	Cleaved
CL	Cytotoxic lymphocyte
CLL	Chronic lymphocytic leukaemia
CML	Chronic myeloid leukaemia
CNS	Central nervous system
CR	Complete response

CRC	Colorectal cancer
CRISPR	Clustered regularly interspaced short palindromic repeats
CSC	Cancer stem cell
CSA	Cyclosporin A
CTLA-4	Cytotoxic T-lymphocyte-associated protein 4
DD	Death domain
DIABLO	Direct IAP-Binding *protein* with Low PI
DLT	Dose limiting toxicity
DMEM	Dulbecco's modified Eagle's medium
DNA	Deoxyribonucleic acid
EC	Enterochromaffin
EC_{50}	Half maximal effective concentration
ECL	Enhanced chemiluminescence
EDTA	Ethylenediaminetetraacetic acid
ERK	Extracellular signal-regulated kinase
ESCC	Esophageal squamous carcinoma
FACs	Florescence-activated cell sorting
FADD	FAS-associated death domain
FCS	Fetal calf serum
FDA	U.S Food and Drug Administration
FDH	Fluphenazine dihydrochloride
Fl	Full-length
GI	Gastrointestinal
GPCR	G-protein coupled receptor
gRNA	Guide RNA
GS	TNF-based gene expression signature
HBV	Hepatitis B virus
HDI	Hydrodynamic injection
HGSC	High-grade serous ovarian cancer
HIV	Human immunodeficiency virus
HNSCC	Head and neck squamous cell carcinoma
HOAC	Human ovarian adenocarcinoma

HoxA9	Homeobox protein 9
HSPCs	Haematopoietic stem and progenitor cells
IAP	Inhibitor of apoptosis protein
IBC	Inflammatory breast cancer
IBM	IAP binding motif
IC_{50}	Half maximal inhibitory concentration
ICI	Immune checkpoint inhibitors
ICV	Intracerebroventricular
IKK	IκB kinase
ILP-2	IAP-like protein 2
IP	Intraperitoneal
IV	Intravenous
K_i	Inhibitory constant
LPS	Lipopolysaccharide
LSC	Leukaemia stem cell
LSK	$Lineage^{-}Sca\text{-}1^{+}cKit^{+}$
LUBAC	Linear ubiquitin chain assembly complex
M	Membrane
MAPK	Mitogen-activated protein kinases
Meis1	Meis Homeobox 1
MEK	Mitogen-activated protein kinase kinase
MDR	Multidrug resistance
MDR1	Multidrug resistance protein 1
MDS	Myelodysplastic syndrome
ML-IAP	Melanoma IAP
MLKL	Mixed lineage kinase domain-like protein
MLL	Mixed leukaemia lineage
MM	Multiple myeloma
mRNA	messenger RNA
MRP1	Multidrug resistance-associated protein 1
MS	Median survival
MTD	Maximum tolerated dose

MXR	Multi-xenobiotic resistance protein
NAIP	Neuronal IAP
NBD	Nucleotide binding domain
Nec-1	Necrostatin-1
NF-kB	Nuclear Factor kappa-light-chain-enhancer of activated B cells
NK	Natural killer cell
NOD	Nucleotide-binding oligomerisation domain-containing protein
NSCLC	Non-small-cell lung carcinoma
P	Phosphorylated
PAGE	Polyacrylamide gel electrophoresis
PCR	Polymerase chain reaction
PD-1	Programmed cell death protein 1
PD-L1	Programmed death-ligand 1
P-gp	P-glycoprotein
PI	Propidium iodide
PKA	Protein kinase A
PPTP	Pediatric Preclinical Testing Program
PR	Partial response
RHIM	Respective homotypic interaction motif
RING	Really interesting new gene
RIPK	Receptor-interacting serine/threonine-protein kinase
RMS	Rhabdomyosarcoma
SD	Standard deviation
SDS	Sodium dodecyl sulfate
SEM	Standard error of the mean
SM	Smac-mimetic
Smac	Second mitochondria-derived activator of caspases
SSRIs	Serotonin reuptake inhibitors
TAK1	Transforming growth factor beta-activated kinase
t-AML	Therapy induced secondary acute myeloid leukaemia
Tari	Tariquidar
TCA	Tricyclic antidepressant

TCGA	The Cancer Genome Atlas
TLR	Toll-like receptor
TNBC	Triple negative breast cancer
TNF	Tumour necrosis factor
TNFR1	TNF receptor 1
TNFSF	TNF super family
TRADD	TNF receptor-associated death domain
TRAIL	TNF-related apoptosis-inducing ligand
TRAF2	TNF receptor-associated factor 2
Ub	Ubiquitin
UBA	Ub-associated domain
VMAT	Vesicular monoamine transporter
VSVΔ51	Vesicular stomatitis virus
WB	Western blot
WT	Wild-type
XIAP	X-chromosome linked IAP
Zosu	Zosuquidar

1 Introduction

The basis of this introduction is an invited review titled, ***"Future therapeutic directions targeting Smac-mimetic resistance",*** that has been submitted for publication to the peer-reviewed journal *Cells* on the 21/01/2020 and is currently under revision.

1.1 Abstract

Cell proliferation that is not balanced by programmed cell death is a hallmark of cancer. Strategies to promote cell death as an anti-cancer therapy have been investigated for decades. Overexpression of members of the inhibitor of apoptosis (IAP) protein family is one possible mechanism hindering the death of cancer cells. To promote cell death, drugs that mimic natural IAP antagonists, such as second-mitochondria-derived activator of caspases (Smac/DIABLO) were developed. Smac-mimetics, such as the drug birinapant, have entered clinical trials for haematological and solid cancers, unfortunately with disappointing results so far. This introduction explores the use of Smac-mimetics for the treatment of cancer, in particular the aggressive disease acute myeloid leukaemia (AML), and discusses the current challenges facing this strategy.

1.2 The Relevance of Programmed Cell Death in Cancer

One of the hallmarks of cancer is failure to undergo genetically programmed cell death in response to signals that would normally promote a suicide response in untransformed cells. This failure to undergo cell death allows cancer cells to mutate, evolve and proliferate. Therefore, reactivating their ability to commit

suicide is an appealing anti-cancer treatment strategy and has been explored in a variety of chemotherapeutic drug approaches. Apoptosis is one type of programmed cell death, which occurs under normal physiological conditions and is described as being either intrinsic (mitochondria dependent) or extrinsic (death receptor dependent) (Salvesen and Duckett, 2002). Apoptosis is characterised morphologically by cell shrinkage, membrane blebbing, aggregation of chromatin and formation of apoptotic bodies (**Figure 1.1**). The enzymes that cause these phenotypes are cysteine proteases that cleave after an aspartate residue and are therefore known as caspases (Thornberry and Lazebnik, 1998). In contrast, necrosis, an unregulated form of cell death, leads to loss of cell homeostasis and membrane integrity resulting in cell rupture (Edinger and Thompson, 2004; Vandenabeele et al., 2010). Another form of programmed cell death termed necroptosis, that shares features with necrosis such as cell rupture and release of cellular contents, has recently also been explored as an anti-cancer therapeutic strategy (**Figure 1.1**) (Brumatti et al., 2016; Schenk and Fulda, 2015). Necroptosis is implemented during cellular stress when caspases are inhibited, for example genetically or pharmacologically. The proteins that carry out the necroptotic program are the receptor-interacting serine/threonine-protein kinases (RIPK) 1 & 3 and the pseudokinase mixed lineage kinase domain-like protein (MLKL) (Silke et al., 2015).

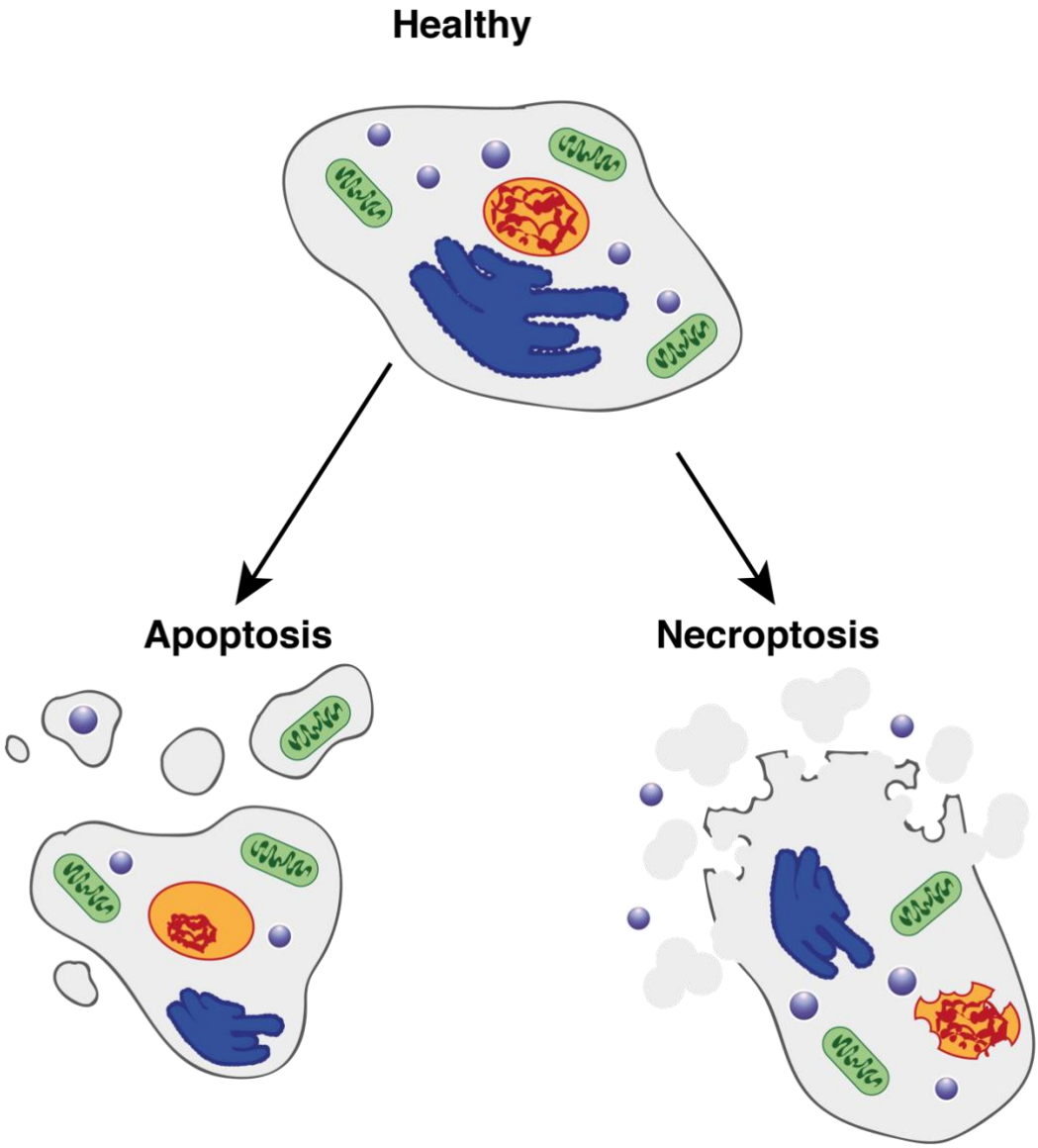

Figure 1.1 Schematic of apoptosis and necroptosis

Healthy cells can undergo programmed cell death, apoptosis or necroptosis, to maintain homeostasis. Characteristics of apoptosis include cell shrinkage, chromatin condensation, membrane blebbing and formation of apoptotic bodies. Characteristics of necroptosis include cell swelling, membrane breakdown and release of cellular contents. Adapted from (Novus Biologicals, 2017).

1.3 Inhibitor of Apoptosis Proteins

The human family of inhibitor of apoptosis (IAP) proteins regulates cell survival in response to a number of stimuli. The IAP family, defined by the presence of one or more baculoviral IAP repeat (BIR) domains, consists of eight members; X-chromosome-linked IAP (XIAP), cellular IAP 1 and 2 (cIAP1 and cIAP2), melanoma-IAP (ML-IAP), neuronal-IAP (NAIP), survivin, BIR-containing ubiquitin-conjugating enzyme (Bruce/Apollon) and IAP-like protein 2 (ILP-2). Only three of these, cIAP1, cIAP2 and XIAP, have major anti-apoptotic roles and this introduction therefore focuses on them (**Figure 1.2**) (De Almagro and Vucic, 2012; Obexer and Ausserlechner, 2014; Vaux and Silke, 2005). These three proteins contain three BIR domains, a really interesting new gene (RING)-finger domain, that has Ubiquitin (Ub) ligase (E3) activity, and a Ub-associated (UBA) domain, which enables their interaction with ubiquitylated proteins (Darding et al., 2011; Gyrd-Hansen et al., 2008). XIAP is able to bind and inhibit caspases 3, 7 and 9, whilst cIAP1 and 2 inhibit apoptosis induced by members of the tumour necrosis factor (TNF) super family (TNFSF), at least in part by regulating RIPK1, a cytoplasmic protein recruited to TNFSF receptors. XIAP is also essential for nucleotide-binding oligomerisation domain-containing protein (NOD) signalling and ubiquitylates the NOD binding protein RIPK2, presumably in a similar manner to the way cIAPs ubiquitylate RIPK1 (Bertrand et al., 2008; Galbán et al., 2009; Mahoney et al., 2008; Silke et al., 2001; Varfolomeev et al., 2007; Vince et al., 2007). However, NOD and RIPK2 do not appear to induce cell death and therefore, XIAP function in this pathway is unlikely to be directly anti-apoptotic.

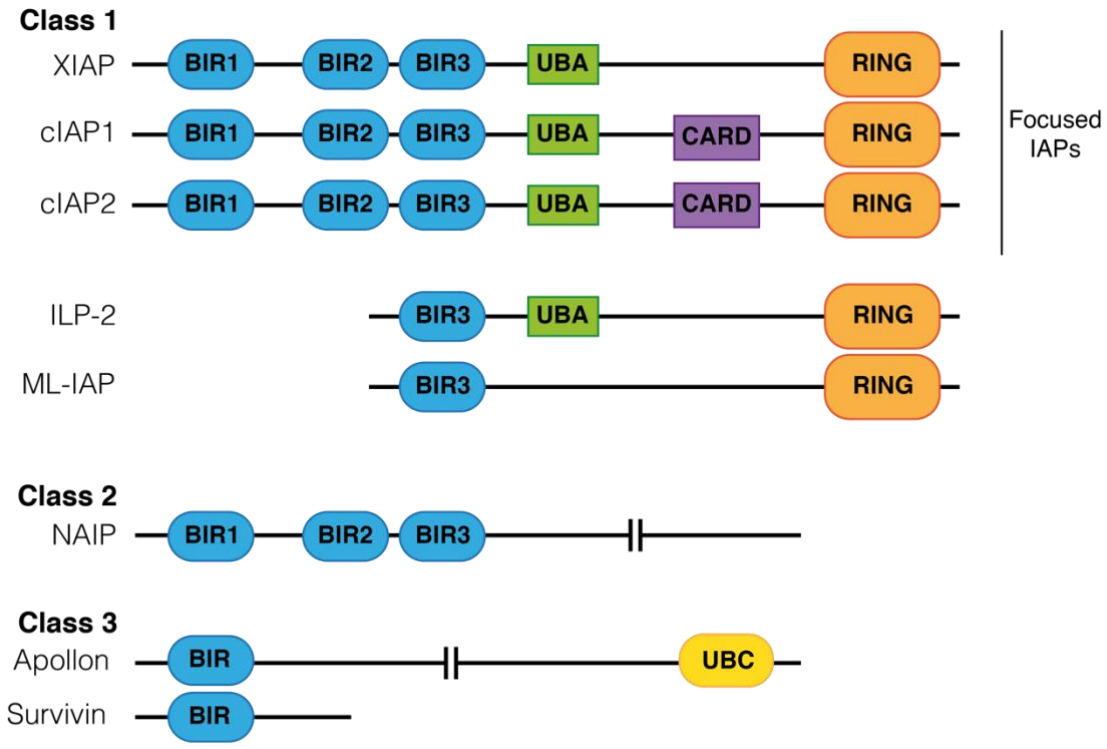

Figure 1.2 Inhibitor of apoptosis proteins

Schematic representation of the structures of the eight-mammalian inhibitor of apoptosis (IAP) proteins. Domains are: BIR1/2/3: Baculovirus IAP repeat, UBA; Ubiquitin binding domain, RING; E3-Ligase RING domain, CARD; caspase recruitment domain, UBC E2-Ligase domain. Adapted from (Obexer and Ausserlechner, 2014).

1.4 TNF Signalling Pathway

TNF is a potent and pleiotropic cytokine responsible for a diverse range of biological functions including inflammation, proliferation and cell death. In most cases, the binding of TNF to its receptor, TNFR1, leads to the recruitment of the TNF receptor-associated death domain (TRADD) and RIPK1 via their respective death domains. TRADD and RIPK1 can apparently bind TNFR1 at the same time, but the relative contribution of each to the signalling complex may depend upon the cell type (Anderton et al., 2019; Dowling et al., 2019; Füllsack et al., 2019). TRADD can recruit the TNF receptor-associated factor 2 (TRAF2) and cIAP1/2 are bound to TRAF2 via a BIR1 interaction with the coiled coil of a TRAF2 trimer (Mace et al., 2010; Zheng et al., 2010). As E3 ubiquitin ligases, cIAP1/2 conjugate components of this complex with ubiquitin. The ubiquitin platform recruits linear ubiquitin chain assembly complex (LUBAC), IκB kinases (IKKs) and transforming growth factor beta-activated kinase 1 (TAK1), resulting in activation of canonical nuclear factor kappa-light-chain-enhancer of activated B cells (NF-κB) and mitogen-activated protein kinases (MAPKs). This leads to transcriptional upregulation and mRNA stabilisation of genes that encode mediators of inflammation and proteins involved in cell survival and proliferation (Fulda and Vucic, 2012; Vanden Berghe et al., 2015; Vince et al., 2007). Although the details are not fully understood, ubiquitylation and phosphorylation of components within this plasma membrane associated, complex 1, limit the formation of the death-inducing complex 2 (**Figure 1.3**) (Annibaldi et al., 2018; Dondelinger et al., 2017; Gerlach et al., 2011; Jaco et al., 2017; Menon et al., 2017).

Natural antagonists of IAPs, such as second mitochondria-derived activator of caspases (Smac/DIABLO), or HtrA2, bind to the BIR domains of IAPs via their IAP-binding motifs (IBMs). Smac and HtrA2 prevent XIAP from binding and inhibiting caspases 3, 7 and 9 (Bratton et al., 2001; Ekert et al., 2001; Hegde et al., 2002; Silke et al., 2002; Wu et al., 2000). IAP antagonists rarely induce XIAP degradation, however in many cases they promote cIAP auto-ubiquitylation and proteasomal degradation (Varfolomeev et al., 2007; Vince et al., 2007). They do this by unleashing the RING domain of cIAPs from BIR3 inhibition allowing it to dimerise (Dueber et al., 2011; Feltham et al., 2011). This activation of the E3 ligase function of cIAPs by an IAP antagonist may also result in ubiquitylation of the antagonist but the physiological significance of this is not clear (Creagh et al., 2004; Hu and Yang, 2003; Wu et al., 2000; Yang and Du, 2004). IAP antagonist induced degradation of cIAPs prevents cIAP-mediated ubiquitylation of components in the TNF signalling pathway and thus converts TNFR1 signalling from pro-survival to pro-apoptotic. In particular, loss of cIAPs allows the formation of a FADD-caspase-8 containing complex-2, leading to caspase-8 activation by oligomerising in a chain like manner (**Figure 1.3**) (Dickens et al., 2012; Kitson et al., 1996; Micheau and Tschopp, 2003).

In the absence of caspase-8 activity, for example through pharmacological antagonism or genetic deletion, and in the presence of IAP inhibitors, a second cell death mediating complex forms, termed complex 2b. RIPK1 binds with RIPK3 via their respective homotypic interaction motif (RHIM) domains, leading to auto-phosphorylation and subsequent recruitment of MLKL. RIPK3 phosphorylation

and oligomerisation of MLKL, leads to its activation and translocation from the cytosol to the plasma membrane, where it disrupts membrane integrity, leading to necroptotic cell death (**Figure 1.3**) (Chen et al., 2016; Murphy et al., 2013; Murphy and Silke, 2014; Vanden Berghe et al., 2015; Wang et al., 2014).

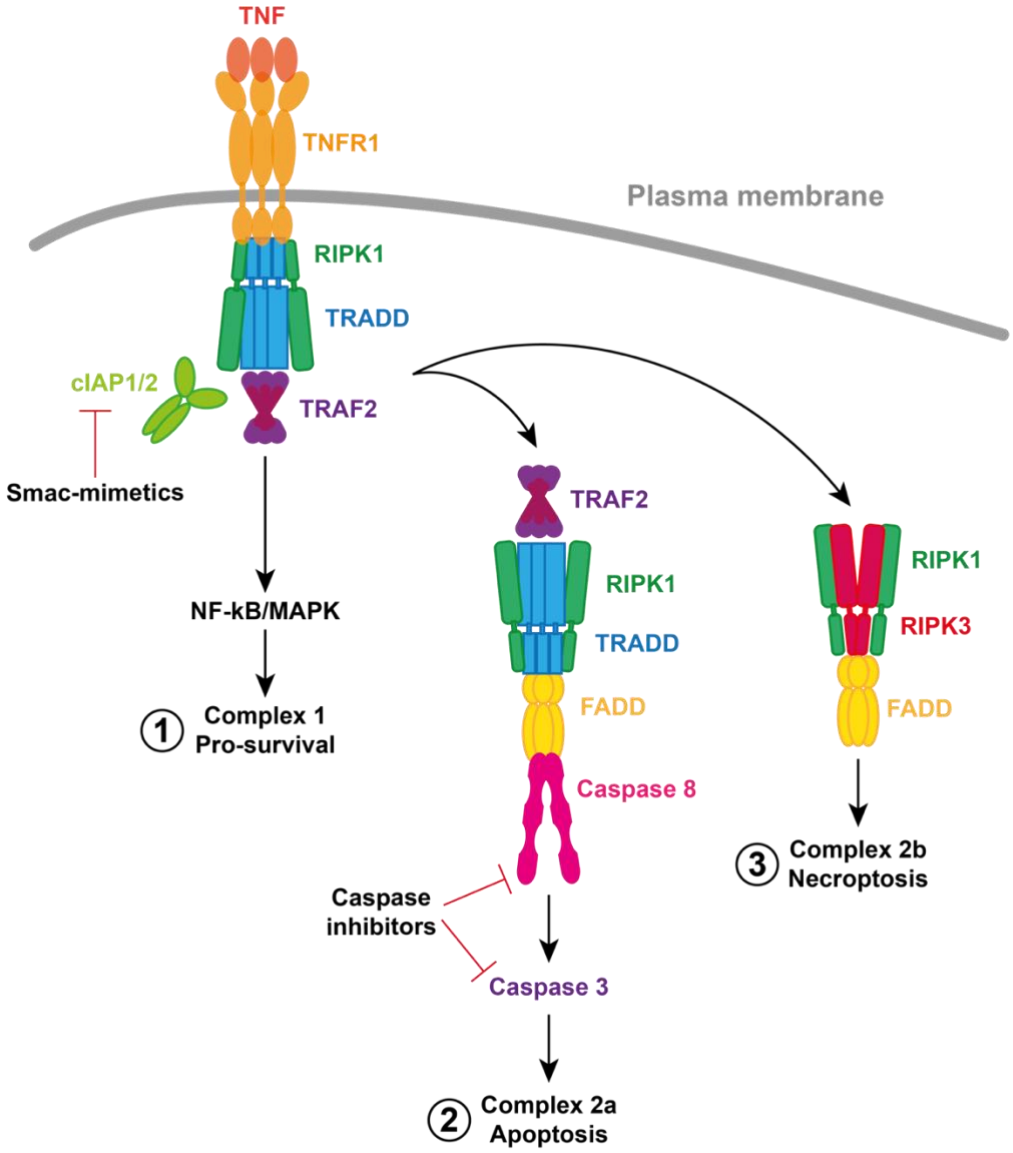

Figure 1.3 Schematic of TNF signalling

Simplified schematic of TNFR1 signalling. Formation of complex 1 can lead to activation of canonical NF-κB and MAPK pro-survival signalling. Loss (or antagonism) of cIAP proteins induced by Smac-mimetics, leads to formation of complex 2a, containing TRADD, RIPK1, FADD and caspase 8. Caspase 8 activation and cleavage, and activation of caspase 3, results in apoptosis. Alternatively, if caspases are inhibited, complex 2b can form via a RHIM motif dependent recruitment of RIPK3. RIPK3 auto-phosphorylates and phosphorylates the pseudokinase MLKL. Phosphorylation of MLKL leads to a conformational change, membrane translocation, oligomerisation, membrane permeabilisation and necroptotic cell death.

1.5 Development of Smac-mimetics

Overexpression of IAPs has been associated with multiple cancers, including haematological and solid cancers, and is indicative of poor prognosis (Condon et al., 2014; Fulda and Vucic, 2012; Zender et al., 2006). Clinically it was observed that patients expressing higher levels of Smac had a more favourable prognosis, with higher remission rates and longer overall survival (Fulda and Vucic, 2012). Proof of principle for targeting IAPs was provided by the demonstration that exogenously expressing Smac in resistant neuroblastoma cells sensitised them to TNF-related apoptosis-inducing ligand (TRAIL) induced apoptosis (Fulda et al., 2002). Subsequent studies using antisense oligonucleotides against XIAP or synthetic Smac peptides, showed that these also sensitised cancer cells to chemotherapy (Arnt et al., 2002; Carter et al., 2003). Together with other studies, this prompted the pharmaceutical development of small molecule, peptide-like mimetics of Smac, termed Smac-mimetics (**Figure 1.4**). Smac-mimetics mimic the minimal N-terminal tetrapeptide (NH_2-AVPI), that constitutes a significant part of the IBM, which binds to the BIR domains of cIAP1/2 and XIAP (Kipp et al., 2002; Silke et al., 2000; Wu et al., 2000). Many of these mimetic compounds have shown anti-cancer effects *in vitro* and *in vivo*, validating the development of clinical Smac-mimetics (Fulda and Vucic, 2012; Li et al., 2004; Oost et al., 2004; Schimmer et al., 2004; Zobel et al., 2006).

Endogenous Smac homodimerises through an extensive hydrophobic interface and is bivalent (Chai et al., 2000). Potent and selective bivalent Smac-mimetics, as well as monovalent compounds, have been developed for the clinic.

Monovalent Smac-mimetics have one AVPI-like binding motif whilst bivalent Smac-mimetics have two. To date, five monovalent compounds; GDC-0152, CUDC-427 (GDC-0917), AT-406 (Debio 1143), LCL161 and BI 891065, and three bivalent compounds; birinapant (TL32711), APG-1387, HGS1029 (AEG40826), have entered clinical trials for the treatment of cancer (**Figure 1.4**).

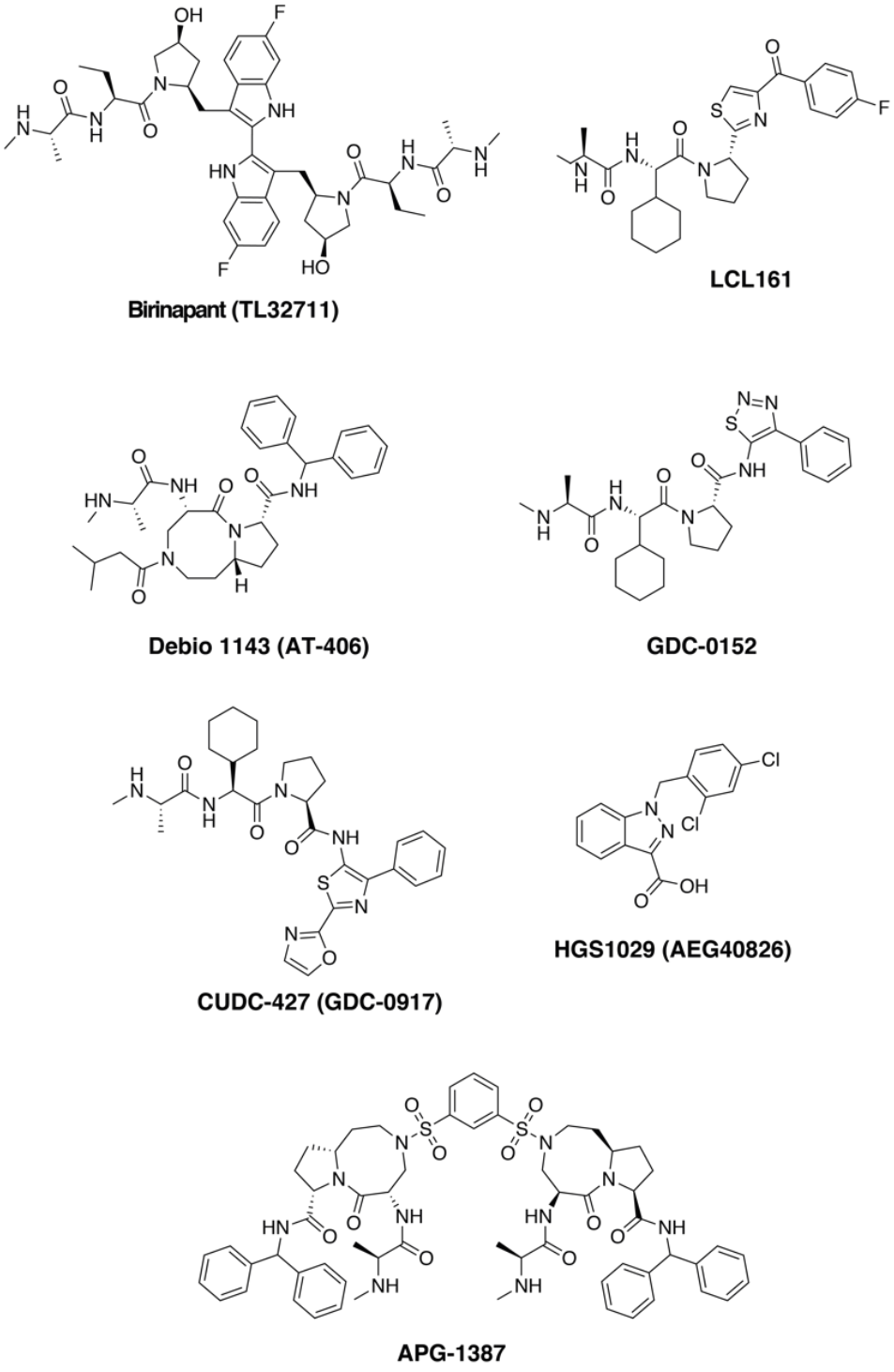

Figure 1.4 Structures of clinical Smac-mimetic compounds

Structures of Smac-mimetic compounds that have progressed to in-human clinical trials. Note the structure of BI 891065 is not publicly available.

1.6 Smac-mimetics as Single-agents in Pre-clinical and Clinical Studies

Triple knock-out *ciap1*$^{-/-}$*ciap2*$^{-/-}$*xiap*$^{-/-}$ and double knock-out *ciap1*$^{-/-}$/*ciap2*$^{-/-}$ animals are embryonic lethal. In contrast, double knock-out *ciap2*$^{-/-}$/*xiap*$^{-/-}$ are viable (Moulin et al., 2012). There are two conflicting reports with regard to *ciap1*$^{-/-}$/*xiap*$^{-/-}$, with one strain being embryonic lethal (Moulin et al., 2012) and another viable (Heard et al., 2015). At the least, these data suggest that inhibiting all three anti-apoptotic IAPs may be undesirable from a safety perspective. Certainly Smac-mimetics that inhibit all three with low nanomolar K_i's tend to have a more inflammatory profile and be more toxic to cells than ones with a more restricted profile (**Table 1**) (Anderton et al., 2017; Condon et al., 2014; Ndubaku et al., 2009; Vince et al., 2012).

Table 1 K_i values for clinically relevant Smac-mimetics

Smac-mimetic	cIAP1	cIAP2	XIAP	ML-IAP	Reference
Birinapant	~1	36	50 ± 23	~1	Condon *et al.,* 2014
LCL161	-	-	-	-	Derakhshan *et al.,* 2016
AT-406	1.9	5.1	66.4	-	Cai *et al.,* 2011
GDC-0152	17	43	28	14	Flygare *et al.,* 2013
CUDC-427	<60	<60	<60	<60	Wong *et al.,* 2013

1.6.1 Birinapant

Birinapant (previously known as TL32711, Tetralogic Pharmaceuticals) is one of the most clinically progressed Smac-mimetics (Condon et al., 2014). Birinapant's higher affinity for the BIR3 of cIAP1 (K_i ~1 nM) than for that of cIAP2 (36 nM) and XIAP (50 ± 23 nM), is likely to contribute to its good safety profile (Condon et al., 2014; Moulin et al., 2012). Birinapant's anti-cancer activity as a single-agent has been extensively investigated *in vitro* and *in vivo*. Benetatos *et al.,* undertook a large-scale screen *in vitro* of 111 different malignancies and observed 18 (16%) were sensitive to birinapant single-agent treatment (Benetatos et al., 2014). Interestingly, single-agent birinapant treatment *in vivo* in 50 patient-derived xenotransplant models of ovarian, colorectal and melanoma cancer, resulted in inhibition of tumour growth in roughly one third (Benetatos et al., 2014). Similarly, although the human melanoma cell lines 451Lu and 1025Lu were both resistant to birinapant single treatment *in vitro*, in xenotransplantation models of these cells, treatment with birinapant single-agent led to significant slowing of tumour growth for both cell lines (Krepler et al., 2013). It is possible that this unexpected improvement of efficacy *in vivo* compared with *in vitro*, is due to elevated levels of TNF in the microenvironment of melanoma lesions due to chronic inflammation (Coussens and Werb, 2002). While TNF has pro-survival effects on melanoma cells, enhancing invasion and migration potential (Katerinaki et al., 2003), Smac-mimetics can convert this advantage to a liability. These results highlight that Smac-mimetics may synergise with an inflammatory environment, whether induced or otherwise, to cause cancer cell death (Beug et al., 2014; Chesi et al., 2016; Michie et al., 2019)

A recent analysis of 279 head and neck squamous cell carcinoma (HNSCC) tumours by The Cancer Genome Atlas (TCGA) identified roughly thirty percent of HNSCC patients have genomic amplifications of Fas-associated death domain (*FADD*), with a subset of these patients also having amplifications in *BIRC2/cIAP1* or *BIRC3/cIAP2* (Cancer Genome Atlas Network, 2015; Eytan et al., 2016). Birinapant was effective as a single-agent both *in vitro* and *in vivo* in HNSCC cells over expressing FADD, with differential expression levels of cIAP1. Interestingly, following overexpression of FADD in the FADD-deficient cell line UM-SCC-38, birinapant treatments were effective at inducing cell death, implicating FADD as an important component in Smac-mimetic mediated killing (Eytan et al., 2016; Eytan et al., 2015). In inflammatory breast cancer (IBC), overexpression of XIAP has been correlated with acquired therapeutic resistance to apoptotic stimulus such as TRAIL (Allensworth et al., 2012). Single-agent treatment with birinapant in TRAIL resistant IBC cell lines was pro-apoptotic, leading to cell death (Allensworth et al., 2013). The authors proposed that this sensitivity was due to birinapant's activity towards XIAP, as a related bivalent Smac-mimetic that binds XIAP less potently (K_d 0.45 and >1 μM respectively) was not as effective at inducing cell death (Allensworth et al., 2013). However, caveats to this conclusion are that cIAP2 binding was not examined and the different physico-chemical properties of the two compounds was not discussed (Allensworth et al., 2013).

The first in-human clinical trial with birinapant was in patients with advanced solid tumours or lymphoma (NCT00993239). Birinapant was administered

intravenously, with a dose-escalation from 0.18 to 63 mg/m$_2$, once a week, every three out of four weeks. The maximum tolerated dose (MTD) was determined as 47 mg/m$_2$, with the maximum dose 63 mg/m$_2$ having adverse effects (AEs) including headache, nausea and vomiting. Intriguingly, 2 out of 3 patients receiving 63 mg/m$_2$ presented with Bell's palsy, a facial nerve paralysis (Amaravadi et al., 2015). Although birinapant accumulated in tumour tissue and had on target effects as an IAP inhibitor, no complete (CR) or partial responses (PR) were observed in the 26 patients who were eligible for evaluation. Stable disease was observed in 7 patients (27%) and 2 patients with colorectal cancer demonstrated radiographic evidence of tumour shrinkage (Amaravadi et al., 2015). A second Phase I/II clinical trial with birinapant was conducted in patients with relapsed acute myeloid leukaemia (AML) or myelodysplastic syndrome (MDS). Birinapant was administered at varying doses (17, 22 or 26 mg/m$_2$) and frequency (weekly, twice weekly or three times weekly) (Frey et al., 2014). One case of Bell's palsy was observed at 22 mg/m$_2$ dosed twice a week, and the three times a week dosing schedule was abandoned due to feasibility concerns. Best responses included a reduction in bone marrow blasts from 60% to 10% (Frey et al., 2014). A Phase II single-agent trial of birinapant in 11 patients with relapsed platinum-resistant or -refractory epithelial ovarian cancer was conducted using the pre-established MTD of 47 mg/m$_2$, administered once a week, three out of four weeks (NCT01681368) (Amaravadi et al., 2015; Noonan et al., 2016). Similar to previous studies, birinapant demonstrated potent on target inhibition of IAPs, but no clinical benefit was observed, and therefore the study was terminated (Noonan et al., 2016). Together, these first in-human studies with birinapant

indicate that as a single-agent, birinapant has some anti-cancer activity but is unlikely to be universally effective in treating cancer. Despite the incidences of Bell's palsy (which is reversible upon birinapant reduction or withdrawal), the good tolerability profile of birinapant suggests it has the potential to be combined with chemotherapy and TNF enhancing therapy.

1.6.2 LCL161

LCL161 (Novartis) is a structural analogue of the Smac-mimetic compound LBW242 and has also progressed into the clinic (Weisberg et al., 2007; Weisberg et al., 2010). It is an orally available monovalent compound that inhibits multiple IAPs including XIAP, cIAP1 and cIAP2 (Condon, 2011; Weisberg et al., 2007; Weisberg et al., 2010). K_i values for individual IAPs do not appear to have been published for this compound, however, like birinapant, it promotes degradation of cIAP1 and appears to have greater activity against cIAP1 and cIAP2 than XIAP (Hird et al., 2015). Initial studies with LCL161 showed its efficacy as a single-agent towards mutant FLT3- and BCR-ABL-positive leukaemia cells (Weisberg et al., 2010). In human hepatocellular carcinoma (HCC) cell lines Hep3B and PLC5, LCL161 had single-agent activity (IC_{50} 10.23 μM and 19.19 μM respectively) and induced cell death (Chen et al., 2012a). Further studies have also identified LCL161 single-agent activity in multiple myeloma (MM) *in vitro* and *in vivo* (Chesi et al., 2016; Ramakrishnan et al., 2014). Although there was a mixed anti-tumour response in LCL161 treated MM cell lines, degradation of cIAP1 and inhibition of XIAP was observed in all cells tested (Ramakrishnan et al., 2014). In the study by Chesi *et al.,* MM cells were resistant *in vitro* to LCL161 except at doses that were not clinically achievable (Chesi et al., 2016). Other

studies have also reported differential responses of tumours to LCL161 treatment. In particular the Pediatric Preclinical Testing Program (PPTP) screened 23 cell lines *in vitro* and 46 xenograft models *in vivo* and reported a variable and limited response to LCL161 within these childhood cancer cell lines (Houghton et al., 2012). The relationship between TNF expression and treatment sensitivity of PPTP cell lines was investigated by the authors (Neale et al., 2008). Although 2 of the most sensitive tumours (anaplastic large cell lymphoma Karpas-299 cell line and medulloblastoma BT-39 xenograft) showed elevated TNF expression, multiple B-precursor acute lymphoblastic leukaemia (ALL) xenografts, which also presented with moderate levels of TNF, were resistant to LCL161 treatment (Houghton et al., 2012). In a later study, Faye and colleagues identified the dependence of rhabdomyosarcoma (RMS) tumours on cIAP1 and observed that LCL161 treatment of mice with established Kym-1 RMS xenograft tumours led to cancer cell death and prolonged survival (mean survival days were 46 vs 77.69 $\pm$ SEM) (Faye et al., 2015). Strikingly, if LCL161 treatment was initiated prior to tumour growth, mice did not develop tumours by 120 days, effectively preventing the establishment of disease (Faye et al., 2015). However, it should be noted that Kym-1 cells are exquisitely sensitive to Smac-mimetic treatment (Vince et al., 2007), for example compound A (a preclinical precursor of birinapant) has an IC_{50} of ~50 pmol (unpublished).

The first in-human clinical trial of LCL161 tested the safety and effectiveness of the Smac-mimetic in patients with advanced solid tumours (NCT01098838). After treating 53 patients with a dose range of 10 to 3000 mg of LCL161, the MTD was

determined as 1800 mg, administered orally once a week. Higher doses led to AEs of cytokine release syndrome, vomiting, nausea, fatigue and anorexia. No patients had an objective response, with 19% having a best response of stable disease (Infante et al., 2014). Degradation of cIAP1 and increased circulating cytokine levels, including TNF, were observed in patients dosed with lower concentrations than the MTD, indicating that the dosage of 1800 mg is sufficient to target IAPs irrespective of individual patient pharmacokinetics. As observed in *in vitro* testing of cancer cell lines, the lack of efficacy of LCL161 in this study correlated with a lack of basal production and insensitivity of tumour cells to TNF. Therefore, future studies with LCL161 should focus on the screening of patients that express and are sensitive to TNF (Infante et al., 2014).

1.6.3 AT-406

AT-406 (also known as Debio 1143) is a monovalent Smac-mimetic that was first described in 2011 and developed by Ascenta Therapeutics. This compound has oral bioavailability and targets cIAP1 > cIAP2 > XIAP with K_i values of 1.9, 5.1 and 66.4 nM respectively (Cai et al., 2011). Initial studies evaluated its single-agent capacity to inhibit cancer cell growth *in vitro* in more than 100 human cancer cell lines and observed that 15% were sensitive. As a single-agent, AT-406 inhibited tumour growth in MDA-MB-231 breast cancer xenograft models (Cai et al., 2011). Further analysis of AT-406 showed it also had single-agent activity in 60% of ovarian cancer cell lines tested *in vitro*. Intriguingly, 3 out of 5 carboplatin resistant ovarian cell lines were sensitive to single-agent treatment. This finding highlights the ability of Smac-mimetics to drive cell death through

molecular mechanisms independent of classical chemotherapy (Brunckhorst et al., 2012).

Analysis of a mouse xenograft model treated with AT-406 showed it was quickly absorbed and distributed after oral administration, and in the lung, blood, kidney and liver it reached maximum serum concentration within 15 minutes (Zhang et al., 2013). AT-406 progressed into first-in-human Phase I clinical trials in patients with advanced metastatic solid cancer (30 patients) and lymphoma (1 patient) (NCT01078649) (Hurwitz et al., 2015). AT-406 was administered orally at a dose range of 5 to 900 mg, daily from days 1-5, then every 14 days and then later every 21 days. A MTD was not confirmed and AEs experienced included fatigue, nausea and vomiting, with 4 patients withdrawing from the trial (Hurwitz et al., 2015). As with birinapant and LCL161, on target activity was seen, with rapid degradation of cIAP1 in tumour tissue and no CRs or PRs were observed. Stable disease as best response was seen in 5 patients. The authors of the study highlight the need for combination approaches and screening of sensitive markers for the clinical progression of IAP inhibitors (Hurwitz et al., 2015).

1.6.4 GDC Smac-mimetics

Compounds by Genentech, GDC-0152 and CUDC-427 (also known as GDC-0917 and currently being developed by Curis) were reported in 2012 and 2013 respectively. Both are pan-selective IAP antagonists with K_i values towards cIAP1, cIAP2, XIAP and ML-IAP of less than 60 nM (Flygare et al., 2012; Wong et al., 2013) The advantage of CUDC-427 over GDC-0152 is its increased oral bioavailability (Wong et al., 2013).

Initial studies with single-treatment of both compounds demonstrated safety towards healthy mammary epithelial tissue and efficacy in inhibiting tumour growth in MDA-MB-231 breast cancer xenograft models (Flygare et al., 2012; Wong et al., 2013). Tchoghandjian and colleagues showed that glioblastoma cell lines and primary human samples all expressed IAP proteins, cIAP1/2, XIAP and ML-IAP, albeit at varying levels (Tchoghandjian et al., 2016). Intriguingly, analysis of two cohorts, totaling 101 primary human glioblastoma samples, indicated that high expression levels of ML-IAP were indicative of worse progression-free and overall survival (Tchoghandjian et al., 2016). Therefore, the authors chose to test the ability of GDC-0152, a Smac-mimetic with high affinity towards ML-IAP, to induce glioblastoma cell death *in vitro* and *in vivo. In vitro* treatment with GDC-0152 decreased the expression levels of IAP proteins, including ML-IAP in 3 out of 4 glioblastoma cell lines, driving apoptotic cell death. *In vivo* studies using the sensitive U87MG glioblastoma cell line orthotopically xenografted into mice, showed that GDC-0152 postponed tumour development and increased survival (Tchoghandjian et al., 2016). The fact that GDC-0152 and CUDC-427 potently target ML-IAP indicates that they may offer benefit to patients suffering from cancer where ML-IAP is a biomarker of poor prognosis.

The progression of GDC-0152 and CUDC-427 into human clinical trials followed positive preclinical modelling and simulation exercises to predict in-human safety (Wong et al., 2013). Although initial data showed GDC-0152 was tolerated, its translation into additional human clinical trials has been delayed due to withdrawal of a Phase I trial for reasons unrelated to safety or anti-tumour activity

(NCT00977067). Similar to GDC-0152, CUDC-427's progression in-human clinical trials has also been arrested. CUDC-427 was tested in a Phase I trial in 42 patients with advanced solid malignancies to determine its safety profile (NCT01226277) (Tolcher et al., 2016). Patients were treated for two out of three weeks with escalating doses of CUDC-427, starting from 5 mg and advancing to 600 mg. AEs included fatigue, nausea, vomiting and rash, with treatment being discontinued in 6 patients due to dose limiting toxicities. Although out of the 36 patients evaluable for response, 34 had no objective response, 2 patients (mucosa-associated lymphoid tissue (MALT) lymphoma of the stomach and the other a BRCA1 (germline) and platinum-refractory ovarian cancer) showed evidence of a durable CR (Tolcher et al., 2016). The profound response experienced by these 2 patients warrants further investigation into patient indications to select sensitive candidates. Despite the initial promising results, progression of GDC Smac-mimetics has halted following a second Phase I trial with CUDC-427 that was discontinued (NCT01908413) (Tolcher et al., 2016).

1.6.5 Other Smac-mimetic drugs

Numerous other Smac-mimetics have been developed and undergone pre-clinical assessment. These include APG-1387, HGS1029 (also known as AEG40826) and BI 891065 (also known as BI5).

APG-1387 (Ascentage Pharma) has shown anti-cancer effects as a single-agent *in vitro* and *in vivo* in nasopharyngeal carcinoma cells and in ovarian cancer cells (Ji et al., 2018; Li et al., 2018; Li et al., 2016). APG-1387 is currently in dose-escalation Phase I/II clinical trials to determine safety, tolerability,

pharmacokinetics and anti-cancer activity in patients with advanced solid tumours or haematological malignancies (**Table 2**) (NCT03386526, ACTRN12614000268640 and CTR20150161) (Rasco et al., 2019; Xu et al., 2018).

HGS1029 (also known as AEG40826) was developed by Aegera Therapeutics Inc. and subsequently licensed to Human Genome Sciences Inc. for commercial development. Preliminary *in vitro* studies with HGS1029 have shown it has some activity as a single-agent in 4 out of 8 pancreatic cancer cell lines tested (Humphreys et al., 2009). The safety and efficacy of HGS1029 was assessed in a Phase I clinical trial in 44 patients with advanced solid tumours (NCT00708006). The most common AEs were nausea, anorexia, pyrexia, vomiting, diarrhea, fatigue and rash, with dose limiting toxicities being observed in 1 out of 9 patients at 1.4 mg/m_2 and in 2 out of 6 patients at 4.8 mg/m_2. Best responses were 1 colon cancer patient presenting with tumour regression and 2 patients, with non-small-cell lung carcinoma (NSCLC) and adrenocortical carcinoma, having stable disease for more than 6 months (Eckhardt et al., 2010; Sikic et al., 2011). Despite these promising results, progression of HGS1029 has been attenuated due to termination of a second Phase I clinical trial (NCT01013818).

BI 891065 (also known as BI5) was developed by Boehringer Ingelheim and has higher selectivity towards cIAP1 and cIAP2 compared to XIAP. BI 891065 has shown modest single-agent efficacy in MBT-2 bladder cancer and EMT6 breast cancer cell lines (Impagnatiello et al., 2017). It is currently in human clinical Phase

I trials to determine safety, tolerability and efficacy (**Table 2**) (NCT03697304, NCT03166631 and NCT04138823).

Table 2 In progress clinical Smac-mimetic trials

Smac-mimetic	Adjuvant therapy	Cancer	Phase	Clinical trial	Date
Birinapant	Pembrolizumab	Solid cancer	I/II	NCT02587962	Aug-17
Birinapant	Radiation	HNSCC	I	NCT03803774	Jan-19
LCL161	None	Myelofibrosis	II	NCT02098161	Dec-14
LCL161	Immunotherapy[a]	Solid tumours[b]	Ib	NCT02890069	Oct-16
LCL161	Immunotherapy[c]	Multiple myeloma	I	NCT03111992	Dec-17
LCL161	Topotecan	Solid tumours[d]	I/II	NCT02649673	Jul-19
AT-406	Nivolumab	Solid cancer	I/II	NCT04122625	Apr-19
AT-406	Pembrolizumab	Solid tumours[e]	I	NCT03871959	Sep-19
AT-406	Avelumab	NSCLC	Ib	NCT03270176	Oct-17
AT-406	Cisplatin/radiotherapy	HNSCC	I/II	NCT02022098	Oct-13
APG-1387	None	Solid cancer/Haem	I/II	NCT03386526	Nov-17
BI 891065	Immunotherapy[f]	Solid tumours[g]	I	NCT03166631	May-17
BI 891065	Immunotherapy[h]	Neoplasm/metastasis	II	NCT03697304	Mar-19

[a] PDR001, Everolimus, Panobinstat, QBM076, HDM201
[b] Colorectal cancer, adenocarcinoma, triple negative breast cancer, renal cell carcinoma
[c] PDR001, CJM112
[d] Topotecan, pegylated GCSF
[e] Small cell lung cancer, ovarian cancer
[f] Adenocarcinoma of the pancreas, colon and rectum cancer
[g] BI 754091, BI 754111
[h] Neoplasms, neoplasm metastasis, NSCLC
[i] BI 754091

1.7 Mechanisms of Resistance to Smac-mimetics and Strategies to Overcome Them

The Phase I/II human clinical trials of Smac-mimetics indicated that they are tolerated as single-agents but have low efficacy. Therefore, pre-clinical and clinical research has been conducted to identify biomarkers of response and combination treatments that can increase the effectiveness of Smac-mimetic treatment.

1.7.1 Importance of TNF

The ability of a tumour to produce and respond to TNF (or another TNFSF death ligand) is vital for the anti-tumour effect of Smac-mimetics, and tumours that lack either of these functions will most likely be resistant to Smac-mimetic treatment (Gaither et al., 2007; Petersen et al., 2007; Varfolomeev et al., 2007; Vince et al., 2007). For this reason, an obvious initial combination therapy was the addition of exogenous TNF (or TRAIL) to overcome Smac-mimetic treatment resistance. The efficacy of TNF and/or TRAIL in combination with birinapant is demonstrated by the sensitisation of 41 out of 93 birinapant resistant malignancies *in vitro* (Benetatos et al., 2014). In HNSCC cell lines with differential expression of FADD and cIAP1, addition of TNF or TRAIL dramatically sensitised all tumours to birinapant-mediated killing (Eytan et al., 2015). Similar results have also been observed in melanoma cell lines where 9 out of 16 birinapant resistant tumours were dramatically sensitised to birinapant-mediated killing with the addition of TNF (Krepler et al., 2013).

Despite these results indicating addition of exogenous TNF *in vitro* is able to sensitise Smac-mimetic resistant tumours to treatment, administrating TNF systemically to patients is not feasible due to extreme toxicities observed at therapeutically relevant doses (Roberts et al., 2011). Isolated limb perfusion (ILP) is one technique that has been used to administer TNF at therapeutically relevant doses in combination with chemotherapies, however the technical challenges and innate limitations of ILP means it is only plausible for a minority of localised cancers and therefore alternative methods have been developed to be used in

combination with Smac-mimetics (Lejeune et al., 2006). For example, to overcome the barrier of systemically safe, tumour specific TNF delivery, Yuan and colleagues developed a novel system whereby systemic delivery of adeno-associated virus bacteriophage-TNF (AAVP-TNF) enables tumour vasculature-targeted gene therapy (Yuan et al., 2013). This system allows delivery of TNF directly to the tumour tissue, minimising systemic toxicity (Hajitou et al., 2007; Hajitou et al., 2006; Yuan et al., 2013). Co-administration of AAVP-TNF and LCL161 to M21 human xenograft mice led to increased expression of TNF specifically in tumour tissue, and not in healthy organs. Combination therapy was synergistic and significantly prolonged survival of mice (Yuan et al., 2013). Similarly, cytokine-engineered oncolytic viruses, such as the TNF-armed attenuated oncolytic vesicular stomatitis virus (VSVΔ51), combined with the Smac-mimetic LCL161, slowed tumour growth and improved survival rates in mouse models of solid tumours (Beug et al., 2018). These findings support the hypothesis that increasing TNF expression *in vivo* potentiates Smac-mimetic treatment.

Another approach has been to enhance the levels of TNF expressed by the tumour, by targeting parallel signalling pathways. A boutique screen of kinase inhibitors in macrophages showed, surprisingly, that 11 distinct p38 MAPK inhibitors synergised with compound A, the preclinical precursor of birinapant, to increase TNF production and macrophage killing (Lalaoui et al., 2016). One of these, LY2228820 (Ralimetinib), was shown to increase induction of TNF by Smac-mimetic treatment leading to synergistic potentiation of birinapant killing of

AML cells both *in vitro* and *in vivo* (Lalaoui et al., 2016). Another approach has been to induce TNF in tumours more conventionally using toll-like receptor (TLR) ligands, such as CpG and poly(I:C). Surprisingly, when combined with LCL161 in an *in vivo* model, peritoneal injection of poly(I:C) was better at curing the mice than intra-tumoural injection. However, when combined with CpG, the best responses were dual intra-tumoural and peritoneal injection (Beug et al., 2014). These results certainly suggest that Smac-mimetics can combine with circulating TNF and not just TNF produced in the tumour micro-environment.

1.7.2 Combination with Radiation

Having established the neccessicity of TNF for Smac-mimetic-mediated killing, and the potential for increased TNF to overcome treatment resistance, novel combination therapies were explored that combined Smac-mimetics with TNF enhancing therapy. Hallahan and colleagues reported that treatment of human sarcoma cells with ionising radiation led to an increase in TNF mRNA and an increased production of TNF protein. The increased production of TNF enhanced radiation-mediated killing through autocrine and paracrine mechanisms (Hallahan et al., 1989). Armed with this knowledge, the combination of Smac-mimetics with radiation was explored to overcome TNF-mediated Smac-mimetic resistance in cancer. Birinapant or radiation single-agent treatment only modestly extended the survival of mice burdened with FADD overexpressing HNSCC UM-SCC-46 xenograft tumours (Eytan et al., 2016). Strikingly however, the combination of Smac-mimetic with radiation cured these mice of HNSCC tumours with no signs of relapse, up to 130 days (Eytan et al., 2016). A potent increase in endogenous TNF levels in the tumours was found, corroborating the hypothesis

that the radiosensitisation effect of birinapant is due to an enhancement of TNF in the environment. Similar findings were observed in esophageal squamous carcinoma cells (ESCC), where the radiosensitising effect of LCL161 was investigated. ESCC cells were differentially sensitive to Smac-mimetic single-agent treatment, however addition of radiation, increased radiation-induced TNF, DNA fragmentation and apoptosis of these cells. The pan-caspase inhibitor zVAD-FMK attenuated apoptosis, therefore the sensitisation mediated by the addition of LCL161 was due to the activation of the TNFR1 extrinsic apoptotic pathway (Qin et al., 2014). Further studies showed that AT-406 significantly enhanced radiosensitisation in NSCLC and HNSCC tumours *in vitro* and *in vivo* (Liu et al., 2014; Matzinger et al., 2015). This sensitisation was driven by an increase in autocrine TNF production and cell death was mediated by caspases (Liu et al., 2014; Matzinger et al., 2015). Due to these promising findings, radiation therapy is being trialed in HNSCC tumours in combination with birinapant (NCT03803774) and AT-406 (NCT02022098) (**Table 2**).

1.7.3 Combination with Chemotherapy

Upon exposure of cells to cytotoxic drugs and DNA-damaging agents, a measurable decrease of endogenous Smac within the mitochondria and an accumulation within the cytosol can be observed (Adrain et al., 2001). Therefore, Smac-mimetics provide a means to augment the natural response to cytotoxic compounds. Chemotherapy remains the front-line treatment for a range of cancers, rationalising the exploration of pairing Smac-mimetics with chemotherapies for combination treatment. Paclitaxel is one of the first-line chemotherapy treatments for NSCLC however, due to its limited efficacy in some

patients, new combination treatments are being investigated (Chu et al., 2005). An increase in expression of cIAP levels has been shown to correlate with poor prognosis and lower overall survival in various types of cancer, including NSCLC (Dai et al., 2003; Esposito et al., 2007; Tanimoto et al., 2005; Yang et al., 2016). Therefore, combining the Smac-mimetic LCL161 with paclitaxel in NSCLC tumours was investigated. Addition of LCL161 to paclitaxel therapy increased TNF expression, degradation of cIAP1/2 and activation of caspase 8 dependent apoptotic signalling, sensitising NSCLC cancer cells to treatment *in vitro* (Yang et al., 2016). Similar findings were observed in mice xenografted with NSCLC tumours where LCL161 plus paclitaxel treatment had better anti-tumour activity than either treatment alone (Yang et al., 2016).

Treatment of HNSCC cell lines with birinapant plus docetaxel was more effective than either treatment alone *in vitro* (Eytan et al., 2015). However, while birinapant plus docetaxel treatment of mice burdened with HNSCC xenografts significantly reduced tumour volume, there was no extension in survival compared to control treated mice (Eytan et al., 2015). Surprisingly however, there was a significant extension in survival with birinapant single-agent treatment, although it was less effective at reducing tumour volume (Eytan et al., 2015). The authors suggested that a different dosing schedule might have increased survival in the combination treated animals, but regardless, the results yet again emphasise that *in vivo* response to birinapant can be better than predicted from *in vitro* studies. In HL-60, OVCAR-3 and HT-1376 cancer cell lines, the effects of birinapant treatment could be enhanced by the addition of chemotherapy agents SN-38 (active

metabolite of irinotecan), gemcitabine or 5-azacytidine, but not pemetrexed, vemurafenib, bendamustine or sorafenib (Benetatos et al., 2014). Interestingly, in the HT-1376 bladder cancer cell line, the potentiation of birinapant and gemcitabine treatment was not attenuated by co-treatment with an anti-TNF antibody, thus indicating that the increase in cell death was via a TNF-independent-mechanism in this tumour (Benetatos et al., 2014).

Platinum-based chemotherapy, commonly carboplatin, is the front-line therapy for ovarian cancer patients, however patients can develop resistance to treatment (Cannistra, 1993, 2004). In high-grade serous ovarian cancer (HGSC) primary samples, a small proportion of cells were platinum resistant and possessed stem cell characteristics of tumour initiation, self-renewal and had high expression of IAP proteins. Co-treatment of birinapant with carboplatin led to sensitisation of these cells and increased killing in a caspase 8 dependent mechanism *in vitro* and in xenograft HGSC models (Janzen et al., 2015). As expected, human ovarian adenocarcinoma (HOAC) cells had a variable response to carboplatin single-agent treatment, with 3 out of 5 being resistant. However, despite resistance to chemotherapy, co-treatment with AT-406 plus carboplatin sensitised these cells to cell death *in vitro* (Thibault et al., 2018). Treatment of carboplatin and AT-406 *in vitro* resistant SKOV-3 HOAC xenograft burdened mice with carboplatin had no effect, whilst treatment with AT-406 single-agent induced a slow-down in tumour growth and complete regression in 1 out of 7 mice. This effect was potentiated with the addition of carboplatin leading to slow-down of tumour growth in 2 mice and complete regression in 5 mice (out of 7)

(Thibault et al., 2018). Furthermore, *in vivo* treatment of OVCAR3ip (cells selected *in vivo* from OVCAR3 parental cells to form ascites) carboplatin-resistant ovarian xenograft models with AT-406 in combination with carboplatin was able to prolong survival of mice better than single treatments (Brunckhorst et al., 2012). The capacity of Smac-mimetics to act as single agents or in combination with carboplatin to kill carboplatin resistant ovarian cancer cell lines validates them as a combination or alternative therapy to overcome resistance (Brunckhorst et al., 2012).

The preclinical data discussed above indicated Smac-mimetics are more efficacious when combined with TNF inducing chemotherapies than alone. For this reason, birinapant was combined with several chemotherapies including, carboplatin/paclitaxel, irinotecan, docetaxel, gemcitabine or liposomal doxorubicin for the treatment of patients with solid tumours. Co-treatment of birinapant with these diverse chemotherapies in 124 patients with refractory/relapsed solid tumours did not limit the dose of chemotherapy administered. Despite 7 patients experiencing reversible Bell's palsy symptoms, overall birinapant was well tolerated in combination with chemotherapy as a treatment. Clinical benefit was observed in numerous patients, with 11 patients having a PR and 61 having stable disease. Of the chemotherapies tested, irinotecan enhanced birinapants activity the most, even in patients that had previously failed irinotecan therapy (NCT01188499) (Amaravadi et al., 2013). Therefore, a Phase II extension study was conducted combining birinapant with irinotecan in irinotecan-relapsed or refractory metastatic colorectal cancer

patients (Senzer et al., 2013). Birinapant was administered at a fixed dose or in an ascending dose schedule (ADS) in combination with irinotecan at a fixed dose. The combination was well tolerated and the ADS appeared to prevent symptoms of Bell's palsy. Two patients achieved a PR, while 27 had stable disease. Together this study supports the idea that combining birinapant with the TNF inducing chemotherapy irinotecan may be a feasible therapeutic strategy for irinotecan resistant tumours (NCT01188499) (Senzer et al., 2013).

As discussed above, the chemotherapy paclitaxel has been shown to potentiate LCL161 mediated killing in solid tumours, including triple negative breast cancer (TNBC) (Bardia et al., 2015; Dienstmann et al., 2012; Firestone et al., 2009; Yang et al., 2016). Phase II clinical trials were initiated (Bardia et al., 2018), following Phase I trials that indicated that LCL161 plus paclitaxel therapy is well tolerated (Dienstmann et al., 2012). Interestingly, for this study the TNF-based gene expression signature (GS) was determined for each patient and used as a predictor of sensitivity to Smac-mimetic mediated cell death (Bardia et al., 2018). Bardia and colleagues conducted a global trial incorporating molecular pre-screening to investigate the neoadjuvant treatment of LCL161 and paclitaxel in TNBC patients assigned as GS-positive (more likely to respond to Smac-mimetic treatment) vs GS-negative (less likely to respond) (Bardia et al., 2018). Of 207 patients, 30.4% had a GS-positive score and combination treatment was more effective than paclitaxel alone treatment. However, in the GS-negative group comprising 69.6% of the patient population, there was an antagonistic effect in combination treatment compared to control arms. This study highlights the

importance of molecular screening to determine eligibility of patients and the analysis of possible increased toxicities (NCT01617668) (Bardia et al., 2018).

1.7.4 Combination with Bcl-2 Inhibitors

B-cell lymphoma 2 (Bcl-2) prevents Bax/Bak mediated disruption of the mitochondrial outer-membrane, preventing cell death and efflux of cytochrome *c* from the mitochondrial inter-membrane space (Delbridge et al., 2016; Kluck et al., 1997; Yang et al., 1997). Efflux of endogenous Smac from within the mitochondria is also regulated by Bcl-2 and cells overexpressing Bcl-2 inhibit the release of Smac from the mitochondria following apoptotic stimulus (Adrain et al., 2001; Ekert et al., 2001). Combining Smac-mimetics with other specific inducers of cell death, such as Bcl-2 inhibitors, might increase efficacy and reduce toxicity. Preliminary studies where the authors knocked down Bcl-2 which led to resistant Huh7 cells becoming sensitised to LCL161 treatment *in vitro*, were nevertheless discouraging because the level of cell death achieved was minimal (less than 20%) (Chen et al., 2012a). More impressive results were obtained combining the putative Bcl-2 inhibitor SC-2001 (a derivative of obatoclax) with LCL161 to treat Huh-7 xenograft tumours *in vivo* (Chen et al., 2012a). MM cells have been shown to have high expression of anti-apoptotic Bcl-2 (Pettersson et al., 1992; Wuilleme-Toumi et al., 2005) and IAP family members (Desplanques et al., 2009; Nakagawa et al., 2006), suggesting that the co-inhibition of these two families of proteins may be beneficial for the treatment of MM. Co-treatment with obatoclax and LCL161 led to a synergistic killing of MM cell lines (Ramakrishnan et al., 2016). However, this synergistic killing may not be due specifically to obatoclax inhibiting Bcl-2 because a number of well controlled studies have shown that

obatoclax kills cells in a Bax-Bak independent manner and does not act as a BH3 mimetic (Villalobos-Ortiz et al., 2019; Vogler et al., 2009). A more recent study combining the specific Bcl-2 inhibitor ABT-199 with Smac-mimetics birinapant or AT-406, showed an increase in human colon adenocarcinoma cell death compared to single-agent treatments (Perimenis et al., 2016). Together these preclinical studies indicate the potential for targeting the intrinsic and extrinsic apoptosis pathways in Smac-mimetic combination therapy.

1.7.5 Combination with Immunotherapy

Immunotherapy harnesses the immune system to kill tumours. Kearney *et al.* 2017, showed that the Smac-mimetic birinapant sensitised tumour cells to TNF dependent killing by cytotoxic lymphocytes (CLs), both CD8+ T cells and natural killer (NK) cells. Upon antigen recognition or NK-activating receptor activation, CLs naturally respond by inducing TNF. Surprisingly, given the data showing the ability of Smac-mimetics to increase TNF levels, birinapant did not increase T-cell production of TNF (Kearney et al., 2017). On the other hand, tumour derived programmed death-ligand 1 (PD-L1) engagement of its receptor, programmed cell death protein 1 (PD-1), expressed on CLs, decreased CL production of TNF. Furthermore, while birinapant didn't increase TNF secretion by CLs, it did sensitise the tumour cells to TNF induced death. Together these results suggested that the combination of the immune checkpoint inhibitor (ICI), anti-PD1, and birinapant would be a very effective way to increase CL killing. And indeed, this is what the authors observed (Kearney et al., 2017). Similarly, Beug and colleagues showed that combining the ICIs, anti-PD1 or anti-cytotoxic T-lymphocyte-associated protein 4 (anti-CTLA-4), with the Smac-mimetic LCL161

greatly increased survival in intra-cranial mouse glioblastoma models and produced durable cures (Beug et al., 2017). These results are particularly significant on several levels. Firstly, they show that the combination therapy works well *in vivo* without any reported toxicity. Secondly, the Smac-mimetic was delivered orally, yet the blood-brain barrier, a significant barrier for many drugs, was not an impediment, thus the combination works in one of the most challenging *in vivo* environments. Thirdly, the authors showed that more than one Smac-mimetic and ICI cocktail was effective, boosting confidence in the general utility of the approach. Lastly, the durable response was associated with immunological memory suggesting the potential of the therapy to deliver long-term cures. As in single-agent studies, TNF was an important part of the cytotoxic response and also required CD8+ T-cells (Beug et al., 2017). Encouragingly, an independent study with the Smac-mimetic BI 891065 in combination with an anti-PD1 antibody also eradicated breast cancer tumours in immunocompetent mice (Impagnatiello et al., 2017).

Clinical trials in solid tumours with diverse Smac-mimetics and immunotherapy are currently in progress; birinapant and Pembrolizumab (NCT02587962), LCL161 and PDR001 (NCT03111992 and NCT02890069), AT-406 and Nivolumab or Avelumab (NCT04122625 and NCT03270176), and BI 891065 and BI 754091 (NCT03697304, NCT03166631 and NCT04138823) (**Table 2**).

1.7.6 Inducing Necroptosis

Smac-mimetics can sensitise cells to both apoptotic and necroptotic cell death pathways mediated by TNFR1. As previously discussed, the majority of current

cancer chemotherapies utilise the intrinisic apoptotic pathway to induce cell death. As many cancers have evolved resistance to cell death via apoptosis, the ability of Smac-mimetics to regulate the TNF cell death pathways through promoting both apoptosis and necroptosis provides a promosing novel therapeutic avenue towards resistant malignancies (Fulda, 2012; Laukens et al., 2011). Proof of principle for this concept has been shown as an effective way to kill AML cells both *in vitro* (Steinwascher et al., 2015) and also safely *in vivo* (Brumatti et al., 2016). Specifically Brumatti and colleagues induced necroptosis by combining birinapant with the U.S Food and Drug Administration (FDA) approved caspase inhibitor IDN-6556 (Emricasan) (Brumatti et al., 2016). However, Smac-mimetic-mediated necroptotic cell death does not always require pharmaceutical inhibition of caspases. Birinapant has been observed to mediate cell death through dual action of apoptotic and necroptotic mechanisms in ALL (McComb et al., 2016). Similarily, addition of AT-406 with the chemotherapy carboplatin led to ovarian cancer cell apoptotic or necroptotic cell death, depending on the cell line (Thibault et al., 2018). Together these studies suggest a double activity (apoptotic and non-apoptotic) of birinapant in cancer cells, making it an attractive drug for the treatment of apoptotic resistant cancers.

1.8 Mechanical Resistance: ABC transporters

Despite the promise and optimism surrounding Smac-mimetics as single-agents and in combinations, there has been variable and limited success to date. One common failure to all of these treatment regimens is drug resistance. Multidrug resistance (MDR) is a phenomenon that has been observed in both patients naïve to treatment and in patients that have received extensive treatment. A

potential cause of MDR is upregulation of ATP-binding cassette (ABC) transporter family members, so called due to the presence of a common, highly conserved ATP-binding cassette (Higgins, 1992). Alternative names for ABC transporters include ATPases and P-glycoproteins (Borst and Elferink, 2002). These transporters are able to actively pump out exogenous toxic substrates from within the cell into the extracellular space, protecting cells from possible toxicity (Fletcher et al., 2010). ABC transporters are the largest transmembrane superfamily and consist of 48 members in humans, dived into 7 subfamilies, labelled A to G, according to their sequence and structure homology (Fletcher et al., 2010). The most well described ABC transporters are ABCB1 (MDR1 or P-glycoprotein), ABCC1 (MRP1) and ABCG2 (BCRP) (Fletcher et al., 2010).

1.8.1 MDR1

The multidrug resistance protein 1 (MDR1) also known as P-glycoprotein (P-gp), was first identified in the 1970's and its upregulation has been correlated with drug resistance, disease relapse and poor prognosis (Abraham et al., 1993; Juliano and Ling, 1976; van Helvoort et al., 1996). Due to the known importance of MDR1, there was an impressive scientific community effort to determine its crystal structure. However, due to MDR1's large size, flexibility and insolubility in water, the murine structure was only determined in 2009 and the human structure in 2018 (Aller et al., 2009; Kim and Chen, 2018; Waghray and Zhang, 2017). The overall structure of MDR1 allows molecules to be bound from the intracellular side of a cell, and then released into the extracellular side, following binding and hydrolysis of ATP. In more detail, the structure of MDR1 is produced by two halves, each containing transmembrane alpha-helices and a nucleotide binding

domain (NBD) (**Figure 1.5**). The two halves join to produce the canonical ABC transporter fold, where the two NBDs dimerise and hydrolyse ATP at the interface. This structure allows molecules to bind a cavity created within the inward-facing structure of more than 6000 Å in size. Following dynamic conformational changes of the NBD, driven by ATP binding and hydrolysis, molecules are then released into the extracellular side (Aller et al., 2009; Kim and Chen, 2018).

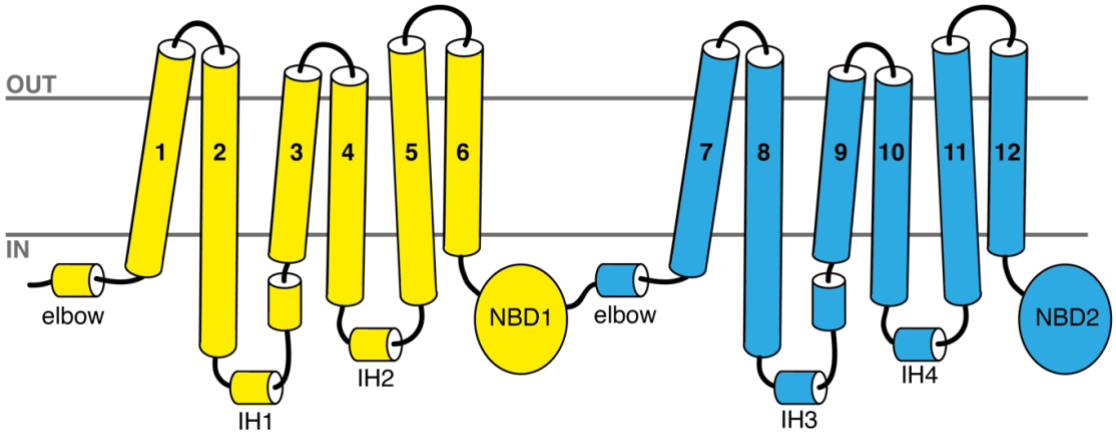

Figure 1.5 MDR1 structure

Topology diagram of human MDR1 illustrating two symmetric halves (yellow and blue). Each contain transmembrane domains and a nucleotide-binding domain (NBD). IH; intracellular helices, OUT; extracellular side, IN; intracellular side. Reproduced from (Kim and Chen, 2018).

An observed phenomenon is the diverse chemical and structural nature of substrates that MDR1 can recognise, including lipids, steroids, peptides, chemotherapeutic drugs and chemical compounds, such as the fluorescent dye Rhodamine-123 (**Table 3**) (Borst and Elferink, 2002; Didziapetris et al., 2003; Seelig, 1998; Takara et al., 2006). Prior to the crystallisation of MDR1, characterisation of different binding sites was described through drug binding and competition studies. These binding sites included the H site (Hoechst-33342 and colchicine), R site (rhodamine-123 and anthracyclines) and P site (prazosin and progesterone) (Martin et al., 2000; Shapiro et al., 1999; Shapiro and Ling, 1997). Generation of compounds derived from natural marine products, the molecule QZ59-RRR and its enantiomer QZ59-SSS, showed for the first time compounds precisely localised in the drug-binding region of MDR1 (Aller et al., 2009). Furthermore, compounds generated based on QZ59-SSS, with systematic increase in size and hydrophobicity, were also able to be bound to MDR1 and inhibit substrate transport, as measured by structure-activity relationship analysis (Aller et al., 2009). These findings led to the reasoning that MDR1 can distinguish between the ligand stereoisomers with distinct binding sites, orientations and stoichiometry and that the binding of compounds is poly-specific. Following these advancements, intense efforts to generate *in silico* approaches and computational models were undertaken to predict substrates and inhibitors of MDR1 (Chen et al., 2012b; Waghray and Zhang, 2017; Wang et al., 2011). However, to date it has not been possible to discern a common chemical feature recognised by MDR1, and therefore, whether a molecule is a substrate of MDR1

must still be determined empirically (Chen et al., 2012b; Waghray and Zhang, 2017; Wang et al., 2011).

Table 3 Substrates for MDR1

Chemo drugs	Cardiac drugs	Calcium antagonists	Psychoactive	Lipid lowering
Daunorubicin	α-methyldigoxin	Felodipine	Perphenazine	Atorvastatin
Doxorubicin	Digitoxin	Nicardipine	Spiperone	Lovastatin
Irinotecan	Digoxin	Nitrendipine	Thioridazine	Simvastatin
Topotecan	Quinidine	Verapamil	Trifluoperazine	
Etoposide	Nicardipine	Bepridil	Triflupromazine	**Other drugs**
Teniposide		Diltiazem		Calcein-AM
Docetaxel	**Antibiotics**	Gallopamil	**HIV protease inhibitors**	Rhodamine-123
Paclitaxel	Clarithromycin		Amprenavir	Loperamide
Vinblastine	Erythromycin	**Steroids**	Indinavir	Imatinib
Vincristine	Levofloxacin	Aldosterone	Nelfinavir	Domperidone
Vindesine	Sparfloxacin	Dexamethasone	Ritoavir	Cepharanthine
Vinorelbine	Saquinavir	Estradiol	Saquinavir	Dexamethasone
Paclitaxel	Cefazolin	Progesterone		Cinchocaine
Bisantrene	Cefoperazone	Hydrocortisone	**β-adreno antagonists**	Dipyridamole
Catharanthine	Cefotetan		Bunitrolol	Domperidone
Mitoxantrone		**Immune suppressants**	Carvedilol	Emetine
Tamoxifen	**Antihistamine**	Cyclosporin	Celiprolol	Ivermectin
	Cetirizine	Tacrolimus	Talinolol	Methadone
Antifungals	Fexofenadine	Rapamycin		Morphine
Itraconazole	Terfenadine			Ondansetron
Ketoconazole				Phenytoin

1.8.2 MRP1 and BCRP

Other ABC transporter members, multidrug resistance-associated protein 1 (MRP1/ABCC1) and breast cancer resistance protein (BCRP/ABCG2), have been linked to clinically relevant drug resistance. The ABCC sub-family consists of 12 members and the most well documented is MRP1, which was first cloned in 1992 (Cole et al., 1992; Cole, 2014). Following the discovery of MDR1 and MRP1, some cell lines were observed to have drug resistance that was present even in the absence of these transporters, indicating the presence of a novel drug pump. This new drug transporter was identified by three independent groups and is most commonly termed BCRP for its high expression in breast cancer MCF-7 AdVp cells (Doyle et al., 1998). Alternative names include, ABCP for its high expression in placenta (Allikmets et al., 1998) and MXR for its mitoxantrone resistance (Miyake et al., 1999). BCRP also known as ABCG2, is the most well described member of the ABCG family, comprising of 5 members. Similar to MDR1, MRP1 and BCRP both require binding and hydrolysis of ATP to facilitate structural changes to efflux substrates from the intracellular to the extracellular side of a cell (Cole, 2014). The diversity of substrates for MRP1 and BCRP are similarly as diverse as MDR1, and range from small ions to large polysaccharides (Cole, 2014; Velamakanni et al., 2007).

1.8.3 MDR1 in Human Health

ABC transporters are prevalent throughout the body and play a vital role in protecting cells by exporting unwanted endogenous and exogenous toxicities. MDR1 is present in a range of organs including haematopoietic stem and progenitor cells (HSPCs), gut mucosa, liver, the blood-brain barrier and the testis-

blood barrier (Borst and Elferink, 2002; Leslie et al., 2005; Takara et al., 2006). MDR1 has been attributed to physiological functions such as the transport of cytokines, migration of antigen-presenting cells and haematopoietic stem cell self-renewal and loss of differentiation (Bunting et al., 1999; Drach et al., 1996; Randolph et al., 1998). Unlike humans, mice have two Abcb1-type transporters encoded by *Mdr1a* and *Mdr1b*. The protein products of these genes, *Mdr3* and *Mdr1* respectively, functionally combine to fulfil the job of the single ABCB1 protein in humans. *Mdr1a*$^{-/-}$, *Mdr1b*$^{-/-}$ *and Mdr1a/b*$^{-/-}$ mice are viable and fertile although they have altered sensitivity and pharmacokinetics towards drugs (Schinkel et al., 1994; Schinkel et al., 1997; Smit et al., 1993). Together these findings highlight that although MDR1 has alternative functions, its primary physiological role is to export xenotoxins to maintain homeostasis and protect cells from possible assault.

1.8.4 MDR1 in Human Disease

Due to the essential role ABC transporters play in protecting cells against possible toxicities, it is not unexpected that disfunction of these transporters results in disease. Indeed, 24 members have been associated with disease, including Parkinson's disease (Furuno et al., 2002), inflammatory bowel disease (Brant et al., 2003) and Tangier disease (Fitzgerald et al., 2010). However, most famously ABC transporters, in particular MDR1, are upregulated in cancer (Baker et al., 2005; Chauncey et al., 2000; Fletcher et al., 2010; Greenberg et al., 2004; Guerci et al., 1995; Leith et al., 1999). For example, recent work by Christie and colleagues identified multiple genetic transcriptional fusions of the *ABCB1* gene in high-grade serous ovarian and breast cancer. Presence of *ABCB1*

transcriptional fusions and overexpression of MDR1 was strongly correlated with the number of lines of MDR1-substrate therapy patients had received previously. Furthermore, ovarian cancer cells harbouring an *ABCB1* fusion were sensitised to paclitaxel treatment with inhibition of MDR1 (Christie et al., 2019). This study highlights the previous finding that chemotherapy treatment in a range of different cancers induces overexpression of MDR1, leading to an increase in drug resistance and disease relapse (Takara et al., 2006). A higher expression of MDR1 has been correlated with worse prognosis and response in haematological and solid cancers, such as acute myeloid leukaemia, multiple myeloma, lung, breast and neuroblastoma (Chan et al., 1991; Koh et al., 1992; Poulain et al., 1999; Segawa et al., 1993; Ucci et al., 1992). Similar to HSPCs, cancer stem cells (CSC) have high expression of ABC transporters, including MDR1. This initial discovery was observed from their ability to export the florescent dye, Hoechst 33342 (Goodell et al., 1996). Altogether, the presence of MDR1 is detrimental to treatment regimens and reduces the efficacy of numerous standard-of-care chemotherapy treatments.

1.8.5 MDR1 Inhibitors

The negative impact MDR1 has on the clinical treatment of cancer, drove the desire to pharmaceutically modulate MDR1-mediated efflux of chemotherapy drugs (**Figure 1.6**). This led to the development of clinical MDR1 inhibitors. First generation inhibitors, including verapamil (Rogan et al., 1984; Tsuruo et al., 1981, 1982) and cyclosporin A (CSA) (Slater et al., 1986a; Slater et al., 1986b), were already approved for clinical use and observed to have inhibition of MDR1. These early observations *in vitro* led to clinical trials in haematological and solid cancer

patients, combining verapamil or CSA with chemotherapies known to be MDR1 substrates. However, the results from these trials were variable (Belpomme et al., 2000; List et al., 2001; Ozols et al., 1987; Verweij et al., 1991) and prompted the development of more specific second-generation inhibitors of MDR1. Of this class of drugs, valspodar (PSC833) developed by Novartis, is the most well-known (Kusunoki et al., 1998; Twentyman and Bleehen, 1991). Valspodar entered into numerous clinical trials in different countries in combination with chemotherapies (Advani et al., 2001; Advani et al., 1999; Baer et al., 2002; Lee et al., 1999). However, the results from these trials indicated an increase in toxicity and mortality in the MDR1 inhibitor arm, with no improvement in clinical response or overall survival observed. The increase in toxicity was due to inhibition of MDR1-mediated intestinal transport, biliary excretion and enzyme-mediated hepatic and intestinal metabolism, leading to a change in pharmacokinetics of the chemotherapy drugs (Kirn et al., 1999; Wacher et al., 1995; Yasuda et al., 2002). The toxicity observed with this class of inhibitors prompted the development of third-generation specific MDR1 inhibitors with decreased toxicity profiles. These include the drugs zosuquidar (LY335979) and tariquidar (XR9576), which following promising *in vitro* results, entered clinical trials in combination with chemotherapies in haematological and solid cancer patients (Fox and Bates, 2007; Gerrard et al., 2004; Marcelletti et al., 2009; Mistry et al., 2001; Pusztai et al., 2005; Starling et al., 1997). However, as with the first- and second-generation compounds, there was variable and limited ability of these inhibitors, in combination with MDR1-substrate therapies, to improve the outcome of patients.

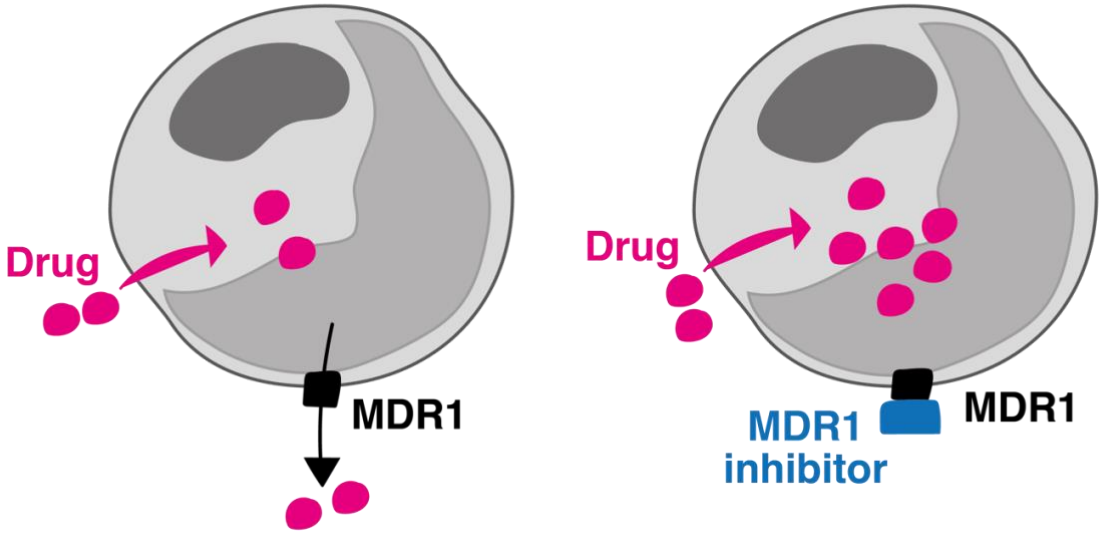

Figure 1.6 Schematic of MDR1 pump efflux

MDR1 substrates, such as drugs (pink), are pumped out of cells that have an MDR1 pump. In the presence of an MDR1 inhibitor (blue), efflux is inhibited and the intracellular concentration of the drug is increased inside the cell.

1.9 Leukaemia

Leukaemia is a broad term which encompasses a range of cancerous diseases that affect the haematopoietic and lymphoid systems. They fall into four main classes distinguished by their aggressiveness and by the main population of cells they affect; acute myeloid (AML), acute lymphoblastic (ALL), chronic myeloid (CML) and chronic lymphocytic (CLL) (Chiorazzi et al., 2005; Lowenberg et al., 1999; Pui et al., 2004; Sawyers, 1999). The incidence of all four types of leukaemia is rare, with AML and CLL being the most prevalent, each accounting for an estimated 1.2% of new cancer cases in the U.S each year (NCI, 2016). AML, CML and CLL are most common in older adults, with the median age of diagnosis being more than 65 years of age. In contrast, ALL predominantly affects children and the median age of diagnosis is 16 years old (NCI, 2016). AML is the most-deadly of the four types, having a 5-year survival rate of only 28.3% and accounting for 1.8% of all cancer deaths annually in the U.S (NCI, 2016).

1.9.1 Acute Myeloid Leukaemia

AML is a heterogenous clonal disorder of haematopoietic progenitor cells, characterised by the presence of immature myeloid cells, termed “blasts”. Blasts infiltrate and occupy space within the bone marrow, leading to insufficient haematopoiesis. In turn, this leads to granulocytopenia, thrombocytopenia or anemia, in the presence or absence of leucocytosis, depending on the cell type predominantly affected (Lowenberg et al., 1999). The clinical presentation of AML can be diverse but commonly includes symptoms of fatigue, haemorrhage, fever or infections (Lowenberg et al., 1999; PDQ, 2019). As described above,

AML most commonly affects older adults more than 60 years of age, with the median age of diagnosis being 68 and the highest rate of death among patients aged 75-84 years, however AML may also affect children (Juliusson et al., 2012; NCI, 2016; Ossenkoppele and Löwenberg, 2015; PDQ, 2019). Although the majority of AML is diagnosed as primary 'de novo' AML, there is also a smaller proportion of patients who develop 'secondary' AML due to a haematological disorder, an inherited disease, therapy related AML (t-AML) or arising from a previous incidence of myelodysplastic syndrome (MDS) (Bhatnagar et al., 2016; Lowenberg et al., 1999; Pedersen-Bjergaard et al., 2002).

1.9.2 MLL-translocation

AML is a complex disease which can originate from a range of cytogenic lesions. Knowledge of cytogenetic lesions resulting in AML and characterisation of their survival profile can enable prognosis and targeted therapeutic treatments for patients. One of the cytogenic lesions that can lead to the development of an acute leukaemia with poor prognosis, is the mixed lineage leukaemia translocation (MLL) (Gu et al., 1992; Tkachuk et al., 1992). Chromosomal rearrangements of the MLL gene located on chromosome 11q23, are prevalent in more than 70% of childhood leukaemia, ~10% of adult primary AML, up to 85% of t-AML and have been associated with low overall survival (Krivtsov and Armstrong, 2007; Lowenberg et al., 1999). Currently, there are around 80 distinct translocation partner genes which have been identified to interact with MLL, these rearrangements produce an in-frame chimeric protein that deregulates the haematopoietic system, transforming haematopoietic stem cells (HSCs) into leukaemic stem cells (LSCs) (Krivtsov and Armstrong, 2007; Meyer et al., 2018;

Meyer et al., 2013). Of these 80 translocation partners, only 5 rearrangements are responsible for ~80% of all MLL-translocation initiated leukaemia; MLL-AF4; t(4;11)(q21;23), MLL-AF9; t(9;11)(p22;q23), MLL-ENL; t(11;19)(q23;p13.3), MLL-AF10; t(10;11)(p12;q23) and MLL-AF6; t(6;11)(q27;q23 (Krivtsov and Armstrong, 2007; Meyer et al., 2018; Meyer et al., 2013). These translocations can acquire further mutations, altering their profile, for example the accelerant Ras mutation is found in 15-20% of all AML cases and is associated with an aggressive and resistant disease profile (Ofran and Rowe, 2013).

1.9.3 HoxA9/Meis1

The homeobox A9 (HoxA9) protein is a homeo-domain-containing transcription factor that is involved in embryonic development and HSC expansion. It is overexpressed in ~50% of all AML cases, in conjunction with its cofactor homeobox protein Meis 1 (Meis1), and correlates strongly with a poor prognosis (Collins et al., 2014; Krumlauf, 1994; Thorsteinsdottir et al., 2001).

Due to the prevalence and the clinical relevance of the MLL and HoxA9/Meis1 lesions, in both adult and childhood acute leukaemia, we have developed experimental models of these AMLs that recapitulate disease (**Figure 1.7**) (Brumatti et al., 2016; Lalaoui et al., 2016; Zeisig et al., 2012; Zuber et al., 2009). These models provide the invaluable tool of primary murine leukaemic cells exhibiting specific AML genetic profiles. Furthermore, these models enable the translation of *in vitro* cell based findings into *in vivo* treatment experiments. The majority of data presented in this thesis was conducted in the clinically relevant MLL-AF9, MLL-AF9-Nras^{G12D}, MLL-ENL and HoxA9/Meis1 models.

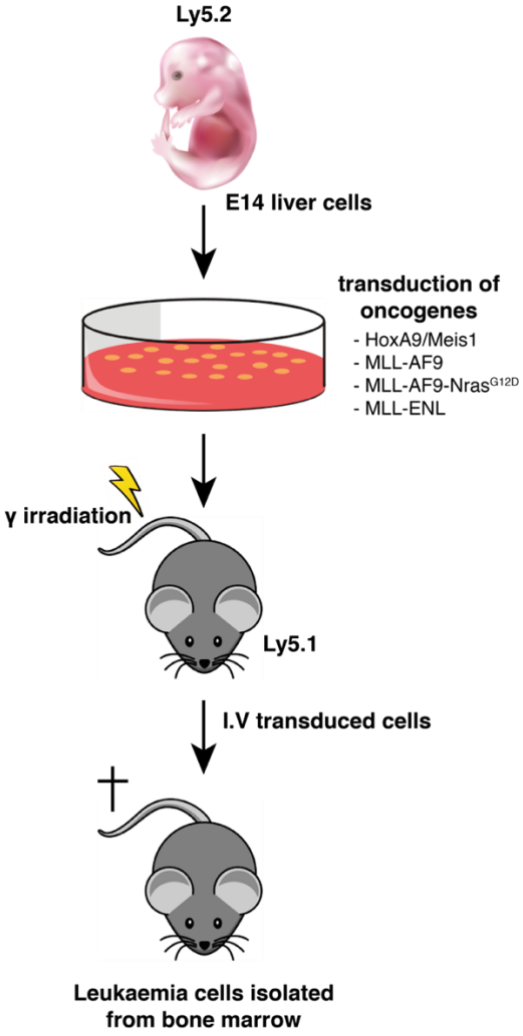

Figure 1.7 Schematic of generation of murine models

Embryonic day 14 (E14) liver cells from Ly5.2 are transduced with oncogenes, HoxA9/Meis1, MLL-AF9, MLL-AF9-Nras$_{G12D}$ and MLL-ENL. Cells are intravenously (I.V) injected into the tail vein of Ly5.1 γ irradiated mice. Cells from leukaemic burdened mice are harvested from bone marrow and used *in vitro* or transplanted into recipient mice.

1.9.4 AML Current Therapies

AML is a complex heterogenous and clonal disease, that currently has a 5-year survival rate of less than 30% (NCI, 2016). Therefore, targeted therapies towards refractory AML are urgently needed. The current therapeutic strategy for AML is induction therapy to induce remission, defined as less than 5% leukaemic blast cells in the bone marrow, and to prevent relapse (Lowenberg et al., 1999). One of the leading standard-of-care treatments is the combination of chemotherapies cytarabine (also known as Ara-c) and daunorubicin. This combination treatment regimen, commonly referred to as 7+3, involves cyclic treatments of Ara-c for days 1-7 and daunorubicin for days 1-3 (Lowenberg et al., 1999). It is incredibly proficient in promoting remission in 70-80% of patients less than 60 years of age. The outcome efficiency is reduced to 50% with an increase in patient age of more than 60 years or with refractory AML (Lowenberg et al., 1999). These relatively good remission rates however, are succumbed by AMLs high relapse rate, leading to an overall survival rate of only 5% for patients with refractory AML (Lowenberg et al., 1999; Ossenkoppele and Löwenberg, 2015; Reese and Schiller, 2013; Schiller, 1998). For these reasons, intense effort has been undertaken to improve the standard-of-care 7+3 therapy, such as the substitution of daunorubicin with other chemotherapies doxorubicin, idarubicin or mitoxantrone (Arlin et al., 1990; Berman et al., 1991; Vogler et al., 1992; Wiernik et al., 1992). Another option that has been explored is an increase in the dose of Ara-c used from 0.2 to 3 g/m_2, however, these studies have had variable success, that was only superior in patients with already favourable prognoses (Bishop et al., 1996; Grimwade et al., 1998; Mayer et al., 1994; Mrózek et al., 1997; Weick

et al., 1996). Succeeding a patient successfully entering into chemotherapy-induced remission, an allogenic bone marrow transplantation is a possible sequential treatment option. When successful, this procedure can radically reduce the rate of relapse to less than 20% and therefore, can effectively cure 50-60% of recipients. However, the inherent risks associated, including infection and graft vs. host disease, and the limited number of eligible patients, means there are severe restraints limiting the practice of this therapy (Appelbaum et al., 1984; Champlin et al., 1985; Thomas et al., 1979). When an appropriate donor is not available for an allogenic transplant, an autologous bone marrow transplant supported by myeloablative treatment has been widely used. Survival rates from this procedure have been reported to be 45-55% (Burnett et al., 1984; Löwenberg et al., 1984; Löwenberg et al., 1990). Studies have attempted to evaluate and compare the overall survival benefit of these three main treatment options; chemotherapy, allogenic or autologous bone marrow transplant. However, results have been variable and no significant differences have been found (Cassileth et al., 1998; Ravindranath et al., 1996). Therefore, there is an obvious need to develop more efficient combination treatment options for AML patients that are effective towards refractory disease, prevent relapse and sustain patients within remission.

In an effort to provide a novel therapeutic strategy, Smac-mimetics and in particular the drug birinapant, have been tested in leukaemia including AML and MDS. As detailed above, these studies have focused on the combination of birinapant with other anti-cancer agents to potentiate therapy. These studies

have shown promise *in vitro* (Brumatti et al., 2016; Lalaoui et al., 2016; McComb et al., 2016), however, there has been variable and limited results to date in in-human clinical trials (NCT02147873, NCT01486784).

1.9.5 Leukaemic Stem Cells

Relapse occurs following a period of remission when a patient's blast count exceeds 5% in the bone marrow, and it is one of the main challenges of treating AML. Patients with the most favourable prognosis are less than 60 years of age, have a positive cytogenic profile and experienced a remission period of more than one year. However, even these patients have only a ~20% chance of survival following relapse (Lowenberg et al., 1999). Therefore, the main therapeutic goal must be to prevent relapse in the first place.

Relapse can occur due to LSCs remaining in the body. These cells have a stem-cell phenotype, are mostly quiescent and have the potential to proliferate extensively to repopulate disease (Guan et al., 2003; Jordan et al., 2006). Targeting LSCs is known to be crucial for efficient eradication of AML disease and preventing relapse (Ho et al., 2016; Leith et al., 1999). LSCs are highly resistant to many currently used anti-cancer therapies and our understanding of LSC resistance to treatment and their ability to generate relapse is developing (Costello et al., 2000; Ishikawa et al., 2007; Shlush et al., 2017; van Rhenen et al., 2005). Previously, a commonly held belief was that treatment pressures, such as chemotherapy drugs, led to mutations and subsequent generation of resistant LSCs to treatment, leading to a patient relapsing and developing refractory disease (Goldie and Coldman, 1984). However, new findings have come to light

indicating the pre-existence of initial resistant LSC sub-clones and that treatment only enables selection of these resistant cells (Bachas et al., 2012; Ding et al., 2012; Garg et al., 2015; Krönke et al., 2013; Parkin et al., 2013). One mechanism that enables LSCs to have drug resistance is their high expression of ABC transporters, including MDR1 (Drenou et al., 1993; Kim et al., 2002; Scharenberg et al., 2002; Zhou et al., 2001).

1.9.6 MDR1 in AML

In AML, MDR1 plays a major role in LSC and blast cell resistance to chemotherapy treatment. MDR1 expression has been reported in ~35% of AML patients less than 60 years of age and ~70% of older patients (Leith, 1998). Patients with secondary or refractory relapse AML are more likely to have a higher expression of MDR1, therefore chemotherapy treatment can select for MDR1 high cancer (Chauncey et al., 2000; Chitnis et al., 1991; Zhou et al., 1995). This high expression of MDR1 is predictive of treatment resistance, poor prognosis, relapse and low overall survival in AML (Leith et al., 1999; Leith et al., 1997; Samdani et al., 1996). For example, patients with a higher expression of MDR1 and CD34+ (stem-like) cells had a significantly worse complete remission rate than those who were MDR1 and CD34+ negative, 5% and 63% respectively (Te Boekhorst et al., 1993). Therefore, novel treatments developed for AML must be able to overcome the burden of LSC MDR1-mediated efflux of anti-cancer therapies to be effective and generate a cure.

1.10 Conclusions

In this introduction, I have highlighted the progression of Smac-mimetics from bench to bed-side and described the challenges that Smac-mimetic therapy faces. Smac-mimetics are a promising class of drugs, that due to their unique specificity and tolerability, interest in them continues. Eight compounds have been tested in humans, all with a good tolerability and safety profile. However, a common draw back for all compounds is their limited clinical activity as single-agents. Extensive investigation has been conducted over the last decade to enhance the efficacy of Smac-mimetics as anti-cancer therapy. The strengths and weaknesses of Smac-mimetic therapy are complex and intertwined. TNF is an essential component for Smac-mimetic mediated cell death and tumours that do not produce and respond to TNF are inherently resistant to Smac-mimetic treatment, limiting therapy. Various combinations have been investigated to enhance the levels of TNF in the tumour tissue either through addition of exogenous TNF, chemotherapy, radiation, immunotherapy or activating necroptosis. However, a commonalitly between these treatments is drug resisitance that can be mediated by members of the ABC transporter family, in particular MDR1. AML is an aggressive disease, characterised by a high relapse rate, low overall survival and expression of ABC transporters, including MDR1. The treatment of AML with Smac-mimetic therapy has been investigated and shows promise, however, as with other tumour types, the response has been minimal. Therefore, this thesis cohesively describes my investigation into mechanisms of resistance AML cells use to evade Smac-mimetic therapy and

the development of novel therapy combinations that are effective towards resistant blast cells and LSCs.

2 Materials and Methods

2.1 Nomenclature

Although I am aware of the changes in HUGO gene nomenclature, for simplicity and readability, I have used the following gene nomenclature: MLL (KMT2A); ENL (MLLT1) and AF9 (MLLT3).

2.2 High Throughput Viability Screen Strategy

To identify bioactive compounds that could overcome resistance to birinapant in AML cells, we conducted a high throughput viability screen of more than 5,700 compounds in two independent birinapant resistant murine HoxA9/Meis1 leukaemias. Cells were subjected to a three-phase viability screen. In Phase I, cell viability was compared between birinapant single treatment and in the presence of library compounds. Drugs that were able to induce more than 50% cell death were selected for further testing (~300 compounds). To determine the toxicity of these compounds as single agents, in Phase II, AML cells were treated with these drugs with or without birinapant. Compounds that were able to synergise with birinapant and kill more than 50% of AML cells, but had no effect as single-agents, were then selected (~20 compounds). In Phase III of the screening, the ~20 compounds were subjected to dose-response testing to select for drugs that were able to synergise with birinapant at clinical achievable doses (less than 1μM).

2.3 Tissue Culture

Primary murine leukaemia models were established and generated as previously described (Brumatti et al., 2016; Zuber et al., 2009). Briefly, fetal liver (E14.5) progenitor/stem cells from wild-type, *Tnfr1*$^{-/-}$, *Ripk3*$^{-/-}$ or *Caspase8*$^{-/-}$*Ripk3*$^{-/-}$ C57BL/6 Ly5.2 mice were cultured in α-minimum essential medium (α-MEM, Gibco) supplemented with 10% fetal calf serum (FCS), 2 mM L-glutamine, murine stem cell factor, (100 ng/ml, PeproTech), IL-6 (10 ng/ml), thrombopoietin (50 ng/ml), and FMS-related tyrosine kinase 3 (FLT) (10 ng/ml) (all produced in house at WEHI). Retroviral oncogene constructs for MLL-ENL, HoxA9/Meis1, MLL-AF9 and MLL-AF9-Nras^{G12D} were previously published (Brumatti et al., 2016; Lalaoui et al., 2016). Fetal liver cells were transduced with viral supernatant produced in 293T cells co-transfected with oncogene constructs and packaging vectors following the RetroNectin protocol (Brumatti et al., 2016). Following infection, transduced cells were tail vein injected intravenously (IV) into sub-lethally g-irradiated (7.5 Gy) C57BL/5 Ly5.1 mice. Upon signs of a leukaemic phenotype (lethargy, hunched posture, hind leg paralysis, enlarged spleen and liver) mice were culled and leukaemic cells harvested from the bone marrow and cultured in Iscove's modified Dulbecco's medium (IMDM, Gibco) supplemented with 10% FCS and 3 ng/ml IL-3 (Peprotech). In contrast, lineage negative (L^-), Sca-1 positive (S^+) and c-Kit positive (K^+) (LSK) cells from C57BL/6 mice were cultured in α-MEM supplemented with murine stem cell factor (SCF) (100 ng/ml, PeproTech), IL-6 (10 ng/ml, WEHI), thrombopoietin (50 ng/ml, WEHI) and FMS-related tyrosine kinase 3 (FLT, WEHI) (10 ng/ml). The human AML cell lines KG1, HL60, MV4-11 and HEL were cultured in Roswell Park Memorial Institute

medium (RPMI, Gibco) supplemented with 10% FCS. HEK-293T cells were cultured in Dulbecco modified Eagle's medium (DMEM, Gibco) and were also supplemented with 10% FCS. All cells were cultured at 37°C in a 10% CO_2 humidified atmosphere. Cell culture medias were purchased from Thermo Fisher Scientific.

2.4 Reagents

Smac-mimetics were sourced from different companies; birinapant (SelleckChem), deuterium labelled birinapant (kindly provided by TetraLogic Pharmaceuticals), GDC-0152 (Genetech), LCL-161 (Novartis), AT-406/Debio1143 (Ascenta) and AEG-40730 (Aegera Therapeutics) (Bertrand et al., 2008). Necrostatin-1 (Nec-1), cytarabine (Ara-c; *in vitro*), reserpine, tariquidar, U0126, JQ1, ABT-199 and the compound library for screening were purchased from SelleckChem. Zosuquidar trihydrochloride, CGP-71683 hydrochloride, Fluphenazine dihydrochloride and PD098059 were purchased from MedChemExpress. Rhodamine-123, reversan, Fum-C and Ara-c (*in vivo*) were purchased from Sigma. SDZ-21009, LP-44 and LP-12 were purchased from Tocris. LP-44 and GR-127935 were purchased from Abcam. TNF was produced within the Silke laboratory at the WEHI.

2.5 *In vitro* AML Viability Assays

For short-term cell death assays (murine AML cells for 24 hours and human AML cells for 48 hours) 2.5-5 x 10_4 cells were plated per well in a 96 well flat bottom plate and treated as described per experiment. MDR1 inhibitors were added 15

minutes prior to Smac-mimetic treatment. For cell viability analysis, samples were spun at 300 g for 5 minutes at room temperature (RT) and cells resuspended in Phosphate-buffered solution (PBS) containing propidium iodide (PI) (1 μg/ml). Long-term viability time courses were conducted by culturing 1 x 10^6 (murine) or 2.5 x 10^5 (human) leukaemic cells in 1 ml containing the specific drug treatments for the indicated time points. Cells were used for cell viability analysis by flow cytometry (Calibur BD Biosciences), generation of cell lysates and/or clonogenic assays. For murine AML cells, cell death was determined by quantification of PI uptake, whilst cell viability of human AML cell lines and primary patient samples, was determined by PI exclusion and change in cell volume (forward-scattered light, FSC). Flow cytometry data was analysed with FlowJo 10.0.8, 10.5 or 10.6 software.

2.6 Clonogenic Assays

AML cells were pre-treated for 6 hours prior to being plated for clonogenic assays as follows; 1 x 10^5 cells per 100 μl was plated and treated with compounds as specified per experiment. Different dilutions of cells were cultured in growth medium containing 10% Agar (0.3 μg/ml), 20% FCS, 3 ng/ml IL-3, 70% IMDM and drug compounds added as specified per experiment. Plates were left to set for a minimum of 30 minutes before ddH_20 was added to the central space within plates. After 10-12 days in culture, colonies were imaged by the Chemidoc Touch Imaging System (Bio-Rad).

2.7 Western Blot Protein Analysis

Cells were lysed at 1 x 10^7 cells/ml in 1 x SDS buffer (SDS buffer; 50 mM tris-HCl (pH 6.8), 2% SDS, 10% glycerol, and 2.5% b-mercaptoethanol) and boiled for 7 minutes at 100°C. Samples were loaded onto a 10-12% SDS-polyacrilamide gel and transferred to a nitrocellulose membrane. Membranes were blocked (to limit non-specific binding) for a minimum of 1 hour at RT in 5% (w/v) non-fat milk in Tris-buffered saline Tween-20 buffer (TBS-T) (TBS-T buffer; 0.1% Tween, 150 mM NaCl, 10 nM Tris-HCl, pH 7.5). Membranes were rinsed in TBS-T prior to incubation with primary antibodies for between 24 and 72 hours at 4°C. For a detailed list of antibodies used please see Appendix 1. Following washing in TBST, immunoblots were probed with the specific secondary (anti-rabbit IgG, anti-mouse IgG or anti-rat IgG) antibody conjugated to horseradish peroxidase (HRP) (Southern Biotech). Bound antibodies were visualised by x-ray film or Chemidoc Touch Imaging System (Bio-Rad) using enzyme-linked chemiluminescence (ECL; Immobilion Western, Millipore or Amersham ECL, GE Healthcare Life Sciences).

2.8 Rho-123 Retention Assay

1 x 10^6 cells/ml were resuspended in Rho buffer (Rho buffer; PBS + 10% FCS (+ 3 ng/ml IL-3 for murine cells)) containing 250 nM Rho-123 for 20 minutes. Cells were then spun at 300 g for 5 minutes at RT, resuspended in Rho buffer containing the specific MDR1 inhibitors and incubated for 1-2 hours at 37°C at 10% CO_2. Rho-123 fluorescence (FL-1 channel) was measured by flow cytometry

on a BD-Calibur and data were analysed using FlowJo 10.0.8, 10.5 or 10.6 software.

2.9 TNF ELISA

AML cells were plated at 1 x 10_6 cells/ml and treated with the specific compounds for the indicated time points. Cells were harvested, pelleted at 300 g for 5 min at RT and the pellet frozen at -80°C. Cell pellets were washed once in PBS and lysed with 55 μl ice-cold protein DISC lysis buffer (DISC buffer; 150 mM sodium chloride, 2 mM EDTA, 1% Triton X-100, 10% glycerol, 20 mM tris (pH 7.5) and protease inhibitors). TNF content in whole-cell lysates was measure by ELISA (enzyme-linked immunosorbent assay) according to the manufacturer's instructions (eBioscience).

2.10 Plasmids, Cloning, Transfection and Lentiviral Infection

Gene-deleted cell lines were generated using clustered regularly interspaced short palindromic repeats (CRISPR)/CRISPR-associated protein 9 (Cas9) technology. Two independent CRISPR guide-RNAs (gRNAs) for the targeting of MDR1 (human; *ABCB1*) (5'TTTATAGTAGGATTTACACG and 5'AATGTTTTCAGCTATCGTGG) were designed using programs MIT (crispr.mit.edu) and benchling (www.benchling.com). gRNAs were cloned into LentiCRISPRv2 containing two expression cassettes (hSpCas9 and the chimaeric gRNA) and DNA prepared by midi-prep (Qiagen). Lentiviral particles were generated by transient transfection of 0.75 x 10_6 293T cells in a 10 cm plate with 2.5 μg of packaging vector (pCMV δR8.2), 1 μg of envelope vector (pMD2G-

VSVG) and 1.5 μg of LentiCRISPRv2-MDR1-gRNA, using Effectene (Qiagen) according to the manufacturer's instructions. Media was changed the following day and cells were left for 24 hours before the supernatant was filtered. Lentiviruses were used immediately to infect leukaemic cells via spinoculation at 32°C for 90 minutes at 2,500 rpm in RPM1 with 10% FCS medium containing 5 μg/ml polybrene (Sigma). Twenty-four hours after infection, cells were collected, washed and cultured in RPMI with 10% FCS for 72-96 hours prior to puromycin (2 μg/ml) selection.

2.11 *In vivo* AML Treatments

The Walter and Eliza Hall Institute Animal Ethics Committee approved the following *in vivo* biosafety and treatment experiments. Birinapant was prepared to 6 mg/ml in 12% captisol and diluted in PBS for intraperitoneal injection (IP). Tariquidar was prepared at 10 mg/ml in 30% Propylene glycol + 5% Tween 80 + 65% D5W (dextrose 5% sterile H_20) and diluted in PBS for oral gavage (OG). All vehicles were prepared at the same time but without the active compound. For drug tolerability experiments, healthy wild-type C57BL/6 mice were treated 3 times a week for 4 weeks. Mice were pre-treated with the MDR1 inhibitor tariquidar (5 mg/kg) or vehicle by OG. Birinapant (5 or 10 mg/kg) or vehicle was then administered 2 hours later by IP.

For treatment experiments, C57BL/6 mice were intravenously injected (IV) with 0.3-5 x 10_5 MLL-AF9 $MDR1_H$ leukaemia cells and 48 hours following re-transplant, mice received MDR1 inhibitor tariquidar (10 mg/kg) or vehicle by OG

four days a week. Birinapant (5 or 10 mg/kg) or vehicle were administered via IP 2 hours after OG twice a week, for 4-5 weeks. For Ara-c pre-treatment experiments, 48 hours following re-transplant mice received Ara-c (50 mg/kg, diluted in PBS) for five days, followed by treatment of tariquidar (10 mg/kg) five days a week combined with birinapant (10 mg/kg) either twice (Ara-c + 2xCombo) or three (Ara-c + 3xCombo) times a week. Upon signs of a leukaemic phenotype (lethargy, hunched posture, hind leg paralysis, enlarged spleen and liver) mice were culled at a pre-determined ethical end point and blood (cardiac bleed) and organs (liver, spleen and sternum) removed for histological analysis. To limit bias, animal technicians familiar with the leukaemic models and phenotype were ultimately responsible for determining the ethical end point of the animals.

2.12 Quantification of Intracellular birinapant

For each treatment group cells were washed 3 times in ice-cold PBS and resuspended in 90% methanol (-20°C), cells were divided into 4 samples then spiked with a titration of stable isotope labelled birinapant (‘heavy’ birinapant; birinapant-d6) at 4 different concentrations (0.001, 0.01, 0.1 and 1 μM). Samples were incubated overnight at -20°C before centrifugation at 21,000 g for 10 minutes at 4°C. The supernatants were collected and lyophilised to dryness. C18 StageTips (3 plugs) were equilibrated with 100 μl methanol prior to being washed sequentially with 100 μl 80% acetonitrile (ACN) / 5% formic acid in water (FA), 50% ACN / 5% FA and 5% FA. Peptides were loaded onto StageTips in 100 μl 5% FA and centrifuged for 3 minutes at 500 g. StageTips were washed with 2 x 100 μl 5% FA and were sequentially eluted with 50 μl 50% ACN / 5% FA then

80% ACN / 5% FA into clean PCR tubes by centrifugation for 5 minutes at 500 g. Samples were transferred to mass spectrometry sample vials and lyophilised to dryness. Samples were analysed by nanoflow LC-MS on an EASY-nLC 1200 (Thermo Fisher Scientific) coupled to a Q-Exactive mass spectrometer (Thermo Fisher Scientific) through a nano-electrospray ion source (Thermo Fisher Scientific). Samples were resuspended in MilliQ water containing 3% ACN and 1% FA before being directly injected into a 250 mm x 75 µm analytical column packed into a silica emitter tip (Aurora series, 1.6 µm C18; IonOpticks) at 100% buffer A (buffer A; 97.9% MilliQ water, 2% ACN, 0.1% FA), and separated by reverse-phase chromatography on a 30 min linear gradient from 2% to 60% buffer B (buffer B; 90% ACN, 9.9% MilliQ water, 0.1% FA) at a 400 nl/min constant flow rate. Full-scans (m/z 200-1000) were acquired with a resolution of 140,000 at 200 m/z. The AGC target was set at 1e6 with a maximum IT of 150 ms.

Skyline software (MacLean et al., 2010) (version 4.1.0.11714) was used for data analysis. The quantification was based on the area under the curves of the charge $2+$ species for each compound. The ratio of heavy:light birinapant was calculated for each sample before multiplication by the heavy birinapant dilution factor and averaging across the titration series to determine the quantity of birinapant per sample.

2.13 MLL-AF9 Blasts and LSC Assays

Previously published MLL-AF9 leukaemic stem cells (LSCs) and matching blasts were kindly provided by Prof. Mark Dawson, Peter MacCallum Cancer Centre,

Melbourne Australia (Fong et al., 2015). They were investigated in short-term cell death assays (24 hours), Rho-123 retention assays and Western blot analysis following the protocols described above.

2.14 LSK Cell Isolation and Treatment

To obtain haematopoietic cells, bones from legs and hips of healthy wild-type C57BL/6 mice were flushed and crushed using FACs buffer (FACs buffer; PBS + 1% FCS + 2.5 nM EDTA), and passed through a 100 µl filter. Cells were spun at 300 g for 10 minutes at 4°C and the pellet was resuspended in 1 ml of FACs buffer. Cells were stained for 15 minutes at 4°C with an antibody cocktail mix containing biotinylated lineage marker antibodies (antibodies against CD3, CD4, CD8, TER119, B220, Ly6G, CD11b; made in house at the WEHI). Cells were washed in 8 ml of FACs buffer, centrifuged at 300 g for 5 minutes at 4°C and the pellet resuspended in streptavidin beads (Mitenyi Biotec) diluted 1:9 in FACs buffer (10 µl beads per $1x10^7$ cells). Following incubation for 15 minutes at 4°C, cells were washed again with 8 ml FACs buffer and resuspended in 500 µl separation buffer (separation buffer; PBS + 2.5 nM EDTA). Magnetic separation with LD Columns (MACs Miltenyi Biotech) was then completed following the manufacturer's instructions. Samples passed through the column were centrifuged at 300 g for 10 minutes at 4°C and resuspended in 300 µl of the same biotinylated lineage marker specific antibodies as previously described. After 20 minute incubation at 4°C, samples were washed by centrifugation in FACs buffer and pellets resuspended in a mixture of antibodies to detect haematopoietic stem and progenitor cells (HSPCs) for 20 minutes at 4°C. For a detailed list of

antibodies used please see Appendix 2. Cells were washed again and resuspended in 200 µl FACs buffer and the cell population sorted for an enrichment of LSK positive cells (LSK; lineage marker low/negative (L^-), Sca-1 positive ($Sca\text{-}1^+$) and c-KIT positive ($c\text{-}KIT^+$), on BD-Influx Cell Sorter. Please see Appendix 3 for the flow cytometry gating strategy to isolate LSK cells. Sorted cells were recovered by centrifugation (300 g for 5 minutes at 4°C) and plated at 500-1,500 cells per well in a 96 U-bottom plate. Following treatment for 48 hours, cell death was measured by PI uptake on a FACs BD-Calibur and analysed with FlowJo 10.0.8 software.

2.15 *Ex vivo* Drug Testing on Patient Derived AML Samples

Human AML samples were obtained from patients diagnosed with AML after informed consent according to institutional guidelines, and studies were approved by the Alfred Health Ethics Committee approved Alfred Haematology Tissue bank protocol 29/05 and low risk application 87/14 or the Royal Adelaide Hospital Human Research Ethics Committee (RAH Protocol No: 20010516 and 041009). Mononuclear cells from apheresis product were isolated by Ficoll-Hypaque density-gradient centrifugation and resuspended in IMDM containing 0.5% FCS. Ficoll-purified leukaemia cells were plated in RPMI and 15-20% FCS at 2.5 x 10^5 cells/ml and drugs tested as described. After 24-48 hours, cell viability was determined by flow cytometric analysis of cellular exclusion of annexin V–fluorescein (BD Biosciences) and/or decrease of blast cell volume using flow cytometry (Gallios, Beckman Coulter or BD LSR-Fortessa). Flow cytometry data was analysed using the FlowJo 10.0.8 or 10.5 software.

2.16 AOCS Cell Fusion Specific RT-PCR and Viability Assays

Ovarian cancer patient derived cell lines have been established from Australian Ovarian Cancer Study (AOCS) patient ascites, authenticated and Mycoplasma tested as previously described (Christie et al., 2019; Etemadmoghadam et al., 2017). Testing for the presence of the SLC25A40-ABCB1 fusion transcript was performed using nested RT-PCR with primers to exon 1 of SLC25A40 and exon 3 of ABCB1 using an assay described previously (Patch et al., 2015). Briefly, PCR conditions were as follows: 98ºC for 30 seconds, 30 cycles of 98ºC for 10 seconds, 60ºC for 30 seconds, 72ºC for 10 seconds, and 72ºC for 10 minutes. PCR product from first PCR was purified using QIAquick PCR purification kit (QIAGEN), for use as template in the second PCR. The PCR product from the second PCR was run on a 2% agarose gel. RT-PCR for the SLC25A40-ABCB1 fusion was performed on 20 cell lines, and one fusion positive line was identified, AOCS18.5. A fusion negative line, AOCS21.2, was used as a control. Cells were seeded in triplicate at 5 x 10_3 cells per well, in 96 well black-walled plates, 24 hours prior to drug treatment. Cells were treated for 72 hours with a 10-point dilution series of birinapant with or without 250 nM tariquidar and with or without 20 ng/ml TNF in antibiotic-free medium. Cell viability was determined via DAPI staining and high content imaging on the Cellomics ArrayScan Vti platform. Briefly, cells were fixed with 4% PFA for 10 minutes, then permeabilised with 0.2% Triton X and stained with DAPI (1:1000 dilution). IC_{50} doses of birinapant were approximated by fitting a 4-parameter dose-response curve (Hill equation) and all parameters used in curve comparison using Prism 7 (GraphPad) as previously described (Cowin et al., 2012).

2.17 *In vivo* Analysis of Hepatitis B Virus

The Walter and Eliza Hall Institute Animal Ethics Committee approved the following *in vivo* treatment experiments within hepatitis B virus (HBV) infected mice. Murine models of HBV infection, analysis of alanine aminotransferase (ALT) and serial serum HBV-DNA analysis were carried out as previously described (Ebert et al., 2015a; Ebert et al., 2015b). Briefly, HBV infection was induced in male C57BL/6 6-8-week-old mice through hydrodynamic injection (HDI). Zosuquidar was prepared at 10 mg/ml in 2% D-mannitol, 0.015% Glycine in sterile H_20 and diluted in saline solution to the appropriate concentration. Five days following induction of infection, mice were pre-treated by IP with the MDR1 inhibitor zosuquidar (5 or 25 mg/kg) for three consecutive days. Five hours following the last dose of zosuquidar, birinapant (3 mg/kg) was delivered by IP injection. For acute ALT analysis, animals were culled 16 hours later and the same experimental plan was followed for uninfected animals. Serum from cardiac bleeds was isolated and analysed for ALT using a Cobas e411 Analyser according to the manufacturer's instructions (Roche). We thank the Research Support Team in Pathology at The Royal Melbourne Hospital for assistance with liver enzyme analysis.

For *in vivo* serial serum HBV DNA analysis, mice were treated as described above for three weeks, where zosuquidar (5 or 25 mg/kg) was administered IP three times a week and birinapant (10 mg/kg) administered IP once a week. Mice were mandible bled once a week prior to treatment for a total of 5 weeks and serum from bleeds was isolated and analysed for HBV DNA content as previously

described (Ebert et al., 2015a; Ebert et al., 2015b). Briefly, the High Pure Viral Nucleic Acid Kit (Roche) or the Invisorb Virus DNA HTS 96 Kit (Stratec) was used to extract viral DNA from prepared serum and real-time PCR (RT-PCR) was used to quantify DNA load. The DNA Amplification SYBR Green Kit (Roche) on a LightCycler 480 II Machine (Roche) with Absolute Quantification Software (Roche) was used to further quantify DNA load. Serial dilutions of pAAV-HBV1.2 were used as the standard. Primers were HBV1745fw (GTTGCCCGTTTGTCCTCTAATTC) and HBV1844rev (TGAGGGAAACATAGAGTTGCCTTGA). The limit of detection of serum HBV DNA was 500 copies/mL and sensitivity threshold was 10^3 copies/mL.

2.18 Preparation of Mouse Organs for Western Blot

Immediately following death, sample tissue from mouse livers was harvested and snap frozen using liquid nitrogen and stored at -20°C. Samples were generated in Cell Lysis Buffer (20 nM Tris HCL pH 7.5, 135 mM NaCl, 1.5 mM Mg2Cl, 1 mM EGTA, 1% Triton X-100, 10% Glycerol, 1 x final concentration of Protease Cocktain (Roche) and 1 x final concentration of PhosSTOP (Roche)). Samples were spun at 15,000 rcf for 5 min at 4°C and the concentration of protein in soluble supernatants was determined by bicinchoninic acid (BCA) assay (Thermo Fisher) according to manufacturer's instructions.

2.19 Statistical analysis

Unless otherwise stated in figure legends, all statistics were calculated using an unpaired two tailed t test with Welch's correction on Prism 7 or Prism 8

(GraphPad) where P* < 0.05, P** < 0.01, P*** < 0.001, P**** < 0.0001 and n.s is non-significant. Where no P value is stated the value was either n.s or not calculated due to irrelevance. Bliss synergy analysis was completed using the Synergy Finder program as described previously (Ianevski et al., 2017). Survival curves throughout the thesis are presented as Kaplan-Meier curves.

2.20 Data availability

The datasets generated during and/or analysed during the current study are available on request.

3 Clinical MDR1 Inhibitors and Smac-mimetics Combine to Kill Leukaemic Stem Cells and Overcome Resistance in Acute Myeloid Leukaemia

Chapter 3 in its entirety contains the manuscript, ***"Clinical MDR1 inhibitors and Smac-mimetics combine to kill leukaemic stem cells and overcome resistance in acute myeloid leukaemia"***, which was submitted for publication to the peer-reviewed journal, *Leukemia* on 29/11/2019 and is currently under review. Please see the Preface for a more detailed description of contributions by co-authors.

3.1 Abstract

The specific targeting of inhibitor of apoptosis (IAP) proteins by Smac-mimetic (SM) drugs, such as birinapant, has been tested in clinical trials of acute myeloid leukaemia (AML) and certain solid cancers. Despite their promising safety profile, these drugs have so far had variable and limited success. Using a library of more than 5,700 bioactive compounds we screened for approaches that could overcome birinapant resistance in AML and identified multidrug resistance protein 1 inhibitors (MDR1i) as a class of clinically approved drugs that can sensitise cancer cells to SM therapy. Inhibition of MDR1 in SM resistant leukaemia cells increased intracellular levels of birinapant and sensitised AML patient samples to birinapant killing. Combination of clinical MDR1 and IAP inhibitors is well-tolerated *in vivo* and more effective against leukaemic cells,

compared to normal haematopoietic progenitors. Importantly, birinapant combined with 3rd generation MDR1i effectively killed leukaemic stem cells (LSCs) and prolonged survival of AML burdened mice, suggesting a therapeutic opportunity for AML. This study identifies a drug combination strategy, that by efficiently killing LSCs, may improve AML patient outcomes.

3.2 Introduction

Inhibitor of apoptosis (IAP) proteins regulate cell survival in response to a number of stimuli. In TNF receptor super family (TNFRSF) signalling they are required to activate the canonical NF-κB pathway and mitogen-activated protein kinases (MAPKs). They also act as repressors of the non-canonical NF-κB pathway and apoptotic cell death (Matsuzawa et al., 2008; Vallabhapurapu et al., 2008; Varfolomeev et al., 2007; Vince et al., 2007). Natural IAP antagonists, such as second mitochondria-derived activator of caspases (Smac/DIABLO), can bind to IAPs to prevent their interaction with specific substrates (Du et al., 2000; Verhagen et al., 2000). In certain conditions, this leads to auto-ubiquitylation and proteasomal degradation of IAPs (Varfolomeev et al., 2007; Vince et al., 2007).

The observation that overexpression of IAPs correlates with cancer progression, poor prognosis and treatment resistance, led to the development of small molecule, peptide-like mimetics of Smac, termed Smac-mimetics (SMs) (Fulda and Vucic, 2012). Birinapant is one of the most clinically advanced SMs and is currently in clinical trials for the treatment of certain solid and haematological cancers. Due to its limited efficacy as a single-agent, birinapant is being tested in

combination with chemotherapeutic drugs and immune checkpoint inhibitors (NCT01188499 and NCT02587962) (Amaravadi et al., 2013; Schilder et al., 2018). Studies by us and others suggest that SMs can also synergise with several drugs, including p38-kinase inhibitors, caspase-8 inhibitors and immunotherapy, to efficiently eliminate cancer cells (Beug et al., 2017; Brumatti et al., 2016; Kearney et al., 2017; Lalaoui et al., 2016; Steinhart et al., 2013). Although combinations of birinapant with other anti-cancer agents show promise for the treatment of several cancers, boosting their efficacy and overcoming resistance are still major challenges.

Using an unbiased high throughput strategy, we screened a library of clinical and pre-clinical compounds, to identify molecules that could overcome birinapant resistance in acute myeloid leukaemia (AML). From several compounds that sensitised resistant AML cells to birinapant, we selected reserpine for further study. Reserpine is an antihypertensive and antipsychotic clinical drug that also inhibits the multidrug resistance protein 1 (MDR1) (Beck et al., 1988; Bleuler and Stoll, 1955; Stitzel, 1976). MDR1 or P-glycoprotein (P-gp), is a member of the ATP-binding cassette (ABC) transporter family that actively exports structurally unrelated substrates out of cells, presumably to protect them from possible toxicities. MDR1 substrates include several chemotherapeutic drugs and chemical compounds, such as the fluorescent dye Rhodamine-123 (Abraham et al., 1993; Borst and Elferink, 2002; Juliano and Ling, 1976; Neyfakh, 1988). Despite the fact that MDR1 exports many xenobiotic compounds, it has not been possible to discern a common chemical feature recognised by MDR1 (Waghray

and Zhang, 2017). Therefore, whether a molecule is a substrate of MDR1 must be determined empirically.

MDR1 is frequently up-regulated in cancer cells and its expression correlates with treatment resistance and disease relapse (Fletcher et al., 2010; Guerci et al., 1995; Leith et al., 1999). In AML, MDR1 expression has been reported in patients of all ages, with prevalence in >50% of relapsed and secondary AML (Leith et al., 1999; Schaich et al., 2005). This led to clinical trials of MDR1 inhibitors (MDR1i) in AML. Although Phase I/II clinical trials have proven the safety of these inhibitors in AML patients, limited success was observed due to changes in chemotherapy pharmacokinetics and increased toxicity (Fletcher et al., 2010; Relling, 1996; Schinkel et al., 1994; Waghray and Zhang, 2017).

Our data provide strong evidence for the re-evaluation of MDR1i therapy in combination with SMs, for the treatment of AML. Here we show that SMs such as birinapant, synergise with 3rd generation MDR1i to enhance killing of AML cells *in vitro* and *in vivo*. Importantly, leukaemic stem cells (LSCs) are highly sensitive to this combination therapy whilst healthy haematopoietic stem/progenitor cells (HSPCs) are resistant. A frequent shortcoming of existing therapies for the cure of AML is that while they effectively target leukaemic blasts, they fail to eradicate LSCs, leading to disease relapse (Costello et al., 2000; Ishikawa et al., 2007; Shlush et al., 2017; van Rhenen et al., 2005). Therefore, therapies that can kill both blasts and LSCs, whilst sparing normal HSPCs, are required for effective treatment of AML.

In this study we explored MDR1 as a biomarker for resistance to birinapant treatment and determine the impact of the clinical MDR1i, tariquidar and zosuquidar, as novel combination therapies to overcome SM resistance and enhance killing of AML cells. Our findings provide a rationale for testing the combination of SM/MDR1i in clinical trials for the treatment of AML.

3.3 Results

3.3.1 Clinical MDR1i Enhance the Efficacy of SM Based Therapy in AML Cells

To identify drugs that could overcome birinapant resistance in AML, we conducted a high throughput screen of >5,700 bioactive compounds in two independent birinapant resistant murine HoxA9/Meis1 leukaemias (**Figure 1A**) (Brumatti et al., 2016). After increasingly stringent tests (see supplemental materials and methods) we identified 12 drugs that can sensitise AML cells to birinapant (bir) (**Supplemental Figure 1A**). One of the most active compounds was reserpine (res) (Bleuler and Stoll, 1955; Stitzel, 1976). Reserpine combined with birinapant and other SMs such as AT-406 and AEG-40730, to effectively kill primary HoxA9/Meis1 and MLL-AF9-driven AML (**Figure 1B; Supplemental Figure 1B-E**). However, reserpine did not consistently increase the killing of AML cells induced by the SMs LCL161 and GDC-0152 (**Supplemental Figure 1F-I**),

Since reserpine can inhibit both the vesicular monoamine transporter and MDR1 (Ahmed et al., 1993; Beck et al., 1988; Stitzel, 1976), we investigated whether the enhanced SM-mediated killing in AML was dependent on MDR1. Using the

3rd generation clinical MDR1i, tariquidar (tari) and zosuquidar (zosu), we tested the impact of specific MDR1 inhibition on birinapant induced killing in AML cells. These inhibitors are molecularly distinct but have both reached phase II/III clinical trials for a range of cancers, including AML (Gerrard et al., 2004; Mistry et al., 2001; Pusztai et al., 2005; Starling et al., 1997). Tariquidar and zosuquidar sensitised AML cells to nanomolar concentrations of birinapant (**Figure 1C,D**). Tariquidar also markedly enhanced the killing of HoxA9/Meis1 AMLs induced by the SMs AT-406 and AEG-40730, but not LCL161 or GDC-0152 (**Figure 1E,F; Supplemental Figure 1J-L**).

To test the specificity of the synergy between the SM peptido-mimetics and MDR1i, we tested whether killing induced by other peptide-mimetics could be enhanced by tariquidar or zosuquidar. MDR1i did not sensitise leukaemia cells to the BH3-mimetic Bcl-2 inhibitor ABT-199 (Souers et al., 2013) (**Figure 1G; Supplemental Figure 1M**) or the BET inhibitor JQ1 (Zuber et al., 2011) (**Figure 1H; Supplemental Figure 1N**), suggesting that these drugs are non-MDR1 substrates. Together these data indicate that the sensitisation mediated by MDR1i is specific to SMs, and not a function of their peptide-like nature.

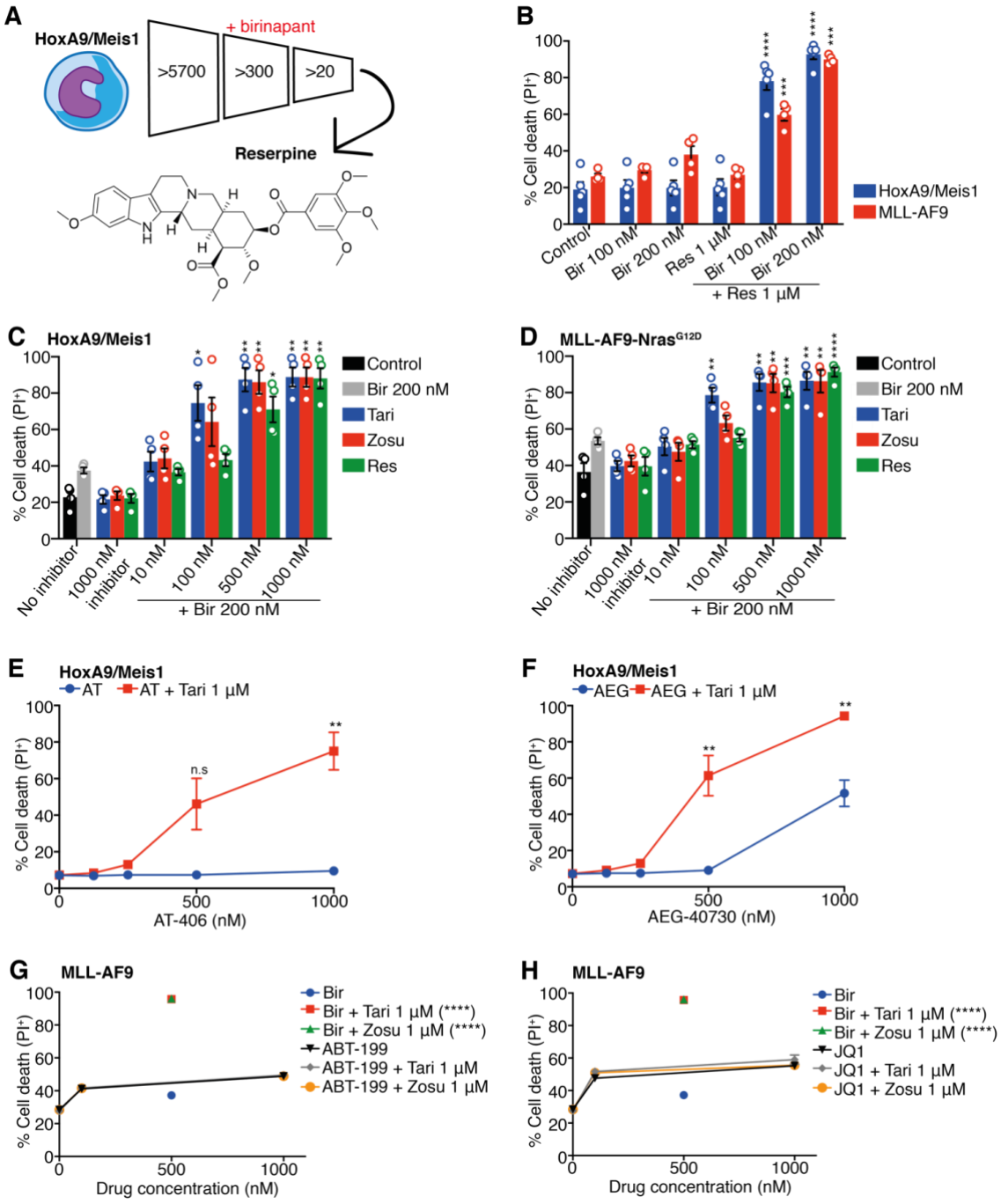
A
HoxA9/Meis1
+ birinapant
>5700
>300
>20
Reserpine
B
% Cell death (PI+)
HoxA9/Meis1
MLL-AF9
Control
Bir 100 nM
Bir 200 nM
Res 1 µM
Bir 100 nM
Bir 200 nM
+ Res 1 µM
C
HoxA9/Meis1
% Cell death (PI+)
Control
Bir 200 nM
Tari
Zosu
Res
No inhibitor
1000 nM inhibitor
10 nM
100 nM
500 nM
1000 nM
+ Bir 200 nM
D
MLL-AF9-Nras^{G12D}
% Cell death (PI+)
Control
Bir 200 nM
Tari
Zosu
Res
No inhibitor
1000 nM inhibitor
10 nM
100 nM
500 nM
1000 nM
+ Bir 200 nM
E
HoxA9/Meis1
AT
AT + Tari 1 µM
% Cell death (PI+)
n.s
AT-406 (nM)
F
HoxA9/Meis1
AEG
AEG + Tari 1 µM
% Cell death (PI+)
AEG-40730 (nM)
G
MLL-AF9
% Cell death (PI+)
Bir
Bir + Tari 1 µM (****)
Bir + Zosu 1 µM (****)
ABT-199
ABT-199 + Tari 1 µM
ABT-199 + Zosu 1 µM
Drug concentration (nM)
H
MLL-AF9
% Cell death (PI+)
Bir
Bir + Tari 1 µM (****)
Bir + Zosu 1 µM (****)
JQ1
JQ1 + Tari 1 µM
JQ1 + Zosu 1 µM
Drug concentration (nM)

Manuscript Figure 1 MDR1i potentiate SM killing in AML cells

(**A**) Approximately 5,700 compounds were screened for their ability to synergise with birinapant and overcome resistance in murine HoxA9/Meis1 AML cells. Compounds that induced cell death in combination with birinapant, but not as single-agents, were selected and their impact determined in a dose response assay. (**B**) Reserpine sensitises primary murine HoxA9/Meis1 and MLL-AF9 AML cells to birinapant. AML cells were treated with birinapant (100 and 200 nM) ± 1 µM reserpine (Res) for 24 h (n=4-5). (**C**) HoxA9/Meis1 and (**D**) MLL-AF9-Nras$_{G12D}$ AML cells were treated with 10, 100, 500 and 1000 nM reserpine, tariquidar or zosuquidar ± birinapant (200 nM) for 24 h (n=4). (**E, F**) HoxA9/Meis1 AML cells were treated with 125, 250, 500 and 1000 nM of (**E**) AT-406 (AT) and (**F**) AEG-40730 (AEG) for 24 h ± 1 µM tariquidar (n=5). MLL-AF9 AML cells were treated with (**G**) ABT-199 and (**H**) JQ1 at 100 and 1000 nM ± 1 µM tariquidar for 24 h. Treatment with birinapant (500 nM) ± tariquidar or zosuquidar (1 µM) was used as a control (n=4). Data are presented as mean ± SEM throughout. Cell death was measured by propidium iodide (PI) uptake or decrease of cell volume (MLL-AF9-Nras$_{G12D}$) and flow cytometry from 3-4 independent tumours. P values were obtained by comparison of treatment with SM alone and with SM in combination with MDR1i at the indicated concentrations.

3.3.2 MDR1 Expression Inversely Correlates with Response to SM Related Therapies in Leukaemia

To establish whether MDR1 expression is a predictor of birinapant resistance, we screened several primary murine leukaemias for MDR1 expression and function. As expected, independent HoxA9/Meis1 and MLL-AF9-Nras^{G12D} leukaemias expressed MDR1, albeit at varying levels (**Figure 2A,B**). Conversely, MLL-ENL AMLs had no detectable MDR1 expression (**Figure 2C**). To confirm that MDR1 was functional we used a Rhodamine-123 (Rho-123) retention assay (Neyfakh, 1988). Consistent with the protein expression, inhibition of MDR1 increased fluorescence in MDR1-high (MDR1$_H$) HoxA9/Meis1 AMLs (**Figure 2D**) and to a lesser extent in MLL-AF9-Nras^{G12D} leukaemias (**Figure 2E**), but Rho-123 levels were unaffected in MDR1-low (MDR1$_L$) MLL-ENL AMLs (**Figure 2F**). In agreement with these results, MDR1i synergistically increased birinapant induced killing of HoxA9/Meis1 (Bliss Synergy Score (BSS) 56.7 and 66.5) and MLL-AF9-Nras^{G12D} AML cells (BSS 38.7 and 49.3) (**Figure 2G,H; Supplemental Figure 2A-F**) but had limited effect in MLL-ENL AMLs (BSS 12.7 and 9) (**Figure 2I; Supplemental Figure 2G-I**).

Human AML cell lines also had variable levels of MDR1 (**Figure 2J**). Consistently**,** addition of MDR1i markedly sensitised MDR1$_H$ KG1 cells to birinapant induced killing (bir EC50 (μM) = 6.86 vs bir/tari EC50 = 0.12 and bir/zosu EC50 = 0.09; **Figure 2K**). In contrast, the MDR1$_L$ HL60 cell line was not significantly affected by tariquidar (bir EC50 (μM) = 0.14; bir/tari EC50 = 0.10; **Figure 2L**). Collectively,

our results show an inverse correlation between MDR1 expression/activity and response of leukaemia cells to birinapant.

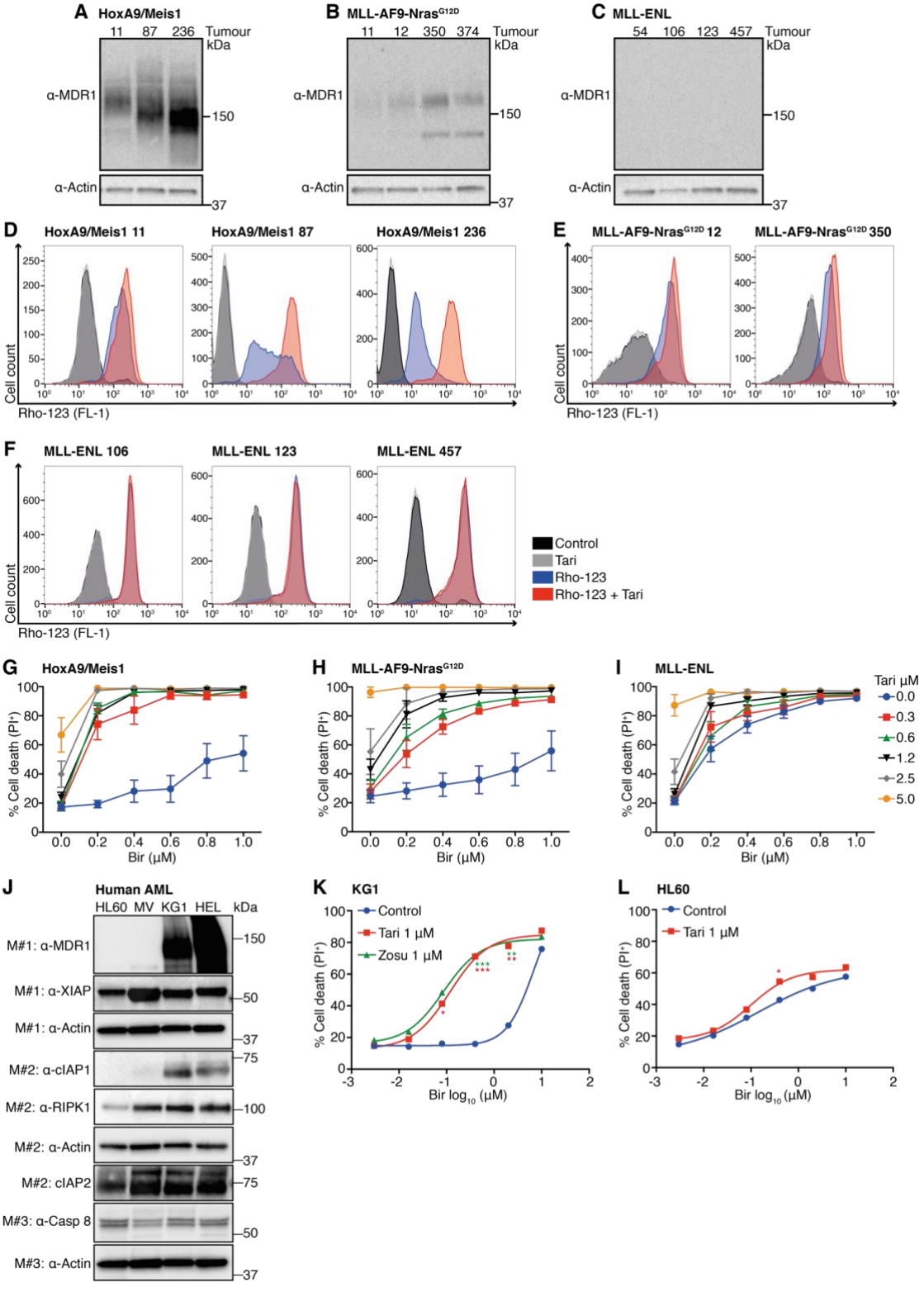
A HoxA9/Meis1
11 87 236 Tumour
kDa
α-MDR1
150
α-Actin
37
B MLL-AF9-Nras^{G12D}
11 12 350 374 Tumour
kDa
α-MDR1
150
α-Actin
37
C MLL-ENL
54 106 123 457 Tumour
kDa
α-MDR1
150
α-Actin
37
D HoxA9/Meis1 11
HoxA9/Meis1 87
HoxA9/Meis1 236
Cell count
Rho-123 (FL-1)
E MLL-AF9-Nras^{G12D} 12
MLL-AF9-Nras^{G12D} 350
Cell count
Rho-123 (FL-1)
F MLL-ENL 106
MLL-ENL 123
MLL-ENL 457
Cell count
Rho-123 (FL-1)
Control
Tari
Rho-123
Rho-123 + Tari
G HoxA9/Meis1
% Cell death (PI+)
Bir (μM)
H MLL-AF9-Nras^{G12D}
% Cell death (PI+)
Bir (μM)
I MLL-ENL
Tari μM
0.0
0.3
0.6
1.2
2.5
5.0
% Cell death (PI+)
Bir (μM)
J Human AML
HL60 MV KG1 HEL kDa
M#1: α-MDR1
150
M#1: α-XIAP
50
M#1: α-Actin
37
M#2: α-cIAP1
75
M#2: α-RIPK1
100
M#2: α-Actin
37
M#2: cIAP2
75
M#3: α-Casp 8
50
M#3: α-Actin
37
K KG1
Control
Tari 1 μM
Zosu 1 μM
% Cell death (PI+)
Bir log$_{10}$ (μM)
L HL60
Control
Tari 1 μM
% Cell death (PI+)
Bir log$_{10}$ (μM)

Manuscript Figure 2 MDR1 expression correlates inversely with response to SM related therapies in leukaemia

Western blot analysis of MDR1 expression in (**A**) HoxA9/Meis1, (**B**) MLL-AF9-Nras$_{G12D}$ and (**C**) MLL-ENL AML cells. (**D**-**F**) Rhodamine-123 (Rho-123) retention analysis of MDR1 activity in (**D**) HoxA9/Meis1, (**E**) MLL-AF9-Nras$_{G12D}$ and (**F**) MLL-ENL AML cells. (**G**) HoxA9/Meis1 (n=5), (**H**) MLL-AF9-Nras$_{G12D}$ (n=4) and (**I**) MLL-ENL (n=3) AML cells were treated with tariquidar (0.3, 0.6, 1.2, 2.5 and 5 μM) ± birinapant (0.2, 0.4, 0.6, 0.8, 1 μM) for 24 h. (**J**) Lysates from human AML cell lines HL60, MV4-11 (MV), KG1 and HEL were probed with the indicated antibodies and probing for actin was used as a loading control, M#1, 2, 3 indicates different membranes. (**K**) KG1 (MDR1$_H$) (n=3) and (**L**) HL60 (MDR1$_L$) (n=2, error bars SD) cells were treated with tariquidar and/or zosuquidar (1 μM) ± birinapant (0.003, 0.016, 0.08, 0.4, 2 and 10 μM) for 48 h. Data are presented as mean ± SEM throughout unless otherwise stated, n=3-4 independent tumours for each AML line, repeated 1-2 times. Cell death was measured by propidium iodide (PI) uptake, decrease of cell volume (MLL-AF9-Nras$_{G12D}$) and flow cytometry.

3.3.3 TNF and MDR1 are Biomarkers of Birinapant Response in AML

Our results suggest that high levels of MDR1 can be used to predict resistance to birinapant-based therapy in different AML sub-types. Considering clonal and sub-clonal variations that appear in patients within an AML sub-type, we correlated MDR1 expression and birinapant sensitivity in independent MLL-AF9 leukaemias. MDR1 expression and activity, as well as sensitivity to birinapant related therapy, was heterogeneous in these leukaemias (**Figure 3A,B**; **Supplemental Figure 3A**). As predicted, $MDR1_L$ MLL-AF9 cells were sensitive to birinapant and addition of tariquidar did not affect their sensitivity (blue bars, **Figure 3B**). In contrast, $MDR1_H$ MLL-AF9 cells were only responsive to birinapant in the presence of MDR1i (red bars, **Figure 3B**; **Supplemental Figure 3B-E**). Of note, some $MDR1_L$ (black bars) and $MDR1_H$ (green bars) AMLs did not respond to bir ($MDR1_L$) or bir/tari ($MDR1_H$) treatment (**Figure 3B**). Because SMs kill cancer cells by autocrine TNF/TNFR1 signalling (Petersen et al., 2007; Varfolomeev et al., 2007; Vince et al., 2007), we hypothesised that the inherent ability of AML cells to produce TNF contributed to their response to birinapant. Indeed, while TNF levels were increased in $MDR1_H$ AML cells (red bars, **Figure 3C; Supplemental Figure 3F,G**) upon bir/tari treatment, no increase in TNF could be observed in $MDR1_H$ MLL-AF9 AML cells that are resistant to the combination therapy (green bars, **Figure 3C; Supplemental Figure 3F**). Addition of exogenous TNF and MDR1i sensitised these cells (green bars) to birinapant, thus confirming that sensitivity to this SM is determined by both TNF and MDR1 expression (**Figure 3B**).

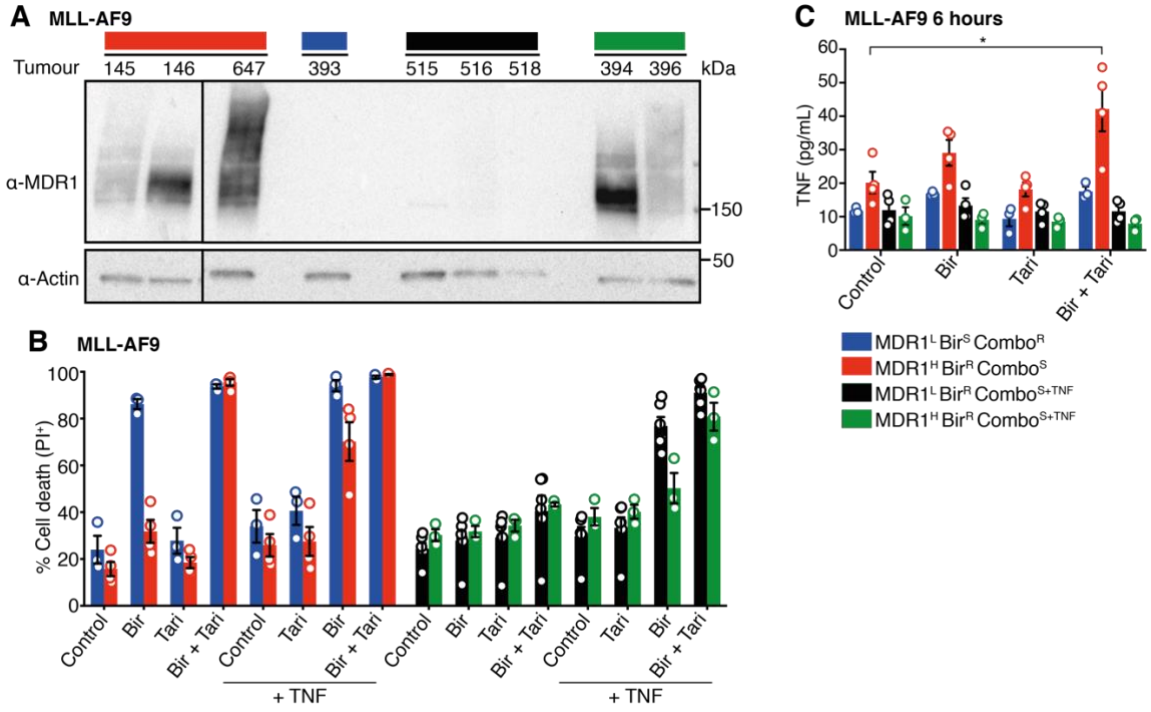

Manuscript Figure 3 TNF and MDR1 expression are biomarkers of birinapant response in AML

(**A**) Western blot analysis of MDR1 in independent MLL-AF9 AML cells. (**B**) $MDR1^{L}$, birinapant-sensitive (Bir^{S}), combination-resistant ($Combo^{R}$) (blue bars); $MDR1^{H}$, birinapant-resistant (Bir^{R}), combination-sensitive ($Combo^{S}$) (red bars); $MDR1^{L}$, Bir^{R}, $Combo^{S+TNF}$ (black bars) and $MDR1^{H}$, Bir^{R}, $Combo^{S+TNF}$ (green bars) AML cells were treated for 24 h with tariquidar (500 nM) ± birinapant (500 nM) ± TNF (100 ng/mL) (1-3 independent tumours for each sub-group, with 2-3 repeats). (**C**) TNF production in the four MLL-AF9 AML sub-groups was determined by ELISA. Cells were treated with tariquidar (500 nM) ± birinapant (500 nM) for 6 h (1-2 independent tumours for each sub-group, with 2-3 repeats). The data are presented as mean ± SEM throughout. Cell death was measured by propidium iodide (PI) uptake, decrease of cell volume and flow cytometry. P values were obtained by comparison of control and combination treatment groups.

3.3.4 MDR1 Inhibition Increases the Intracellular Concentration of Birinapant in AML

The most likely hypothesis to explain the synergistic killing between birinapant and MDR1i is that inhibition of MDR1 increases the intracellular concentration of birinapant, consequently, inducing rapid degradation of SM targets cIAP1/2 and AML cell death (**Figure 4A**). To explore this hypothesis, we analysed the degradation of cIAP1/2, in MDR1$_H$ KG1 AML cells treated with bir or bir/tari. As predicted, combination treatment accelerated cIAP1/2 degradation and induced potent killing of these cells (**Figure 4B,C; Supplemental Figure 4A,B**). The reduction in cIAP levels in AML cells at early time points post combination treatment was unlikely due to cell death, which was negligible during the first 6 h of treatment (**Figure 4C**). Similarly, when combined with the SMs AT-406 or AEG-40730, tariquidar also increased cell death and induced rapid degradation of cIAP1 in KG1 AML cells (**Supplemental Figure 4B-G**).

To further validate that rapid degradation of cIAPs is associated with increased intracellular levels of birinapant, we performed mass spectrometry on MDR1$_H$ KG1 cells treated with bir or bir/tari. For quantification of the intracellular birinapant we used deuterium labelled birinapant as an internal standard. Inhibition of MDR1 increased the intracellular concentration of birinapant 3-fold after 6 h, with SM levels remaining high up to 24 h post-treatment (**Figure 4D**).

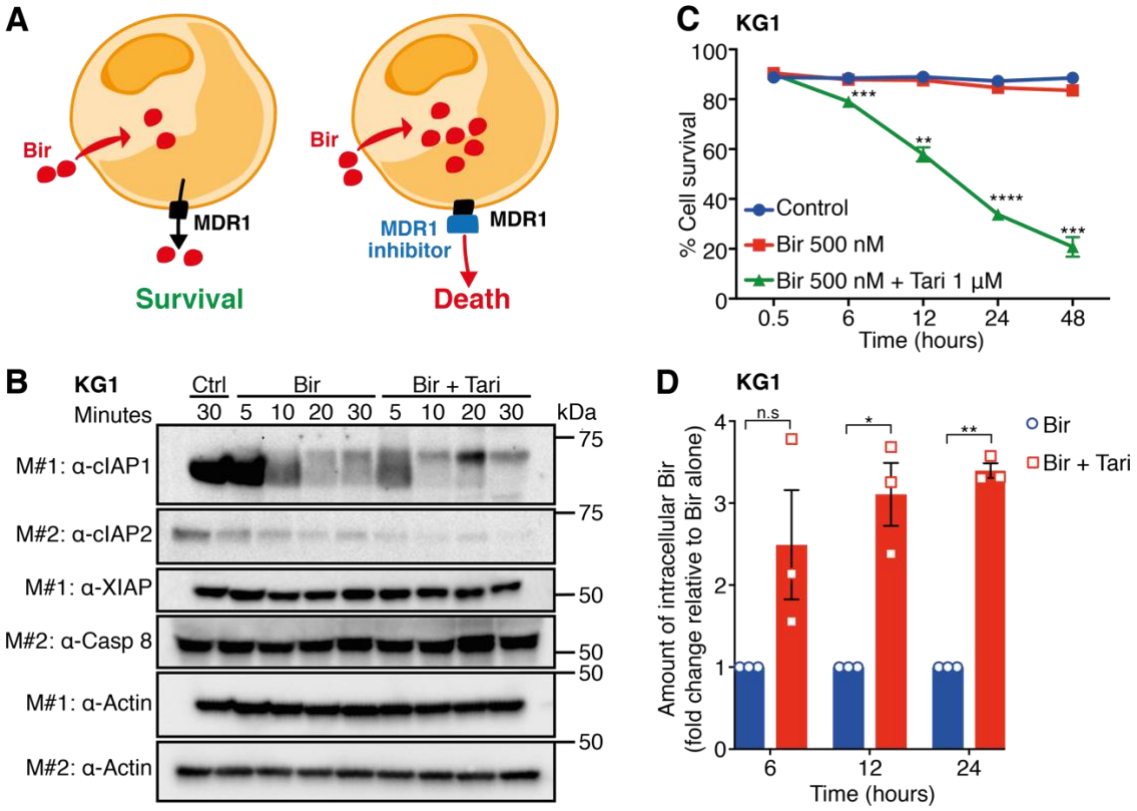

Manuscript Figure 4 MDR1 inhibition increases the intracellular concentration of birinapant in MDR1$_H$ leukaemias

(**A**) Schematic of the proposed mechanism of action of the SM plus MDR1i combination therapy in MDR1$_H$ cells. Birinapant (Bir) is pumped out of cells by MDR1 and inhibition of MDR1 pumps increases the intracellular levels of Bir. (**B**) KG1 AML cells were treated for the indicated times with birinapant (500 nM) ± tariquidar (1 µM). Expression of the indicated proteins was determined by Western blot and probing for actin was used as a loading control, M#1, 2 indicate different membranes. (**C**) KG1 AML cells were treated for up to 48 h with birinapant (500 nM) ± tariquidar (1 µM) (n=4). Cell survival was measured by propidium iodide (PI) exclusion, decrease of cell volume and flow cytometry. (**D**) Deuterium labelled birinapant was used as a standard for intracellular quantification of birinapant by mass spectrometry of KG1 AML cells treated with birinapant (500 nM) ± tariquidar (1 µM) (n=3 independent experiments). Data are presented as mean ± SEM throughout. P values were obtained by comparison of SM alone and in combination with MDR1 inhibitors at the indicated concentrations or time points.

3.3.5 Specific Targeting of MDR1 Sensitises AML Cells to SM Induced Killing

To confirm that the killing mediated by SM/MDR1i was due to specific targeting of MDR1, we took a pharmacological and genetic approach. Other ABC transporters, such as ABCC1 and ABCG2 (also known as MRP1 and BCRP respectively) (Legrand et al., 1999; Westover and Li, 2015), can also mediate efflux of anti-cancer drugs. To determine whether SMs are exclusively MDR1 substrates, we tested the impact of the MRP1 and BCRP inhibitors, reversan (Rev) (Burkhart et al., 2009) and fumitremorgin C (Fum-C) (Rabindran et al., 2000) respectively, on birinapant induced killing. Neither HoxA9/Meis1 nor MLL-AF9 leukaemias were sensitised to birinapant by low doses of these inhibitors (**Figure 5A; Supplemental Figure 5A**). However, higher concentrations of reversan were able to increase birinapant-induced death (**Supplemental Figure 5A**). This is most likely due to the off-target inhibition of MDR1 by high concentrations of reversan (Burkhart et al., 2009; Kannan et al., 2010), suggesting that MDR1 is the ABC transporter responsible for regulating SM concentration in AML cells. To further validate this hypothesis, we generated KG1 *MDR1*$^{-/-}$ cells using two independent guide-RNAs (gRNAs) with CRISPR. Protein analysis confirmed loss of MDR1 in pools of <10 clones transduced with either MDR1 gRNA (**Figure 5B**). The KG1 *MDR1*$^{-/-}$ 3.30 cell line was a complete knock-out for MDR1, whereas the KG1 *MDR1*$^{-/-}$ 2.48 cell line had a small proportion of cells which retained MDR1 activity (**Figure 5B,C; Supplemental Figure 5B,C**). As predicted, genetic loss of MDR1 sensitised KG1 leukaemia to birinapant treatment and MDR1i were able to further increase SM-mediated cell death.

(**Figure 5D-F**). Consistently, cIAP1 degradation mediated by birinapant was faster in KG1 *MDR1*$^{-/-}$ cells, and the addition of tariquidar had no additional effect (**Figure 5G)**. The increased killing of AML cells imparted by MDR1 loss was specific to birinapant treatment because KG1 control and *MDR1*$^{-/-}$ cells were similarly sensitive to the chemotherapy Ara-c, and peptide-mimetics JQ1 and ABT-199 (**Supplemental Figure 5D-F**).

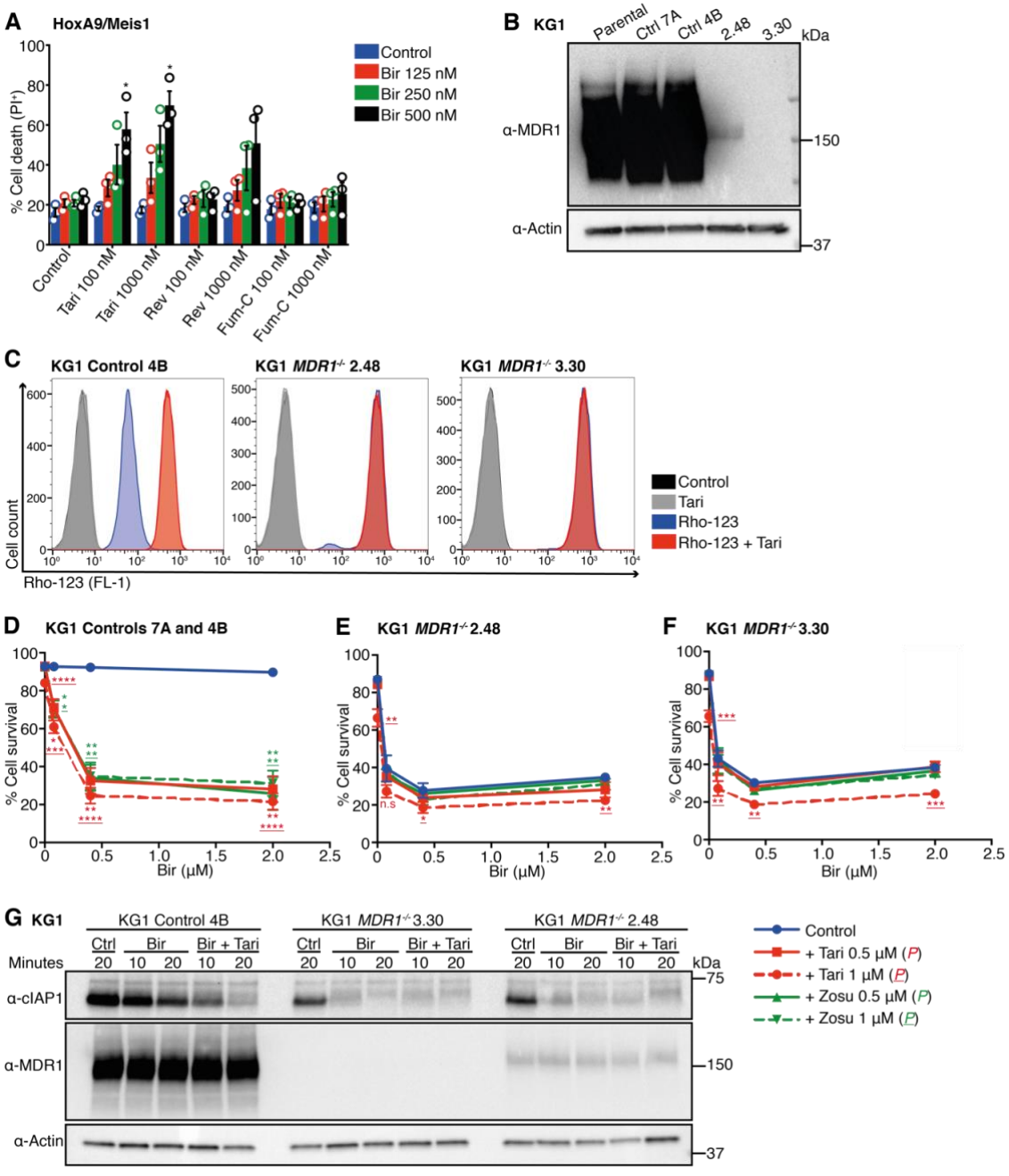
A
HoxA9/Meis1
% Cell death (PI+)
Control
Bir 125 nM
Bir 250 nM
Bir 500 nM
Control
Tari 100 nM
Tari 1000 nM
Rev 100 nM
Rev 1000 nM
Fum-C 100 nM
Fum-C 1000 nM
B
KG1
Parental
Ctrl 7A
Ctrl 4B
2.48
3.30
kDa
α-MDR1
150
α-Actin
37
C
KG1 Control 4B
KG1 MDR1-/- 2.48
KG1 MDR1-/- 3.30
Cell count
Rho-123 (FL-1)
Control
Tari
Rho-123
Rho-123 + Tari
D
KG1 Controls 7A and 4B
E
KG1 MDR1-/- 2.48
F
KG1 MDR1-/- 3.30
% Cell survival
Bir (μM)
G
KG1
KG1 Control 4B
KG1 MDR1-/- 3.30
KG1 MDR1-/- 2.48
Ctrl
Bir
Bir + Tari
Minutes
20
10
20
10
20
kDa
α-cIAP1
75
α-MDR1
150
α-Actin
37
Control
+ Tari 0.5 μM (P)
+ Tari 1 μM (P)
+ Zosu 0.5 μM (P)
+ Zosu 1 μM (P)

Manuscript Figure 5 Specific targeting of MDR1 sensitises AML cells to SM induced killing

(**A**) HoxA9/Meis1 AML cells were treated with ABC transporter inhibitors, Fum-C (inhibits BCRP/ABCG2) and reversan (Rev) (inhibits MRP1/ABCC1 and MDR1), 100 and 1000 nM ± birinapant 125, 250 and 500 nM for 24 h (n=3). (**B**) Western blot analysis of MDR1 expression in KG1 AML parental, control (Ctrl) 7A and 4B, and *MDR1*$^{-/-}$ pools 2.48 and 3.30. (**C**) Rho-123 retention assay in KG1 control 4B and *MDR1*$^{-/-}$ 2.48 and 3.30 AML cells pre-treated with Rho-123 (250 nM) ± tariquidar (1 µM). (**D**) KG1 controls 7A and 4B (n=4-6), (**E**) *MDR1*$^{-/-}$ 2.48 (n=2-3, error bars SD) and (**F**) *MDR1*$^{-/-}$ 3.30 (n=2-3, error bars SD) AML cells were treated with tariquidar or zosuquidar (0.5 and 1 µM) ± birinapant (0.08, 0.4, 2 µM) for 48 h. (**G**) KG1 control 4B, *MDR1*$^{-/-}$ 3.30 and 2.48 AML cells were treated with birinapant (500 nM) ± tariquidar (1 µM) for 10 and 20 min. Expression of the indicated proteins was determined by Western blot analysis. Data are presented as mean ± SEM throughout unless otherwise stated. Cell survival was measured by propidium iodide (PI) exclusion, decrease of cell volume and flow cytometry. P values were obtained by comparison of SM alone and in combination with MDR1/ABC transporter inhibitors at the indicated concentrations or time points. Actin was used as a loading control, M#1, 2 indicate independent membranes. Blots and Rho-123 graphs are representative of 2 independent experiments.

3.3.6 The Bir/MDR1i Combination is Well Tolerated, Efficiently Kills LSCs and Prolongs Survival in AML Models

Short-term cell viability assays are indicative but not necessarily predictive of a therapeutic response, we therefore tested $MDR1^{H}$ MLL-AF9 leukaemias in long-term assays. AML cells treated with bir/zosu were unable to form colonies in agar culture (**Supplemental Figure 6A,B**), suggesting that the combination therapy could be an effective way to treat MDR1 expressing AMLs. While birinapant and MDR1i are all well-tolerated as single-agents, their safety in combination has not been evaluated. To test whether bir/MDR1i treatment is feasible *in vivo*, C57BL/6 mice were treated with the combined drugs three times a week for 4 weeks and analysed immediately upon completion of the treatment regime (acute toxicity) or 6 weeks after completion (chronic toxicity). No signs of distress were observed following injections. Body and liver weights, and white blood cell and lymphocyte counts were unaffected, however there was an increase in neutrophil counts (**Supplemental Figure 6C-G**). Although there was an increase in spleen weights immediately following completion of treatment, this subsided after 6 weeks (**Supplemental Figure 6H,I**). Together these results indicate a high tolerability of bir/MDR1i combination therapy *in vivo*.

Despite these encouraging results, a limiting factor in treating leukaemias is often the toxicity of chemotherapies to healthy HSPCs (Lin^{-}, $Sca\text{-}1^{+}$, $c\text{-}KIT^{+}$ (LSK)). Notably, these cells are known to be $MDR1^{H}$ (Bagger et al., 2019; Oguro et al., 2013) and thus, may be particularly sensitive to MDR1i combination therapies (**Supplemental Figure 7A**). To determine the impact of bir/MDR1i treatment on

HSPCs, LSK cells from healthy C57BL/6 mice were treated for 48 h with bir/tari or with the chemotherapy Ara-c. As predicted, Ara-c potently killed these cells, whereas the viability of LSK cells was unaffected by bir or bir/tari treatment (**Figure 6A**; **Supplemental Figure 7B**)**,** suggesting a therapeutic window for SM/MDR1i therapy.

Similar to normal HSPCs, high levels of MDR1 have also been reported in LSCs and it is known that targeting these cells is crucial for efficient elimination of AML disease and preventing relapse (Ho et al., 2016; Leith et al., 1999). As the aggressive nature of the AML transplant model makes it difficult to assess the ability of the bir/tari therapy to target LSCs, we determined the impact of this treatment *in vitro* in previously established MLL-AF9 LSCs and matching blasts (Fong et al., 2015). Rho-123 efflux assays and protein analysis confirmed high levels of functional MDR1 in LSCs compared to leukaemic blasts (**Figure 6B,C**). As previously observed (**Figure 3**), MLL-AF9 blasts were sensitised to birinapant induced killing by the addition of MDR1i (**Figure 6D**). Strikingly, MLL-AF9 LSCs were highly sensitive to bir/MDR1i treatment but less sensitive to Ara-c chemotherapy (**Figure 6E; Supplemental Figure 7C**). Because MDR1i have shown limited effect in clinical trials in combination with chemotherapies that are MDR1 substrates, such as daunorubicin and etoposide (VP16), we compared the efficacy of bir/tari with VP16/tari in LSCs and blasts. Remarkably, the bir/tari combination was significantly more effective at eliminating LSCs and blast cells than the VP16/tari combination treatment (**Supplemental Figure 7D,E**). These

results suggest that bir/MDR1i combination therapy is stronger at eliminating LSCs to overcome treatment resistance and disease relapse.

Although Ara-c, a front-line chemotherapy for AML, is effective for the elimination of leukaemic blasts, disease relapse occurs in ~50% of patients, possibly due to the presence of Ara-c resistant LSCs (Shlush et al., 2017). Due to bir/tari's strong effect on LSCs, we determined whether this therapy could prolong survival after chemotherapy. Mice transplanted with an aggressive MDR1$_H$ MLL-AF9-GFP AML, were treated with Ara-c (50 mg/kg) for five consecutive days followed either by bir or bir/tari treatment, twice or three times a week (**Supplemental Figure 7F**). Although the MDR1$_H$ MLL-AF9-GFP AML cells are responsive *in vitro* at higher concentrations of bir, *in vivo* the survival advantage is limited. Therefore, in this aggressive model, the bir/tari combination was the only treatment to give a survival benefit, doubling the median survival (MS) when compared to control or single-agent groups (MS of Ara-c + 2xCombo = 34 days; Ara-c + 3xCombo = 40 days vs Ara-c alone = 22 days) (**Figure 6F**). Consistently, histological analysis revealed a remarkable decrease of leukaemic blasts in the spleens and livers of bir/tari treated mice compared to the Ara-c only group (**Figure 6G; Supplemental Figure 8A**). This correlated with a reduction of MLL-AF9-GFP cells in the bone marrow, lower overall white blood cell counts and reduction of organ size (**Figure 6H-J**; **Supplemental Figure 8B-F**), thus confirming the effectiveness of the combination treatment.

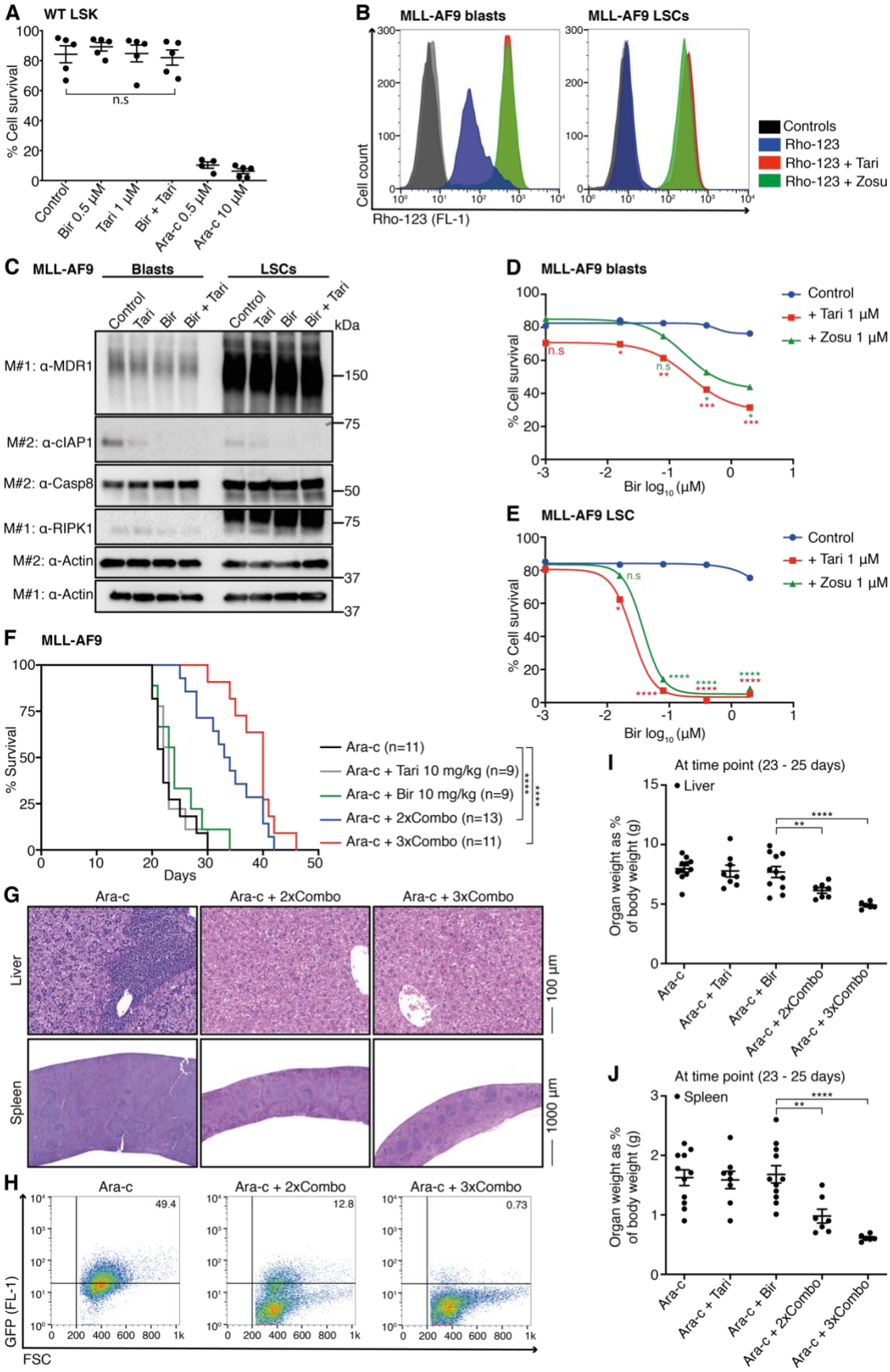
A
WT LSK
% Cell survival
n.s
Control
Bir 0.5 µM
Tari 1 µM
Bir + Tari
Ara-c 0.5 µM
Ara-c 10 µM
B
MLL-AF9 blasts
MLL-AF9 LSCs
Cell count
Rho-123 (FL-1)
Controls
Rho-123
Rho-123 + Tari
Rho-123 + Zosu
C
MLL-AF9
Blasts
LSCs
Control
Tari
Bir
Bir + Tari
kDa
M#1: α-MDR1
M#2: α-cIAP1
M#2: α-Casp8
M#1: α-RIPK1
M#2: α-Actin
M#1: α-Actin
150
75
50
75
37
37
D
MLL-AF9 blasts
% Cell survival
Bir log10 (µM)
Control
+ Tari 1 µM
+ Zosu 1 µM
E
MLL-AF9 LSC
F
MLL-AF9
% Survival
Days
Ara-c (n=11)
Ara-c + Tari 10 mg/kg (n=9)
Ara-c + Bir 10 mg/kg (n=9)
Ara-c + 2xCombo (n=13)
Ara-c + 3xCombo (n=11)
G
Ara-c
Ara-c + 2xCombo
Ara-c + 3xCombo
Liver
Spleen
100 µm
1000 µm
H
Ara-c
Ara-c + 2xCombo
Ara-c + 3xCombo
49.4
12.8
0.73
GFP (FL-1)
FSC
I
At time point (23 - 25 days)
• Liver
Organ weight as % of body weight (g)
Ara-c
Ara-c + Tari
Ara-c + Bir
Ara-c + 2xCombo
Ara-c + 3xCombo
J
At time point (23 - 25 days)
• Spleen
Organ weight as % of body weight (g)

Manuscript Figure 6 The bir/MDR1i combination is well tolerated, efficiently kills LSCs and prolongs survival in murine AML models

(**A**) Lin$^-$Sca-1$^+$c-KIT$^+$ (LSK) HSPCs from wild-type (WT) C57BL/6 mice were treated with birinapant (0.5 µM) ± tariquidar (1 µM) or Ara-c (0.5 µM and 10 µM) for 48 h (n=3-5, 3 independent experiments). (**B, C**) MLL-AF9 LSCs have high expression of MDR1 compared to matching blasts as shown through (**B**) Rho-123 retention assay and (**C**) Western blot analysis of samples treated with tariquidar (1 µM) ± birinapant (500 nM) for 10 min as indicated. MLL-AF9 (**D**) blasts and (**E**) LSCs were treated with 0.001, 0.016, 0.08, 0.4 and 2 µM birinapant ± tariquidar or zosuquidar (1 µM) for 24 h (n=4-7). (**F**) C57BL/6 mice transplanted with MLL-AF9-GFP MDR1$_H$ AML cells were treated with Ara-c (50 mg/kg) for five consecutive days followed either by birinapant single-agent treatment (10 mg/kg), or birinapant plus tariquidar (10 mg/kg) combination therapy, given twice or three times a week (Ara-c + 2xCombo and Ara-c + 3xCombo respectively) (n=9-13, 4 independent experiments). P values were obtained by comparison of Ara-c single treatment and birinapant combination treatments and determined by Log-rank (Mantel-Cox) test. At timepoint 23 – 25 days, mice were taken from all groups and (**G**) histology of spleens and livers of mice and (**H**) percentages of GFP positive cells in the bone marrow were analysed. The weights of (**I**) livers and (**J**) spleens as percentage of body weight (n=6-11) were also determined. The data are presented as mean ± SEM throughout. Cell survival was measured by propidium iodide (PI) exclusion, decrease of cell volume and flow cytometry. P values were obtained by comparison of control or SM alone and in combination with MDR1 inhibitors at the indicated concentrations unless otherwise stated. Probing for actin was used as a loading control, M#1, 2 indicate independent membranes.

3.3.7 Combination Bir/Tari Therapy Kills Human Primary Leukaemias

To further explore the safety of such a combination therapy in humans, we determined the impact of bir and bir/tari treatment on healthy human CD34+ HSPCs *in vitro*. Although human CD34+ cells have MDR1 activity (**Figure 7A**), no increase in birinapant-mediated killing was observed in the presence of an MDR1i (**Figure 7B**). In contrast, VP16/tari treatment was toxic to these cells (**Figure 7B**). Finally, we determined the efficacy of bir/MDR1i treatment in patient-derived primary AML cells. As expected, MDR1 activity was heterogeneous in primary leukaemias (**Figure 7C-O**). Although the amount of cell death achieved was variable among the different primary human $MDR1_H$ AMLs, all were sensitised to birinapant induced killing by the addition of tariquidar (patients 1, 2 and 3) (**Figure 7C-H**). Whereas, $MDR1_L$ AML cells (patient 4 and 5) were sensitive to birinapant alone treatment and addition of tariquidar did not increase killing (**Figure 7I-L**). Lastly, similar to what was observed in murine AMLs, $MDR1_L$ AMLs not responsive to birinapant could be somewhat sensitised in the presence of exogenous TNF (patient 6) (**Figure 7M,N**). There was no correlation between patient cytogenetics and molecular marker profile and response to treatment (**Figure 7O**). These results reinforce the notion that high MDR1 activity may cause resistance to birinapant and that MDR1 levels may be used as a predictor of response of cancer cells to SM drugs.

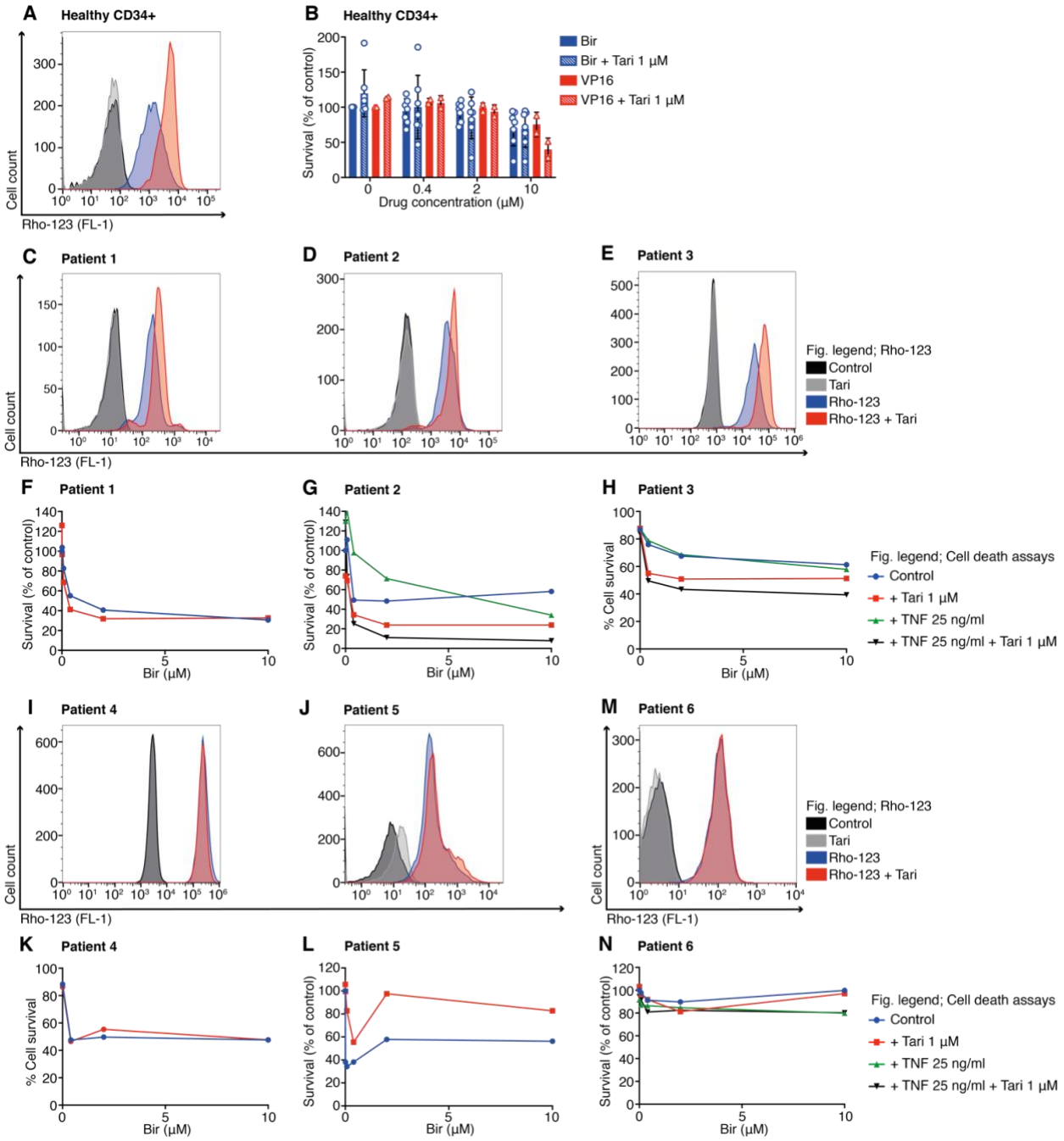

O

Patient	BM/PB	Age	Sex	WCC	Blast (%)	Status	WHO	Cytogenetics	Molecular
1	BM	75	M	2.98	33	Relapsed	AML with MDS related changes	Normal	Not performed
2	BM	64	M	7.44	60	Primary refractory	AML with MDS related changes	Normal	ASXL1, SRSF2, RUNX1
3	Blood	56	M	132	75	De novo	Acute myelomonocytic leukemia	Normal	FLT3-ITD, IDH1, R132H
4	Blood	44	F	221	82	Therapy induced	N/D	t(9;11), 11q23	N/D
5	BM	56	M	1.92	86	De novo	AML without maturation	Normal	IDH2
6	BM	75	M	5.38	93	De novo	AML with mutated NPM1	Normal	IDH2 c.419G>A p.Arg140Gln (R140Q)

Manuscript Figure 7 Combination bir/tari therapy kills human primary leukaemias

(**A**) MDR1 activity was determined in primary human CD34+ HSPCs through Rho-123 retention assay. (**B**) Human CD34+ HSPCs were treated with birinapant or VP16 (0.4, 2 and 10 μM) ± tariquidar (1 μM) for 24-48 h (n=2-7 independent samples, error bars SD). (**C-N**) For patient samples; (**C, F**) patient 1, (**D, G**) patient 2, (**E, H**) patient 3, (**I, K**) patient 4, (**J, L**) patient 5 and (**M, N**) patient 6, MDR1 activity was determined (**C, D, E, I, J and M**) through Rho-123 retention assay. (**F, G, H, K, L and N**) Primary cells were treated with birinapant (0.016, 0.08, 0.4, 2 and 10 μM) ± tariquidar (1 μM) ± TNF (25 ng/ml) for 24-48 h (1 independent experiment for each sample). (**O**) Description of patient samples' cytogenetics and molecular markers. BM; bone marrow, PB; peripheral blood, WCC; white blood cell count; N/D; not determined. Cell survival was determined by Annexin V staining, decrease of cell volume and flow cytometry. Patient 1, 2, 5, 6 and CD34+ data represented as relative to control.

3.4 Discussion

Chemoresistance is a common feature of AML and one of the main causes of disease relapse and poor overall survival (<30% at 5 years). Clinical trial therapies, such as Venetoclax, cytarabine or hypomethylating agent combinations, have been effective in newly diagnosed AML but have shown modest and short-lived responses in chemoresistant patients, thus new therapies are needed for this group. High levels of IAPs have also been linked to drug resistance in AML, and SM drugs that target IAPs, such as birinapant, have entered late phase clinical trials. Unfortunately, despite initial promising results, good safety profiles and their ability to elicit an anti-cancer immune response, the use of SMs as single-agent therapy has not been overwhelmingly successful in MDS and relapse AML (Amaravadi et al., 2013; Fulda and Vucic, 2012; Schilder et al., 2018). Using an unbiased screen of pre-clinical and clinical compounds, we identified MDR1 inhibitors as a class of drugs that can enhance SM therapy and overcome treatment resistance in AML. Expression of MDR1 has extensively been reported to be a predictor of treatment outcome in AML, with high levels of MDR1 being identified in over 50% of patients with relapse or secondary disease, for example MDS, chronic myeloproliferative neoplasia (cMPN) and therapy-related AML (Leith et al., 1999; Mahadevan and List, 2004; Samdani et al., 1996; Schaich et al., 2005). Therefore, this manuscript suggests a drug regimen of SM plus MDR1i therapy, that has activity in chemotherapy relapsed or refractory AML, to improve outcomes for patients.

MDR1 actively expels diverse cytotoxic agents from cells, including chemotherapies, maintaining the quantities of anti-cancer drugs below toxic levels (Van Tellingen et al., 2003; Waghray and Zhang, 2017). Therefore, cancers that express high levels of MDR1 can be selected for by chemotherapy. Clinical trials of new therapies are frequently performed in cancer patients that have failed conventional therapies and thus, their tumours are likely to have high MDR1 activity. This is an important finding because birinapant and other SMs have been unsuccessfully trialed in MDS and AML relapse patients. In this study we show that the combination of birinapant with 3rd generation MDR1-specific inhibitors is well tolerated, efficiently kills LSCs and prolongs survival in $MDR1_H$ leukaemia models. Thus, screening for MDR1 expression and activity would enable bir/MDR1i therapy to be targeted to $MDR1_H$ cancers.

The fact that MDR1 is a member of the large ABC transporter family and is implicated in chemoresistance (Fletcher et al., 2010), has prompted both the U.S. Food and Drug Administration and the European Medicines Agency to mandate that new anti-cancer drugs be assessed for interactions with MDR1 and other drug transporters (Giacomini et al., 2010). However, older anti-cancer agents have not been selected to meet with this requirement. An outstanding question within the field is how ABC transporters select their substrates, as they are structurally diverse (Waghray and Zhang, 2017). We were intrigued that birinapant and other chemically distinct SMs synergised with MDR1i (Hugle et al., 2019; Talbott et al., 2015), however our tests with ABT-199 and JQ1 indicate that not all peptide-mimetic drugs are substrates.

Regulation of cellular mechanisms other than drug efflux, including differentiation and cell survival, have been proposed as possible mechanisms by which inhibition of MDR1 may sensitise cells to chemotherapy (Fletcher et al., 2010). Using mass spectrometry, we showed that co-treatment with the MDR1i tariquidar tripled the intracellular levels of birinapant in MDR1$_H$ AML cells, indicating that regulation of birinapant efflux is the main mechanism by which these drugs enhance birinapant tumour cell killing.

Unfortunately, while MDR1i are well tolerated by patients, their combination with cytotoxic drugs led to increased toxicity towards healthy cells, limiting the clinical use of such combination treatments (Fletcher et al., 2010; Gerrard et al., 2004; Relling, 1996; Schinkel et al., 1994; Waghray and Zhang, 2017). Moreover, given that HSPCs express higher levels of MDR1 than their differentiated progeny, we were concerned that combining birinapant with MDR1i would cause haematopoietic toxicity. However, in addition to observing no adverse effects of bir/MDR1i combination in immunocompetent mice, this treatment did not diminish the survival of mouse or human HSPCs in culture, whereas the current standard-of-care chemotherapy Ara-c or the combination VP16/MDR1i was highly toxic as previously observed (Brumatti et al., 2016). We speculate that this may be explained by the fact that birinapant is not inherently toxic and therefore, increasing doses of this SM in healthy cells has no discernible effect on their viability. Collectively, these results suggest that repurposing of MDR1 inhibitors in combination with SMs might be a safe and efficacious new approach for cancer therapy.

The reason why birinapant preferentially kills transformed cells while leaving normal cells intact remains unclear. One explanation put forward is that, contrary to chemotherapeutic drugs that alter multiple cellular pathways (Adams, 2004; Silke et al., 2008), SMs specifically affect IAP signalling pathways. Another explanation might be that abnormal expression of IAPs and/or TNF by the tumour or stromal cells in its environment, leads to addiction to the NF-κB and/or the TNFR1 signalling pathways. Consistent with the latter idea, our *in vitro* assays with AML revealed that tumours must be able to produce TNF in response to birinapant to be killed efficiently by SMs.

For novel therapies to cure AML they must eradicate LSCs. Yet these cells are highly resistant to many anti-cancer drugs and therefore are often responsible for disease relapse (Costello et al., 2000; Ishikawa et al., 2007; Shlush et al., 2017; van Rhenen et al., 2005). Our discoveries suggest that MDR1 expression is an Achilles heel of LSCs which birinapant is able to exploit if combined with MDR1i, and thereby prevent disease relapse and prolong survival.

Screening tools for MDR1 activity are readily available and inexpensive. Our findings show that MDR1 expression in AML can be used as a biomarker for SM-related therapies to improve patient stratification. This observation combined with the safety and efficacy of the bir/MDR1i drug combination in primary AML patient samples and *in vivo* models of AML, provides the rationale for the clinical testing of this drug combination in AML patients.

3.5 Acknowledgments

We thank the staff of the WEHI Bioservices facilities for technical assistance. We also thank all members of the Silke laboratory, Prof. Andreas Strasser, A/Prof. Paul Ekert and Mr. George Kiossoglou for discussions. This work was supported by a Leukemia & Lymphoma Society [SCOR (Specialized Centre of Research, grant #7015-18 to J.S.), the National Health and Medical Research Council (NHMRC; grants 1025594, 1046010, and 1081376), Cancer Australia and Leukaemia Foundation Australia priority grant (PdCCRS 1162023 to G.B.), NHMRC fellowship (1058190 to J.S.) and a Victoria Cancer Agency (VCA) mid-career fellowship (MCRF 15027 to G.B.). This work was made possible through the Australian Cancer Research Foundation and Victorian State Government Operational Infrastructure Support and Australian Government NHMRC IRIISS (9000433).

3.6 Supplemental Materials and Methods

For Materials and Methods relevant to Chapter 3, please see the main Methods section of this thesis.

3.7 Supplemental Figures

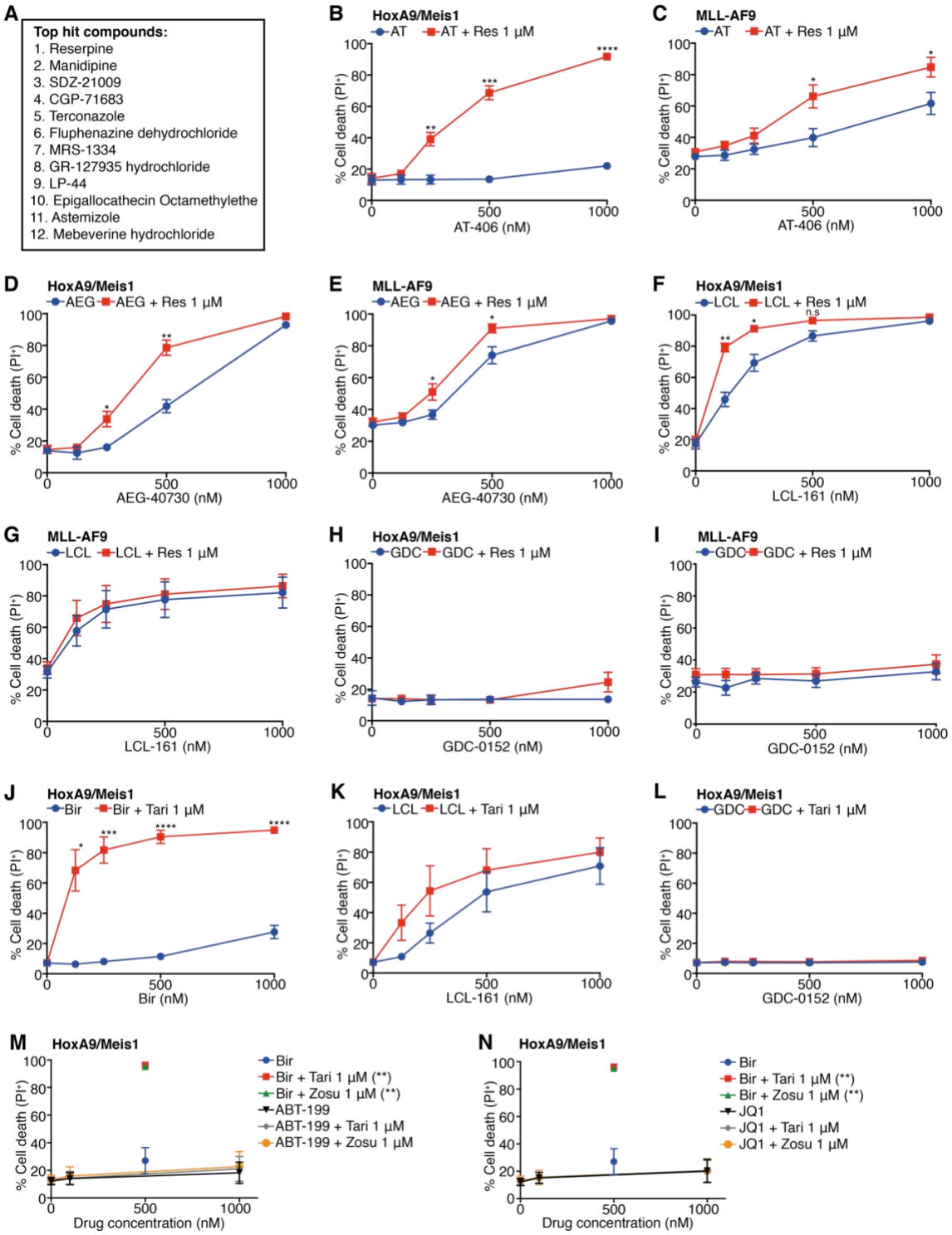
A
Top hit compounds:
1. Reserpine
2. Manidipine
3. SDZ-21009
4. CGP-71683
5. Terconazole
6. Fluphenazine dehydrochloride
7. MRS-1334
8. GR-127935 hydrochloride
9. LP-44
10. Epigallocathecin Octamethylethe
11. Astemizole
12. Mebeverine hydrochloride
B
HoxA9/Meis1
AT
AT + Res 1 µM
% Cell death (PI+)
AT-406 (nM)
C
MLL-AF9
AT
AT + Res 1 µM
% Cell death (PI+)
AT-406 (nM)
D
HoxA9/Meis1
AEG
AEG + Res 1 µM
% Cell death (PI+)
AEG-40730 (nM)
E
MLL-AF9
AEG
AEG + Res 1 µM
% Cell death (PI+)
AEG-40730 (nM)
F
HoxA9/Meis1
LCL
LCL + Res 1 µM
n.s
% Cell death (PI+)
LCL-161 (nM)
G
MLL-AF9
LCL
LCL + Res 1 µM
% Cell death (PI+)
LCL-161 (nM)
H
HoxA9/Meis1
GDC
GDC + Res 1 µM
% Cell death (PI+)
GDC-0152 (nM)
I
MLL-AF9
GDC
GDC + Res 1 µM
% Cell death (PI+)
GDC-0152 (nM)
J
HoxA9/Meis1
Bir
Bir + Tari 1 µM
% Cell death (PI+)
Bir (nM)
K
HoxA9/Meis1
LCL
LCL + Tari 1 µM
% Cell death (PI+)
LCL-161 (nM)
L
HoxA9/Meis1
GDC
GDC + Tari 1 µM
% Cell death (PI+)
GDC-0152 (nM)
M
HoxA9/Meis1
% Cell death (PI+)
Drug concentration (nM)
Bir
Bir + Tari 1 µM (**)
Bir + Zosu 1 µM (**)
ABT-199
ABT-199 + Tari 1 µM
ABT-199 + Zosu 1 µM
N
HoxA9/Meis1
% Cell death (PI+)
Drug concentration (nM)
Bir
Bir + Tari 1 µM (**)
Bir + Zosu 1 µM (**)
JQ1
JQ1 + Tari 1 µM
JQ1 + Zosu 1 µM

Supplemental Figure 1 MDR1 inhibitors increase cell death mediated by structurally distinct SMs

(**A**) Top hit compounds identified by the high throughput screen that synergise with birinapant in the killing of HoxA9/Meis1 AML cells. (**B, D, F, H**) HoxA9/Meis1 and (**C, E, G, I**) MLL-AF9 AML cells were treated with 125, 250, 500 and 1000 nM of (**B, C**) AT-406 (AT) (n=4-8), (**D, E**) AEG-40730 (AEG) (n=4-8), (**F, G**) LCL161 (n=4-6) and (**H, I**) GDC-0152 (GDC) (n=3-6) ± 1 μM reserpine (Res) for 24 h. HoxA9/Meis1 AML cells were treated with 125, 250, 500 and 1000 nM of (**J**) birinapant (Bir), (**K**) LCL161 (LCL) and (**L**) GDC-0152 (GDC) ± tariquidar (1 μM) for 24 h (n=5). HoxA9/Meis1 AML cells were treated with other peptide-mimetic anti-cancer agents (**M**) ABT-199 and (**N**) JQ1 (100 and 1000 nM) ± tariquidar or zosuquidar (1 μM) for 24 h (n=4). Birinapant (500 nM) plus MDR1 inhibitors was used as a control throughout (n=4). Data are presented as mean ± SEM throughout. Cell death was measured by propidium iodide (PI) uptake and flow cytometry (2-4 independent tumours, repeated 1-2 times). P values were obtained by comparison of SM alone and in combination with MDR1i at the indicated concentrations.

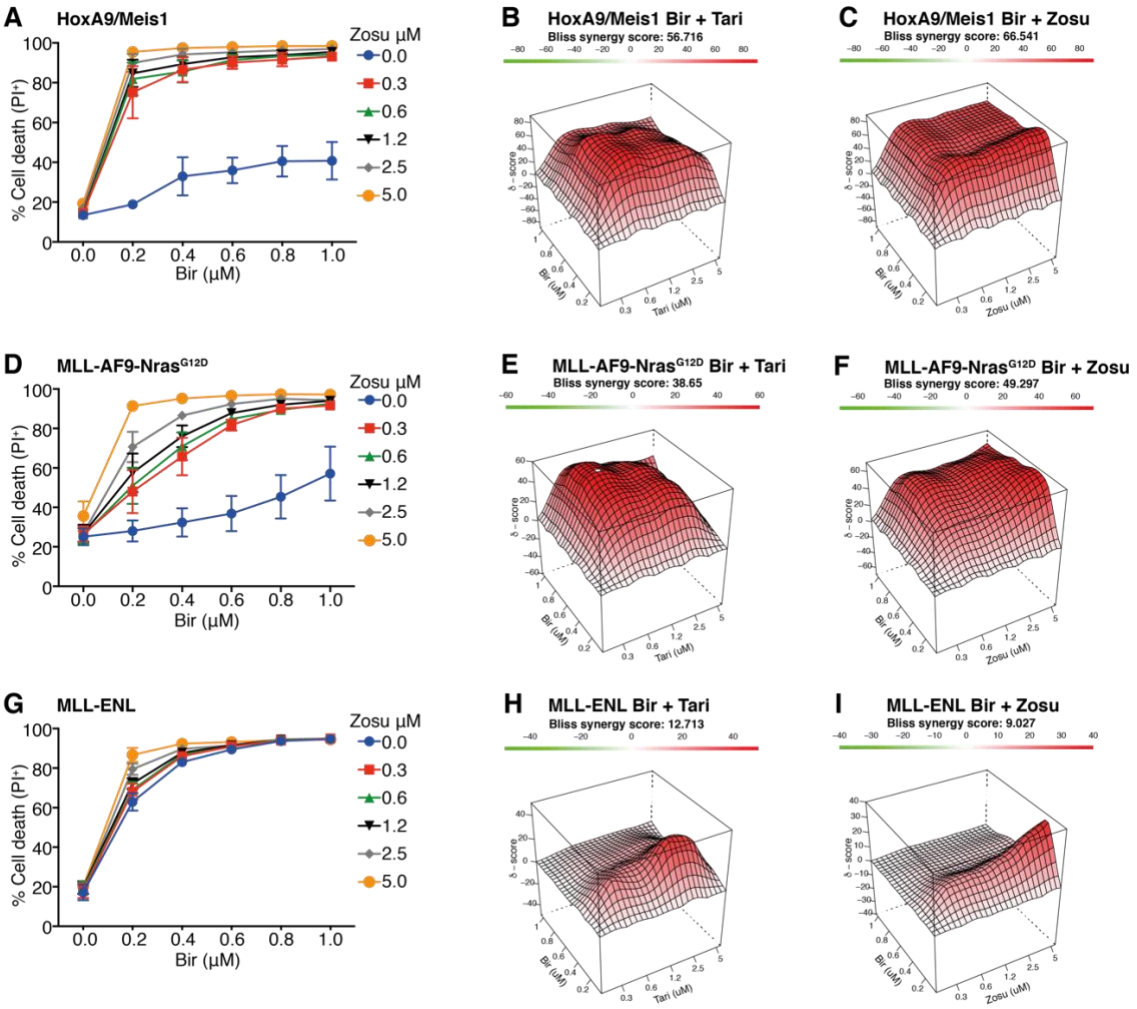

Supplemental Figure 2 MDR1 activity can predict response of AML cells to treatment with birinapant and MDR1i

(**A**) HoxA9/Meis1 AML cells were treated with zosuquidar (0.3, 0.6, 1.2, 2.5 and 5 µM) ± birinapant (0.2, 0.4, 0.6, 0.8, 1 µM) for 24 h (n=4). Bliss synergy analysis of HoxA9/Meis1 AML cells treated with birinapant ± a titration of (**B**) tariquidar or (**C**) zosuquidar. (**D**) MLL-AF9-Nras$_{G12D}$ AML cells were treated as described in (A) (n=4) and Bliss synergy analysis of birinapant ± a titration of (**E**) tariquidar or (**F**) zosuquidar. (**G**) MLL-ENL AML cells were treated as described in (A) (n=4) and Bliss synergy analysis of birinapant ± a titration of (**H**) tariquidar or (**I**) zosuquidar. Data are presented as mean ± SEM throughout. Cell death was measured by propidium iodide (PI) uptake, decrease of cell volume (MLL-AF9-Nras$_{G12D}$) and flow cytometry from 3-4 independent tumours.

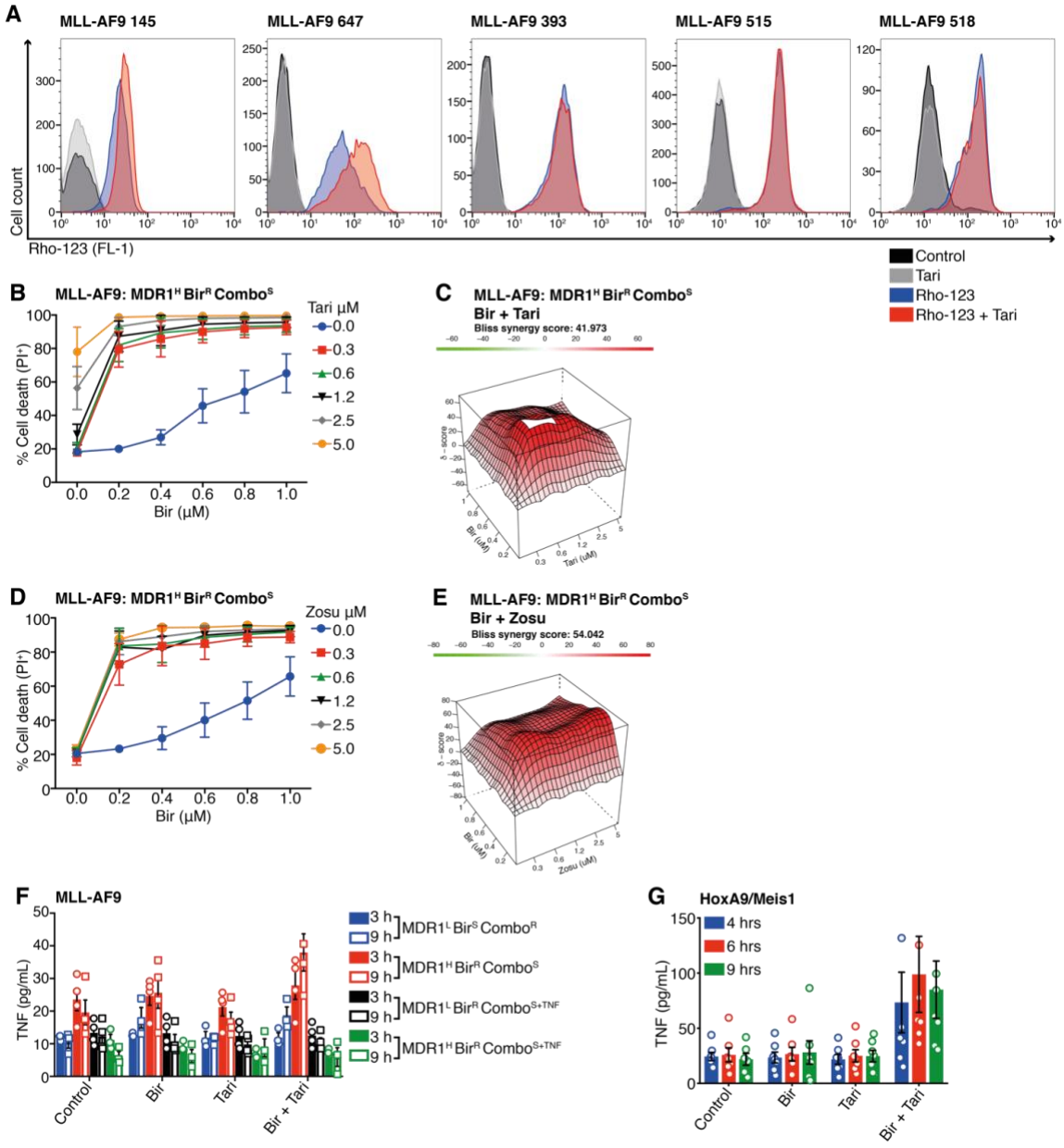
A
MLL-AF9 145
MLL-AF9 647
MLL-AF9 393
MLL-AF9 515
MLL-AF9 518
Cell count
Rho-123 (FL-1)
Control
Tari
Rho-123
Rho-123 + Tari
B
MLL-AF9: MDR1H BirR ComboS
Tari µM
0.0
0.3
0.6
1.2
2.5
5.0
% Cell death (PI+)
Bir (µM)
C
MLL-AF9: MDR1H BirR ComboS
Bir + Tari
Bliss synergy score: 41.973
D
MLL-AF9: MDR1H BirR ComboS
Zosu µM
E
MLL-AF9: MDR1H BirR ComboS
Bir + Zosu
Bliss synergy score: 54.042
F
MLL-AF9
TNF (pg/mL)
3 h
9 h
MDR1L BirS ComboR
MDR1H BirR ComboS
MDR1L BirR ComboS+TNF
MDR1H BirR ComboS+TNF
Control
Bir
Tari
Bir + Tari
G
HoxA9/Meis1
4 hrs
6 hrs
9 hrs

Supplemental Figure 3 Characterisation of MDR1 expression and synergistic cell death of MLL-AF9 sub-groups induced by the combination SM/MDR1i

(**A**) MDR1 activity was determined in MLL-AF9 AML sub-groups through Rho-123 retention assay. (**B**) MLL-AF9 ($MDR1_H$ Bir_R $Combo_S$) AML cells were treated with (0.3, 0.6, 1.2, 2.5 and 5 μM) tariquidar ± birinapant (0.2, 0.4, 0.6, 0.8, 1 μM) for 24 h (n=4) and (**C**) corresponding Bliss synergy analysis. (**D**) MLL-AF9 ($MDR1_H$ Bir_R $Combo_S$) AML cells were treated with (0.3, 0.6, 1.2, 2.5 and 5 μM) zosuquidar ± birinapant (0.2, 0.4, 0.6, 0.8, 1 μM) for 24 h (n=4) and (**E**) corresponding Bliss synergy analysis. (**F**) TNF production by MLL-AF9 AML sub-groups treated with tariquidar (500 nM) ± birinapant (500 nM) for 3 and 9 h as determined by ELISA (1-2 independent tumours for each sub-group, with 2-3 repeats). (**G**) HoxA9/Meis1 AML cells were treated with tariquidar (500 nM) ± birinapant (500 nM) and TNF production measured by ELISA at 4, 6 and 9 h (4 independent tumours, with 1-2 repeats). Data are presented as mean ± SEM throughout. Cell death was measured by propidium iodide (PI) uptake and flow cytometry.

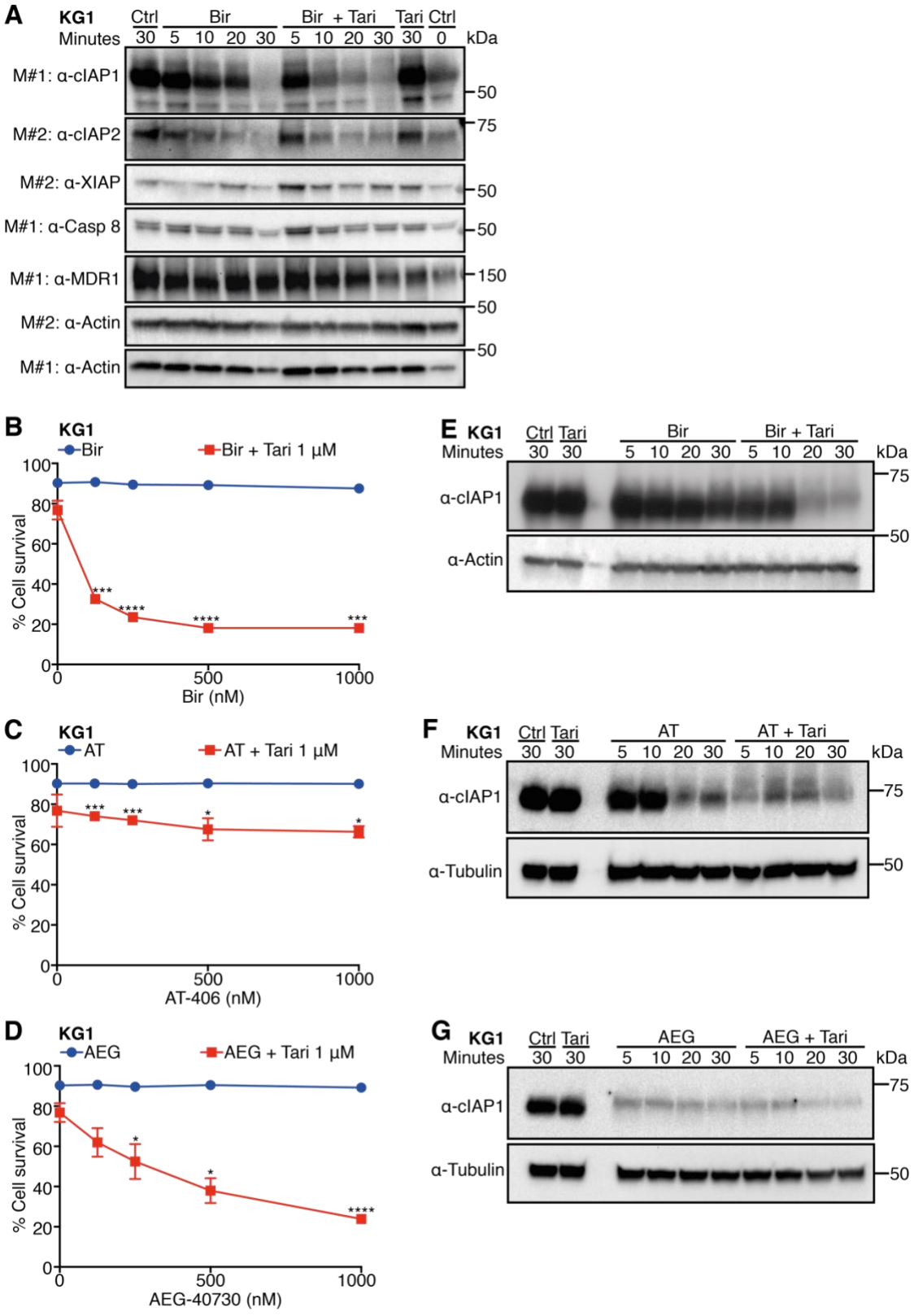
A
KG1
Ctrl
Bir
Bir + Tari
Tari
Ctrl
Minutes
30 5 10 20 30 5 10 20 30 30 0
kDa
M#1: α-cIAP1
M#2: α-cIAP2
M#2: α-XIAP
M#1: α-Casp 8
M#1: α-MDR1
M#2: α-Actin
M#1: α-Actin
50
75
50
50
150
50
50
B
KG1
Bir
Bir + Tari 1 μM
% Cell survival
Bir (nM)
C
KG1
AT
AT + Tari 1 μM
% Cell survival
AT-406 (nM)
D
KG1
AEG
AEG + Tari 1 μM
% Cell survival
AEG-40730 (nM)
E
KG1
Ctrl Tari
Bir
Bir + Tari
Minutes
30 30 5 10 20 30 5 10 20 30
kDa
α-cIAP1
α-Actin
75
50
F
KG1
Ctrl Tari
AT
AT + Tari
Minutes
30 30 5 10 20 30 5 10 20 30
kDa
α-cIAP1
α-Tubulin
75
50
G
KG1
Ctrl Tari
AEG
AEG + Tari
Minutes
30 30 5 10 20 30 5 10 20 30
kDa
α-cIAP1
α-Tubulin
75
50

Supplemental Figure 4 MDR1 inhibition enhances SM-mediated cIAP degradation

(**A**) Human KG1 AML cells were treated for the indicated times, with birinapant (500 nM) ± tariquidar (1 µM) and expression of the indicated proteins was determined by Western blotting. (**B-D**) KG1 AML cells were treated with 125, 250, 500 and 1000 nM of (**B**) birinapant (Bir) (n=3), (**C**) AT-406 (AT) (n=2-3, error bars SD) and (**D**) AEG-40730 (AEG) (n=3) for 24 h ± tariquidar (1 µM). (**E-G**) KG1 AML cells were treated with tariquidar (1 µM) ± 500 nM of Smac-mimetics; (**E**) Bir, (**F**) AT and (**G**) AEG for 5, 10, 20 and 30 min. Cell lysates were analysed by Western blot. Data are presented as mean ± SEM throughout unless otherwise stated. Cell survival was measured by propidium iodide (PI) exclusion, decrease of cell volume and flow cytometry. P values were obtained by comparison of SM alone and in combination with MDR1 inhibitors at the indicated concentrations. Probing for actin or α/β Tubulin was used as a loading control and M#1, 2 indicates independent membranes.

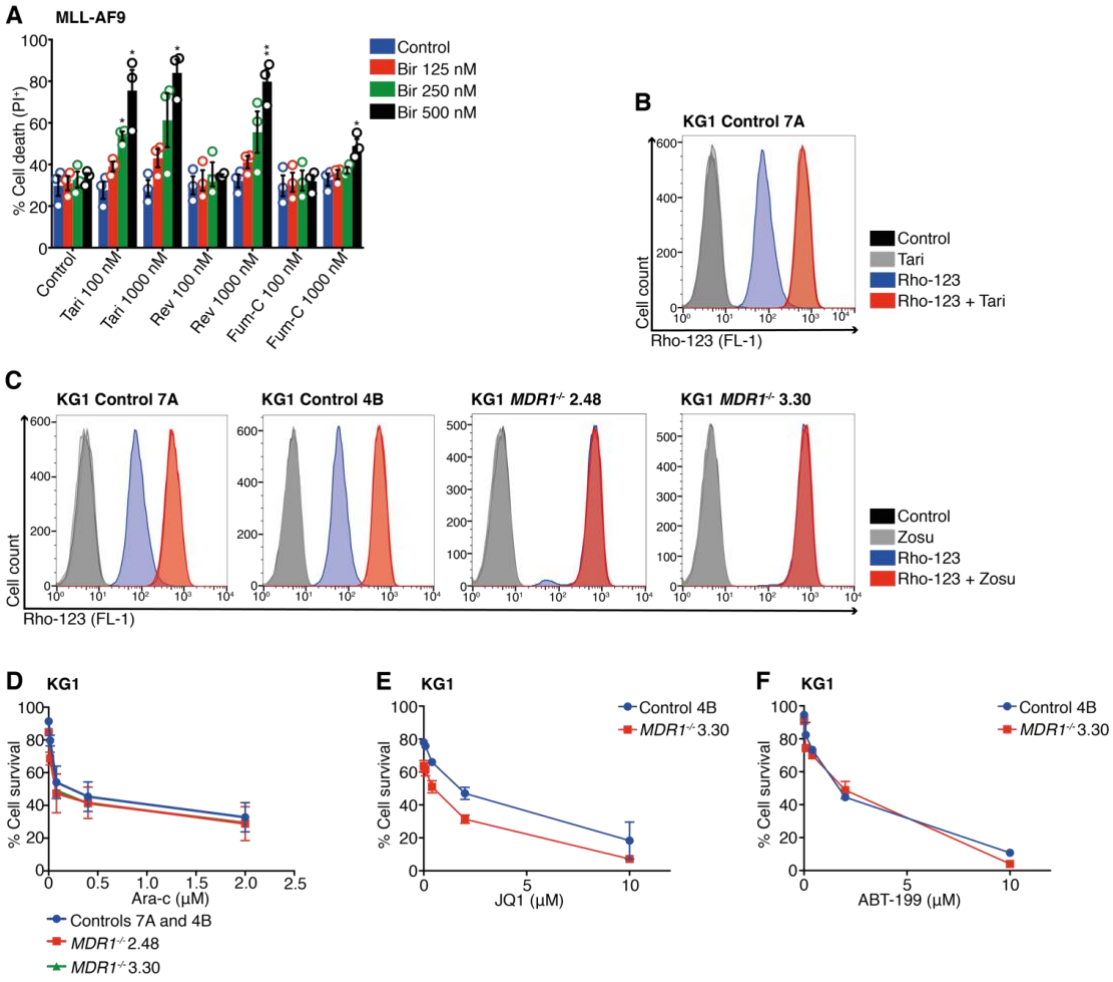

Supplemental Figure 5 Increased killing of AML cells is due to specific targeting of MDR1

(**A**) MLL-AF9 AML cells were treated with ABC transporter inhibitors, Fum-C (ABCG2/BCRP) and reversan (Rev) (ABCC1/MRP1) (100 and 1000 nM), ± birinapant (125, 250 and 500 nM) for 24 h (n=3). (**B, C**) MDR1 activity was determined in KG1 control 7A and 4B, and KG1 *MDR1*$^{-/-}$ 2.48 and 3.30, AML cells through Rho-123 retention assay with (**B**) tariquidar or (**C**) zosuquidar (1 μM). (**D**) KG1 control 7A and 4B, and *MDR1*$^{-/-}$ 2.48 and 3.30 AML cells were treated with Ara-c (0.016, 0.08, 0.4 and 2 μM) for 48 h (n=2-4, error bars SD). (**E, F**) KG1 control 4B and KG1 *MDR1*$^{-/-}$ 3.30 AML cells were treated with 0.08, 0.4, 2 and 10 μM of (**E**) JQ1 and (**F**) ABT-199 for 48 h (n=2, error bars SD). Data are presented as mean ± SEM throughout unless otherwise stated. Cell survival was measured by propidium iodide (PI) exclusion, decrease of cell volume and flow cytometry. P values were obtained by comparison of SM alone and in combination with ABC transporter inhibitors at the indicated concentrations.

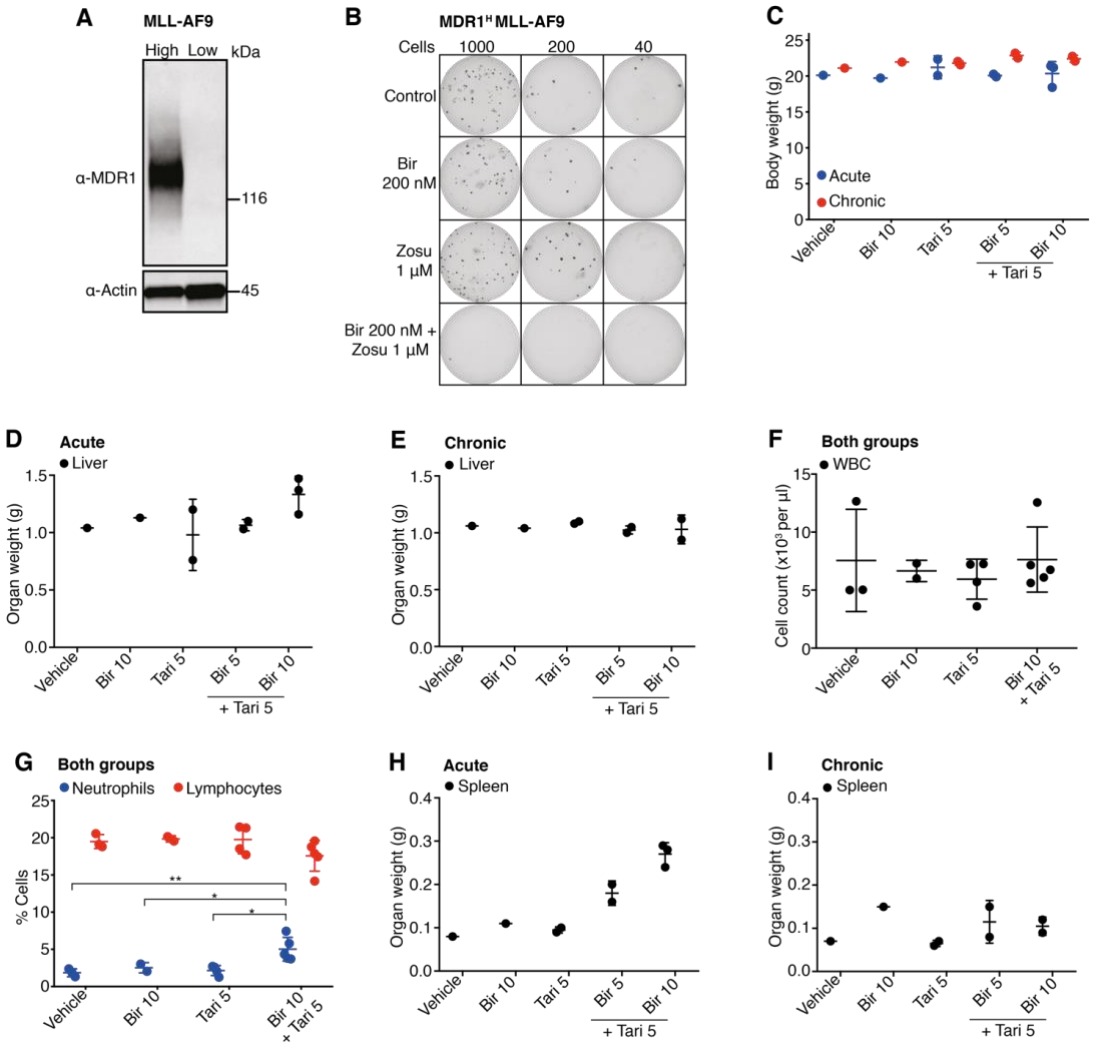

Supplemental Figure 6 Combination SM/MDR1i treatment is safe *in vivo*

(**A**) MLL-AF9 AML cells were determined as MDR1H or MDR1L through Western blot analysis and actin was used as a loading control. (**B**) MDR1H MLL-AF9 AML cells were titrated (1000, 200 and 40) and treated with birinapant (200 nM) ± zosuquidar (1 μM). Colony formation was analysed after 12 days (n=2, representative image). (**C–I**) C57BL/6 mice were treated with birinapant 5 and 10 mg/kg ± tariquidar 5 mg/kg for 4 weeks and analysed immediately following completion of treatment (acute toxicity) or 6 weeks after completion (chronic toxicity). (**C**) Body weights at both time points. Liver weights at (**D**) acute and (**E**) chronic time points. (**F**) white blood cells (WBC) and (**G**) neutrophil and lymphocyte counts at both time points. Spleen weights at (**H**) acute and (**I**) chronic time points (n=1-5, 1 experiment). Data are presented as mean ± SD throughout. P values were obtained by comparison of combination treatment with different single-agent treatments.

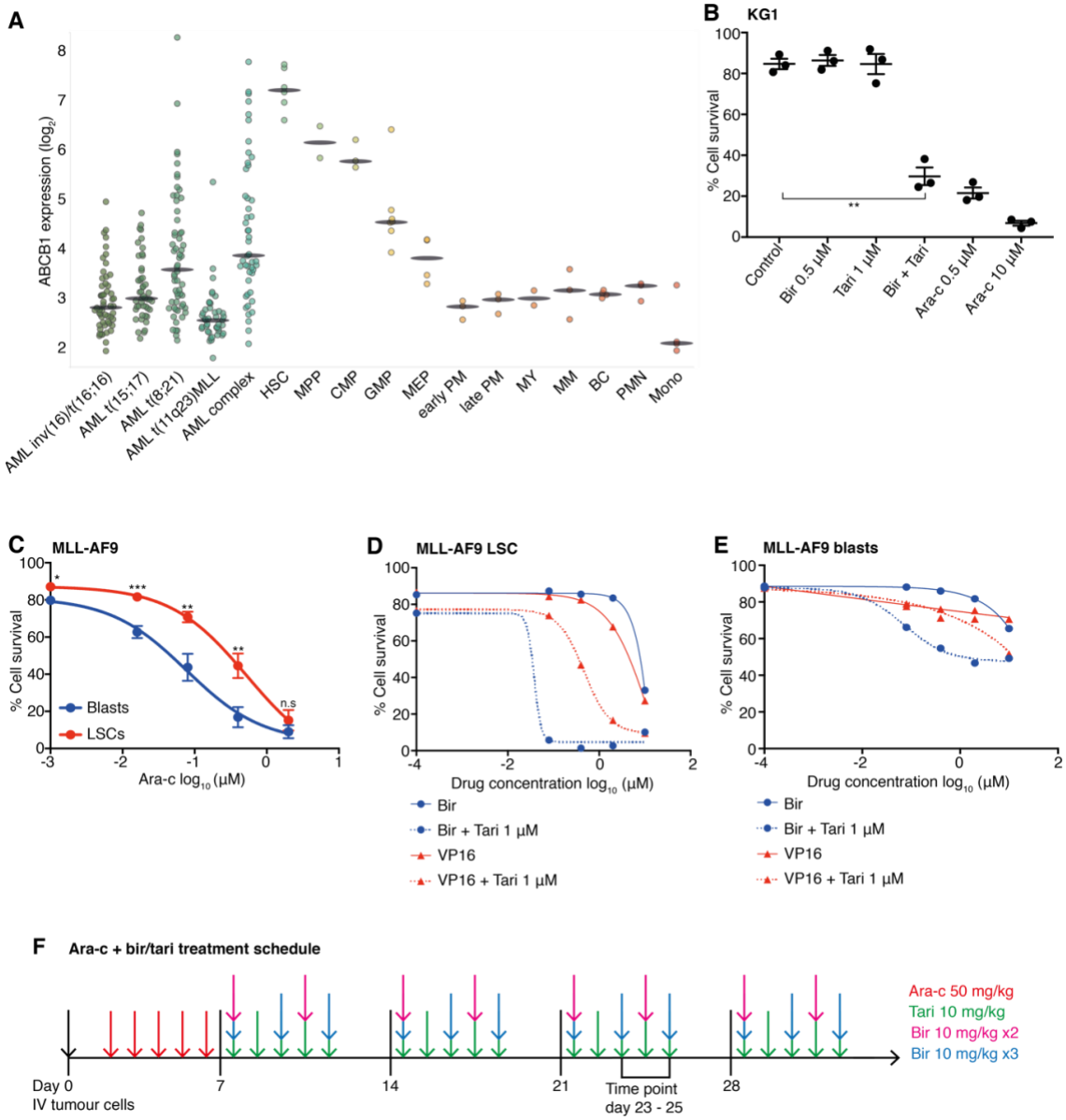
A
ABCB1 expression (log2)
AML inv(16)/t(16;16)
AML t(15;17)
AML t(8;21)
AML t(11q23)/MLL
AML complex
HSC
MPP
CMP
GMP
MEP
early PM
late PM
MY
MM
BC
PMN
Mono
B
KG1
% Cell survival
Control
Bir 0.5 µM
Tari 1 µM
Bir + Tari
Ara-c 0.5 µM
Ara-c 10 µM
C
MLL-AF9
% Cell survival
Blasts
LSCs
n.s
Ara-c log10 (µM)
D
MLL-AF9 LSC
% Cell survival
Drug concentration log10 (µM)
Bir
Bir + Tari 1 µM
VP16
VP16 + Tari 1 µM
E
MLL-AF9 blasts
% Cell survival
Drug concentration log10 (µM)
Bir
Bir + Tari 1 µM
VP16
VP16 + Tari 1 µM
F
Ara-c + bir/tari treatment schedule
Day 0
IV tumour cells
7
14
21
Time point
day 23 - 25
28
Ara-c 50 mg/kg
Tari 10 mg/kg
Bir 10 mg/kg x2
Bir 10 mg/kg x3

Supplemental Figure 7 LSCs have high expression of MDR1

(**A**) ABCB1 expression levels in AML and HSPCs, figure exported from BloodSpot (Bagger et al., 2019). (**B**) In parallel with murine LSK treatments, KG1 AML cells were treated with birinapant (0.5 µM) ± tariquidar (1 µM) or Ara-c (0.5 µM and 10 µM) for 48 h as a positive control (n=3 independent experiments). (**C**) MLL-AF9 AML blasts and matching LSCs treated for 48 h with Ara-c (0.001, 0.016, 0.08, 0.4 and 2 µM) ± tariquidar (1 µM) (n=7). MLL-AF9 (**D**) LSC and (**E**) blasts were treated with birinapant or VP16 (0.08, 0.4, 2 and 10 µM) ± tariquidar (1 µM) for 24 h (n= 2-3, error bars SD). (**F**) Schedule of mice intravenous (IV) injected with $MDR1_H$ MLL-AF9-GFP AML cells treated with Ara-c (50 mg/kg) followed by single or combination treatment of tariquidar (10 mg/kg) ± 2x or 3x birinapant (10 mg/kg) (Ara-c + 2xCombo or Ara-c + 3xCombo respectively). Data are presented as mean ± SEM throughout unless otherwise stated. Cell survival was measured by propidium iodide (PI) exclusion and flow cytometry. P values were obtained by comparison of combination treatment with different single treatments or of MLL-AF9 blasts and LSCs at the indicated concentrations.

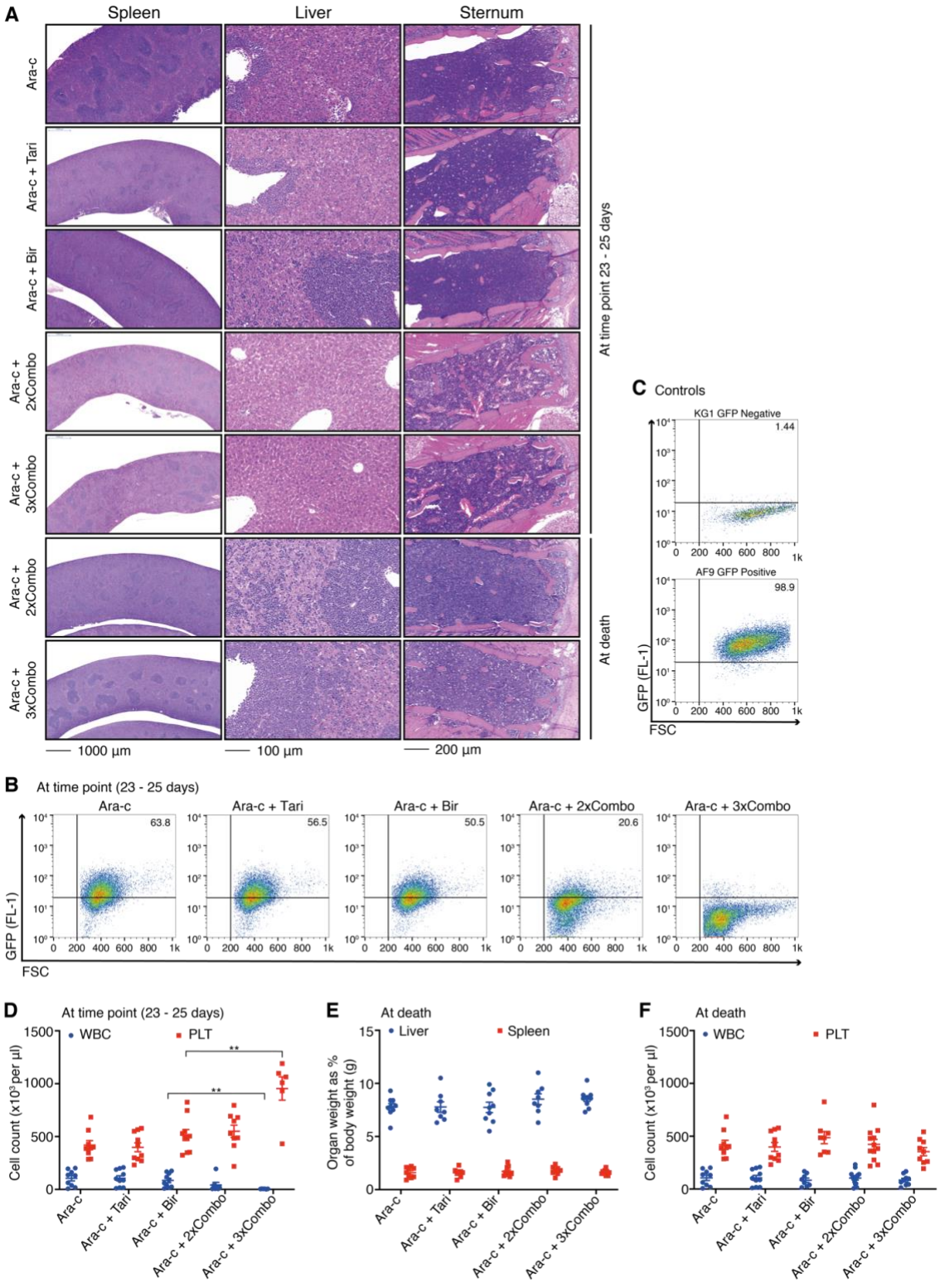
A
Spleen
Liver
Sternum
Ara-c
Ara-c + Tari
Ara-c + Bir
Ara-c + 2xCombo
Ara-c + 3xCombo
Ara-c + 2xCombo
Ara-c + 3xCombo
At time point 23 - 25 days
At death
1000 µm
100 µm
200 µm
C Controls
KG1 GFP Negative
1.44
AF9 GFP Positive
98.9
GFP (FL-1)
FSC
B At time point (23 - 25 days)
Ara-c
Ara-c + Tari
Ara-c + Bir
Ara-c + 2xCombo
Ara-c + 3xCombo
63.8
56.5
50.5
20.6
GFP (FL-1)
FSC
D At time point (23 - 25 days)
WBC
PLT
Cell count (x10³ per µl)
E At death
Liver
Spleen
Organ weight as % of body weight (g)
F At death
WBC
PLT
Cell count (x10³ per µl)

Supplemental Figure 8 Pre-treatment with Ara-c followed by SM/MDR1i combination therapy significantly extends the survival of mice transplanted with MLL-AF9-GFP MDR1$_H$ AML cells

Mice that had been transplanted with MLL-AF9-GFP MDR1$_H$ AML cells were treated with Ara-c (50 mg/kg) followed by single or combination treatment of tariquidar (10 mg/kg) ± 2x or 3x birinapant (10 mg/kg) (Ara-c + 2xCombo or Ara-c + 3xCombo respectively). (**A**) H&E staining of histology sections of the spleen, liver and sternum of mice at time point (23 - 25 days) after receiving 2 weeks of combination treatment and at death. (**B**) FACs analysis of bone marrow-GFP positive cells taken from mice at the time point (23 - 25 days) after receiving 2 weeks of combination treatment. (**C**) Controls for GFP analysis; KG1 AML cells (GFP negative) and MLL-AF9-GFP AML cells (GFP positive). (**D**) White blood cell (WBC) and platelet (PLT) cell count (n=6-10) analysed at the time point (23 – 25 days). (**E**) Liver and spleen weights as percentage of body weight taken at time of death (n=8-10). (**F**) WBC and PLT cell count at time of death (n=7-13). Data are presented as mean ± SEM throughout. Representative images.

3.8 Supplemental Information Outside the Scope of the Submitted Manuscript

3.8.1 MDR1i do not Potentiate *in vitro* Killing by the Chemotherapy Ara-c

To further test the specificity of the bir/MDR1i combination, we tested whether *in vitro* killing mediated by the chemotherapy Ara-c could be potentiated by the addition of MDR1 inhibitors reserpine, tariquidar or zosuquidar. Ara-c is not an MDR1 substrate (NØrgaard et al., 1998), therefore we hypothesised there would be no synergistic increase in cell death. Indeed, Ara-c was toxic as a single-agent in a dose dependent manner in MLL-AF9-Nras$_{G12D}$ and HoxA9/Meis1 AML cells and addition of an MDR1i was unable to enhance Ara-c mediated cell death (**Figure 3.1A-D**).

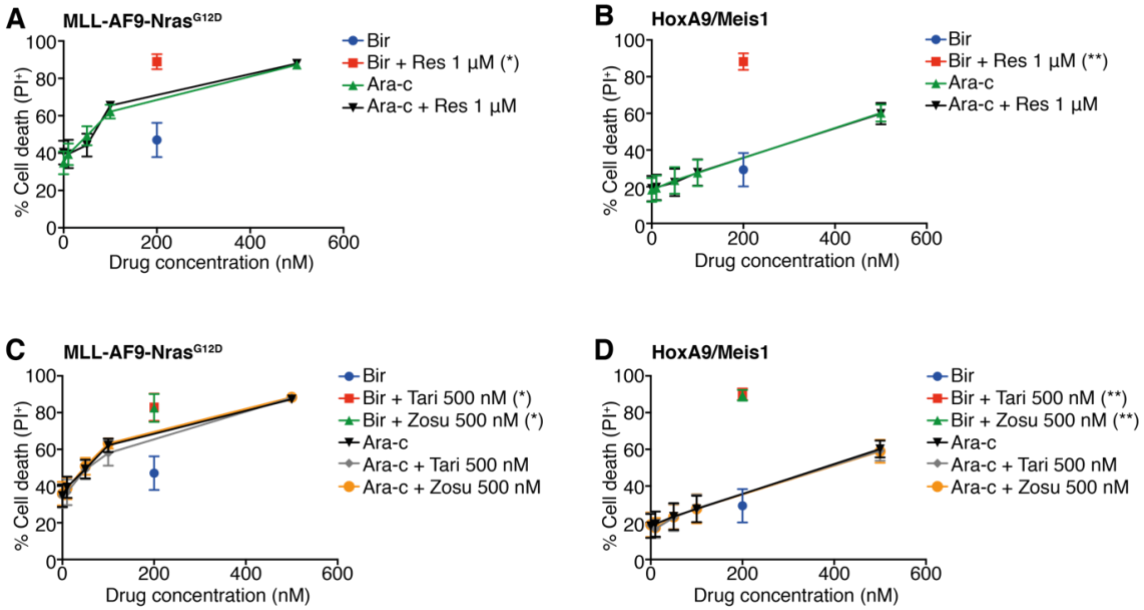

Figure 3.1 MDR1i do not sensitise AML cells to Ara-c killing *in vitro*

(**A**) MLL-AF9-Nras$_{G12D}$ and (**B**) HoxA9/Meis1 AML cells were treated with Ara-c (10, 50, 100 and 500 nM) ± reserpine (Res) (1 µM) for 24 h (n=4). (**C**) MLL-AF9-Nras$_{G12D}$ and (**D**) HoxA9/Meis1 AML cells were treated with the same concentrations of Ara-c as in (A, B) ± tariquidar or zosuquidar (500 nM) for 24 h (n=4). Birinapant (200 nM) plus MDR1 inhibitors was used as a control throughout (n=4). Data are presented as mean ± SEM throughout. Cell death was measured by propidium iodide (PI) uptake, decrease of cell volume (MLL-AF9-Nras$_{G12D}$) and flow cytometry from 3-4 independent tumours. P values were obtained by comparison of birinapant and birinapant plus MDR1 inhibitor.

3.8.2 The Bir/Tari Combination Treatment Extends Survival of Mice *in vivo*

Since the combination of tariquidar and birinapant appeared to be safe and tolerable in healthy mice *in vivo* (**Supplemental Figure 6**), we next investigated whether it was also effective at killing leukaemia *in vivo*. We transplanted MDR1$_H$ MLL-AF9-GFP leukaemias into healthy C57BL/6 mice, leading to a rapidly lethal disease (Brumatti et al., 2016; Lalaoui et al., 2016). Treatment of mice with two different doses of birinapant (5 or 10 mg/kg) in combination with tariquidar (10 mg/kg) led to a significant increase in median survival compared to vehicle treated mice (29 days vs 22 days respectively) (**Figure 3.2A**). Eventually, however, all mice succumbed to disease, exhibiting a leukaemic phenotype with hunched posture, enlarged spleen, liver infiltrated with blasts, decreased platelet and increased white blood cell count (**Figure 3.2A-E**).

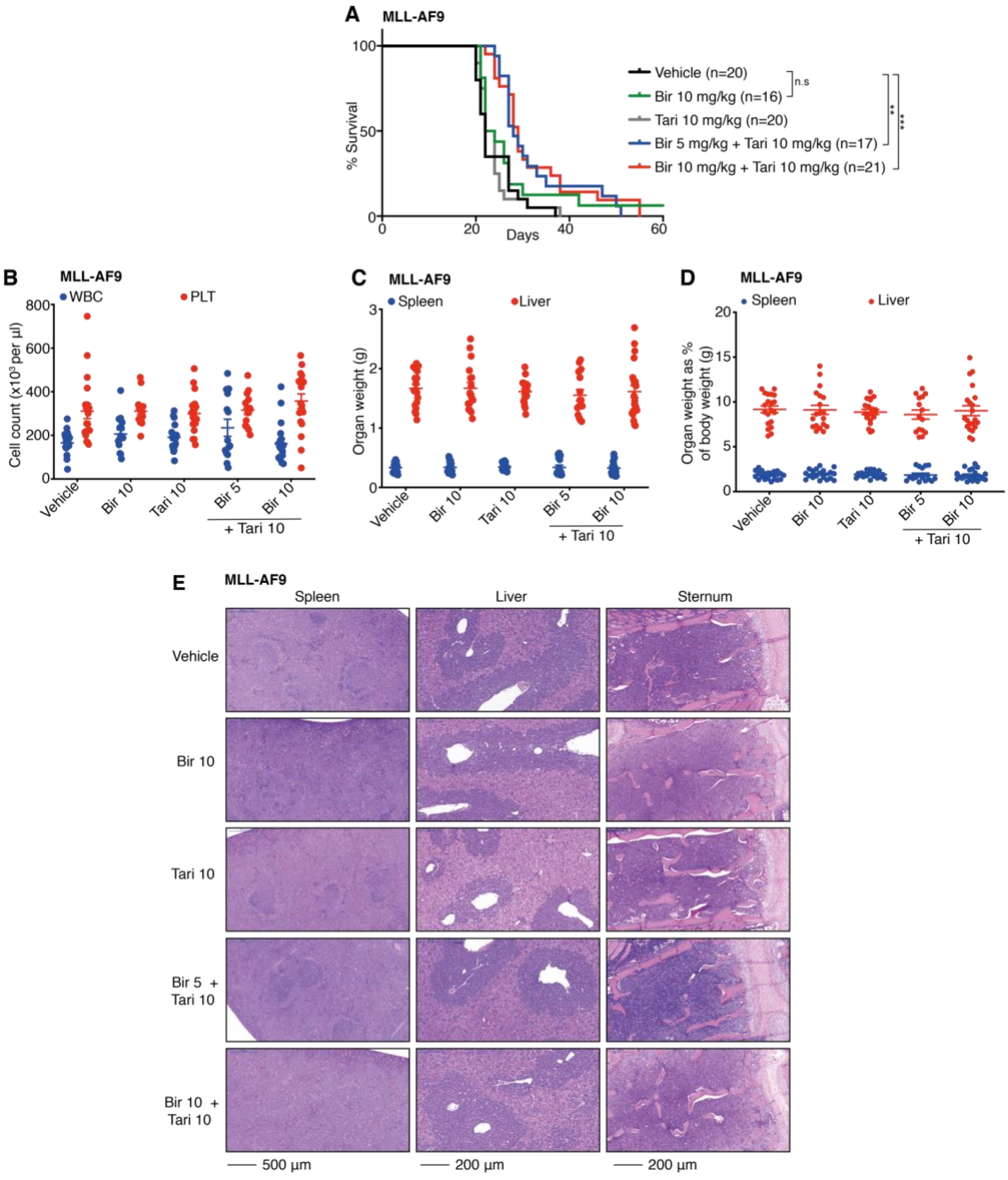
A
MLL-AF9
% Survival
Days
Vehicle (n=20)
Bir 10 mg/kg (n=16)
Tari 10 mg/kg (n=20)
Bir 5 mg/kg + Tari 10 mg/kg (n=17)
Bir 10 mg/kg + Tari 10 mg/kg (n=21)
n.s
**
***
B
MLL-AF9
WBC
PLT
Cell count (x10³ per µl)
Vehicle
Bir 10
Tari 10
Bir 5
Bir 10
+ Tari 10
C
MLL-AF9
Spleen
Liver
Organ weight (g)
D
MLL-AF9
Spleen
Liver
Organ weight as % of body weight (g)
E
MLL-AF9
Spleen
Liver
Sternum
Vehicle
Bir 10
Tari 10
Bir 5 + Tari 10
Bir 10 + Tari 10
500 µm
200 µm
200 µm

Figure 3.2 The bir/tari combination therapy extends survival of mice *in vivo*

(**A-E**) All experimental MLL-AF9 treated mice were taken at the ethical end point exhibiting a leukaemic phenotype. (**A**) Mice were treated with 5 or 10 mg/kg birinapant ± 10 mg/kg tariquidar and survival represented as a Kaplan-Meier curve (n=16-21). P values were obtained by comparison of vehicle and birinapant combination treated animals using a Log-rank (Mantel-Cox) test. Leukaemic burden was analysed by (**B**) white blood cell (WBC) and platelet (PLT) counts (n=14-19), (**C**) spleen and liver weights (n=15-21) and (**D**) spleen and liver weights as a percentage of body weight (n=15-21). (**E**) H&E histology staining of spleen, liver and sternum (scale bars 500 or 200 μm) (representative images).

3.8.3 Tariquidar Potentiates Birinapant-mediated Killing of Ovarian Cancer Cells

Similar to our findings in primary patient AML samples, MDR1 expression in ovarian cancer samples correlates with birinapant resistance. A recent Australian Ovarian Cancer Study (AOCS) of 92 ovarian cancer patients identified *ABCB1* fusions that led to increased MDR1 expression and chemotherapy resistance (Patch et al., 2015). In phase II clinical trials in patients with refractory ovarian cancer, birinapant did not show single-agent activity (Noonan et al., 2016). Based on the findings from our studies of mouse and human AML, we tested the birinapant plus MDR1 inhibitor combination treatment in patient-derived cell lines AOCS21.2 and AOCS18.5, established from AOCS patient ascites (Christie et al., 2019). AOCS21.2 (MDR1$_L$) and AOCS18.5 (MDR1$_H$-fusion) cells were treated with different concentrations of birinapant either on its own or together with tariquidar and/or TNF (**Figure 3.3A-D**). As expected, birinapant induced degradation of cIAP1 and cell death was not affected by the addition of tariquidar in AOCS21.2-MDR1$_L$ cells (**Figure 3.3A and B**), whereas loss of cIAP1 was accelerated in AOCS18.5-MDR1$_H$-fusion cells treated with the bir/tari combination (**Figure 3.3C**). Nevertheless, these MDR1$_H$-fusion cells were not killed by this drug combination (**Figure 3.3D**). As discussed previously, one likely explanation for the failure of this drug combination to kill these cells is the lack of TNF production and hence autocrine TNF/TNFR1 cell death signalling in response to birinapant. Consistent with this hypothesis, the addition of TNF sensitised these ovarian cancer cells to treatment with birinapant alone and their killing was significantly enhanced in the presence of tariquidar (**Figure 3.3D**).

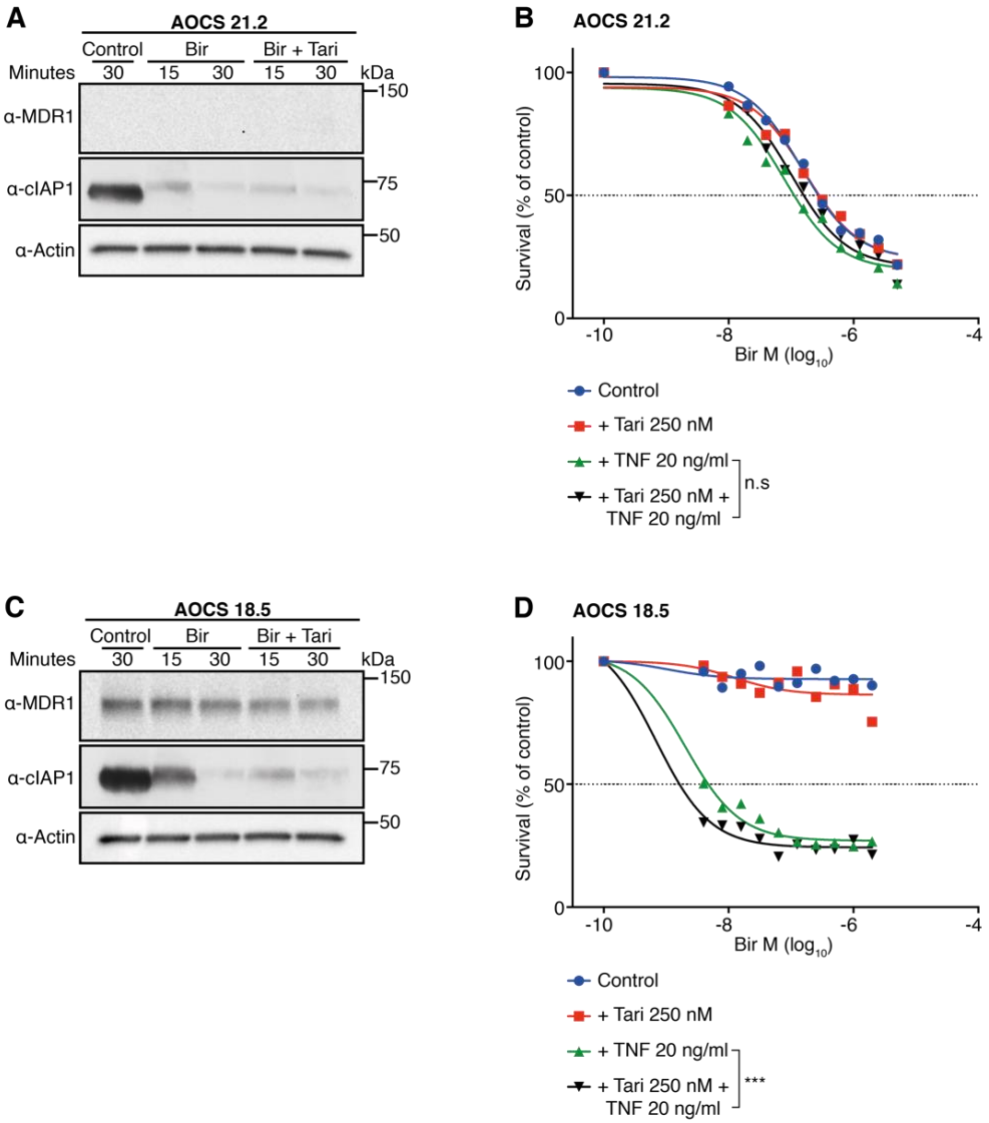

Figure 3.3 The bir/tari combination is effective in human ovarian cancer patient cells

(**A**) AOCS21.2 ovarian cancer cells were treated with birinapant (500 nM) ± tariquidar (1 μM) for 15 or 30 min. Samples were analysed by Western blotting and probed as indicated. (**B**) AOCS21.2 ovarian cancer cells were treated with tariquidar (250 nM) ± TNF (20 ng/ml) ± a titration of birinapant for 72 h. (**C, D**) AOCS18.5 ovarian cancer cells were treated as described in (A, B), respectively. Cell survival was determined via DAPI staining and high content imaging on the Cellomics ArrayScan Vti platform. IC_{50} doses of birinapant were approximated by fitting a 4-parameter dose-response curve (Hill equation) (n=3-4 independent experiments). Probing for actin was used as a loading control. P values were obtained by comparison of SM + TNF and SM + TNF + tariquidar.

4 Investigating the Efficacy of MDR1 Inhibitors to Potentiate Smac-mimetic Treatment in Chronic Hepatitis B Virus (HBV) disease

4.1 Introduction

Viral pathogens frequently use TNF receptor pathways to manipulate molecular processes within host cells to evade control and promote their propagation (Herbein and O'brien, 2000). Chronic infection of Hepatitis B virus (HBV) has been shown to promote high levels of both TNF and TNFR1 in hepatocytes. This has been partly explained by the HBV viral protein HBx, and its ability to transcriptionally upregulate the production of TNF in HBV infected hepatocytes (Herbein and O'brien, 2000). Intriguingly, HBx has also been shown to sensitise cells to TNF mediated apoptotic killing (Herbein and O'brien, 2000). Following these findings, investigations into how the TNFR1 pathway could be harnessed to develop new clinically relevant therapies to target HBV were undertaken.

The observation that IAPs limit TNF mediated apoptosis in HBV infected hepatocytes, promoting disease progression, led to the study of Smac-mimetics as a treatment strategy for HBV (Ebert et al., 2015a; Ebert et al., 2015b). Genetic loss of cIAPs or their degradation through birinapant treatment, promoted death of HBV infected hepatocytes. Furthermore, birinapant therapy enhanced HBV-DNA serum clearance in an *in vivo* murine model of chronic HBV infection (Ebert et al., 2015a; Ebert et al., 2015b). These results were not limited to birianapant, as another Smac-mimetic APG-1387 has also shown efficacy in killing HBV

infected cancer cells (Liu et al., 2018; Pan et al., 2018). These results promted initiation of in-human clinical trials of the Smac-mimetics, birinapant (NCT02288208) and APG-1387 (NCT03585322), for the treatment of chronic HBV (Rasco et al., 2019; Xu et al., 2018). Although the studies with APG-1387 are still underway, unfortunately the trials conducted with birinapant have not been successful due to cranial nerve palsies, such as Bell's palsy, being observed in patients and trials being subsequently ceased. A possible strategy to overcome dose related birinapant side effects could be to potentiate the efficacy of birinapant treatment, resulting in a reduction of Smac-mimetic dose.

Following the results detailed in Chapter 3 of this thesis, describing that birinapant is a substrate of MDR1 and addition of a MDR1 inhibitor can potentiate Smac-mimetic therapy in cancer, I sought to understand whether these findings could be transposed to a viral HBV disease model. Therefore, this Chapter describes my investigation into the safety and efficacy of combining a MDR1 inhibitor with a reduced dose of birinapant to treat murine models of chronic HBV.

4.2 Expression Levels of cIAP1 and MDR1 in Mouse Livers Following Birinapant plus MDR1 Inhibitor Treatment

Prior studies indicated Smac-mimetics are effective towards killing HBV infected liver cells (Ebert et al., 2015a; Ebert et al., 2015b). Therefore, we hypothesised that addition of the 3rd generation specific MDR1 inhibitor zosuquidar to birinapant could enhance treatment in HBV disease. Ebert and colleagues have previously shown that a 30 mg/kg dose of birinapant induces degradation of cIAP1 in HBV infected and uninfected hepatocytes (Ebert et al., 2015a). We therefore chose a

10-fold lower dose to test whether zosuquidar could enhance birinapant-mediated cIAP degradation. C57BL/6 mice were hydrodynamic injected (HDI) with a plasmid containing the HBV genome to establish chronic HBV infection (day 0) (Ebert et al., 2015a). Mice were then preloaded with zosuquidar 5 or 25 mg/kg for three days (day 5, 6 and 7) prior to birinapant 3 mg/kg treatment (day 7). Mice were culled 16 hours following birinapant treatment (day 8) and livers were collected for analysis of cIAP1 and MDR1 expression (**Figure 4.1A)**. As previously reported, liver cIAP1 expression was significantly reduced in birinapant treated HBV infected and uninfected mice (**Figure 4.1B and C**) (Ebert et al., 2015a; Ebert et al., 2015b). However, in both HBV infected and uninfected animals, there was no further increase in cIAP1 degradation in mice treated with birinapant plus zosuquidar combination, compared to birinapant single-agent treatment (**Figure 4.1B and C**). MDR1 expression appeared consistent between HBV infected and uninfected animals and between treatment groups. However, due to the complexity of the hepatocyte samples, and the natural smear pattern of MDR1, we couldn't obtain a clear detection of MDR1 protein.

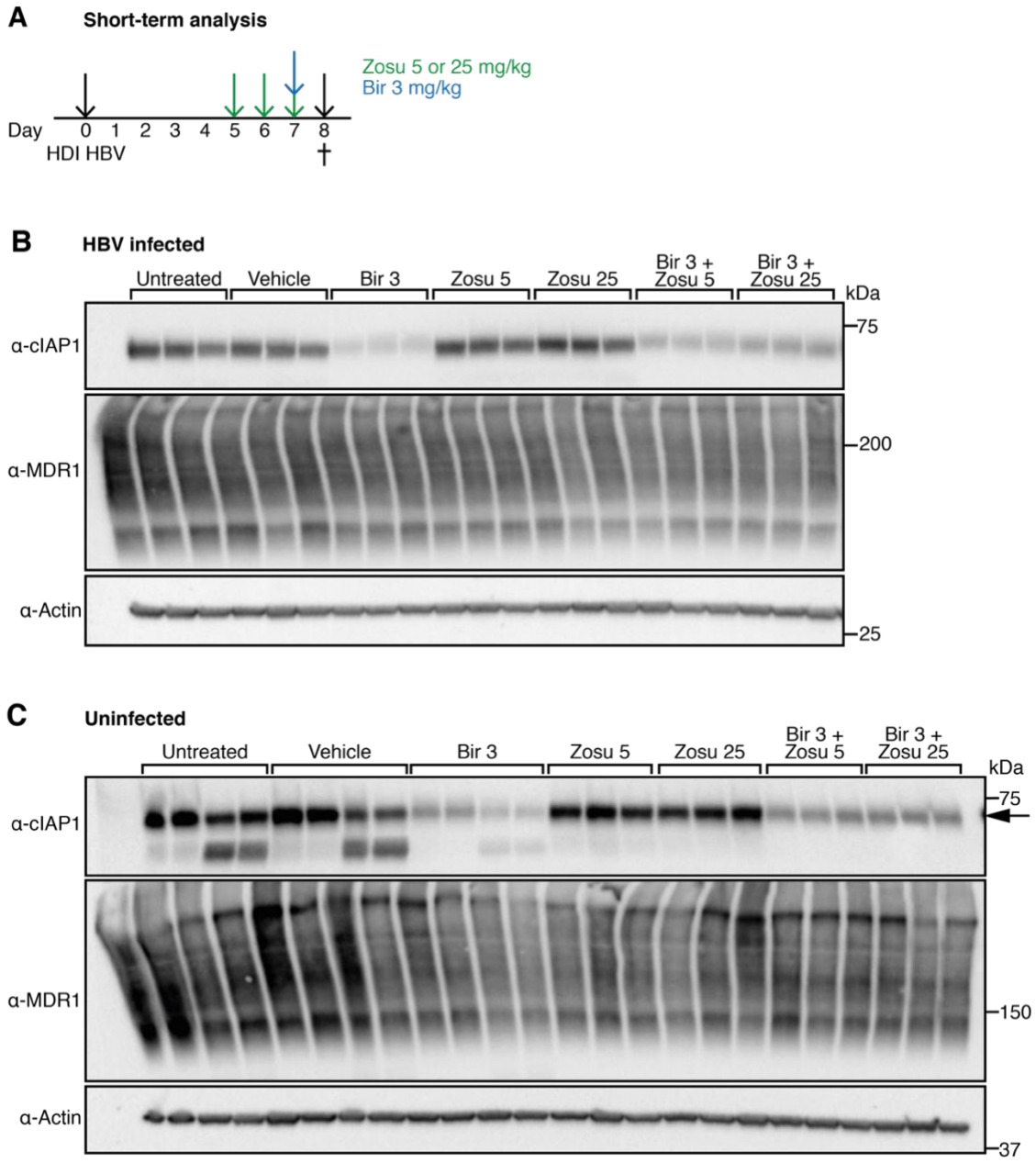

Figure 4.1 HBV infected and uninfected hepatocytes express cIAP1 and MDR1

(**A**) Short-term analysis treatment scheme. C57BL/6 mice were hydrodynamic injected (HDI) with HBV virus (day 0) and preloaded with zosuquidar (Zosu) 5 or 25 mg/kg for three days (day 5, 6 and 7) prior to ± birinapant (Bir) 3 mg/kg treatment (day 7). Mice were culled 16 hours following birinapant treatment (day 8). (**B**) Livers were taken from mice, lysed and analysed by Western blotting. Samples were probed for cIAP1 and MDR1 and actin was used as a loading control (3 independent experiments). (**C**) C57BL/6 mice uninfected with HBV were treated as described in (A) and livers analysed as described in (B) (2 independent experiments).

4.3 Birinapant and MDR1 Inhibitor Combination Treatment Increases ALT Levels in HBV Infected but not Uninfected Mice

A sensitive measurement of liver-cell damage is alanine aminotransferase (ALT) levels, where an increased level indicates elevated liver-cell death. ALT analysis is used routinely in the clinic to monitor liver damage due to alcohol, medication, haemochromatosis and chronic hepatitis B and C infection (Pratt and Kaplan, 2000). We therefore analysed ALT levels to determine the efficacy of our combination treatment to kill HBV infected liver cells, reducing HBV disease burden. Furthermore, we also analysed the specificity and safety of the combination treatment by treating HBV infected and uninfected mice in parallel. Using the treatment scheme previously described (**Figure 4.1**), co-treatment with an MDR1 inhibitor and birinapant was well tolerated in uninfected and infected animals. Similar to our leukemia models, both HBV infected and uninfected groups showed no signs of distress or discomfort following injections. In infected HBV animals, ALT levels were not changed with birinapant single-agent treatment but were significantly increased with birinapant and zosuquidar combination treatment (**Figure 4.2A**). Although there was a reduction in ALT levels in uninfected mice treated with birinapant and the lower dose of zosuquidar (5 mg/kg), there was no change in ALT levels observed in the birinapant plus the higher dose of zosuquidar (25 mg/kg) group (**Figure 4.2B**). Together these data indicate birinapant and MDR1 inhibitor treatment is able to potentiate liver-cell death in HBV infected cells, with less toxicity to uninfected healthy cells.

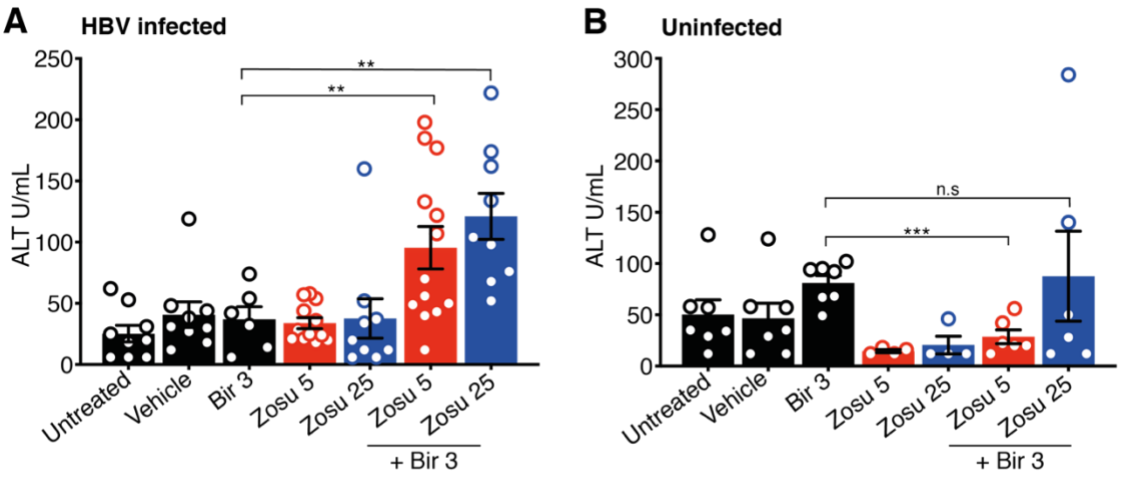

Figure 4.2 MDR1 inhibitor plus birinapant combination treatment increases ALT levels in HBV infected but not uninfected mice

(**A**) C57BL/6 mice were hydrodynamic injected (HDI) with HBV virus (day 0) and preloaded with zosuquidar (Zosu) 5 or 25 mg/kg for three days (day 5, 6 and 7) prior to ± birinapant (Bir) 3 mg/kg treatment (day 7). Mice were culled 16 hours following birinapant treatment (day 8) and cardiac blood was analysed for ALT levels (n=6-13, 3 independent experiments). (**B**) Uninfected C57BL/6 mice were treated as described in (A) and cardiac blood was analysed for ALT levels (n=4-7, 2 independent experiment). Data presented as mean ± SEM throughout. P values were obtained by comparison of birinapant alone and in combination with zosuquidar.

4.4 Zosuquidar Enhances the Efficacy of Birinapant to Reduce HBV-DNA Serum Levels

Monitoring the level of HBV disease burden is an important method to track disease progression or treatment-induced disease reduction. Traditional methods of analysis favoured hepatic histology to assess the stage of liver disease and etiology. However, as this assessment requires serial liver biopsies, alternative methods to monitor HBV disease burden were developed. Similar to human immunodeficiency virus (HIV), there is a correlation between HBV viral replication and HBV disease burden. This led to the practice of measuring HBV-DNA levels to track disease progression in the clinic and in animal models of chronic HBV infection (Mommeja-Marin et al., 2003).

Having established the tolerance of the birinapant and MDR1 inhibitor combination, and its ability to enhance Smac-mimetic mediated liver-cell death, we investigated whether this therapeutic approach could increase the clearance of HBV-DNA in a chronic HBV infection model. Ebert and colleagues have previously shown that treatment of HBV infected mice with birinapant (injections once a week of 30 mg/kg for 3 weeks) rapidly induces clearance of HBV-DNA in the serum (Ebert et al., 2015a). Therefore, we chose to compare this previously described dose with a 3-fold lower dose of birinapant of 10 mg/kg to investigate the potential of MDR1 inhibitors to enhance Smac-mimetic treatment (**Figure 4.4A**). C57BL/6 mice infected with HBV were preloaded with zosuquidar (25 mg/kg) for three days prior to receiving birinapant (10 mg/kg) treatment. This was repeated for 3 weeks and HBV-DNA serum levels determined each week (**Figure 4.4A**). Analysis of HBV-DNA levels revealed no difference in clearance rates

between untreated, vehicle and zosuquidar single-agent treated animals (Median clearance = 5 weeks). Addition of zosuquidar to 10 mg/kg birinapant treatment significantly reduced the time taken for animals to clear HBV virus compared to 10 mg/kg birinapant alone treatment (Median clearance 3.5 weeks vs 4 weeks respectively) (**Figure 4.4B**). Interestingly, the median clearance rate of 10 mg/kg birinapant plus MDR1 inhibitor combination therapy was the same as 30 mg/kg birinapant single-agent treatment (3.5 weeks). These data suggest addition of a MDR1 inhibitor increases the efficacy of birinapant to mediate clearance of HBV-DNA in a chronic HBV model.

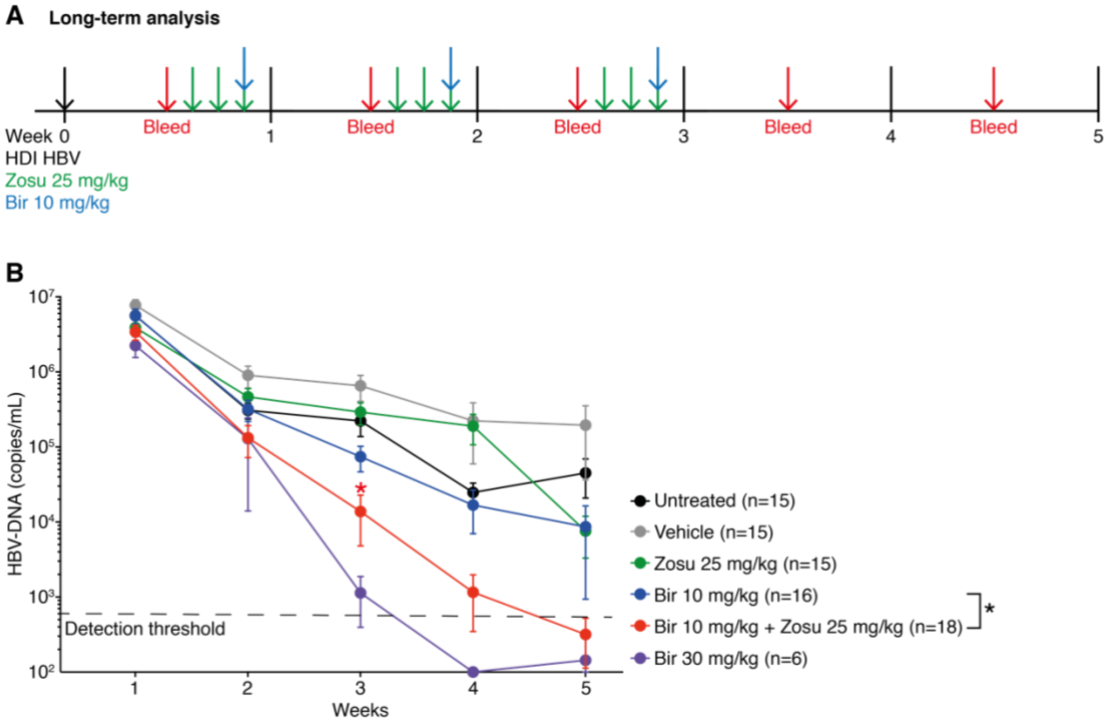

Figure 4.3 Zosuquidar enhances the efficacy of birinapant to control serum HBV DNA levels

(**A**) Long-term analysis treatment scheme. C57BL/6 mice were hydro dynamic injected (HDI) with HBV virus and preloaded with zosuquidar (Zosu) 25 mg/kg for three days prior to ± birinapant (Bir) 10 mg/kg, treatment was repeated for 3 weeks. Birinapant 30 mg/kg was used as a positive control. Animals were mandible bled each week prior to treatment and serum HBV DNA levels analysed. (**B**) Animals were treated as described in (A) and serum HBV DNA levels analysed (n=15-19, 2 independent experiments). Data presented as mean ± SEM throughout. P values were calculated using an unpaired t test, two-tailed comparing birinapant alone and in combination with zosuquidar.

4.5 Conclusions

HBV remains an endemic disease, with 3.5% of the world population having been exposed to HBV and an estimated 257 million people suffering from chronic HBV infection (WHO, 2017). Unlike in primary self-limiting HBV infections, where there is complete clearance of virus from the body, in persistent chronic HBV infection virus production continues indefinitely (Ganem and Prince, 2004). Furthermore, HBV is an oncovirus that is responsible for the development of HBV-related liver cancer (McGlynn et al., 2015). Therefore, investigation into novel strategies to overcome chronic HBV infection are required.

Prior work by Ebert and colleagues demonstrating Smac-mimetics have efficacy in HBV (Ebert et al., 2015a; Ebert et al., 2015b), propelled us to determine whether the 3rd generation specific MDR1 inhibitor zosuquidar, could be used to increase the efficacy of birinapant treatment in a chronic HBV model. Initially, I investigated the levels of MDR1 expression in murine infected and uninfected liver samples treated with the combination and did not observe any differences. Although degradation of cIAP1 was present in all birinapant treatment groups, this was not enhanced with the addition of zosuquidar.

To investigate the ability of zosuquidar to potentiate the liver-cell killing potential of birinapant, we utilised a short-term analysis of HBV liver-cell death. We observed an increase in ALT levels in animals treated with a low dose of birinapant in combination with the MDR1 inhibitor zosuquidar, compared to birinapant single-agent treatment. An increase in ALT indicates an increase in

HBV positive liver cell death and therefore, a reduction in HBV disease burden. Furthermore, this result was only present in the HBV infected animals, with the uninfected healthy animals having no increase in ALT levels with combination treatment compared to birinapant alone. This indicates specificity of the combination treatment to HBV infected liver cells and not uninfected liver cells. These data are important as it indicates the safety and tolerability of the treatment and therefore the applicability of the translation of this combination therapy in to the clinic.

Lastly, we investigated the clinical potential of the combination to clear HBV-DNA from serum. Importantly, our results show a significant improvement in the clearance of HBV-DNA in mice treated with birinapant plus zosuquidar, compared to birinapant single-agent treatment. Impressively, the median clearance rate of low dose 10 mg/kg birinapant combination treatment was the same as the previously published high dose concentration of birinapant 30 mg/kg. These data suggests MDR1 inhibitors potentiate the effect mediated by Smac-mimetics in a chronic HBV model and these findings could offer an alternative to high-dose Smac-mimetic treatment. Moreover, these findings highlight MDR1 inhibition to enhance Smac-mimetic efficacy, is transferable across oncogenic and viral diseases.

5 Understanding the Molecular Mechanisms by which Psychoactive Drugs Potentiate Smac-mimetic Mediated Killing in Acute Myeloid Leukaemia

5.1 Introduction

To date, I have introduced and discussed my finding that birinapant is a substrate of MDR1 and that inhibition of MDR1 can potentiate birinapant-mediated killing in cancer and HBV disease models (Chapters 3 and 4). Despite the success of this combination, we observed some primary human AML samples had resistance to birinapant plus MDR1 inhibitor combination treatment, even in the presence of exogenous TNF (Chapter 3 **Figure 7**). Therefore, to identify other possible mechanisms of resistance that AML cells use to evade Smac-mimetic therapy, and new molecular strategies to overcome resistance, we investigated the remaining hit compounds identified by the high throughput screen. As discussed in Chapter 3, the clinical antipsychotic and antihypertensive drug reserpine was the first compound we investigated and it is a known MDR1 inhibitor. Intriguingly, from the 12 top compounds identified, we observed half of them (including reserpine) are psychoactive. That is, they are capable of altering central nervous system functions resulting in changes to mood, anxiety, consciousness and behaviour. These compounds include the clinical drug fluphenazine dihydrochloride (Prolixin) and the preclinical compounds LP-44, SDZ 21009 (Carpindolol), GR-127935 and CGP-71683. Some psychoactive compounds, in particular antidepressant and antipsychotic drugs, have been

shown to have anti-proliferative and pro-apoptotic effects (Nordenberg et al., 1999). Therefore, we were intrigued to further investigate the molecular mechanisms behind the synergy observed between these psychoactive drugs in combination with birinapant.

5.2 Anti-cancer Effects of Psychotropic Compounds

Psychoactive compounds are used to modify the brains functions to temporarily influence behaviour, mood, consciousness and perception (Gelenberg et al., 2013). Psychotropic compounds for the treatment of clinical neurological disorders, including depression, anxiety, schizophrenia and bipolar disorder, act principally on the dopamine and serotonin (5-hydroxytryptamine; 5-HT) pathways (Miyamoto et al., 2004). Large scale epidemiology studies have described schizophrenic patients that are prescribed antidepressants and/or antipsychotics have lower incidences of developing cancer, compared to age- and gender-matched individuals without schizophrenia or the general population (Chou et al., 2011; Mortensen, 1989, 1994). Numerous papers and patents echo these findings, describing the anti-neoplastic properties of psychotropic compounds (Nordenberg et al., 1999).

The phenothiazine antipsychotics work by antagonising dopamine receptors (Seeman and Lee, 1975). In mammals, five subtypes of dopamine receptors, D1 to D5, have been identified (Sibley and Monsma Jr, 1992). Several of these phenothiazine antipsychotics have been observed to have potent pro-apoptotic and anti-proliferative effects in different cancer models, including AML, with little toxicity towards healthy tissue (Burgess, 2012; Cheng et al., 2015; Sachlos et al.,

2012; Schleuning et al., 1993; Zhelev et al., 2004) (patent US-20130065887A1). The majority of these findings have been observed using the drug thioridazine, however the clinical drug fluphenazine dihydrochloride identified in our screen, is also a member of the phenothiazines and has shown anti-proliferative effects (Sachlos et al., 2012; Schleuning et al., 1993). The molecular mechanisms driving these phenothiazine-mediated anti-cancer effects remains unclear. In one study, these effects were attributed to thioridazine's ability to induce differentiation to overcome neoplastic self-renewal in AML cancer stem cells (CSCs). It was proposed that this effect was due to antagonism of the dopamine receptor, suggesting development of some cancers may be dopamine receptor dependent (Sachlos et al., 2012). Cheng and colleagues also observed that thioridazine had anti-stem cell properties in glioblastoma, however their data indicated that its cytocidal effects were independent of dopamine receptor antagonism and were rather due to induction of autophagy and upregulation of AMP-activated protein kinase activity (Cheng et al., 2015). Interestingly, data from these and other studies, indicates the anti-cancer effects observed with thioridazine are specific to cancer cells with no influence on healthy cells (Sachlos et al., 2012; Zhelev et al., 2004).

The other major pathway principally acted on by antidepressant and/or antipsychotic drugs is the serotonin signalling pathway. Similarly to dopamine, in mammals there are several serotonin receptors. Perhaps unsurprisingly therefore, it has been observed that serotonin can have opposing effects on cancer cells, being either pro-cancer or anti-cancer (Vicaut et al., 2000). The

tricyclic antidepressants (TCAs), which act primarily through blocking the serotonin and norepinephrine transporters, have been shown to have pro-apoptotic actions in human lymphocytes (Xia et al., 1996, 1998). Combination of TCA drugs with the chemotherapy actinomycin D potentiated apoptosis in human lymphocytes. Similarly, serotonin re-uptake inhibitors have been shown to have potent anti-cancer potential *in vitro*, however the effective concentration required is seldom reached within patients at clinically therapeutic doses (Rosetti et al., 2006). Mice bearing large methylcholanthrene-induced fibrosarcomas responded favourably with serotonin treatment, having strong inhibition of tumour growth and increased overall survival (Burtin et al., 1982). In contrast, Cattaneo and colleagues observed an increase in cancer cell growth in small lung carcinoma due to serotonin's suggested stimulation of DNA synthesis and mitogenesis (Cattaneo et al., 1993; Cattaneo et al., 1994; Vicaut et al., 2000). These disparities highlight the complexity of serotonin signalling and likely reflect the fact that there are multiple receptors that can be targeted by these drugs, which will therefore, affect which cancers respond (Vicaut et al., 2000).

Our screen identified three different compounds that act on the serotonin pathway; the agonist LP-44 and antagonists SDZ 21009 and GR-127935. Therefore, my initial attention and curiosity was focused on investigating the molecular mechanisms by which these compounds synergise with birinapant. The strongest synergy observed in combination with birinapant was with the agonist LP-44 and therefore, my initial focus was to investigate how this compound synergised with birinapant.

5.3 Serotonin

Serotonin (5-HT) is an important neurotransmitter implicated in a large variety of central and peripheral physiological and pathological processes, including regulation of perception, pain, mood, anxiety, gastrointestinal regulation (GI) and inflammation. Surprisingly, the vast majority of 5-HT (~95%) is found outside of the central nervous system and is predominantly produced by enterochromaffin cells in the intestinal tract where it regulates many aspects of digestion (Gershon and Tack, 2007). Serotonin also plays a role in vasculature, haemostasis, cardiac function and reproductive biology among other activities (Berger et al., 2009; Dray, 1995; Gershon and Tack, 2007; Spiller, 2007). The mammalian 5-HT receptor family consists of 14 structurally and pharmacologically distinct members designated by a number and letter (e.g. 5-HT_{1A} receptor). The family is divided into 7 groups ranging from 5-HT_1 to 5-HT_7 and further receptor heterogeneity is achieved through RNA editing, alternative splicing and the formation of hetero- and homo- dimers (Barnes and Neumaier, 2011). With the exception of 5-HT_3, which is a ligand-gated ion channel, all family members are G-protein coupled receptors (GPCR) (Boess et al., 1995; Hoyer et al., 2002). As their name suggests, GPCRs couple to a G-protein to modulate intracellular signalling. The seven 5-HT receptor families have diverse and specific signalling pathways that utilise different families of G-proteins; 5-HT_1 and 5-HT_5 receptors couple to $G_{i/o}$-type proteins, inhibiting adenylyl cyclase (AC); 5-HT_2 receptors couple to G_q-type G proteins, activating phosphoinositide hydrolysis; and 5-HT_4, 5-HT_6 and 5-HT_7 receptors couple to G_s, stimulating AC (**Table 4**) (Johnson-Farley et al., 2005; Leon-Ponte et al., 2007).

Table 4 5-HT receptor subtypes and associated signals

* Not present in humans. Excerpt from (Leon-Ponte et al., 2007).

Receptor Subtype	Signal
5-HT_{1A}	$G_{i/o}$
5-HT_{1B}	$G_{i/o}$
5-HT_{1D}	$G_{i/o}$
5-HT_{1E}	$G_{i/o}$
5-HT_{1F}	$G_{i/o}$
5-HT_{2A}	$G_{q/11}$
5-HT_{2B}	$G_{q/11}$
5-HT_{2C}	$G_{q/11}$
5-HT_{3}	Ion channel
5-HT_{4}	G_{s}
5-HT_{5A}	$G_{i/o}$
5-HT_{5B}*	Unknown
5-HT_{6}	G_{s}
5-HT_{7}	G_{s}

5.4 5-HT$_7$ Receptor

The 5-HT$_7$ receptor gene is located on human chromosome 10q23.3-q24.3 and is 445 amino acids in length (Bard et al., 1993; Lovenberg et al., 1993; Ruat et al., 1993). As previously described, the 5-HT$_7$ GPCR is coupled to the stimulatory G$_s$ protein. Upon receptor stimulation, AC is activated leading to a rise in cyclic adenosine monophosphate (cAMP) and Ca^{2+} dependent activation of both protein kinase B (Akt) and extracellular signal-regulated kinase (ERK)/MAPK signalling pathways. Agonist activation of the 5-HT$_7$ receptor, leading to an increase in cAMP, has been shown to activate both ERK and Akt independent of protein kinase A (PKA) (Errico et al., 2001; Guseva et al., 2014b; Lin et al., 2003; Shen et al., 1993). The 5-HT$_7$ receptor has also been described to couple to the heterotrimeric G$_{12}$-protein, resulting in the selective activation of the small GTPases, RhoA and Cdc42 (**Figure 5.1**) (Kobe et al., 2012; Kvachnina et al., 2005).

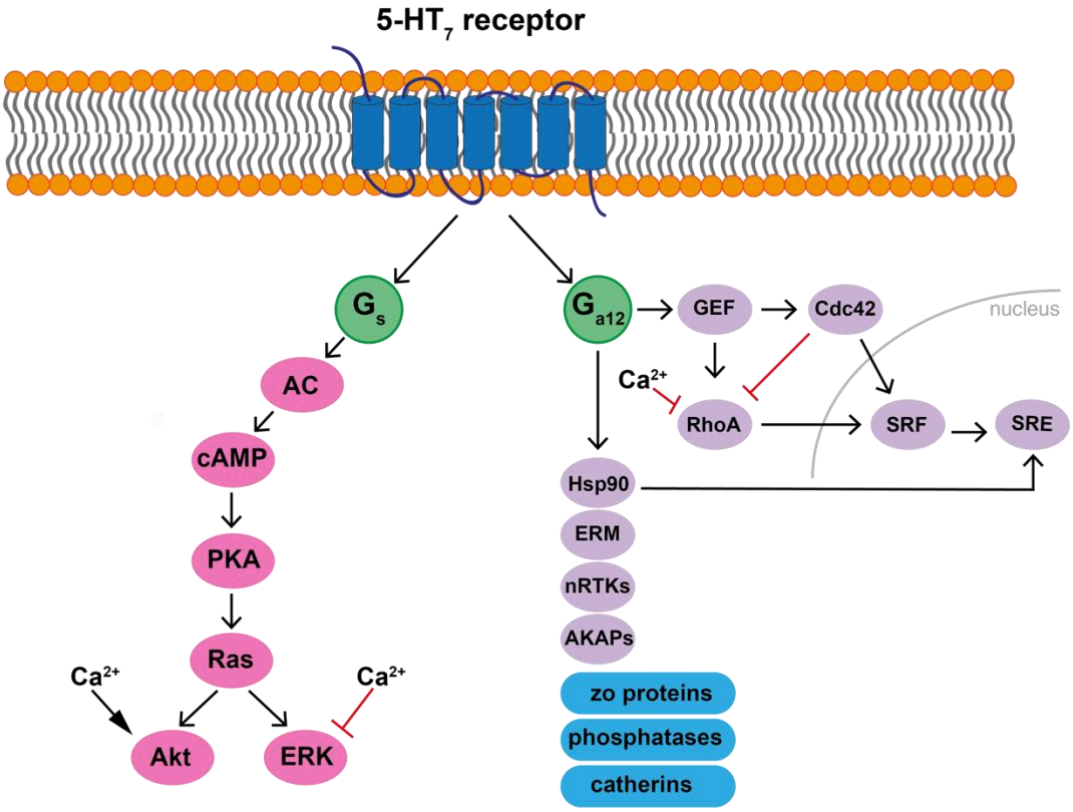

Figure 5.1 Schematic of 5-HT$_7$ receptor signalling pathway

The 5-HT$_7$ G-protein coupled receptor (GPCR) can be coupled to G$_s$ or Gα_{12} proteins. AC; adenylyl cyclase, cAMP; cycli adenosine monophosphate, PKA; protein kinase A, ERK; extracellular signal-regulated kinases, Akt; protein kinase B, Hsp; heat shot shock protein 90, ERM; proteins of the ezrin-radixin-moesin family, GEF; guanine-nucleotide exchange factor, nRTKs; non-receptor tyrosine kinases, AKAPs; a kinase anchoring proteins, ZO; zona occludens proteins, SRF; serum response factor, SRE; serum response element. Adapted from (Guseva et al., 2014b).

5-HT$_7$ receptors were identified in the central nervous system, and are mainly expressed in discrete areas of the brain including the hypothalamus, thalamus, hippocampus and specific areas related to pathological psychiatric disorders (Mullins et al., 1999). Furthermore, it was observed that some antipsychotic and antidepressant drugs had a high affinity towards the 5-HT$_7$ receptor and chronic administration of these drugs down regulated the expression of 5-HT$_7$ receptors in rat hypothalamus (Mullins et al., 1999; Sleight et al., 1995). Following these findings, the 5-HT$_7$ receptor has been investigated as a potential target for the clinical conditions of depression, schizophrenia, sleep disorders, migraines and neuropathic pain (Atanes et al., 2013; Di Pilato et al., 2014; Guscott et al., 2005; Hedlund, 2009; Hedlund et al., 2005; Mullins et al., 1999).

The role of 5-HT$_7$ receptors is not limited to psychotropic alterations as they are located in a diverse range of tissues and have been attributed to the regulation of many complex processes. 5-HT$_7$ receptors are expressed in peripheral tissues of the ileum, spleen, endocrine glands and the smooth muscle cells of blood vessels and the GI tract (Guseva et al., 2014a; Leopoldo et al., 2011). It is believed that 5-HT$_7$ receptor signalling plays an important role in the regulation of circadian rhythm, rapid eye movement, mood, thermoregulation, nociception, contextual learning and memory processing (Di Pilato et al., 2014; Eriksson et al., 2008; Hedlund et al., 2003; Hedlund, 2009; Hedlund et al., 2005; Lovenberg et al., 1993; Mullins et al., 1999). Furthermore, 5-HT$_7$ receptors are also expressed on immune cells (Dürk et al., 2005; Leon-Ponte et al., 2007). Agonist activation of 5-HT$_7$ receptors has been shown to dose dependently reduce the

secretion of TNF in resting monocytes and increase the release of inflammatory cytokines IL-6, IL-8 and IL-1β in lipopolysaccharide stimulated monocytes (Dürk et al., 2005). Naïve T-cells have been shown to predominantly express 5-HT_7 receptors and activation leads to increased expression, as well as the initiation of 5-HT_{1B} and 5-HT_{2A} receptor expression (Gordon and Barnes, 2007; Leon-Ponte et al., 2007). The specific activation of 5-HT_7 receptors on naïve T-cells has been shown to contribute to T-cell activation, specifically through phosphorylation of ERK1/2, leading to canonical NF-κB signalling (Leon-Ponte et al., 2007). Using the database portal http://servers.binf.ku.dk/bloodspot/, I found that 5-HT_7 receptors are present on haematopoietic progenitor/stem cells (HSPCs) and AML cancer cells (**Figure 5.2**) (Bagger et al., 2019). However, there is very little known about their function in blood cancers, although there has been some research into their role in other cancers. For example, 5-HT mediated activation of 5-HT_7 receptors on the triple negative breast cancer cell line MDA-MB-231 promoted invasion and proliferation of cancer cells, and knock down of the 5-HT_7 receptor suppressed this phenotype (Gautam et al., 2017; Gautam et al., 2016).

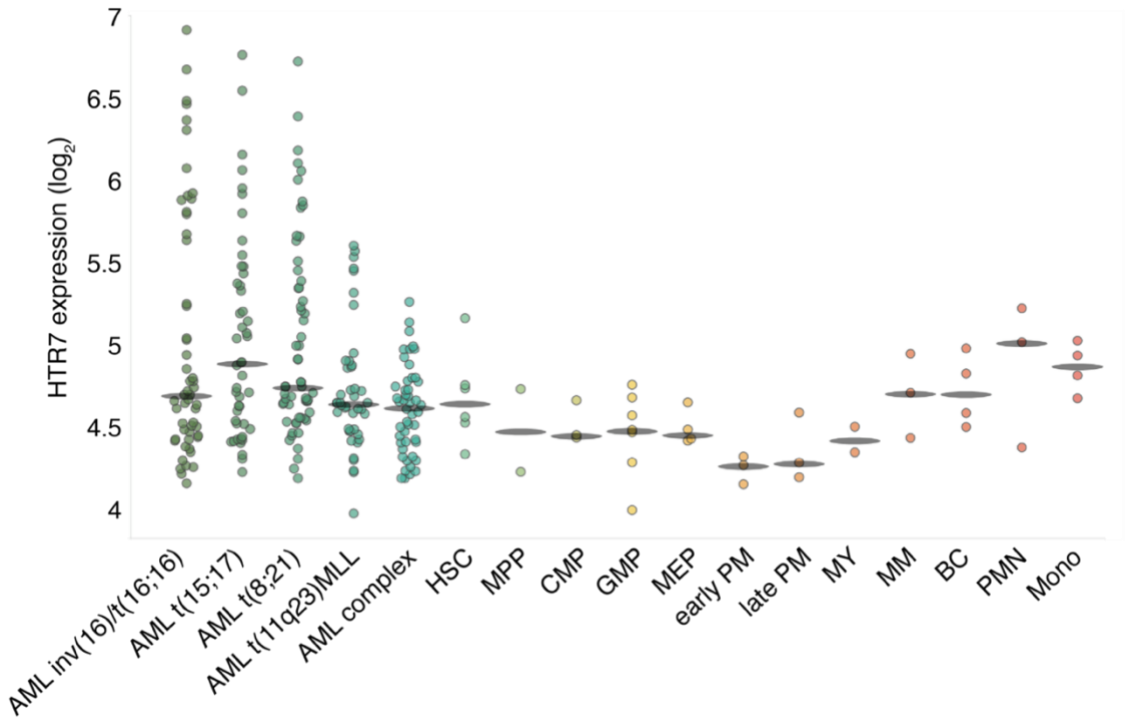

Figure 5.2 Expression levels of the 5-HT$_7$ receptor in AML and haematopoietic cells

Expression levels of the human 5-HT$_7$ receptor (gene name HTR7) in different types of AML (first 5 data sets) and healthy haematopoietic cells (remaining data sets). HSC; haematopoietic stem cell, MPP; multipotential progenitors, CMP; common myeloid progenitor cell, GMP; granulocyte monocyte progenitors, MEP; megakaryocyte-erythroid progenitor cell, early_PM; early promyelocyte, late_PM; late promyelocyte, MY; myelocyte, MM; metamyelocytes, BC; band cell, PMN; polymorphonuclear cells, Mono; monocytes. Output from (Bagger et al., 2019).

5.5 LP-44

Potent and highly specific agonists and antagonists towards the 5-HT_7 receptor have been developed as tools to investigate its role in physiological regulation. Agonists include LP-44, LP-12, LP-211 and AS-19, whilst commonly used antagonists include SB-269970, SB-258719 and SB-656104 (Di Pilato et al., 2014; Hagan et al., 2000; Monti and Jantos, 2014). LP-44 was reported in 2004 as a high-affinity ligand for the rat 5-HT_7 receptor (K_i = 0.22 nM) (Leopoldo et al., 2004). It has a 200-fold selectivity over the 5-HT_{1A} receptor and >1000-fold selectivity over the 5-HT_{2A} receptor (Gang et al., 2014; Leopoldo et al., 2008). Three years following the report of LP-44, another high-affinity agonist towards the 5-HT_7 receptor was reported called LP-12. The K_i of LP-12 is comparable to LP-44 (K_i = 0.13 nM) however, it has a higher selectively over the 5-HT_{1A} receptor at ~450-fold (**Figure 5.3**) (Di Pilato et al., 2014; Leopoldo et al., 2008). LP-44 has been used extensively in preclinical *in vitro* and *in vivo* studies to investigate the role of 5-HT_7 receptors in thermoregulation, urination, depression, mood and sleep, however to our knowledge it has not entered clinical trials (Di Pilato et al., 2014).

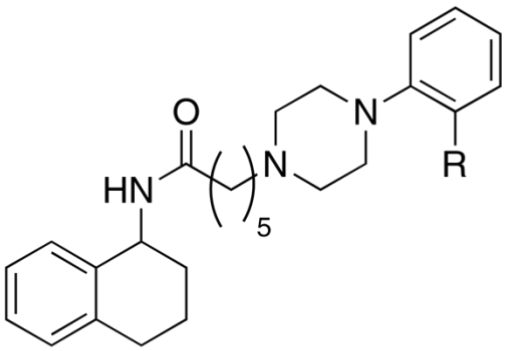

LP-44: R = SCH_3
LP-12: R = Ph

Target receptor	LP-44	LP-12
5-HT_7	0.22	0.13
5-HT_{1A}	52.7	60.9
5-HT_{2A}	326	1464

Figure 5.3 Comparison of the structures and K_i values for LP-44 and LP-12

LP-44 (R = SCH_3) and LP-12 (R = Ph) structures. K_i (nM) values for human cloned receptors (except where specified); 5-HT_7 (rat), 5-HT_{1A} and 5-HT_{2A} (rat cortex membrane for LP-44). Data from (Leopoldo et al., 2007).

In summary, half of the compounds identified by the high throughput screen have psychoactive activity. Previous studies showing that psychotropic drugs can have anti-cancer effects as single-agents, supports the notion that addition of these compounds to Smac-mimetic therapy may potentiate killing of cancer cells. This Chapter details my investigation into testing this hypothesis and exploring the molecular mechanisms by which psychoactive drugs potentiate Smac-mimetic mediated killing in AML.

5.6 The Psychoactive Compound LP-44 Potentiates Birinapant-mediated Cell Death

I first validated the high throughput screens identification of LP-44 by treating HoxA9/Meis1 AML cells with LP-44 alone and in combination with birinapant (**Figure 5.4A**). When combined with birinapant (at 250 or 500 nM), all concentrations of LP-44 tested were able to significantly increase the amount of cell death (**Figure 5.4A**). These findings were reproduced in MLL-AF9-Nras^{G12D} leukaemias, although in these cells 5 μM of LP-44 alone was toxic (**Figure 5.4B**). Therefore, the lower concentration of 2 μM of LP-44 was chosen to minimise single-agent toxicity. Altogether, these results confirm and extend the original screen and indicate that LP-44 is able to synergise with birinapant in different AML sub-types.

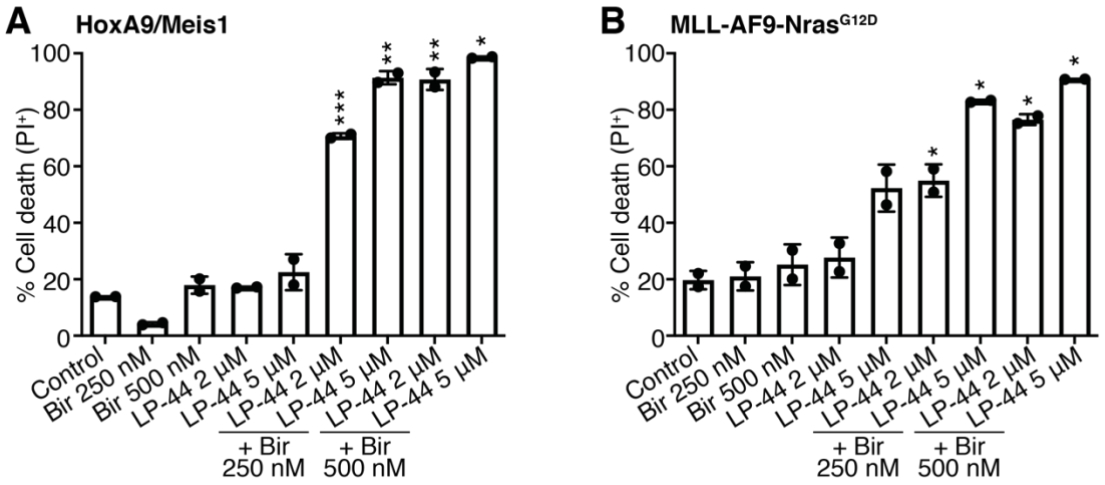

Figure 5.4 The psychoactive compound LP-44 potentiates birinapant-mediated cell death in AML

(**A**) HoxA9/Meis1 and (**B**) MLL-AF9-Nras^{G12D} AML cells were treated with LP-44 (2 and 5 µM) ± birinapant (250 and 500 nM) for 24 hours. Data are presented as mean ± SD throughout (2 biologically independent tumours). Cell death was measured by propidium iodide (PI) uptake, decrease of cell volume (MLL-AF9-Nras^{G12D}) and flow cytometry. P values were obtained by comparison of birinapant alone and birinapant plus LP-44 at the indicated concentrations.

5.7 LP-12 can Synergise with Birinapant, Albeit to a Lesser Extent than LP-44

A second potent highly-specific 5-HT$_7$ receptor agonist, LP-12, was described three years following the report of LP-44 (Di Pilato et al., 2014; Leopoldo et al., 2004; Leopoldo et al., 2008). LP-12 is structurally related to LP-44 and has similar K_i values for the 5-HT$_7$ receptor (**Figure 5.3**), however LP-12 boasts more specificity towards the 5-HT$_7$ receptor over the 5-HT$_{1A}$ receptor, compared to LP-44 (~450 vs ~200-fold respectively). LP-12 was not a compound included in the initial high throughput screen so I tested it to see whether its increased specificity towards the 5-HT$_7$ receptor would lead to a more powerful synergy profile with birinapant. Similar to LP-44, LP-12 was not toxic alone at 2 μM and increased cell death mediated by 250 and 500 nM of birinapant in HoxA9/Meis1, MLL-AF9 and MLL-AF9-Nras^{G12D} leukaemias (**Figure 5.5A-C**). However, the increase in cell death in all leukaemias was either comparable or less than that observed with LP-44. Therefore, I focused on the LP-44 plus birinapant combination.

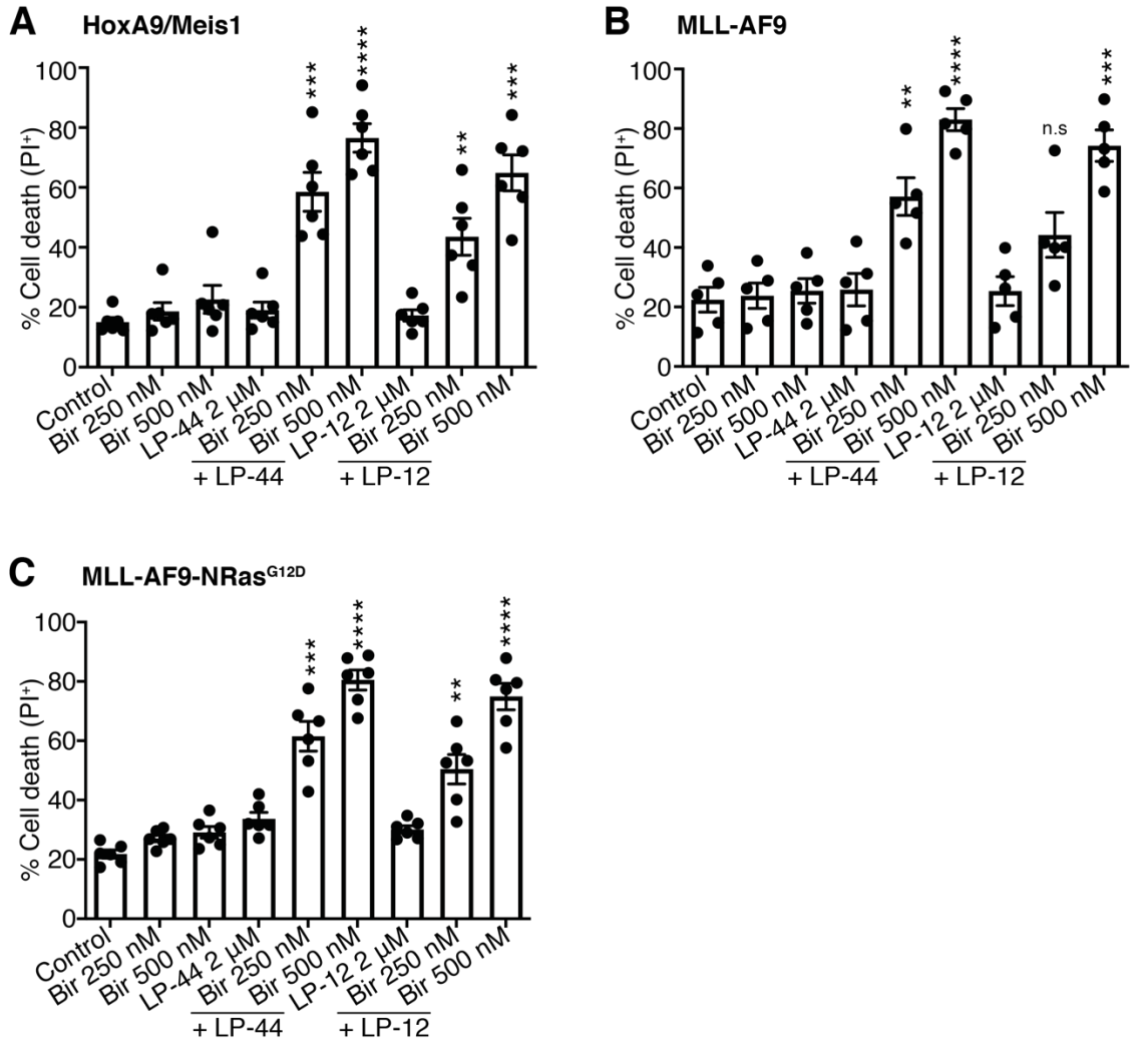

Figure 5.5 LP-12 can synergise with birinapant, albeit to a lesser extent than LP-44

(**A**) HoxA9/Meis1 (n=6) (**B**) MLL-AF9 (n=5) and (**C**) MLL-AF9-Nras$_{G12D}$ (n=6) AML cells were treated with LP-44 or LP-12 (2 µM) ± birinapant (250 and 500 nM) for 24 hours. Data presented as mean ± SEM throughout (3-4 independent tumours, repeated 1-3 times). Cell death was measured by propidium iodide (PI) uptake, decrease of cell volume (MLL-AF9-Nras$_{G12D}$) and flow cytometry. P values were obtained by comparison of birinapant alone and in combination with LP-44 or LP-12 at the indicated concentrations.

5.8 LP-44 Synergises with Different Monovalent and Bivalent Smac-mimetics

Similar to my earlier studies (Chapter 3 **Figure 1**), I tested whether LP-44 was able to synergise with different Smac-mimetics. LP-44 potentiated cell death mediated by the monovalent Smac-mimetic AT-406 (AT) and the bivalent Smac-mimetic AEG-40730 (AEG) in HoxA9/Meis1 and MLL-AF9 AML cells, although the combination of AEG plus LP-44 in MLL-AF9 cells was not significant (**Figure 5.6A-D**). Similarly, LP-44 did not consistently increase the killing of AML cells induced by Smac-mimetics LCL161 (LCL) and GDC-0152 (GDC) (**Figure 5.6E-H)**. Although there was a suggestion of an increase in cell death in AMLs treated with LP-44 plus the monovalent Smac-mimetic LCL, this was not significant (**Figure 5.6E and F**) and the cell death observed in AML cells treated with single-agent GDC or in combination with LP-44 was minimal (**Figure 5.6G and H**). These results show that LP-44, a psychoactive drug, increases the killing mediated by some, but not all, structurally distinct, Smac-mimetics in AML.

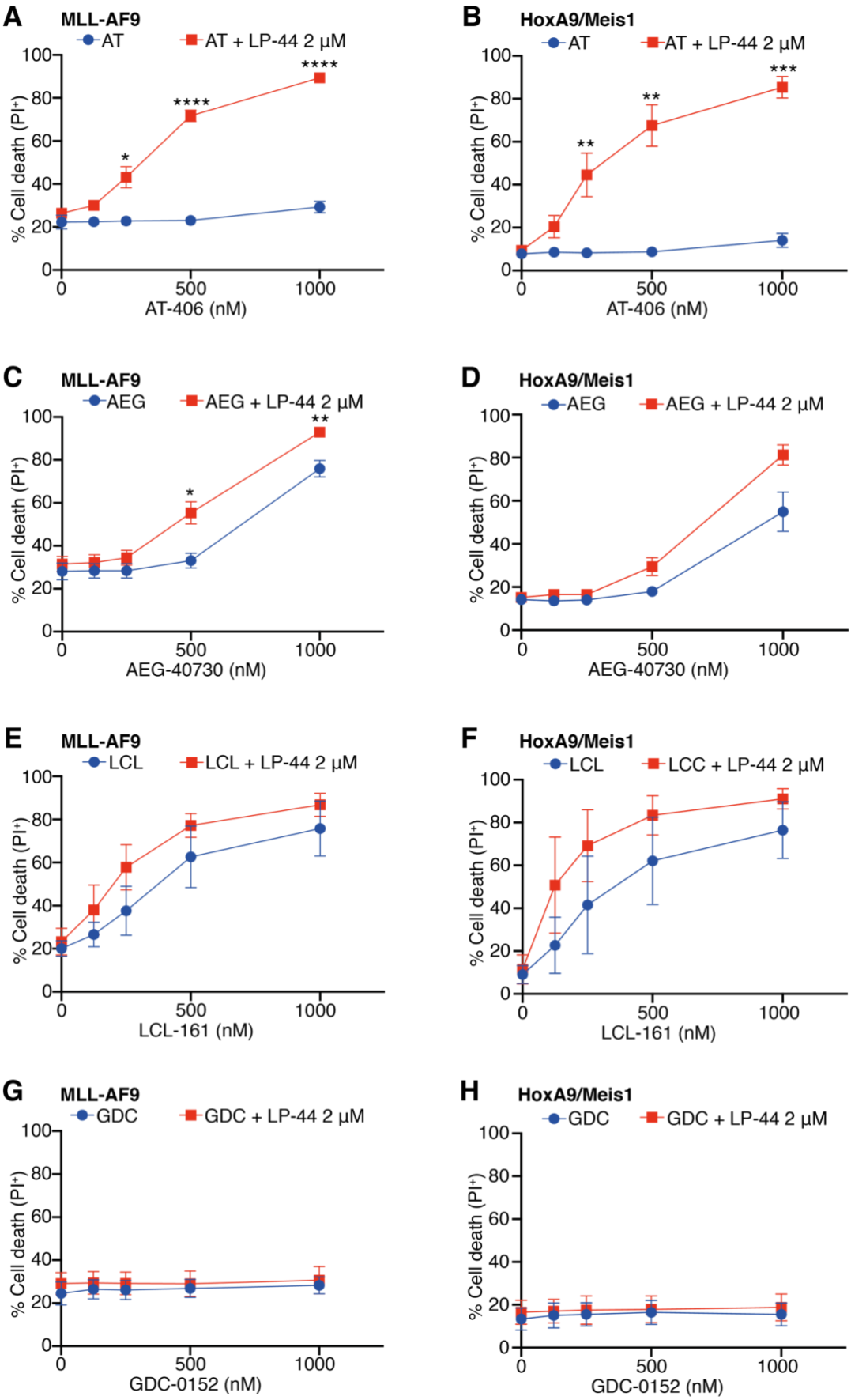
A
MLL-AF9
AT
AT + LP-44 2 µM
% Cell death (PI+)
AT-406 (nM)
B
HoxA9/Meis1
AT
AT + LP-44 2 µM
% Cell death (PI+)
AT-406 (nM)
C
MLL-AF9
AEG
AEG + LP-44 2 µM
% Cell death (PI+)
AEG-40730 (nM)
D
HoxA9/Meis1
AEG
AEG + LP-44 2 µM
% Cell death (PI+)
AEG-40730 (nM)
E
MLL-AF9
LCL
LCL + LP-44 2 µM
% Cell death (PI+)
LCL-161 (nM)
F
HoxA9/Meis1
LCL
LCC + LP-44 2 µM
% Cell death (PI+)
LCL-161 (nM)
G
MLL-AF9
GDC
GDC + LP-44 2 µM
% Cell death (PI+)
GDC-0152 (nM)
H
HoxA9/Meis1
GDC
GDC + LP-44 2 µM
% Cell death (PI+)
GDC-0152 (nM)

Figure 5.6 LP-44 synergises with different monovalent and bivalent Smac-mimetics

MLL-AF9 and HoxA9/Meis1 AML cells were treated with LP-44 (2 µM) ± 125, 250, 500 and 100 nM of (**A, B**) AT-406 (AT) (n=4), (**C, D**) AEG-40730 (AEG) (n=4-6), (**E, F**) LCL161 (LCL) (n=2-4, error bars SD) and (**G, H**) GDC-0152 (GDC) (n=4-5) for 24 hours. Data presented as mean ± SEM throughout unless otherwise stated (2-3 independent tumours, repeated 1-3 times). Cell death was measured by propidium iodide (PI) uptake, decrease of cell volume and flow cytometry. P values were obtained by comparison of Smac-mimetic alone and in combination with LP-44 at the indicated concentrations.

5.9 Peptide-mimetics, the BET Inhibitor JQ1 and the BH3 Mimetic ABT-199, do not Synergise with LP-44 or LP-12

Having observed LP-44 can combine with peptide-like Smac-mimetics, I tested whether LP-44 or LP-12 (LP-44/12) could synergise with other peptide-mimetics such as the BET-inhibitor JQ1 (Chaidos et al., 2015; Zuber et al., 2011) or the BH3-mimetic Bcl-2 inhibitor ABT-199 (Merino et al., 2018; Souers et al., 2013). JQ1 was toxic as a single-agent at 200 nM in all AML cells tested (**Figure 5.7A-C**). The cell death mediated by LP-44/12 in combination with 25 nM of JQ1 was less than that mediated by LP-44/12 plus birinapant (**Figure 5.7A-C**). ABT-199 only induced a small level of cell death as a single-agent up to doses of 1000 nM in HoxA9/Meis1, MLL-AF9 and MLL-AF9-Nras^{G12D} AML cells (**Figure 5.7D-F**), and LP-44/12 did not increase the killing mediated by ABT-199 at the concentrations tested (**Figure 5.7D-F**). Therefore, suggesting that LP-44 and LP-12 do not have the capacity to synergistically increase cell death mediated by all peptide-mimetic based therapies.

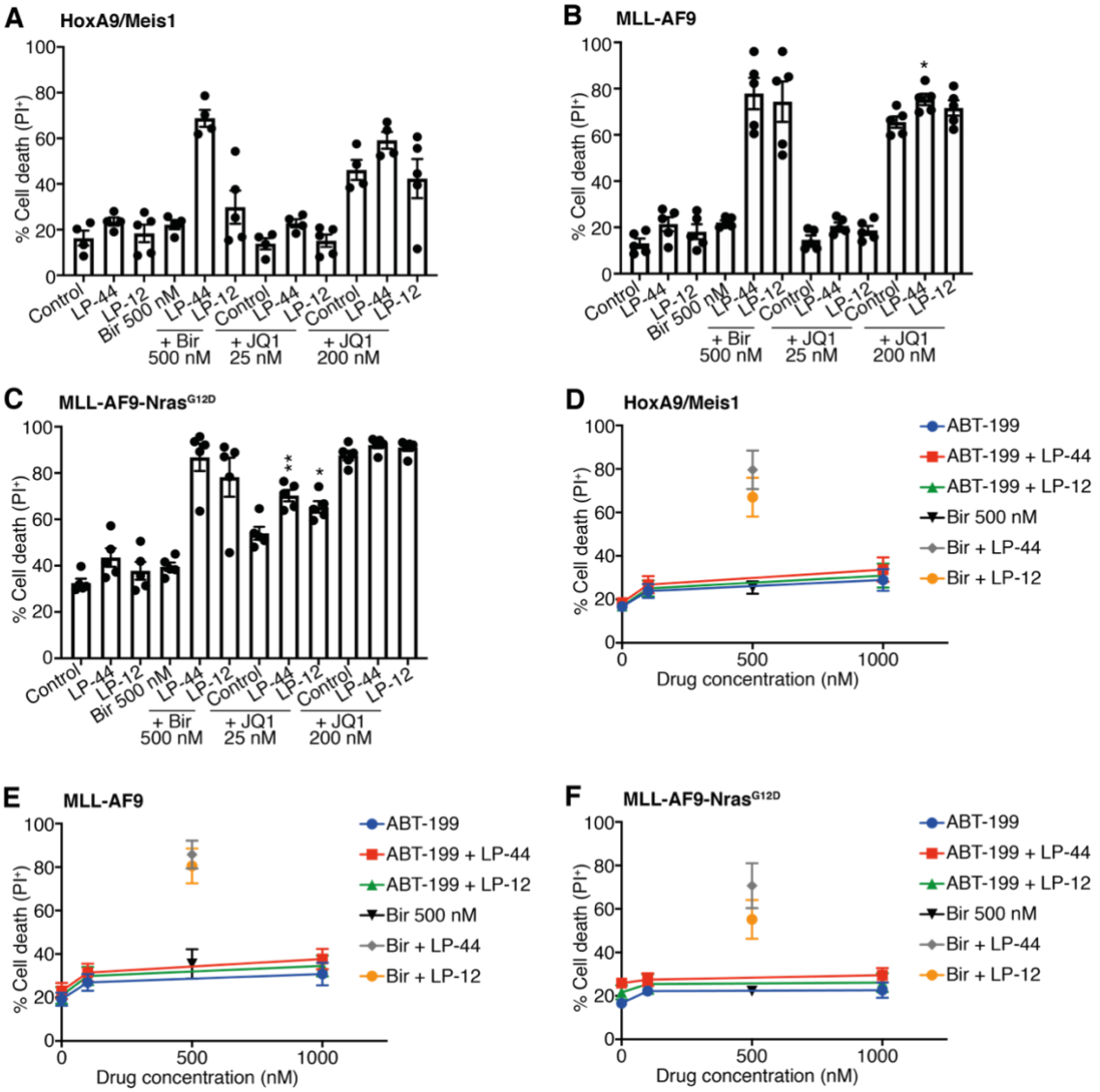

Figure 5.7 The BET inhibitor JQ1 and the BH3 mimetic ABT-199, do not synergise with LP-44 or LP-12

(**A**) HoxA9/Meis1 (n=4), (**B**) MLL-AF9 (n=4) and (**C**) MLL-AF9-Nras^{G12D} (n=4) cells were treated with LP-44 or LP-12 (2 μM) ± JQ1 (25 or 200 nM) for 24 hours. (**D**) HoxA9/Meis1 (n=4), (**E**) MLL-AF9 (n=4) and (**F**) MLL-AF9-Nras^{G12D} (n=3) cells were treated with LP-44 or LP-12 (2 μM) ± ABT-199 (100 or 1000 nM) for 24 hours. Birinapant (500 nM) in combination with LP-44 or LP-12 (2 μM) was used as a positive control. Data presented as mean ± SEM throughout (2-4 independent tumours, repeated 1-3 times). Cell death was measured by propidium iodide (PI) uptake, decrease of cell volume (MLL-AF9-Nras^{G12D}) and flow cytometry. P values were obtained by comparison of JQ1 or ABT-199 alone and in combination with LP-44 or LP-12.

5.10 LP-44 and LP-12 do not Potentiate Ara-c Chemotherapy Mediated Cell Death

As discussed previously, cytarabine (Ara-c) is a current standard-of-care chemotherapy for AML patients. One way to improve therapy outcomes for patients, is to try and combine existing chemotherapies, such as Ara-c, with other drugs (Reese and Schiller, 2013). Having established that LP-44 and LP-12 do not synergise with the peptide-mimetics JQ1 and ABT-199, I tested whether the 5-HT_7 receptor agonists could potentiate cell death induced by Ara-c. Ara-c was toxic as a single-agent in a dose dependent manner in HoxA9/Meis1, MLL-AF9 and MLL-AF9-$Nras_{G12D}$ AML cells and addition of LP-44/12 was unable to enhance Ara-c mediated cell death (**Figure 5.8A-C**).

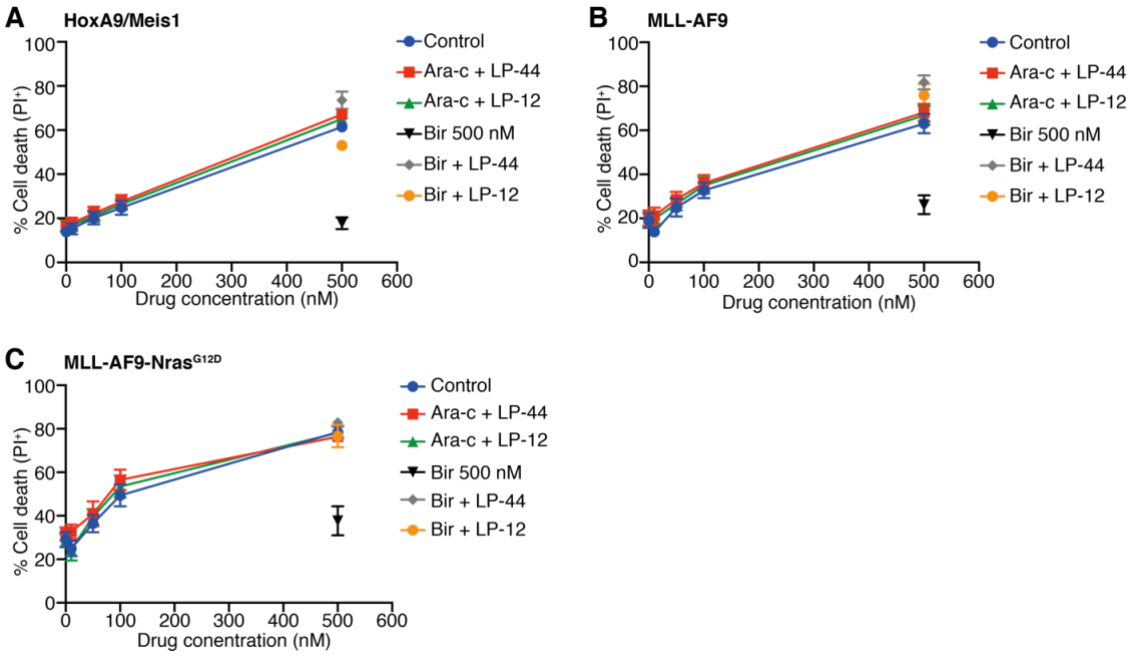

Figure 5.8 LP-44 and LP-12 do not potentiate Ara-c chemotherapy mediated cell death

(**A**) HoxA9/Meis1 (n=5), (**B**) MLL-AF9 (n=4) and (**C**) MLL-AF9-Nras^{G12D} (n=4) cells were treated with LP-44 or LP-12 (2 μM) ± Ara-c (10, 50, 100 or 500 nM) for 24 hours. Birinapant (500 nM) in combination with LP-44 or LP-12 (2 μM) was used as a positive control. Data presented as mean ± SEM throughout (3 independent tumours, repeated 1-2 times). Cell death was measured by propidium iodide (PI) uptake, decrease of cell volume (MLL-AF9-Nras^{G12D}) and flow cytometry.

5.11 LP-44 plus Birinapant Combination Induces TNF Receptor 1, Caspase 8 and 3 Dependent Apoptosis

To interrogate the molecular mechanisms by which LP-44 plus birinapant treatment induced killing of AML cells, I tested HoxA9/Meis1 cells derived from gene-deleted mice lacking different components of the TNFR1 cell death pathway. As discussed in the introduction, the Smac-mimetic birinapant promotes cell death through degradation of IAPs, leading to the formation of the TNFR1 downstream pro-apoptotic complex 2a (RIPK1 and caspase 8/3) or the pro-necroptotic complex 2b (RIPK3 and MLKL) pathways (Ofengeim and Yuan, 2013) (**Figure 5.9A**). Therefore, I initially tested HoxA9/Meis1 *Tnfr1*$^{-/-}$ cells and observed loss of TNFR1 attenuated LP-44 plus birinapant killing (**Figure 5.9B**). Birinapant has previously been shown to mediate RIPK3/MLKL dependent necroptosis alone or when caspases are inhibited, for example with the caspase inhibitor IDN-6556 (Emricasan) (Brumatti et al., 2016; McComb et al., 2016). However, HoxA9/Meis1 *Ripk3*$^{-/-}$ cells (red bars) were equally sensitive to LP-44 plus birinapant combination treatment compared to wild type (blue bars), indicating cell death is independent of RIPK3 and therefore not necroptotic (**Figure 5.9C**). Caspase 8 deficient animals are embryonic lethal, however the additional loss of RIPK3 can be used to generate viable *Casp8*$^{-/-}$*Ripk3*$^{-/-}$ animals (Kaiser et al., 2011; Varfolomeev et al., 1998). Having established the redundancy of RIPK3, I treated HoxA9/Meis1 *Casp8*$^{-/-}$*Ripk3*$^{-/-}$ AML cells with the LP-44 plus birinapant combination (green bars). I observed combination cell death was significantly reduced compared to wild type HoxA9/Meis1 cells (blue bars), indicating combination-mediated cell death is caspase 8 dependent

(**Figure 5.9C**). Western blot analysis confirmed that expression of the relevant proteins was absent in the *Casp8*$^{-/-}$*Ripk3*$^{-/-}$ and *Ripk3*$^{-/-}$ AML cells (**Figure 5.9D**).

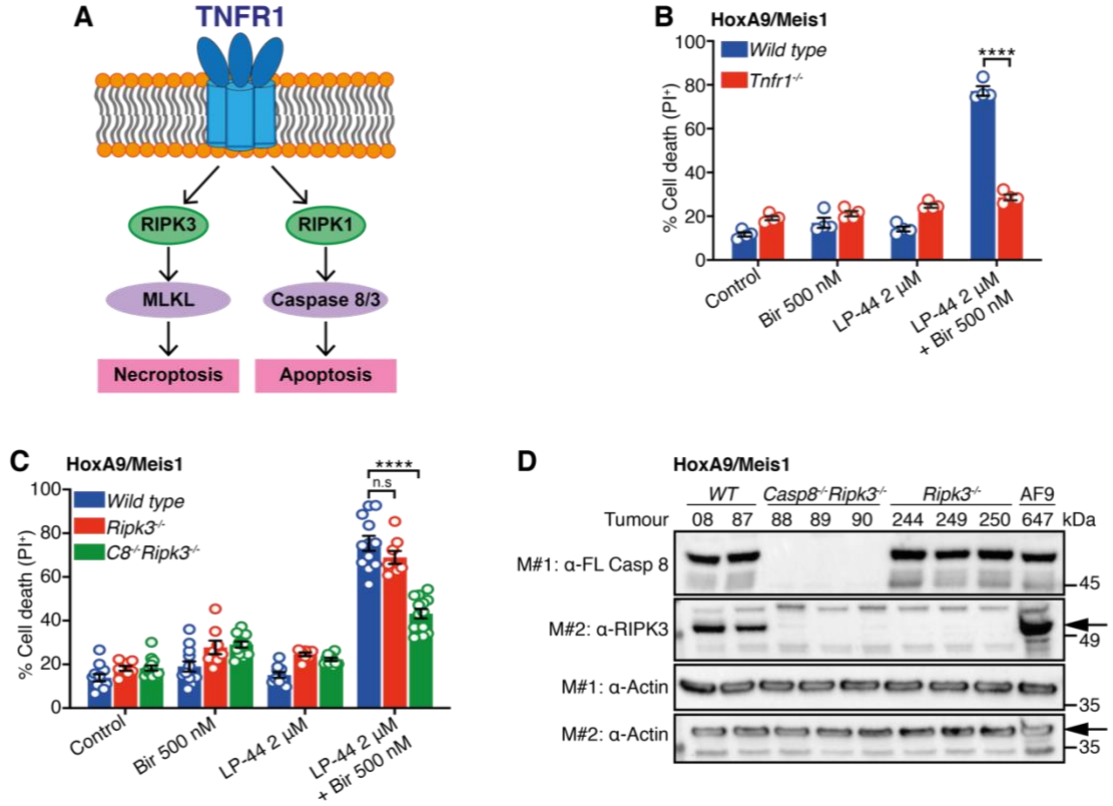

Figure 5.9 Combination cell death is TNFR1 and caspase 8 dependent

(**A**) Schematic of TNFR1 signalling pathways. RIPK3/MLKL are essential for necroptosis whilst RIPK1/caspase8/3 are essential for apoptosis. (**B**) HoxA9/Meis1 wild-type (WT) and knock out AML cells deficient for TNF receptor 1 (*Tnfr1*$^{-/-}$) were treated with LP-44 (2 µM) ± birinapant (500 nM) for 24 hours (n=4). (**C**) HoxA9/Meis1 WT and knock out AML cells deficient for RIPK3 (*Ripk3*$^{-/-}$) and Caspase 8/RIPK3 (*Casp8*$^{-/-}$*Ripk3*$^{-/-}$) were treated with LP-44 (2 µM) ± birinapant (500 nM) for 24 hours (n=6-10). (**D**) HoxA9/Meis1 WT and knock out AML cells deficient for *Ripk3*$^{-/-}$ and *Casp8*$^{-/-}$*Ripk3*$^{-/-}$ were analysed by Western blotting to confirm lack of RIPK3 and caspase 8 protein. An MLL-AF9 AML was used as a positive control. FL; full length, CL; cleaved, Casp; caspase. M#1, 2 indicate independent membranes. Actin was used as a loading control. Cell death was measured by propidium iodide (PI) uptake and flow cytometry. Data presented as mean ± SEM throughout (2-3 independent tumours, repeated 2-3 times). P values were obtained by comparison of treatments in different cell lines as indicated.

The results above using genetic models of HoxA9/Meis1 AML cells lacking key components of the TNFR1 signalling pathway strongly suggested LP-44 plus birinapant combination-mediated cell death is dependent on TNFR1 and is driven by the caspase 8 apoptotic pathway. To further validate these findings, I analysed protein expression of the key targets of the TNFR1 apoptotic pathway following LP-44 plus birinapant treatment. In HoxA9/Meis1 AML cells, cIAP1 degradation was enhanced and sustained for longer with combination treatment, compared to birinapant single-agent treatment (**Figure 5.10A**). In contrast, cIAP1 was equally degraded in birinapant alone and birinapant plus LP-44 combination treatment in MLL-AF9 cells at the time points tested (**Figure 5.10B**). Indicators of cell death activation, such as cleavage of caspases 8, 3 and the downstream caspase 3 substrate PARP, were detected at stronger intensities in the LP-44 plus birinapant co-treated cells for both leukaemias (**Figure 5.10A and B**). Together, these data corroborate earlier findings and indicate LP-44 plus birinapant combination-mediated cell death is TNFR1 dependent apoptosis, mediated by the activation of caspases 8 and 3.

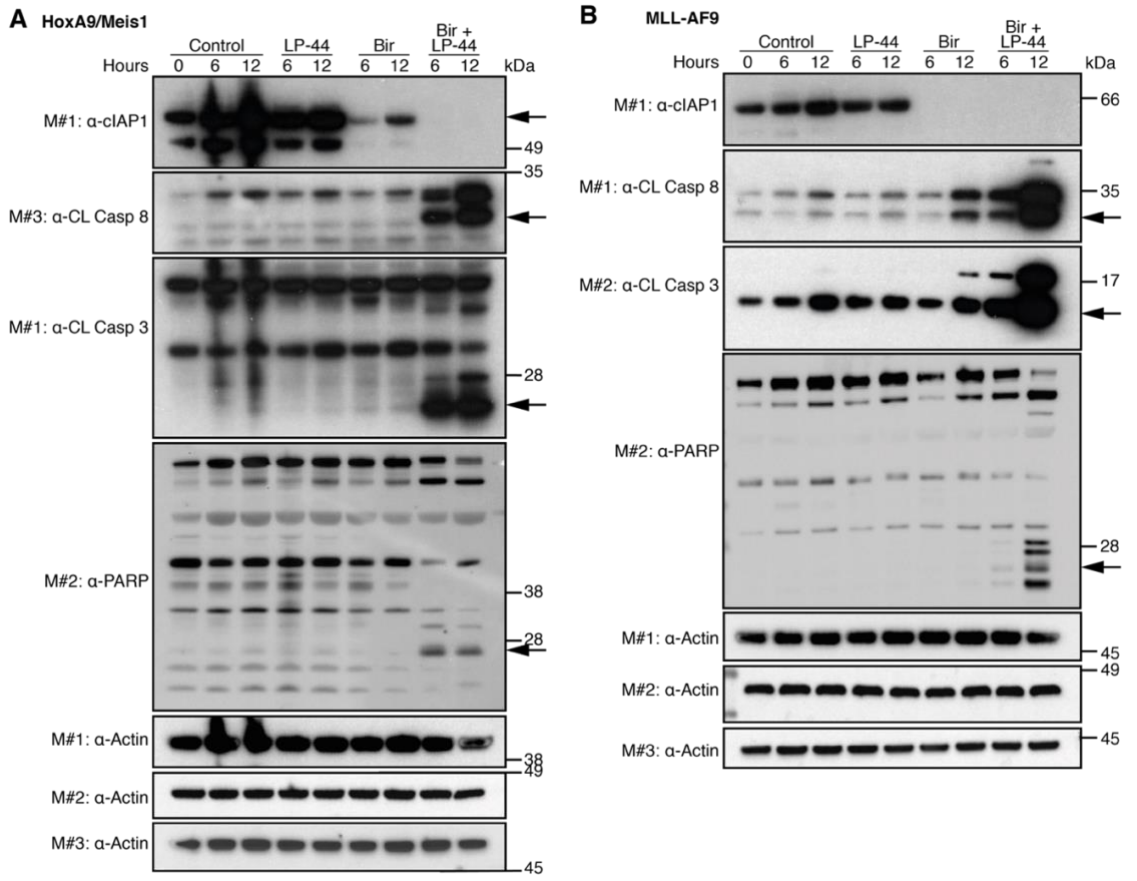

Figure 5.10 Protein analysis confirms LP-44 plus birinapant combination cell death is caspase 8/3 dependent apoptosis

(**A**) HoxA9/Meis1 and (**B**) MLL-AF9 AML cells were treated with LP-44 (2 μM) ± birinapant (250 nM) for 6 and 12 hours. Samples were probed by Western blot with the antibodies described. FL; full length, CL; cleaved, Casp; caspase. M#1, 2 indicate independent membranes. Actin was used as a loading control.

5.12 Nec-1 Attenuates LP-44/12 plus Birinapant Combination Cell Death and TNF Production

Having established that combination cell death is TNFR1 and caspase 8/3 dependent, but independent of RIPK3, I next investigated the role of RIPK1 in LP-44/12 plus birinapant cell death. RIPK1 is involved in regulating signalling pathways downstream of TNFR1, including both the transcriptional response and the formation of the pro-apoptotic complex 2a. This complex is formed following loss of cIAPs and drives activation of caspase 8 and 3, leading to apoptotic cell death (Dickens et al., 2012; Kitson et al., 1996; Micheau and Tschopp, 2003). Therefore, I hypothesised that RIPK1 would be necessary for LP-44/12 plus birinapant mediated apoptotic killing. Pre-treatment of HoxA9/Meis1, MLL-AF9 and MLL-AF9-Nras^{G12D} AML cells with the RIPK1 inhibitor necrostatin-1 (Nec-1) (Degterev et al., 2008), was able to block LP-44/12 plus birinapant-mediated cell death (**Figure 5.11A-C**). Analysis of TNF levels in HoxA9/Meis1 cells treated with LP-44 plus birinapant in the presence or absence of Nec-1 at 4, 6 and 9 hours showed Nec-1 attenuated TNF production (**Figure 5.11D**). These findings are in agreement with previous reports that show Nec-1 mediated RIPK1 inhibition leads to attenuation of TNF production, which is essential for Smac-mimetic killing and therefore results in an inhibition of cell death (Brumatti et al., 2016; Wong et al., 2014).

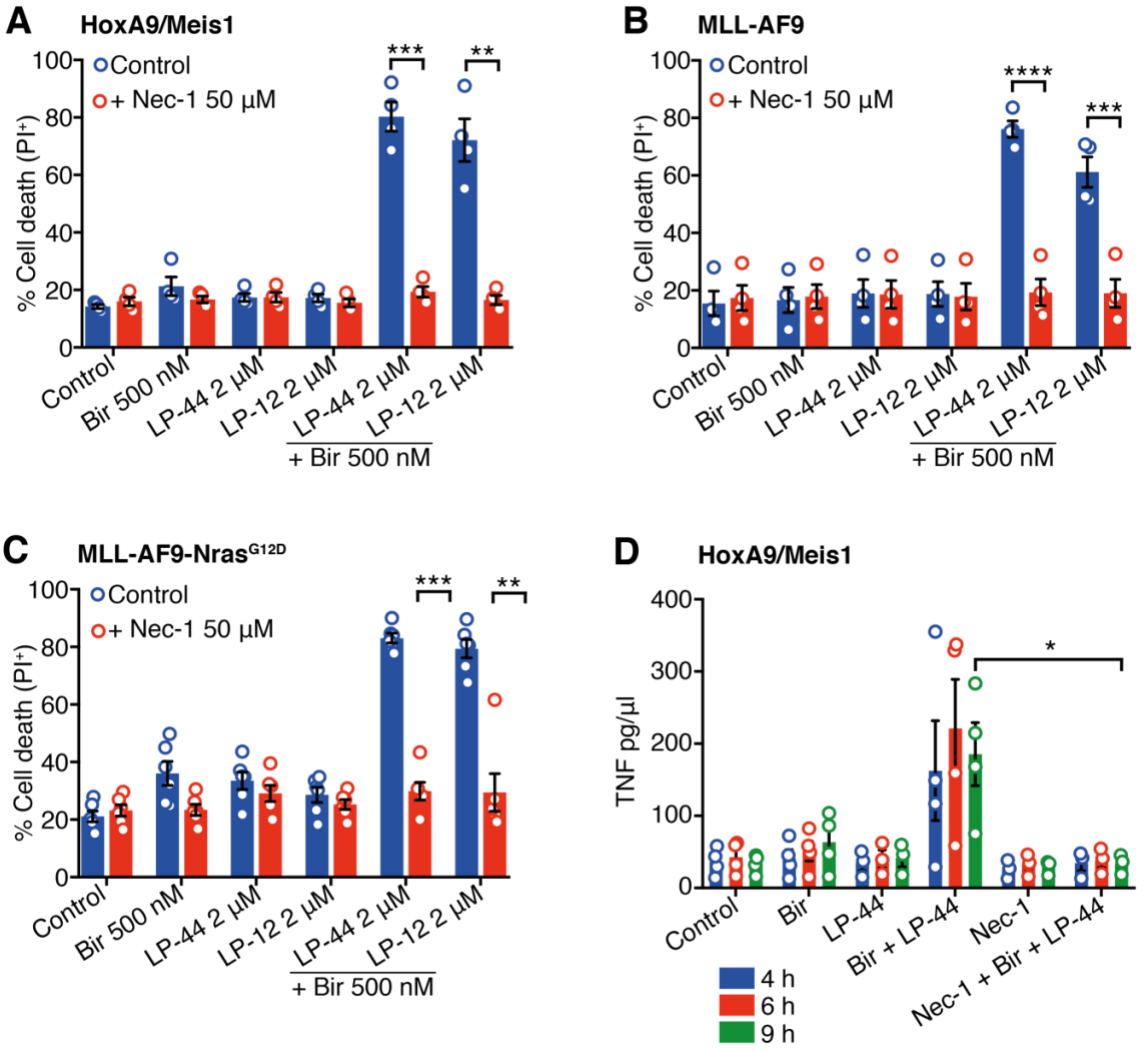

Figure 5.11 Nec-1 attenuates LP-44/12 plus birinapant combination cell death and TNF production

(**A**) HoxA9/Meis1 (n=4), (**B**) MLL-AF9 (n=4) and (**C**) MLL-AF9-Nras^{G12D} (n=6) AML cells were treated with LP-44 or LP-12 (2 µM) ± birinapant (500 nM) ± Nec-1 (50 µM) for 24 hours. (**D**) HoxA9/Meis1 AML cells treated with LP-44 (2 µM) ± birinapant (500 nM) for 4, 6 or 9 hours were analysed by ELISA for TNF levels. Cell death was measured by propidium iodide (PI) uptake, decrease of cell volume (MLL-AF9-Nras^{G12D}) and flow cytometry. Data presented as mean ± SEM throughout (2-4 independent tumours, 1-2 repeats). P values were obtained by comparison of LP-44/12 plus birinapant treatment and in combination with Nec-1.

5.13 Investigating the Role of MAPK/ERK Signalling in LP-44 plus Birinapant Treatment

The canonical signalling pathway of the 5-HT_7 receptor involves it's coupling to a G_s-protein and activation of AC. This activates the production of cAMP, resulting in the stimulation of PKA and leads to the activation of multiple signalling cascades, including the MAPK/ERK pathway (Errico et al., 2001; Guseva et al., 2014b; Johnson-Farley et al., 2005). Alternatively, the 5-HT_7 receptor can be coupled to a G_{12}-protein to activate members of the Rho family of small GTPases (Rho, Rac, and Cdc42) (**Figure 5.1**) (Kobe et al., 2012; Kvachnina et al., 2005). Previous studies have shown inhibition of MAPK p38 with the inhibitor LY2228820 (Ralimetinib) can enhance birinapant-mediated killing of AML cells (Lalaoui et al., 2016). Consequently, I investigated the importance of the MAPK/ERK pathway in LP-44 and birinapant combination cell death. This was achieved by interrogating the phosphorylation, and therefore the activation, of ERK in response to short-term LP-44 plus birinapant combination treatment in AML cells. Detection of phosphorylated ERK was present for all treatment conditions, in both HoxA9/Meis1 and MLL-AF9 leukaemias, however the signal intensity was reduced by LP-44 plus birinapant treatment at 120 minutes, most prominently in HoxA9/Meis1 AML cells (**Figure 5.12A and B**). Detection of total ERK confirmed equivalent protein loading between samples (**Figure 5.12A and B**). cIAP1 was degraded at all time points with birinapant alone or LP-44 plus birinapant combination treatment, in both cell lines (**Figure 5.12A and B**). There was no detectable cleaved caspase 8 in all samples at the time points tested, indicating that up to 2 hours, caspase 8 is not activated in those conditions.

Therefore, the lower levels of phosphorylated-ERK are unlikely to be due to cell death (**Figure 5.12A and B**).

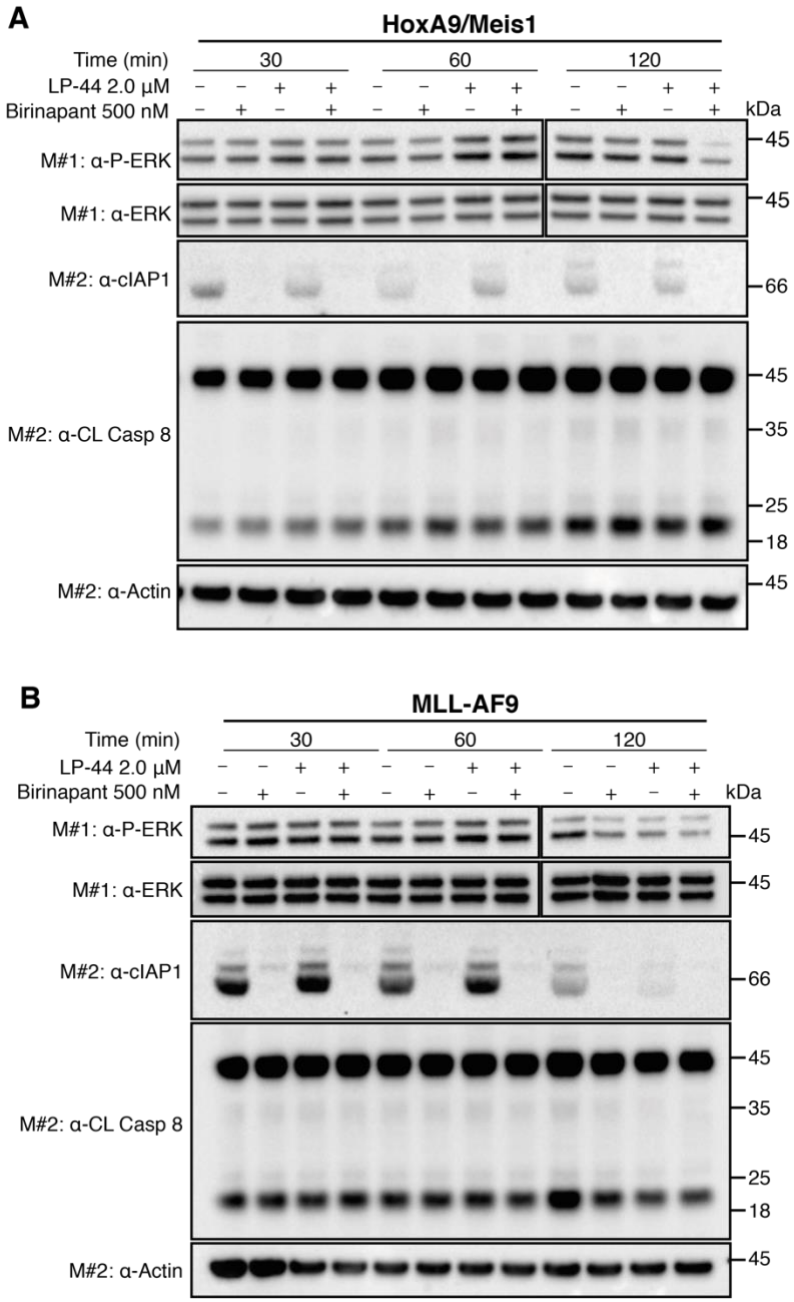

Figure 5.12 Investigating the role of MAPK/ERK signalling in LP-44 plus birinapant combination treatment

(**A**) HoxA9/Meis1 and (**B**) MLL-AF9 AML cells were treated with LP-44 (2 μM) ± birinapant (500 nM) for 30, 60 and 120 minutes. Samples were probed by Western blot with antibodies described. CL; cleaved, P; phosphorylated. Actin and total ERK was used as a loading control. M#1, 2 indicate independent membranes.

Although the presence of phosphorylated ERK was variable between leukaemias tested, its reduction in the LP-44 plus birinapant treated cells led me to further investigate the role of the MAPK/ERK signalling pathway in combination-mediated cell death. To test whether antagonism of the MAPK/ERK pathway is essential for LP-44 plus birinapant treatment, I used the mitogen-activated protein kinase kinase (MEK) inhibitors U0126 and PD098059 to disrupt the MAPK/ERK (also known as the Ras-Raf-MEK-ERK) signalling pathway (**Figure 5.13A**) (Alessi et al., 1995; Dudley et al., 1995; Favata et al., 1998). U0126 and PD098059 were not toxic as single-agent treatments and pre-treatment with them prior to LP-44 and birinapant treatment was unable to increase cell death in HoxA9/Meis1 and MLL-AF9 leukaemias (**Figure 5.13B and C**). To confirm the efficacy of U0126 and PD098059 to inhibit the activation of MAPK/ERK, I probed for expression of phosphorylated ERK (**Figure 5.13D**). Following 60 minutes of treatment, U0126 inhibited phosphorylation of ERK even in the presence of LP-44 plus birinapant treatment and this inhibition was more efficient compared to PD098059 at both concentrations tested (**Figure 5.13D**). These data suggest that the MAPK/ERK signalling pathway does not play an essential role in LP-44 and birinapant combination-mediated cell death.

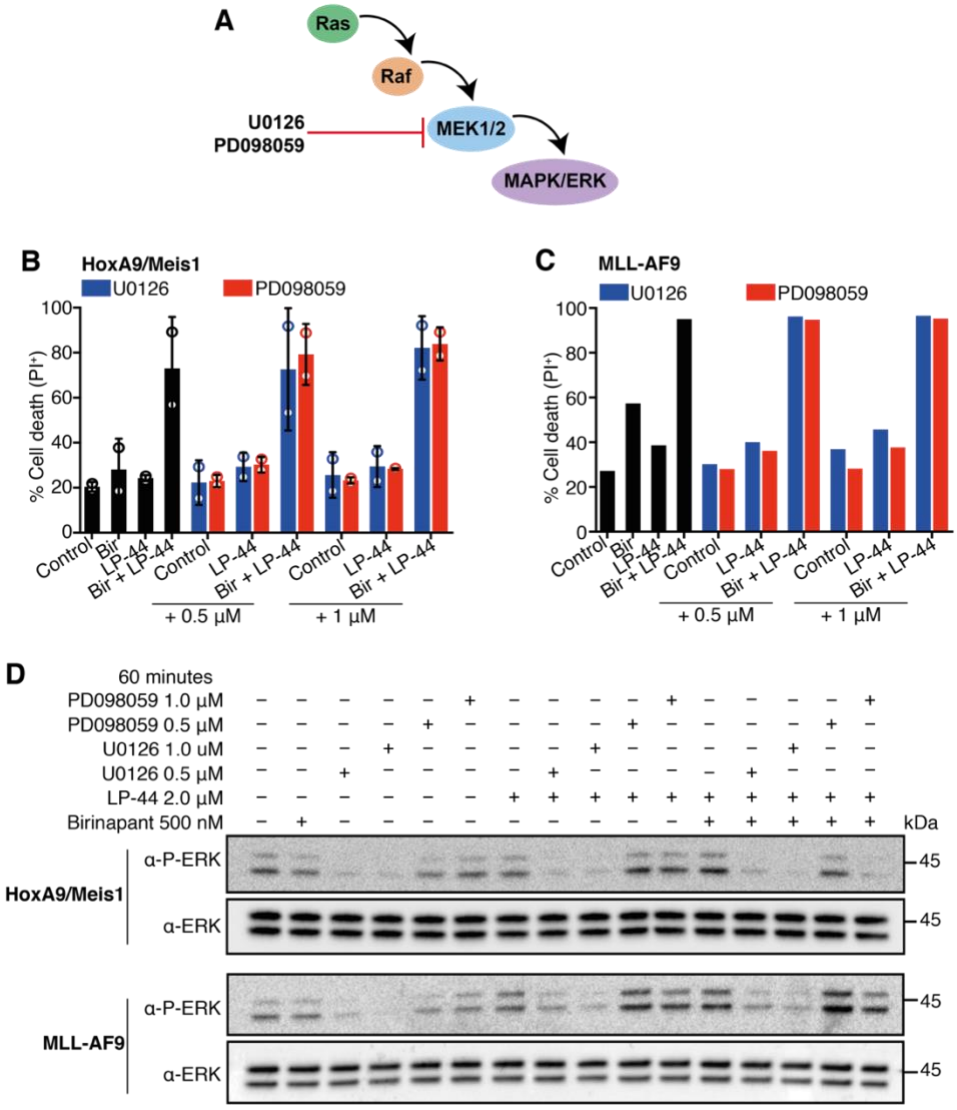

Figure 5.13 The MAPK/ERK signalling pathway does not play an essential role in LP-44 plus birinapant combination mediated cell death

(**A**) Schematic of the Ras/Raf/MEK/ERK signalling pathway. Inhibition of MEK1/2 by U0126 or PD098059 disrupts MAPK/ERK phosphorylation and activation. (**B**) HoxA9/Meis1 and (**C**) MLL-AF9 AML cells were treated with LP-44 (2 µM) ± birinapant (500 nM) ± MEK inhibitors U0126 (blue bars) or PD098059 (red bars) (0.5 or 1 µM) for 24 hours. Cell death was measured by propidium iodide uptake (PI), decrease of cell volume and flow cytometry. Data presented as mean ± SD throughout (1-2 independent tumours, 1-2 repeats). (**D**) HoxA9/Meis1 and MLL-AF9 AML cells were treated as described in (A) for 60 minutes. Samples were analysed by Western blotting for levels of phosphorylated and total ERK (P-ERK and ERK respectively).

5.14 LP-44 and LP-12 are MDR1 Inhibitors

The finding that antagonism of the MAPK/ERK signalling pathway is not important for LP-44 plus birinapant-mediated cell death led us to consider alternative explanations for the mechanism of combination synergy. Surprisingly, the initial results with LP-44 in combination with birinapant mirrored the findings observed with the MDR1 inhibitor plus birinapant combination, described in Chapter 3. For example, both LP-44 and MDR1 inhibitors can synergise with structurally distinct Smac-mimetics, but not peptide-mimetics JQ1 and ABT-199, or the chemotherapy Ara-c. Furthermore, both of the LP-44 and MDR1 inhibitor plus birinapant-combination mediated cell death is TNFR1, RIPK1 and caspase 8/3 dependent apoptosis. Interestingly, during my research of psychotropic compounds, I discovered that there has been some speculation of a correlation between the efficacy of antipsychotics and MDR1 inhibition (Boulton et al., 2002; Moons et al., 2011; Wang et al., 2006). Whilst the MDR1 inhibitory potential of the psychoactive compounds LP-44, SDZ 21009, GR-127935 and CGP-71683 is not known, similar to reserpine, fluphenazine is known to inhibit MDR1 function (Ford et al., 1989; Jaszczyszyn et al., 2012). We therefore hypothesised that LP-44/12 may act as MDR1 inhibitors and that this previously undescribed action of LP-44 and LP-12 enables them to synergise with birinapant to potentiate cell death.

To definitively test this hypothesis, I used the techniques and tools developed in Chapter 3 to investigate the potential of LP-44/12 to inhibit MDR1. Initially I used Rho-123 retention assays to test the MDR1 inhibitory potential of LP-44/12 in the

KG1 control and KG1 *MDR1*$^{-/-}$ cells previously generated (Chapter 3 **Figure 5**). Supporting my hypothesis and correlating with the previously generated data, LP-44 inhibited MDR1 at 1 μM and 10 μM, whilst LP-12 only inhibited MDR1 at 10 μM (**Figure 5.14A and B**). As expected, there was no difference in the shift between Rho-123 alone and in combination with LP-44 or LP-12 in KG1 *MDR1*$^{-/-}$ cells (**Figure 5.14A and B**). Treatment of cells with tariquidar was used as a positive control (**Figure 5.14C**). Together, these data indicate LP-44 and LP-12 can inhibit MDR1, albeit less potently than tariquidar.

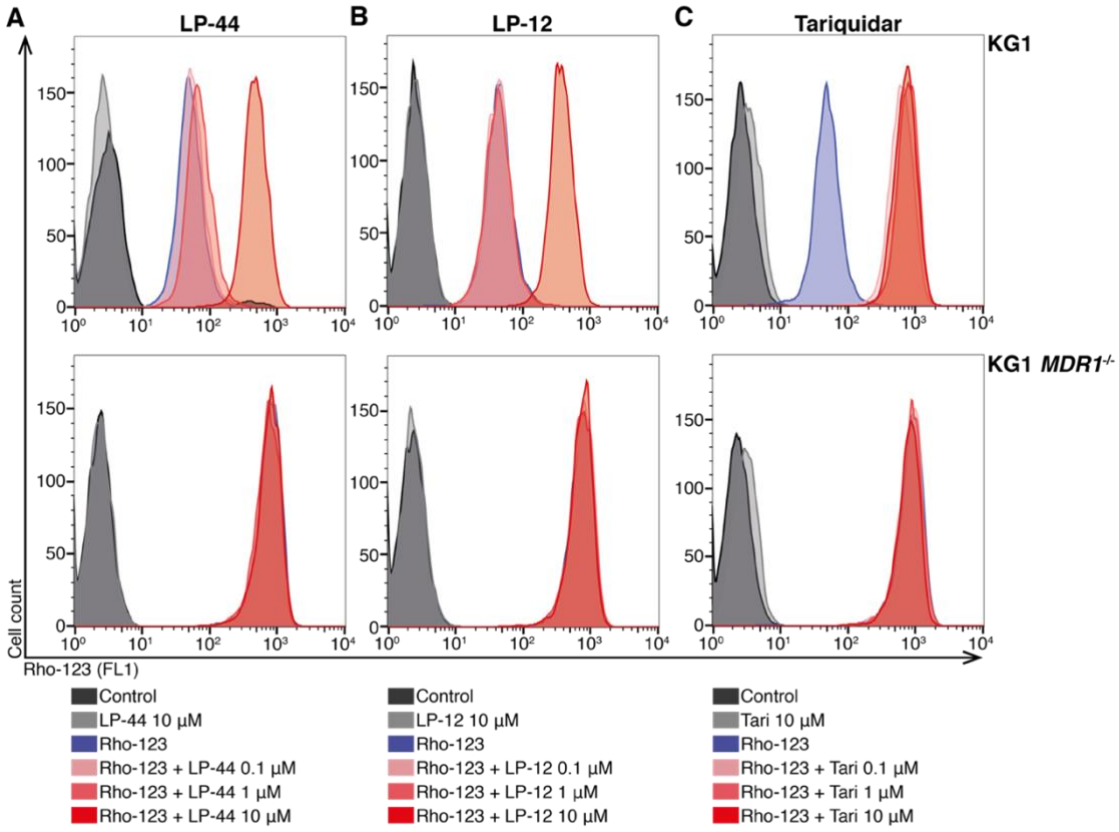

Figure 5.14 LP-44 and LP-12 are MDR1 inhibitors

KG1 control and KG1 *MDR1*$^{-/-}$ AML cells were pre-treated with Rhodamine-123 (Rho-123) 250 nM ± 0.1, 1 or 10 µM of (**A**) LP-44, (**B**) LP-12 and (**C**) tariquidar for 2 hours. Rho-123 florescence was analysed by flow cytometry (FL1 channel).

5.15 MDR1 Expression Correlates Inversely with Response to LP-44 and Birinapant Treatment in AMLs

To confirm that the MDR1 inhibition potential of LP-44 translates to an increase in birinapant mediated cell death, I treated KG1 control and KG1 *MDR1*$^{-/-}$ AML cells with LP-44 plus birinapant for 48 hours and analysed cell death by flow cytometry. As expected from the Rho-123 retention assay results (**Figure 5.14**), there was an increase in KG1 cell death when birinapant was combined with 2 or 10 μM of LP-44. However, KG1 *MDR1*$^{-/-}$ AML cells, which were more sensitive to birinapant alone treatment, did not have an increase in cell death following the addition of LP-44 at any of the concentrations tested (**Figure 5.15A**). Treatment of both cell lines with tariquidar was used as a positive control (**Figure 5.15B**). These data are in agreement with the hypothesis that LP-44 inhibition of MDR1 is responsible for birinapant-mediated synergistic cell death and therefore in the absence of *MDR1* synergy is not possible.

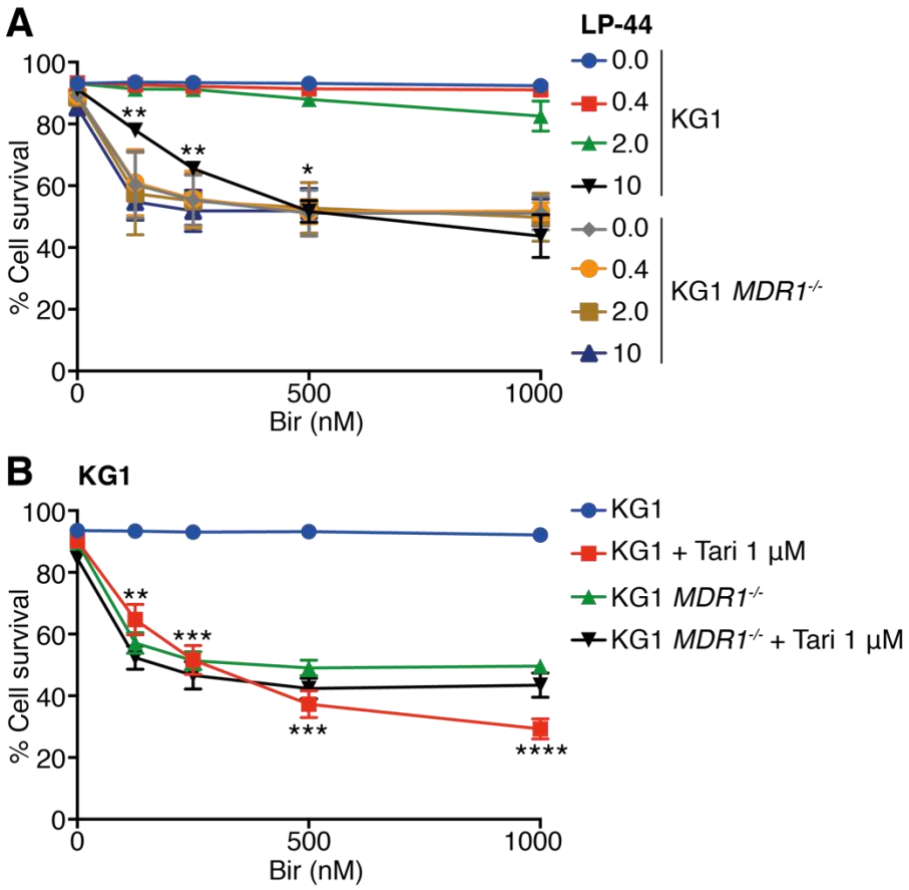

Figure 5.15 LP-44 potentiates birinapant-mediated cell death in KG1 but not KG1 *MDR1*$^{-/-}$ AML cells

(**A**) KG1 control and KG1 *MDR1*$^{-/-}$ AML cells were treated with LP-44 (0, 0.4, 4 and 10 µM) ± birinapant (125, 250, 500 and 1000 nM) for 48 hours (n=2, data presented as mean ± SD). (**B**) KG1 control and KG1 *MDR1*$^{-/-}$ AML cells were treated with tariquidar (1 µM) ± birinapant (125, 250, 500 and 1000 nM) for 48 hours as a control (n=5, data presented as mean ± SEM). Cell survival was measured by propidium iodide (PI) exclusion, decrease of cell volume and flow cytometry. P values were obtained by comparison of birinapant alone and birinapant plus LP-44 or tariquidar at the indicated concentrations.

As described in Chapter 3, we have identified that the expression and function of MDR1 is a biomarker of response for birinapant treatment. Following my findings in Figure 5.15, describing that LP-44 plus birinapant synergy is dependent on MDR1 expression/function in KG1 cells, I next investigated whether this is also true in different AMLs. To test this, I treated our known $MDR1_H$ and $MDR1_L$ murine leukaemias (discussed in Chapter 3 **Figure 2**) with the combination to determine whether their MDR1 profile correlated with their response. Corroborating our earlier findings (**Figures 5.4 and 5.5**), LP-44 synergised with the $MDR1_H$ leukaemias HoxA9/Meis1 and MLL-AF9-$Nras_{G12D}$ (BSS 29.2 and 30.4 respectively; **Figures 5.16A-F**). Whilst, in the $MDR1_L$ MLL-ENL AMLs, cell death was not increased with the addition of LP-44 (BSS -4.6; **Figure 5.16G-I**). These results suggest that MDR1 expression correlates inversely with response to LP-44 plus birinapant treatment in different leukaemias.

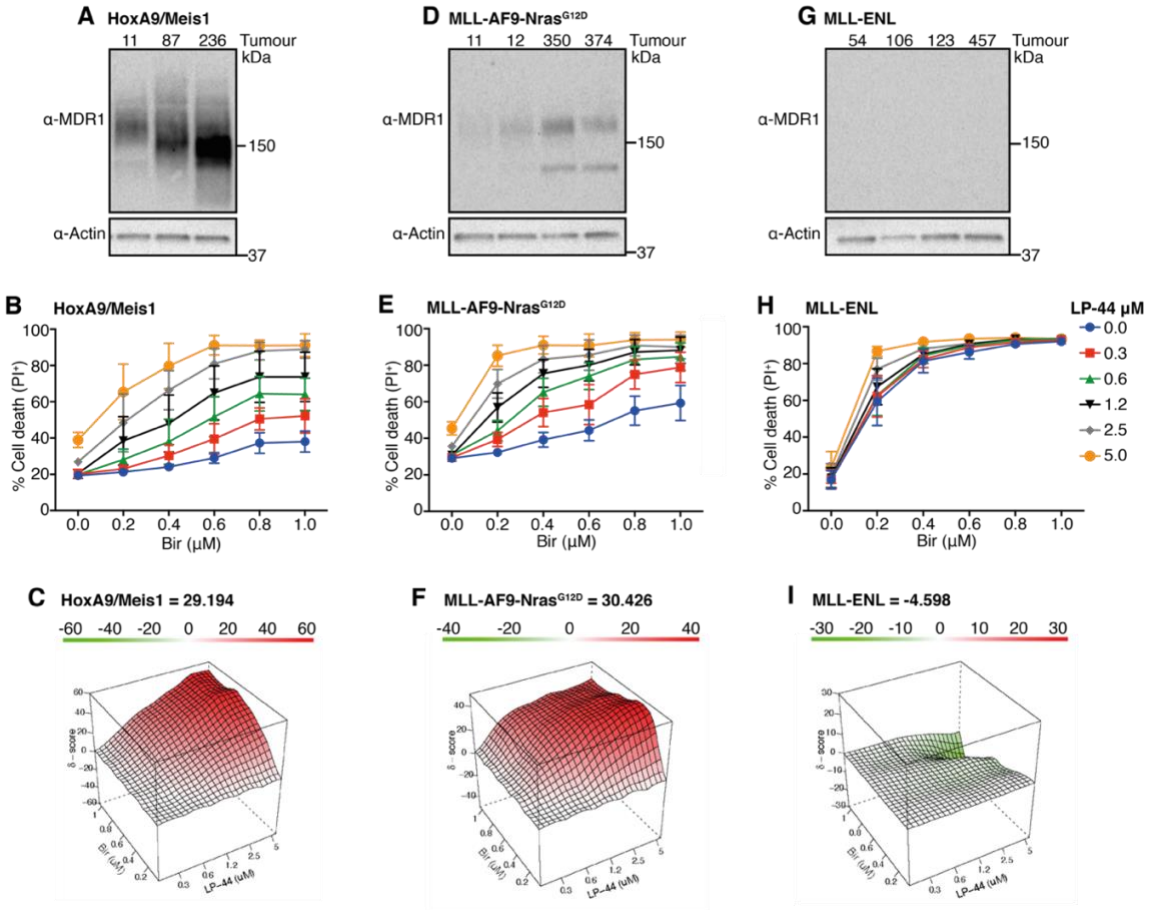

Figure 5.16 MDR1 expression correlates inversely with response to LP-44 plus birinapant treatment in AMLs

(**A-C**) HoxA9/Meis1, (**D-F**) MLL-AF9-Nras^{G12D} and (**G-I**) MLL-ENL AML cells (reiterated from Chapter 3). (**B**) HoxA9/Meis1 (n=4), (**E**) MLL-AF9-Nras^{G12D} (n=3-4) and (**H**) MLL-ENL (n=4) AML cells were treated with LP-44 (0.3, 0.6, 1.2, 2.5 and 5 μM) ± birinapant (0.2, 0.4, 0.6, 0.8, 1 μM) for 24 hours. (**C, F and I**) Bliss synergy score (BSS) analysis was calculated for each leukaemia treated with LP-44 and birinapant. Data presented as mean ± SEM throughout (2-4 independent tumours, repeated 1-3 times). Cell death was measured by propidium iodide (PI) uptake, decrease of cell volume (MLL-AF9-Nras^{G12D}) and flow cytometry.

5.16 MDR1 Expression and TNF are Biomarkers of LP-44 plus Birinapant Treatment Response in AML

Following the finding that the MDR1 profile of different leukaemias can be used to predict their sensitivity to LP-44 plus birinapant treatment, I next investigated the role TNF plays in this specific combination. Smac-mimetic treatment requires autocrine TNF/TNFR1 signalling to kill (Petersen et al., 2007; Varfolomeev et al., 2007; Vince et al., 2007), therefore, I hypothesised that similar to the MDR1 inhibitor plus birinapant combination, TNF would also be a biomarker for the LP-44 plus birinapant combination therapy. To test the hypothesis that both MDR1 and TNF are biomarkers of response, I treated different MLL-AF9 AML sub-groups, with varying MDR1 and TNF profiles (introduced in Chapter 3 **Figure 3**), with LP-44, birinapant and recombinant TNF. As expected, $MDR1_L$ MLL-AF9 cells were sensitive to birinapant single-agent treatment and addition of LP-44 did not affect their sensitivity (blue bars, **Figure 5.17A and B**). In contrast, $MDR1_H$ MLL-AF9 cells were only responsive to birinapant in the presence of LP-44 (red bars, **Figure 5.17A and B**). Of note, some $MDR1_L$ (black bars) and $MDR1_H$ (green bars) AML cells required addition of TNF to be efficiently killed by birinapant ($MDR1_L$) or birinapant plus LP-44 ($MDR1_H$) (**Figure 5.17A and B**). These results confirm that autocrine TNF must be produced by AML cells for LP-44 plus birinapant treatment to be effective. Corroborating these findings, TNF levels were increased in $MDR1_H$ MLL-AF9 AML cells upon treatment with LP-44 plus birinapant (red bars) but not in the $MDR1_H$ MLL-AF9 AML cells that were resistant to combination treatment (green bars) (**Figure 5.17C-E**). An analysis of the synergy between LP-44 and birinapant in $MDR1_H$ birinapant resistant (Bir_R) and combination sensitive ($Combo_S$) MLL-AF9 AML cells (red bars) was also

determined (BSS 44.5; **Figure 5.17F and G**). Together these data support the findings that sensitivity to LP-44 plus birinapant treatment is determined by both TNF and MDR1 expression.

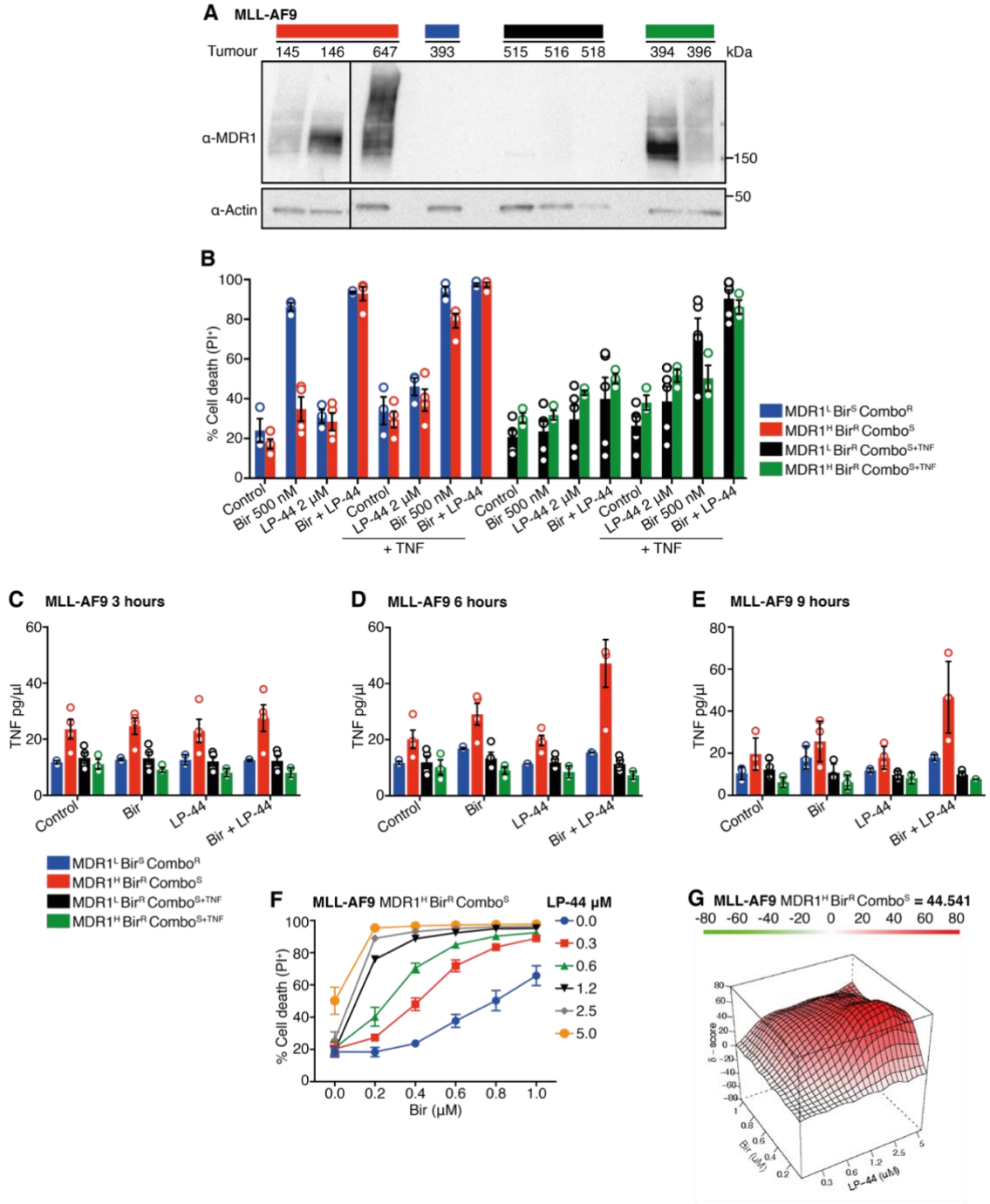
A MLL-AF9
Tumour 145 146 647 393 515 516 518 394 396 kDa
α-MDR1
α-Actin
150
50
B
% Cell death (PI+)
Control
Bir 500 nM
LP-44 2 μM
Bir + LP-44
+ TNF
MDR1L BirS ComboR
MDR1H BirR ComboS
MDR1L BirR ComboS+TNF
MDR1H BirR ComboS+TNF
C MLL-AF9 3 hours
D MLL-AF9 6 hours
E MLL-AF9 9 hours
TNF pg/μl
Control
Bir
LP-44
Bir + LP-44
F MLL-AF9 MDR1H BirR ComboS
LP-44 μM
0.0
0.3
0.6
1.2
2.5
5.0
% Cell death (PI+)
Bir (μM)
G MLL-AF9 MDR1H BirR ComboS = 44.541
-80 -60 -40 -20 0 20 40 60 80
δ - score
Bir (μM)
LP-44 (μM)

Figure 5.17 TNF and MDR1 expression are biomarkers of LP-44 and birinapant treatment response in AML

(**A**) Western blot analysis of MDR1 in different MLL-AF9 AML sub-groups (reiterated from Chapter 3). (**B**) $MDR1_L$, birinapant-sensitive (Bir_S), combination-resistant ($Combo_R$) (blue bars); $MDR1_H$, birinapant-resistant (Bir_R), combination-sensitive ($Combo_S$) (red bars); $MDR1_L$, Bir_R, $Combo_{S+TNF}$ (black bars) and $MDR1_H$, Bir_R, $Combo_{S+TNF}$ (green bars) AML cells were treated with LP-44 (2 μM) ± birinapant (500 nM) ± TNF (100 ng/mL) for 24 hours (1-2 independent tumours for each sub-group, with 2-3 repeats, error bars SD). (**C-E**) TNF production in the four MLL-AF9 AML sub-groups was determined by ELISA. Cells were treated with LP-44 (2 μM) ± birinapant (500 nM) for (**C**) 3, (**D**) 6 and (**E**) 9 hours (1-2 independent tumours for each sub-group, with 2-3 repeats, error bars SD). (**F**) $MDR1_H Bir_R Combo_S$ MLL-AF9 AML cells were treated with LP-44 (0.3, 0.6, 1.2, 2.5 and 5 μM) ± birinapant (0.2, 0.4, 0.6, 0.8, 1 μM) for 24 hours (n=3, error bars SEM). (**G**) Bliss synergy analysis was calculated for $MDR1_H Bir_R Combo_S$ MLL-AF9 AMLs as treated in (F). Data presented as mean ± SD throughout unless otherwise stated. Cell death was measured by propidium iodide (PI) uptake, decrease of cell volume and flow cytometry.

Having observed the correlation between TNF and MDR1 expression and the response of leukaemias to LP-44 plus birinapant treatment, I tested whether these findings also applied to the LP-12 plus birinapant combination. I treated $MDR1_{H}Bir_{R}Combo_{S}$ MLL-AF9 and $MDR1_{L}$ MLL-ENL AML cells with LP-12 plus birinapant treatment. Similar to findings with LP-44, LP-12 synergistically increased cell death mediated by birinapant in $MDR1_{H}Bir_{R}Combo_{S}$ MLL-AF9 cells to a greater extent than in the $MDR1_{L}$ MLL-ENL cells (BSS 34.3 and 8.8 respectively; **Figure 5.18A-D**).

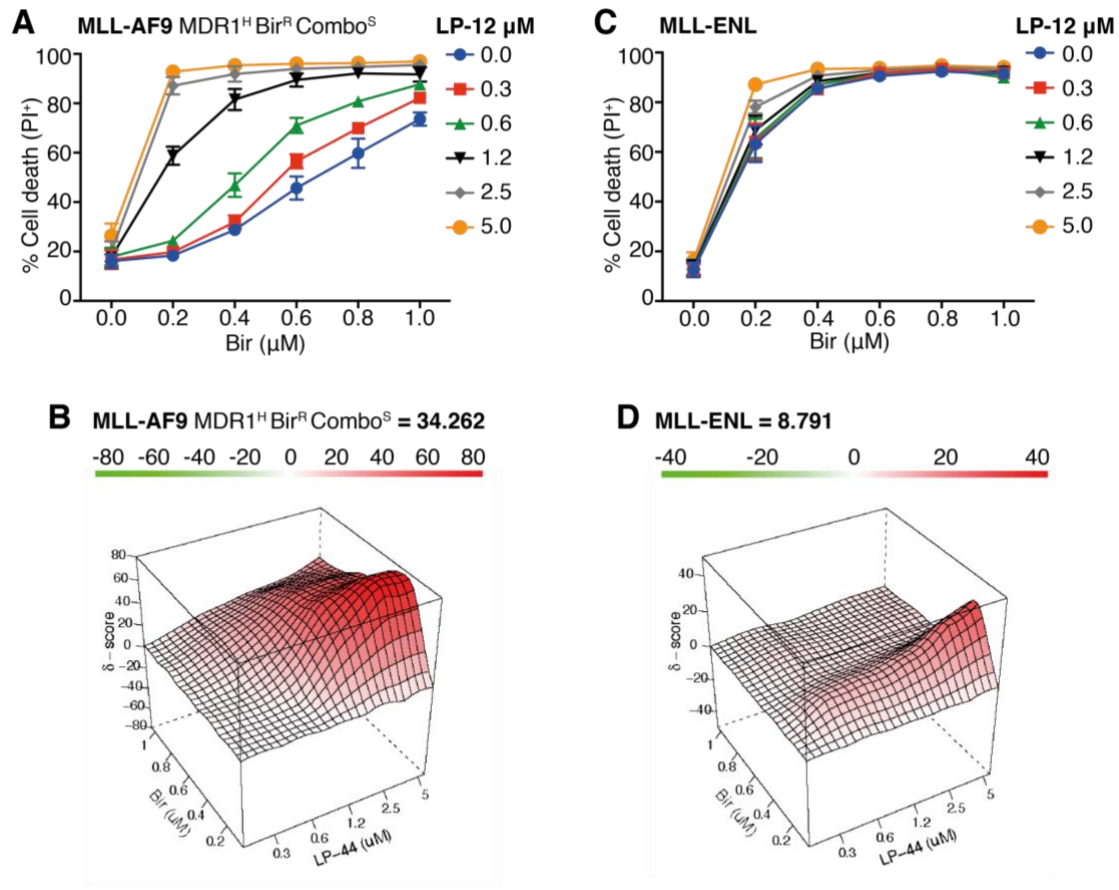

Figure 5.18 MDR1 expression correlates inversely with response to LP-12 plus birinapant treatment in AML

(**A**) MLL-AF9 MDR1$_H$Bir$_R$Combo$_S$ AML cells were treated with LP-12 (0.3, 0.6, 1.2, 2.5 and 5 µM) ± birinapant (0.2, 0.4, 0.6, 0.8, 1 µM) for 24 hours and (**B**) bliss synergy score (BSS) analysis calculated. (**C**) MDR1$_L$ MLL-ENL AML cells were treated as described in (A) and (D) BSS analysis calculated. Data presented as mean ± SEM throughout (2-4 independent tumours, repeated 1-3 times). Cell death was measured by propidium iodide (PI) uptake, decrease of cell volume (MLL-AF9-Nras$_{G12D}$) and flow cytometry.

5.17 LP-44 plus Birinapant Combination Therapy is not Toxic to Wild-type Bone Marrow

As described in Chapter 3, a limiting factor in developing novel AML therapies for the clinic is their potential toxicity towards healthy bone marrow, in particular HSPCs. In Chapter 3 we established the safety of the MDR1 inhibitor plus birinapant combination treatment in murine and human HSPCs (Chapter 3 **Figures 6A and 7B**). However, as LP-44 is a pre-clinical compound, with unique physico-chemical properties to the clinical MDR1 inhibitors tested, analysis of this combination's toxicity towards wild-type bone marrow (WT-BM) cells and HSPCs is warranted. To determine the safety potential of the LP-44 plus birinapant combination treatment, we treated whole WT-BM from C57BL/6 mice with LP-44 and birinapant alone or in combination for 24 and 48 hours. At both time points, there was no toxicity observed for either LP-44, birinapant or the combination in WT-BM cells (**Figure 5.19A**). In contrast, the chemotherapy Ara-c was very toxic towards these cells (**Figure 5.19A**). To confirm activity of the compounds, HoxA9/Meis1 AML cells were treated alongside WT-BM cells (**Figure 5.19A**). The most important population within the haematopoietic system, responsible for regeneration of all cell types, are the HSPCs, which are described as having expression of c-KIT (Oguro et al., 2013). To investigate the toxicity of LP-44 plus birinapant combination towards these cells, we treated whole WT-BM with the combination and analysed cell death in the c-KIT+ population at 24 and 48 hours. There was no toxicity observed with single or combination treatments, however as expected, the chemotherapy Ara-c was very toxic towards these cells (**Figure 5.19B**) (Chapter 3 **Figure 6A** and (Brumatti et al., 2016)). Together these data

suggest treatment with LP-44 and birinapant specifically targets cancer cells, sparing healthy c-KIT+ HSPCs of toxic effects.

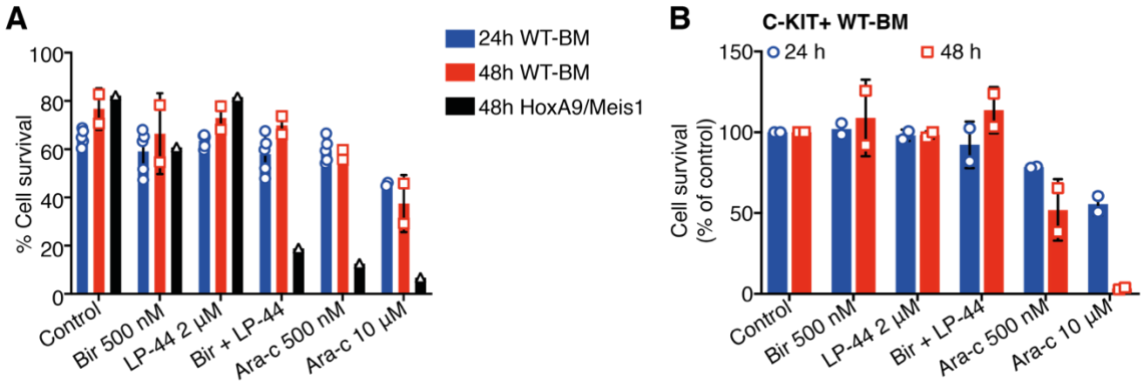

Figure 5.19 LP-44 and birinapant combination therapy is not toxic to wild type bone marrow cells

(**A**) Wild type bone marrow (WT-BM) (n=2-5 independent samples) and HoxA9/Meis1 cells (n=1) were treated with LP-44 (2 µM) ± birinapant (500 nM) or Ara-c (500 nM or 10 µM) for 24 and 48 hours. (**B**) WT-BM cells were treated as described in (A) and samples were analysed by flow cytometry at 24 and 48 hours for c-KIT positivity. (n=2 independent samples). Data presented as mean ± SD throughout. Cell survival was measured by propidium iodide (PI) exclusion, decrease of cell volume and flow cytometry. Data presented as survival, percent of control (B).

5.18 Treatment with Birinapant in Combination with LP-44 is Not Toxic and is Tolerated *In Vivo*

Having established the tolerability of LP-44 plus birinapant treatment towards healthy BM and HSPCs, I next assessed its toxicity in an *in vivo* model. Establishing *in vivo* safety of a novel combination is an important consideration in order to investigate its ability to be translated to the clinic. As discussed in the introduction, the safety of birinapant as a single-agent in murine studies *in vivo* and in human clinical trials has already been established (Amaravadi et al., 2015; Benetatos et al., 2014). Although LP-44 has been administered to mice systemically through intraperitoneal (IP) and intravenous (IV) injection, and directly into the brain through intra-cerebroventricular (ICV) injection, to our knowledge LP-44 has not entered human clinical trials (Di Pilato et al., 2014; Leopoldo et al., 2008; Naumenko et al., 2011). Therefore, to test whether the LP-44 plus birinapant combination was tolerated, we treated healthy C57BL/6 mice with the combination 3 times a week for 4 weeks, and analysed mice immediately after completion of treatment (acute toxicity) or 5 weeks after treatment had ceased (chronic toxicity) (**Figure 5.20A**). Mice did not show any signs of distress following injections. The LP-44 plus birinapant combination groups' body weights were not significantly different to the control groups, either immediately upon completion of the treatment regime (acute) or 5 weeks later (chronic) (**Figure 5.20B**). Overall, the platelet counts were not significantly affected (**Figure 5.20C**), and although there was an increase in white blood cells in the birinapant treated groups immediately after completion of treatment, this subsided after 5 weeks (**Figure 5.20D**). Similarly, despite some variation in liver, spleen and thymus weights between acute and chronic groups, there was not a significant difference

between control and LP-44 plus birinapant groups at these time points (**Figure 5.20E-G**). Furthermore, histological analysis of spleen, liver and sternum indicated no difference between treatment groups at both time points (**Figure 5.21A**). While only a small number of mice were tested, these results indicate that the combination of LP-44 plus birinapant is well tolerated *in vivo*.

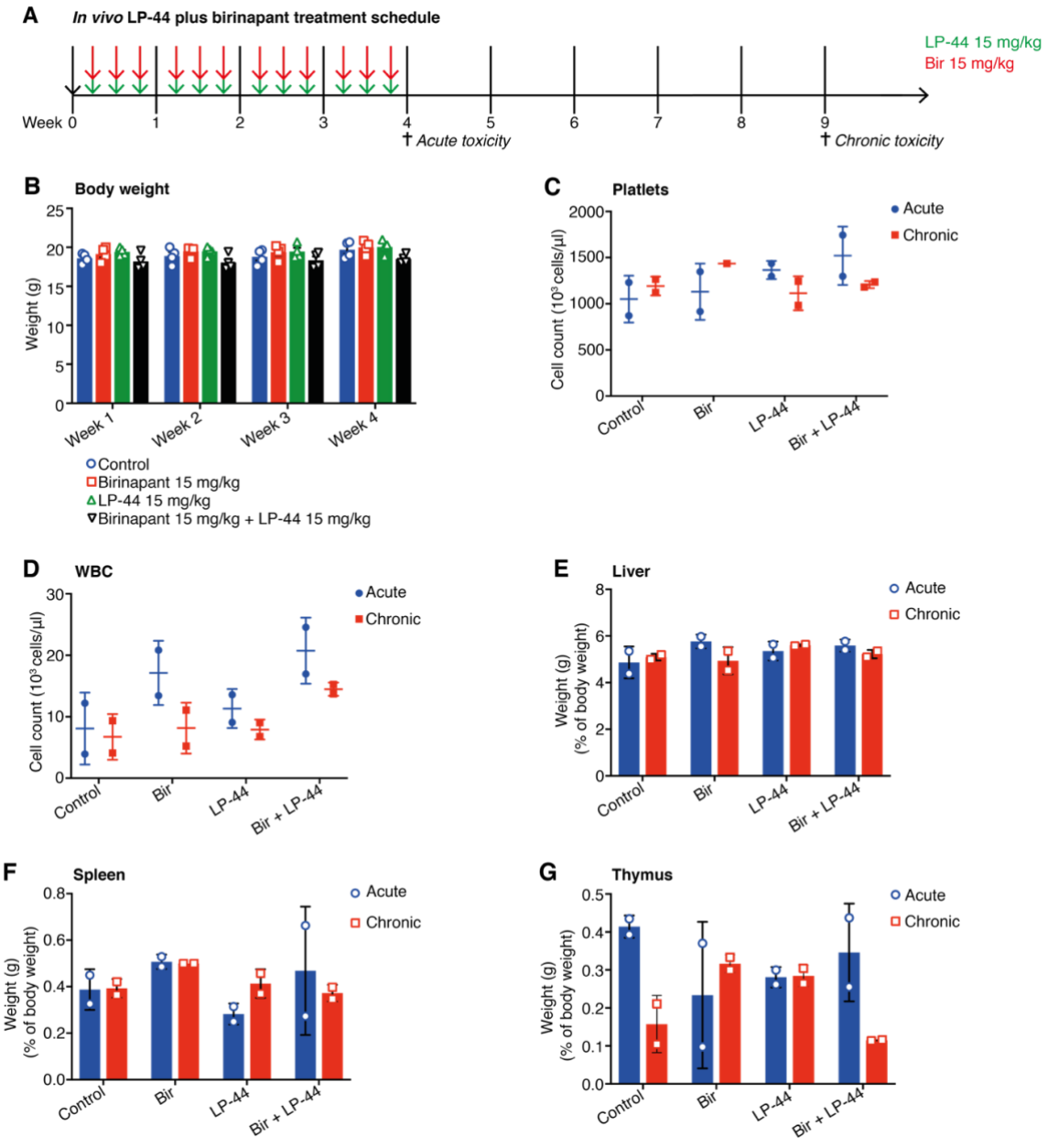

Figure 5.20 Treatment with LP-44 plus birinapant is not toxic and is well tolerated by mice *in vivo*

(**A**) C57BL/6 mice were treated with birinapant 15 mg/kg ± LP-44 15 mg/kg for 4 weeks and analysed immediately following completion of treatment (acute toxicity) or after 5 weeks (chronic toxicity). (**B**) Body weights of mice during the 4 weeks of treatment. (**C**) Platelets and (**D**) white blood cell (WBC) counts at both time points. (**E**) Liver, (**F**) spleen and (**G**) thymus weight measurements at both time points. Data presented as mean ± SD throughout (n=2, one experiment)

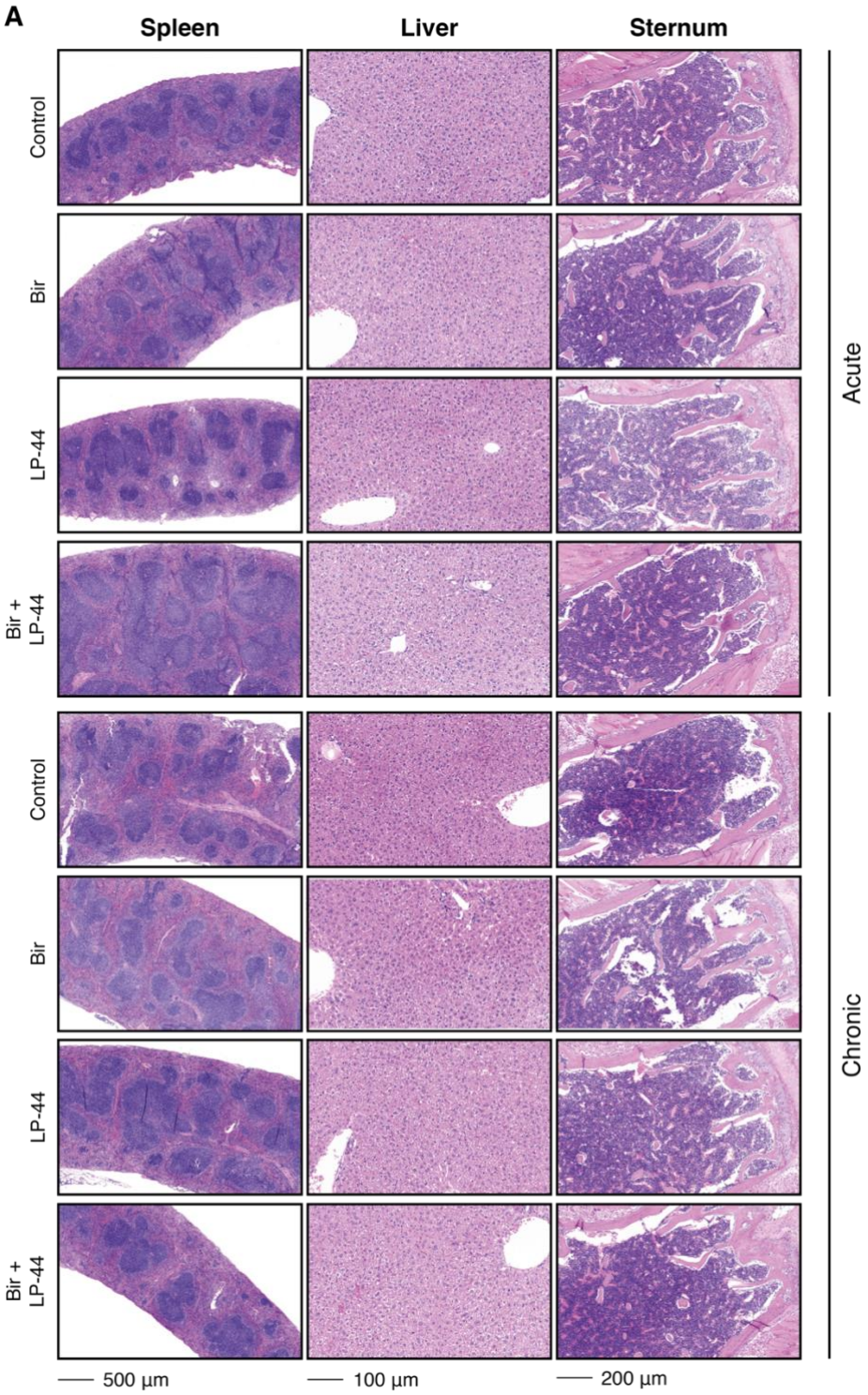

Figure 5.21 Histological analysis of LP-44 plus birinapant treated mice

(**A**) Histological analysis of C57BL/6 mice treated with birinapant 15 mg/kg ± LP-44 15 mg/kg for 4 weeks and analysed immediately following completion of treatment (acute toxicity) or 5 weeks after cessation of treatment (chronic toxicity). Organs analysed were spleen (500 µm), liver (100 µm) and sternum (200 µm). Representative images.

5.19 Validation of Alternative Psychoactive High Throughput Screen Hit Compounds

Surprisingly, the data above shows that the psychoactive compounds LP-44 and LP-12 can inhibit MDR1, leading to a dramatic increase in cell death when these compounds are combined with the Smac-mimetic birinapant. As mentioned in the beginning of this Chapter, half of the compounds identified through the high throughput screen were psychoactive. Therefore, I was very interested in investigating the mechanisms of synergy the other psychotropic drugs, fluphenazine, SDZ 21009, GR-127935 and CGP-71683, use to potentiate birinapant-mediated cell death. As fluphenazine has already been described to inhibit MDR1 function (Ford et al., 1989; Jaszczyszyn et al., 2012), I hypothesised it would share the same mechanism of synergy as reserpine and LP-44. However, due to the distinct chemical and structural characteristics of the remaining compounds, and their lack of previously described MDR1 inhibition potential, I hypothesised that these compounds would not inhibit MDR1 and would synergise with birinapant via different mechanisms. To test this hypothesis, I used the Rho-123 retention assay in KG1 control and KG1 *MDR1*$^{-/-}$ cells to investigate the ability of these compounds to inhibit MDR1. Importantly, I also performed cell death assays in these cells to investigate whether MDR1 inhibition contributes to synergistic cell death when these psychoactive compounds are combined with birinapant.

5.20 Fluphenazine dihydrochloride's Inhibition of MDR1 Potentiates Birinapant Killing

Fluphenazine dihydrochloride (also known as Prolixin) was approved by the FDA in 1967 and has been used exstensively for decades for the management of manifestastions of psychotic disorders (High et al., 1960). Fluphenazine's antipsychotic capacity, including de-escalation of schizophrenia-associated hallucinations and delusions, is due to its ability to inhibit the postsynaptic dopamine D2 receptors in the limbic system, cortical system and basal ganglia (High et al., 1960). In addition to acting on the dopaminergic system, it can also inhibit the serotonin receptor 1B (5-HT_{1B}) (NCI, 2019). Fluphenzine is a member of the oldest synthetic antipsychotic drug family called the phenothiazines, which includes the drug thioridazine (High et al., 1960; Jaszczyszyn et al., 2012) (**Figure 5.22A**). This class of antipsychotic drugs have been established to possess anti-proliferative and potential MDR1 inhibitory effects (Ford et al., 1989; Ganapathi et al., 1991; Jaszczyszyn et al., 2012). Fluphenazine could inhibit MDR1 in KG1 control cells, albeit only at the highest concentration of 10 μM and had no effect in KG1 *MDR1*$^{-/-}$ cells (**Figure 5.22B**). Of note, even at the highest concentration of fluphenazine (10 μM), the level of Rho-123 intensity was less in KG1 control cells compared to KG1 *MDR1*$^{-/-}$ cells. This indicates fluphenazine is unable to completely inhibit MDR1 at these concentrations (**Figure 5.22B**). To interrogate the potential of fluphenazine to sensitise leukaemia cells to birinapant treatment independent of MDR1, KG1 control and *MDR1*$^{-/-}$ AML cells were treated with the fluphenazine plus birinapant (**Figure 5.22C**). Lower concentrations of fluphenazine, that were unable to inhibit MDR1 in the Rho-123 efflux assay, were also unable to increase birinapant-mediated cell death in KG1 control cells. In

contrast, 10 μM of fluphenazine increased cell death in these cells (**Figure 5.22C**). Furthermore, there was no increase in cell death in KG1 *MDR1*$^{-/-}$ AML cells with the combination treatment at all concentrations tested (**Figure 5.22C**). Together these data indicate fluphenazine inhibits MDR1 and the increase in birinapant-mediated cell death observed is likely to be due to MDR1 inhibition. However, fluphenazine has previously been used clinically in humans up to 800-1,200 mg per day (Itil et al., 1970; Quitkin et al., 1975). As these dosages would equate to being greater than 10 μM *in vitro*, it would be reasonable to test higher concentrations of fluphenazine to see whether this would enhance its MDR1 inhibition potential and therefore ability to synergise with birinapant.

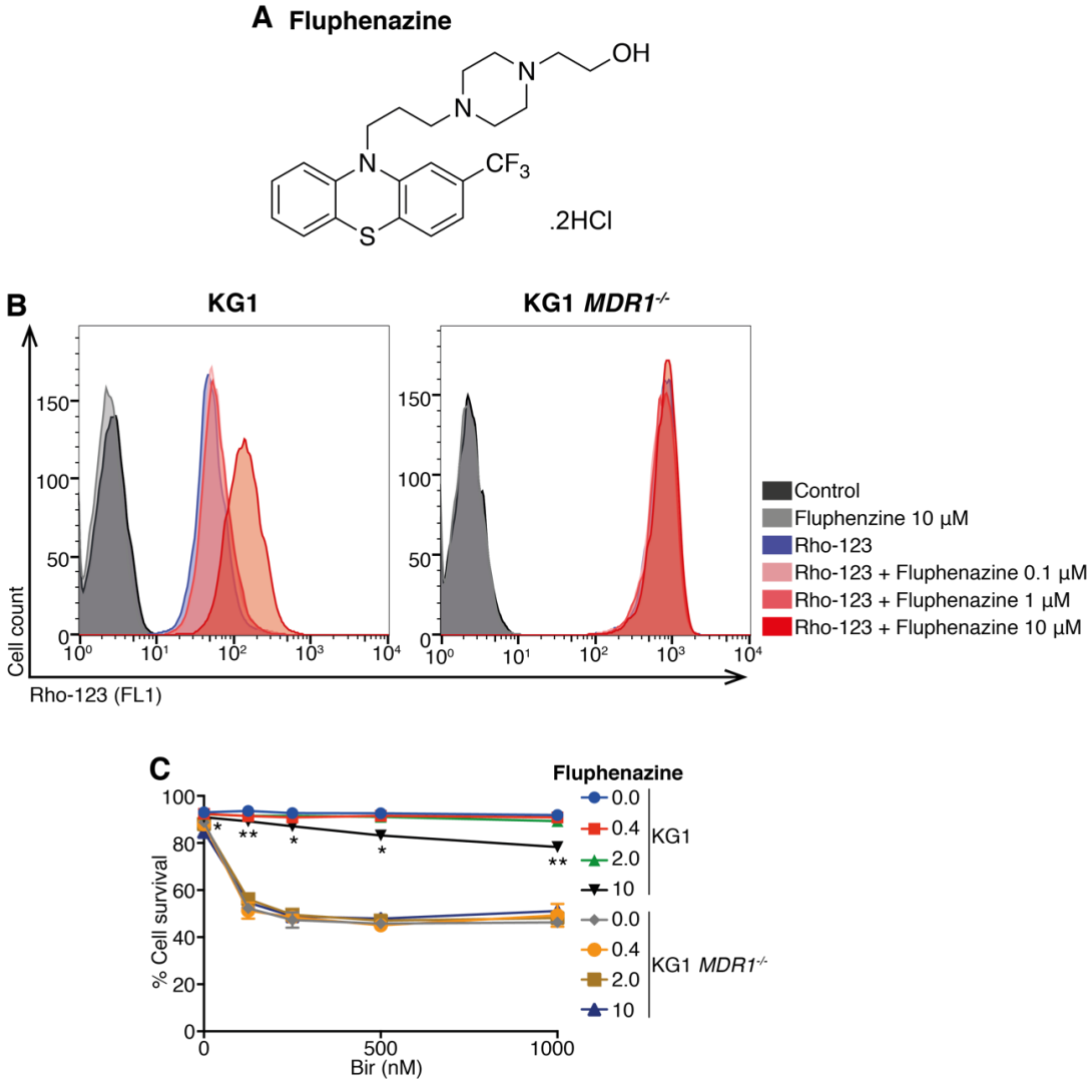

Figure 5.22 Fluphenazine dihydrochloride's inhibition of MDR1 potentiates birinapant killing

(**A**) Structure of Fluphenazine dihydrochloride (fluphenazine). (**B**) KG1 control and KG1 *MDR1*$^{-/-}$ AML cells were pre-treated with Rhodamine-123 (Rho-123) 250 nM ± 0.1, 1 or 10 µM of fluphenazine for 2 hours. Rho-123 florescence was analysed by flow cytometry (FL1 channel). (**C**) KG1 control and KG1 *MDR1*$^{-/-}$ AML cells were treated with fluphenazine (0, 0.4, 4 and 10 µM) ± birinapant (125, 250, 500 and 1000 nM) for 48 hours (n=2). Data are presented as mean ± SD throughout. Cell survival was measured by propidium iodide (PI) exclusion, decrease of cell volume and flow cytometry. P values calculated with Multiple t tests were obtained by comparison of birinapant alone and birinapant plus fluphenazine at the indicated concentrations.

5.21 SDZ 21009 can Inhibit MDR1 to Potentiate Birinapant-mediated Cell Death

SDZ 21009 (also known as Carpindolol) is a β-adrenoceptor blocker, however it is also a high affinity antagonist towards serotonin receptors 5-HT_{1A} and 5-HT_{1B} (**Figure 5.23A**) (Hoyer et al., 1985). SDZ 21009 has been used to establish the role of 5-HT_{1A} receptors in the anticonflict effect. This has been achieved by using the anticonflict drinking test paradigm, an experiment that can evaluate a drugs ability to act as an anxiolytic (Chojnacka-Wójcik and Klodzińska, 1992; Chonjnacka-Wójcik and Przegalinski, 1991; Molderings et al., 1990). SDZ 21009 was another compound that synergised with birinapant to kill AML cells in our screen, but to confirm that SDZ 21009 did increase birinapant-mediated killing, I treated HoxA9/Meis1, MLL-AF9 and MLL-AF9-$Nras_{G12D}$ AML cells with a titration of SDZ 21009 and a fixed concentration of birinapant (**Figure 5.23B-D**). All leukaemias tested were resistant to birinapant single-agent treatment and addition of SDZ 21009 significantly increased killing (**Figure 23B-D**). To date, SDZ 21009 has not been reported to inhibit MDR1, however somewhat surprisingly, SDZ 21009 was yet another compound that was able to inhibit MDR1 at concentrations of 1 and 10 μM in KG1 control cells as determined through Rho-123 retention assay (**Figure 5.23E**). As seen with the previous MDR1 inhibitory compounds, SDZ 21009 at higher concentrations was able to enhance birinapant killing in KG1 control cells but no change was observed in the KG1 *MDR1*$^{-/-}$ AML cells (**Figure 5.23F**). These results indicate that yet another psychoactive compound identified through the high throughput screen is able to inhibit MDR1 to sensitise AML cells to birinapant-mediated killing.

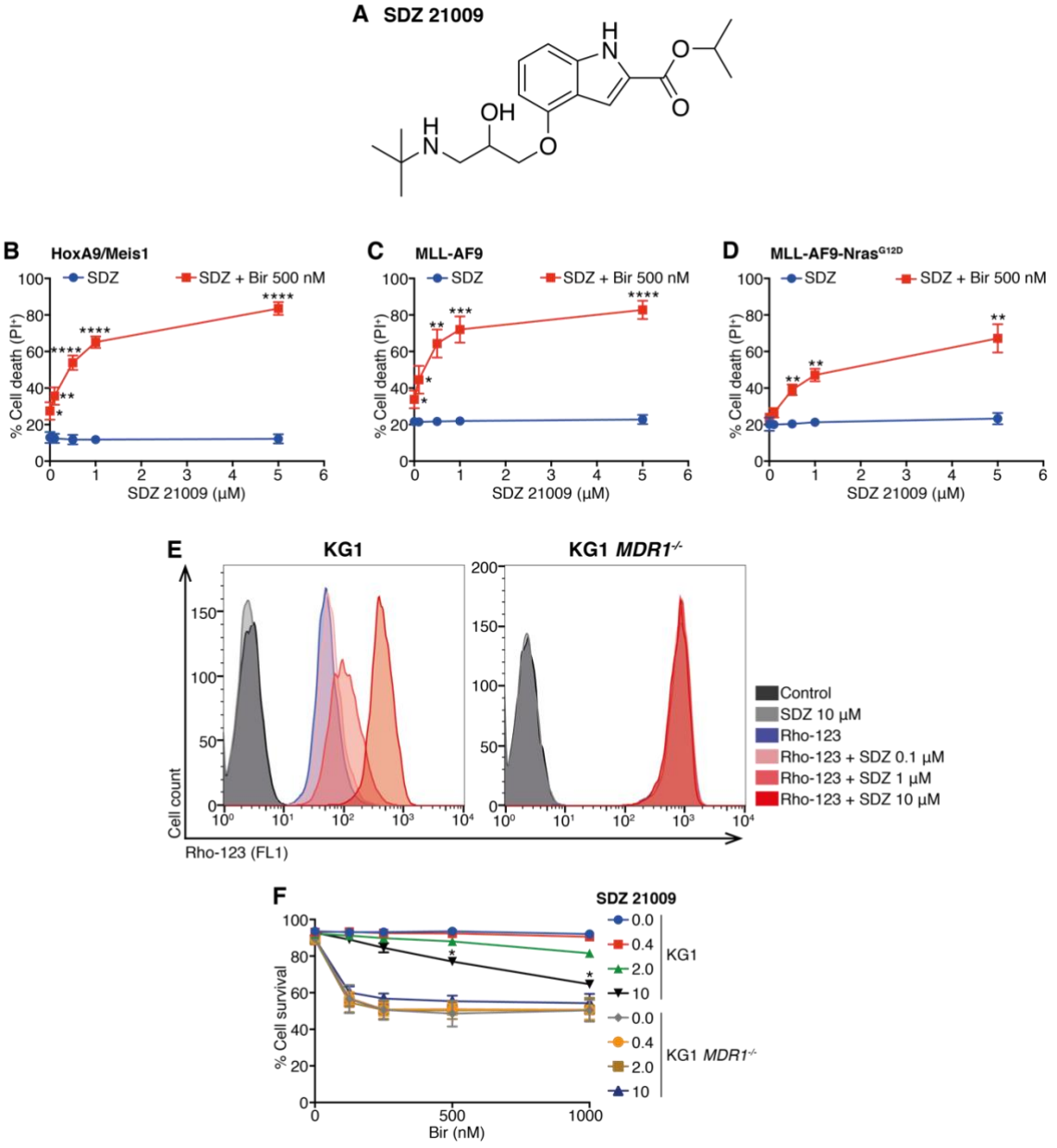
A SDZ 21009
B HoxA9/Meis1
C MLL-AF9
D MLL-AF9-Nras^{G12D}
SDZ
SDZ + Bir 500 nM
% Cell death (PI+)
SDZ 21009 (μM)
E
KG1
KG1 MDR1-/-
Cell count
Rho-123 (FL1)
Control
SDZ 10 μM
Rho-123
Rho-123 + SDZ 0.1 μM
Rho-123 + SDZ 1 μM
Rho-123 + SDZ 10 μM
F
SDZ 21009
0.0
0.4
2.0
10
KG1
KG1 MDR1-/-
% Cell survival
Bir (nM)

Figure 5.23 SDZ 21009 can inhibit MDR1 to potentiate birinapant-mediated cell death

(**A**) Structure of SDZ 21009. (**B**) HoxA9/Meis1 (n=5), (**C**) MLL-AF9 (n=6) and (**D**) MLL-AF9-$Nras_{G12D}$ (n=4) AML cells were treated with SDZ 21009 (SDZ) (0.1, 0.5, 1 and 5 μM) ± birinapant (500 nM) for 24 hours (3-5 independent tumours, repeated 1-2 times). (**E**) KG1 control and KG1 *MDR1*$^{-/-}$ AML cells were pre- treated with Rhodamine-123 (Rho-123) 250 nM ± 0.1, 1 or 10 μM of SDZ for 2 hours. Rho-123 florescence was analysed by flow cytometry (FL1 channel). (**F**) KG1 control and KG1 *MDR1*$^{-/-}$ AML cells were treated with SDZ (0, 0.4, 4 and 10 μM) ± birinapant (125, 250, 500 and 1000 nM) for 48 hours (n=2, error bars SD). Data are presented as mean ± SEM throughout unless otherwise stated. Cell survival was measured by propidium iodide (PI) exclusion or cell death was measured by PI uptake, decrease of cell volume and flow cytometry. P values calculated with Multiple t tests were obtained by comparison of birinapant alone and birinapant plus SDZ 21009 at the indicated concentrations.

5.22 GR-127935 can Inhibit MDR1 to Potentiate Birinapant-mediated Cell Death

Similar to LP-44 and SDZ 21009, which mediate their psychoactive effects by modulating serotonin signalling pathways, GR-127935 is a potent and selective inhibitor of 5-HT_{1D} and 5-HT_{1B} receptors (**Figure 5.24A**) (Skingle et al., 1995). In guinea pigs, GR-127935 antagonism of the 5-HT_{1B} and 5-HT_{1D} receptors has been shown to produce an antidepressant effect, measured by the latency to immobility in the forced swim test, an assay that can identify treatments with antidepressant effects (Porsolt et al., 1978; Porsolt et al., 1977; Rex et al., 2008). To date, GR-127935 has also not been reported to have MDR1 inhibition potential. However, in a Rho-123 retention assay, GR-127935 was able to inhibit MDR1 in KG1 control cells at 2 and 10 μM and it had no effect in KG1 *MDR1*$^{-/-}$ AML cells (**Figure 5.24B**). GR-127935 induced killing of KG1 control and KG1 *MDR1*$^{-/-}$ AML cells as a single-agent at 10 μM (**Figure 5.24C**). It was not toxic as a single-agent at 2 μM and increased birinapant-mediated killing in KG1 control but not in KG1 *MDR1*$^{-/-}$ AML cells (**Figure 5.24C**). These data indicate that the antidepressant compound GR-127935 can also act as a MDR1 inhibitor, leading to the potentiation of cell death when combined with birinapant.

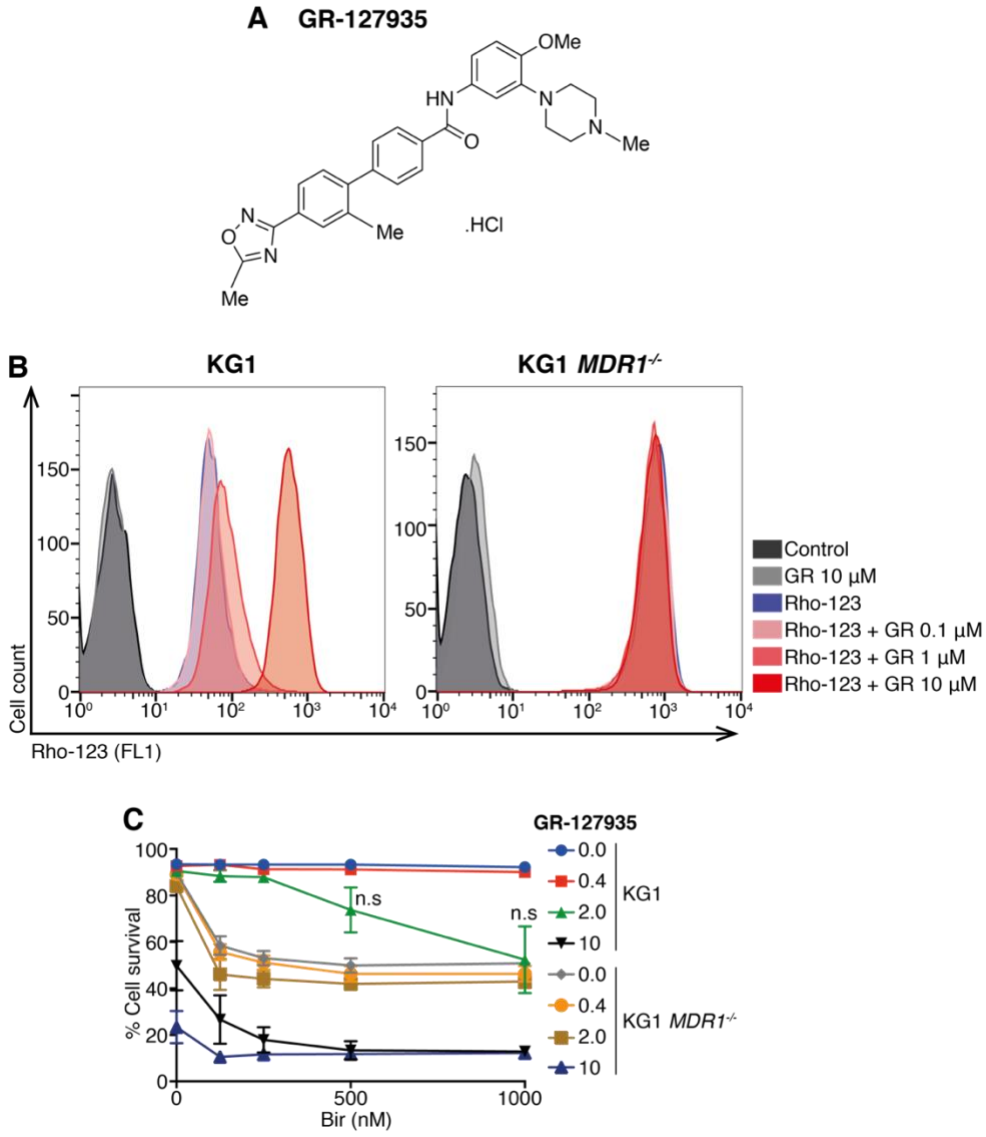

Figure 5.24 GR-127935 can inhibit MDR1 to potentiate birinapant mediated-cell death

(**A**) Structure of GR-127935. (**B**) KG1 control and KG1 *MDR1*$^{-/-}$ AML cells were treated with Rhodamine-123 (Rho-123) 250 nM ± 0.1, 1 or 10 µM of GR-127935 (GR) for 2 hours. Rho-123 florescence was analysed by flow cytometry (FL1 channel). (**C**) KG1 control and KG1 *MDR1*$^{-/-}$ AML cells were treated with GR-127935 (0, 0.4, 4 and 10 µM) ± birinapant (125, 250, 500 and 1000 nM) for 48 hours (n=3-4). Data are presented as mean ± SEM throughout. Cell survival was measured by propidium iodide (PI) exclusion, decrease of cell volume and flow cytometry. P values calculated with Multiple t tests were obtained by comparison of birinapant alone and birinapant plus GR-127935 at the indicated concentrations.

5.23 CGP-71683 can Inhibit MDR1 to Potentiate Birinapant-mediated Cell Death

All psychoactive compounds tested so far identified by the high throughput screen inhibited MDR1 and it appears to be this activity that enables their synergism with birinapant, although we cannot discount that their alternative activities may also contribute to killing. Following these findings, I next tested CGP-71683 to investigate whether it too could inhibit MDR1. Neuropeptide Y (NPY) is one of the most prevalent peptides in the brain and its action through 8 different receptors (Y_1-Y_8) regulates a range of physiological functions including stress, anxiety and feeding behaviours (Reichmann and Holzer, 2016). CGP-71683 is a potent and specific antagonist towards the Y_5 receptor and has been shown to inhibit food intake in rodents (**Figure 5.25A**) (Criscione et al., 1998; Dumont et al., 2000). As measured through the Rho-123 retention assay, CGP-71683 could inhibit MDR1 only at the highest concentration tested (10 μM) (**Figure 5.25B**). Similar to fluphenazine, even at this concentration, CGP-71683 could not completely inhibit MDR1 in KG1 control cells, resulting in a lower Rho-123 intensity detected compared to KG1 *MDR1*$^{-/-}$ cells. Birinapant-mediated cell death in KG1 control cells, but not KG1 *MDR1*$^{-/-}$ cells, was dramatically increased with the addition of CGP-71683 10 μM. These data indicate CGP-71683 can inhibit MDR1 and that it is this activity that is responsible for birinapant-mediated combination synergy. Furthermore, together these findings highlight that psychoactive compounds identified through the screen, that act on distinct signalling pathways, can act as MDR1 inhibitors.

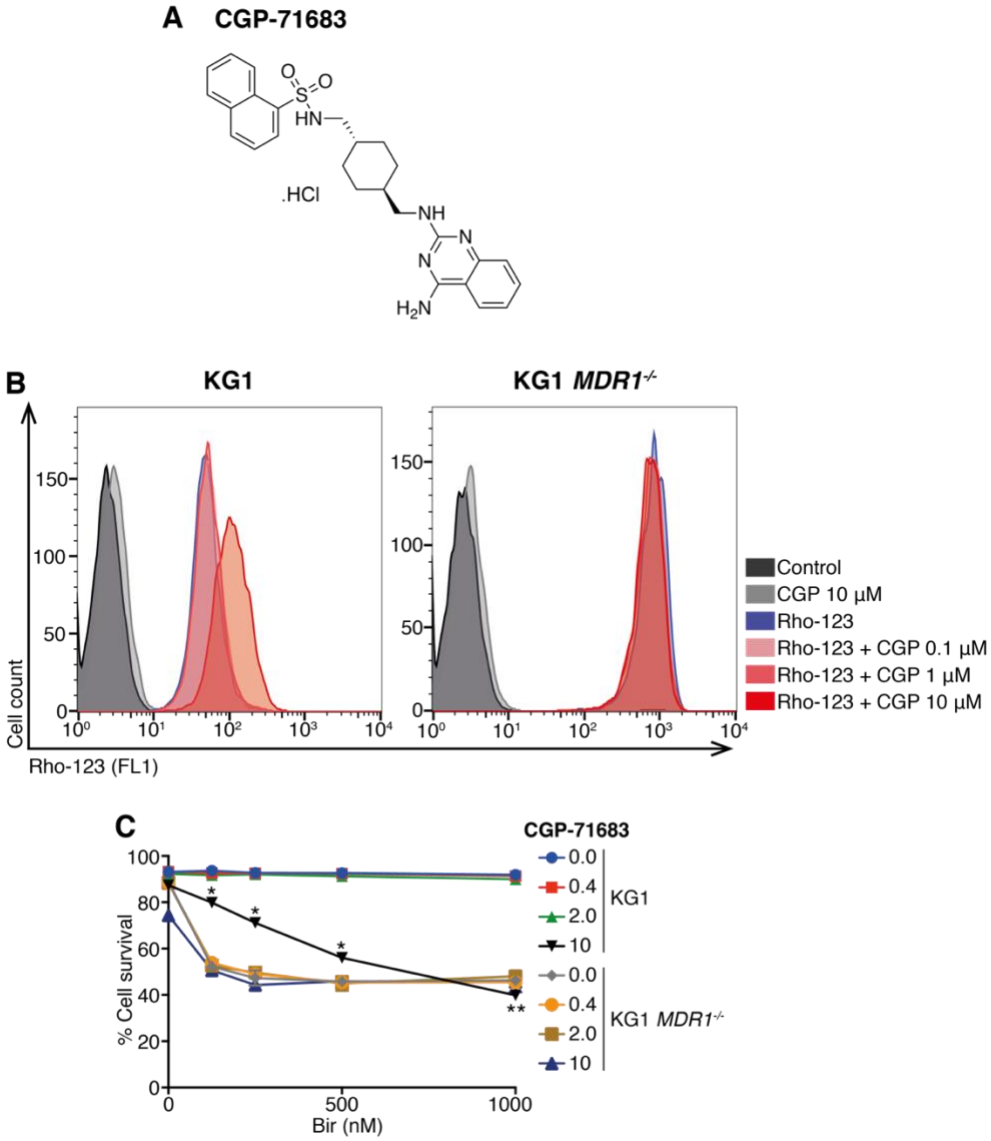

Figure 5.25 CGP-71683 can inhibit MDR1 to potentiate birinapant mediated-cell death

(**A**) Structure of CGP-7930. (**B**) KG1 control and KG1 *MDR1*$^{-/-}$ AML cells were pre-treated with Rhodamine-123 (Rho-123) 250 nM ± 0.1, 1 or 10 µM of CGP-7930 (CGP) for 2 hours. Rho-123 florescence was analysed by flow cytometry (FL1 channel). (**C**) KG1 control and KG1 *MDR1*$^{-/-}$ AML cells were treated with CGP (0, 0.4, 4 and 10 µM) ± birinapant (125, 250, 500 and 1000 nM) for 48 hours (n=2). Data are presented as mean ± SD throughout. Cell survival was measured by propidium iodide (PI) exclusion, decrease of cell volume and flow cytometry. P values calculated with Multiple t tests were obtained by comparison of birinapant alone and birinapant plus CGP-71683 at the indicated concentrations.

5.24 Conclusions

The fact that some clinical psychoactive drugs have anti-neoplastic effects has led to some of them being repurposed for anti-cancer treatment (Burgess, 2012; Cheng et al., 2015; Gil-Ad et al., 2004; Nordenberg et al., 1999; Sachlos et al., 2012). Suprisingly, out of the hundreds of different drug classes examined in the high throughput screen, half of the hit compounds were psychotropic. To understand novel mechanisms of resistance AML cells use to evade Smac-mimetic treatment, I investigated the mechanisms of action these compounds target to overcome birinapant resistance in AML. To date, I have tested half of the hit compounds and rather suprisingly, all of them inhibit MDR1, leading to potentiated birinapant-mediated cell death. This indicates that our screen was particularly adept at identifying MDR1 inhibitors and underlines that MDR1 expression is a key determinant of whether a cell is resistant to the cytotoxic affects of birinapant.

In this Chapter, I focused on LP-44, a 5-HT_7 receptor agonist that has antidepressant activity (Di Pilato et al., 2014; Leopoldo et al., 2004). LP-44 was able to synergise with birinapant and other monovalent and bivalent Smac-mimetics in primary murine AML cells, but could not potentiate killing mediated by the peptide-mimetics JQ1 and ABT-199 or the chemotherapy Ara-c. Agonist activation of the 5-HT_7 receptor leads to activation of the canonical signalling pathway, resulting in the activation of multiple signalling cascades, including the MAPK/ERK pathway (Errico et al., 2001; Guseva et al., 2014b; Johnson-Farley et al., 2005). My observation that LP-44 plus birinapant treatment reduced the

level of phosphorylated ERK detected by Western blotting, led me to investigate the role of the Ras-Raf-MEK-ERK pathway in combination-mediated killing. Addition of the MEK inhibitors, U0126 or PD098059, to LP-44 plus birinapant treatment, did not change or increase combination-mediated killing, suggesting the ERK/MAPK signalling pathway does not play an essential role in this type of cell death.

Due to the similarities observed between the LP-44 plus birinapant and the MDR1 inhibitor plus birinapant combinations (discussed in Chapter 3), I hypothesised that LP-44 was also acting as an MDR1 inhibitor. My studies utilising the previously generated KG1 control and KG1 *MDR1*$^{-/-}$ AML cells in Rho-123 retention assays and cell death assays, confirmed this hypothesis. Similar to the findings in Chapters 3 and 4, combination of LP-44 and birinapant did not have acute or chronic toxicity and was tolerated by healthy C57BL/6 mice *in vivo*. Altogether these studies identified a novel function for the LP-44 and LP-12 compounds to inhibit MDR1, albeit to a lesser extent than the 3rd generation specific MDR1 inhibitor tariquidar. Furthermore, these studies identified that it is LP-44/12's inhibition of MDR1 that allows for their synergisitic combination with birinapant to potentiate cell death.

Fluphenazine dihydrochloride, SDZ 21009, GR-127935 and CGP-71683 are structurally distinct psychoactive drugs that act on the dopamine, serotonin or neuropeptide Y signalling pathways. Fluphenazine is a member of the phenothiazine class of antipsychotics and has previously been described to

inhibit MDR1 function (Ford et al., 1989; Ganapathi et al., 1991). In contrast SDZ 21009's, GR-127935's and CGP-71683's activity towards MDR1 has not been previously reported. Following the surprising findings with LP-44 and LP-12, my studies using KG1 control and KG1 *MDR1*$^{-/-}$ cells confirmed all four of these compounds can inhibit MDR1 to potentiate birinapant-mediated cell death. Given the structurally distinct nature of these drugs, it is quite surprising that all of them are MDR1 inhibitors. Some studies have noted that several antipsychotics have MDR1 activity and that this might affect differences in the concentration of these drugs in the brain. Additionally, a study has shown that the concentration and efficacy of antipsychotic medication in schizophrenic patients is affected by their *ABCB1* genotype (the gene for MDR1) (Moons et al., 2011; Vijayan et al., 2012). Therefore, my findings described in this Chapter highlight the fact that some psychotropic drugs may be unaccounted for as MDR1 inhibitors and that this potential may affect their pharmacokinetics and bioavailability.

Altogether, the findings presented in this Chapter highlight the surprising result that all compounds validated from the high throughput screen so far inhibit MDR1. Despite previously published results showing that some psychotropic drugs are either substrates or inhibitors of MDR1, the frequency that we observed is thought provoking and raises the question of what percentage of psychotropic drugs inhibit MDR1. Furthermore, it prompts the question of how much their inhibition of MDR1 affects their activity and efficacy against their intended targets, such as serotonin and dopamine receptors. Our results also highlight the major contribution that MDR1 expression makes to the resistance of AML cells to

birinapant mediated killing and, as discussed in Chapter 3, opens up the possibility that this is an Achilles heel that can be exploited to treat cancer cells with high MDR1 expression, such as leukaemic stem cells and chemotherapy resistant cells.

6 Discussion and Future Directions

Chemoresistance is a common feature of AML and many other cancers, and is one of the main causes of disease relapse and poor patient survival (~30% at 5 years for AML) (NCI, 2016). High levels of IAPs have been linked to drug resistance in several cancers, including AML, and Smac-mimetic drugs that target IAPs, such as birinapant, have entered late phase clinical trials. Unfortunately, despite some promising results, the use of Smac-mimetics as a single-agent therapy, or in combination with anti-cancer treatments, has not been overwhelmingly successful. However, the high specificity of Smac-mimetics against cancer cells, resulting in a good safety profile, and their ability to elicit an anti-cancer immune response, means that there is still much interest in them. Therefore, a better understanding of the mechanisms that lead to Smac-mimetic resistance is crucial for their further progression in clinical trials.

6.1 Psychoactive Compounds and MDR1 Inhibition

In this study, using an unbiased screen of pre-clinical and clinical compounds, we identified MDR1 inhibitors as a class of drugs that can synergise with Smac-mimetics to overcome resistance. The compounds we identified were reserpine, LP-44, fluphenazine dihydrochloride, SDZ 21009, GR-127935 and CGP-71683. Of note, the screen compound library did not include specific MDR1 inhibitors, therefore, the compounds identified had off-target MDR1 inhibitory actions. Although reserpine and fluphenazine are known inhibitors of MDR1, this was a novel finding for the remaining four compounds. Interestingly, half of the compounds identified through the screen were psychoactive, that is they are able

to modify the brains functions to temporarily influence behaviour, mood, consciousness and perception (Gelenberg et al., 2013). It has been noted that some psychoactive drugs also have MDR1 inhibitory activity (Boulton et al., 2002; Moons et al., 2011; Wang et al., 2006). However, the frequency with which these psychoactive compounds were identified by our screen is still surprising. Out of the hundreds of different drug classes analysed in the high throughput drug-screening, all compounds validated synergised with birinapant through inhibition of MDR1. These findings emphasise that Smac-mimetic resistant AML cells are very sensitive to perturbations in MDR1 efflux and that MDR1 may be an Achilles heel to overcome resistance in AML cells.

Although the remaining 6 compounds identified through the screen are yet to be validated, research into their mechanisms of action indicates MDR1 may also play a role. The remaining compounds are not psychoactive and include manidipine (antihypertensive), terconazole (antifungal), MRS 1334 (adenosine A_3 receptor antagonist), epigallocathecin Octamethyl ether (green tea derivative), astemizole (antihistamine) and mebeverine hydrochloride (antispasmodic). Manidipine and astemizole are reported inhibitors of MDR1 (Keogh and Kunta, 2006; Takara et al., 2002). Epigallocatechin Octamethyl ether is a derivative of epigallocatechin gallate (ECEG), the main flavonoid present in green tea, which has been reported to inhibit MDR1 activity (Qian et al., 2005; Rodriguez-Proteau et al., 2006). Terconazole is an MDR1 substrate (Prasad et al., 2016) whilst, MRS 1134 and mebeverine hydrochloride have no reported MDR1 association. Further studies are required to investigate the mechanism of synergy these compounds

use to combine with birinapant, but it is tempting to suggest that inhibition of MDR1 may be a common mechanism between all compounds identified.

6.2 Clinical Relevance of MDR1 Association

Expression of MDR1 has been reported to be a predictor of treatment outcome in AML, with high levels of MDR1 being identified in over 50% of patients with relapse or secondary disease, for example MDS and t-AML (Beck et al., 1996a; Beck et al., 1996b; Leith et al., 1999; Mahadevan and List, 2004; Samdani et al., 1996; Schaich et al., 2005). Of note, clinical trials of new therapies are frequently performed in cancer patients that have failed conventional therapies and thus their tumours are more likely to present with high levels of MDR1 (Leith et al., 1999). This is an important finding because birinapant and other Smac-mimetics have been unsuccessfully trialed in MDS and AML relapse patients.

In order to overcome ABC transporter mediated resistance, a greater understanding of how these pumps select their substrates is required. Intriguingly, not all drugs are substrates of these pumps and those that are, are chemically and structurally diverse (Waghray and Zhang, 2017). This has prompted both the FDA and the European Medicines Agency to mandate that new anti-cancer drugs be assessed for interactions with MDR1 and other drug transporters (Giacomini et al., 2010). The fact that birinapant and other chemically distinct peptide-like IAP binding compounds synergised with MDR1 inhibitors (Hugle et al., 2019; Talbott et al., 2015), led to the hypothesis that other small peptide-like drugs might also be substrates of MDR1. And therefore, addition of an MDR1 inhibitor might potentiate these peptide-mimetic anti-cancer

drugs. Our tests with the clinical peptide-mimetic drugs ABT-199 (Bcl-2 inhibitor) and JQ1 (BET inhibitor) indicate that this is not, however, the case.

My studies clearly emphasise that it is paramount to assess whether a drug is an MDR1 inhibitor. Similar to understanding whether a drug is a substrate of MDR1, it is near impossible to predict whether a drug in an MDR1 inhibitor. Through our screen, we identified four psychoactive compounds, LP-44, GR-127935, SDZ 21009 and CGP-71683, to be novel MDR1 inhibitors through their off-target effects. Studies have shown drugs that inhibit MDR1 manipulate the concentration of themselves and other metabolites, including other drugs, within the human body (Vijayan et al., 2012). An example of how hidden MDR1 actions can be detrimental, is the combination of digoxin and quinidine, both are clinical antiarrhythmic drugs used for a range of heart conditions. Digoxin has a narrow therapeutic window and as an MDR1 substrate, is dependent on MDR1 function for its elimination. When these two drugs were combined, unexplained toxicities were observed due to an increase in the serum concentration of digoxin (Angelin et al., 1987; Bolme and Otto, 1977; Hedman et al., 1990; Pedersen et al., 1983a; Pedersen et al., 1983b; Pedersen et al., 1985). The discovery that quinidine can inhibit MDR1, provided a rational explanation for the observed clinical interaction (Koren et al., 1998). Therefore, our findings strengthen the apparent need to assess whether novel clinical compounds are MDR1 substrates and also their potential to act as MDR1 inhibitors.

The results presented in Chapters 3 and 5, indicate multiple structurally diverse Smac-mimetics can be potentiated by the addition of an MDR1 inhibitor. These include the monovalent AT-406 (Debio 1143) and bivalent AEG-40730 Smac-mimetics. Although there was some increase in cell death mediated by LCL161 with the addition of the MDR1 inhibitor tariquidar, this was not as synergistic and potent as observed with the other compounds. Therefore, this may indicate LCL161 is not pumped out of cells by MDR1 as effectively as other Smac-mimetic compounds. These findings prompt the discussion of whether a Smac-mimetic, that is not a substrate of MDR1, and which therefore is not affected by the presence of MDR1, would be a superior drug. Although immunity to pump efflux is deemed to be a desirable attribute for anti-cancer compounds, efficacy, safety, specificity and tolerability are other necessary qualities required for a successful anti-cancer drug. My results suggest that a drug that is an MDR1 inhibitor, but which is specific and well tolerated, can be safely combined with clinical MDR1 inhibitors. Furthermore, this regimen may even be a strategy to more selectively target cancers and particularly, leukaemic stem cells. Although a current barrier to this approach is that many people perceive MDR1 inhibitors to have irretrievably failed, because they increased toxicity of chemotherapy drugs (discussed below), hopefully my studies can cause a re-evaluation of this point of view.

6.3 Mechanism of Synergy

Regulation of cellular mechanisms other than drug efflux, including differentiation and cell survival, have been proposed as possible mechanisms by which inhibition of MDR1 may sensitise cells to chemotherapy (Fletcher et al., 2010).

To investigate the mechanism by which MDR1 inhibitors synergise with birinapant, we performed a quantitative analysis of the intracellular concentration of birinapant in MDR1$_H$ KG1 AML cells treated with tariquidar and birinapant. Using a heavy-labelled version of birinapant as an internal control, we used mass spectrometry to show that co-treatment of cells with birinapant and tariquidar tripled the intracellular levels of birinapant in MDR1$_H$ AML cells, compared to birinapant alone treated cells. These findings appear to indicate that regulation of birinapant efflux is the main mechanism by which MDR1 inhibitors enhance tumour cell killing. Moreover, these findings suggest that a 3-fold increase in the intracellular levels of birinapant is sufficient to dramatically increase cell death. However intriguingly, addition of tariquidar to birinapant in MDR1$_H$ KG1 AML cells results in a greater amount of cell death, compared to cells treated with a 3-fold increase in birinapant as a single-agent. This suggests that the 3-fold increase in the intracellular concentration of birinapant mediated by MDR1 inhibitors may be an underestimation. This may be due to technical limitations of the experimental analysis, such as a lack of accounting for cell death. Alternatively, these results may suggest that in parallel with increasing the intracellular concentration of birinapant within a leukaemia cell, MDR1 inhibitors also sensitise cells to death through alternative mechanisms.

6.4 Combination Specificity to MDR1

MDR1 is a member of the large ABC transporter family and fellow members such as ABCC1 and ABCG2, have also been implicated in multidrug and chemotherapy resistance (Fletcher et al., 2010). To establish the specificity of the birinapant plus MDR1 inhibitor drug combination, we tested the impact of

ABCC1/MRP1 and ABCG2/BCRP inhibition in AML cells subjected to Smac-mimetic treatment. Our results with the inhibitors reversan and Fum-C revealed that these transporters are likely to have no impact on birinapant induced killing of AML cells. Two caveats to interpreting these results is that we do not know whether ABCC1 and ABCG2 are expressed at meaningful levels in these cells. The second limitation is the lack of a positive control to confirm activity of the inhibitors reversan and Fum-C and therefore caution should be taken when interpreting negative results.

To mitigate the limitations of the pharmacological studies, we also implemented a genetic strategy to investigate the role of MDR1 in birinapant-mediated cell death. In Chapter 3, I described the development of KG1 *MDR1*$^{-/-}$ AML cells using the CRIPSR/Cas9 system. These cells, alongside their KG1 control partners, offer a unique tool to effectively and efficiently investigate the ability of novel compounds to inhibit MDR1. Tests with these cells revealed that genetic loss of *MDR1* can sensitise AML cells to birinapant single-agent treatment and addition of MDR1 inhibitors cannot enhance cell death, indicating synergy observed between birinapant and MDR1 inhibitors is specific to MDR1. Additional use of these cells in Chapter 5 in Rho-123 retention assays enabled analysis of whether LP-44, LP-12, fluphenazine, SDZ 21009, GR-127935 and CGP-71683 can inhibit MDR1. Cell death assay experiments in KG1 control and KG1 *MDR1*$^{-/-}$ human AML cells also allowed me to conclude that the synergistic action between these different combinations is specific to MDR1.

6.5 Combination Safety and Efficacy *in vivo*

ABC transporters principally function to protect a cell by maintaining the levels of poisonous agents, including anti-cancer drugs, below toxic levels (Van Tellingen et al., 2003; Waghray and Zhang, 2017). Following the identification that prominent AML chemotherapies such as, daunorubicin and the topoisomerase inhibitor etoposide (VP16) (Didziapetris et al., 2003; Seelig, 1998; Takara et al., 2006), are substrates for MDR1, significant efforts have been taken in the past to combine these chemotherapies with MDR1 inhibitors to improve efficacy (CALGB: 19808, 9720) (Baer et al., 2002; Kolitz et al., 2004; Kolitz et al., 2010; Shaffer et al., 2012). Unfortunately, this approach results in a dramatic increase in toxicity due to the accumulation of cytotoxic drug in healthy cells, such as HSPCs. For example, in one study comparing daunorubicin/etoposide/Ara-c combination therapy, mortality rates increased from 20% in the chemotherapy arm, to 44% with the addition of a MDR1 inhibitor (CALGB: 9720) (Baer et al., 2002). Furthermore, to mitigate these toxicities, significant reductions in both daunorubicin (90 to 40 mg/m_2) and etoposide (100 to 40 mg/m_2) doses have been required when in combination with a MDR1 inhibitor, undermining the potential for benefit (CALGB: 19808) (Baer et al., 2002; Kolitz et al., 2004; Kolitz et al., 2010; Shaffer et al., 2012). These side effects have limited the clinical use of such combination treatments and understandably, we were very keen to establish the safety and tolerability of the birinapant plus MDR1 inhibitor combination.

Given that HSPCs express higher levels of MDR1 than their differentiated progeny, we were concerned that combining birinapant with MDR1 inhibitors

would cause haematopoietic toxicity. However, co-treatment of murine WT-BM or HSPCs with birinapant plus a MDR1 inhibitor or LP-44, was not toxic, whereas the current standard-of-care chemotherapy Ara-c was highly toxic to these cells, as previously reported (Brumatti et al., 2016). Similarly, treatment of human $MDR1_H$ CD34+ cells with tariquidar did not increase the amount of birinapant-mediated cell death, whilst in combination with the topoisomerase inhibitor VP16, there was an increase in toxicity. Further, our *in vivo* biosafety experiments demonstrated the systemic safety and tolerability of the birinapant plus tariquidar or LP-44 combination. Despite the fact that the LP-44 plus birinapant treatment was well tolerated by mice, further studies with this combination in AML burdened mice are unlikely due to the superior specificity, potency and clinical viability of 3_{rd} generation MDR1 inhibitors such as tariquidar and zosuquidar.

There are many future experiments that can be considered for a comprehensive analysis of the safety of the MDR1 inhibitor plus birinapant combination. Long term clonogenic assays of WT-BM and HSPCs under treatment pressure would indicate which HSPC populations are sensitive to treatment, and therefore the eligibility of the treatment in patients who require preservation of HSCs for haematopoietic recovery (Morrison et al., 1995). The importance of a cells' ability to produce and respond to TNF for Smac-mimetic-mediated killing has been discussed at length within this thesis. Therefore, in our studies testing the killing potential of the MDR1 inhibitor plus birinapant treatment in human CD34+ HSPCs, incorporating analysis of whether addition of TNF would enhance combination-mediated cell death would be very interesting. These findings would

help predict the tolerability and safety of the combination treatment in a human setting.

Experiments in Chapter 3 demonstrate the efficacy of the tariquidar plus birinapant combination to extend survival in the aggressive MDR1$_{H}$ MLL-AF9 AML model (Chapter 3 **Figure 3.2**). Although tariquidar plus birinapant therapy extended survival of AML burdened mice, pre-treatment with the chemotherapy Ara-c prior to Smac-mimetic combination therapy, had a greater efficacy, suggesting a therapeutic opportunity following standard-of-care treatments (**Figure 6F**). As we have shown here, and previously reported (Brumatti et al., 2016), Ara-c is very effective at killing AML cells, leading to a reduction in the bulk blast population. Our data shows that de-bulking the tumour burden initially, followed by birinapant combination treatment, can double the median survival (Ara-c + 3xCombo = 40 days vs Ara-c alone = 22 days). We hypothesise that the extension of survival may be due to the ability of the tariquidar plus birinapant treatment to potently target LSCs, reducing this aggressive leukaemia cell population, resulting in improved survival. Furthermore, it is important to notice that despite the efficacy of Ara-c to kill blast cells, the Ara-c single-agent treatment does not lead to a prolongation of survival in this aggressive model. MDR1 inhibitor plus birinapant treatment is the only one that was able to significantly extend survival (Chapter 3 **Figure 6F and 3.2**). These findings not only highlight the toxicity and lack of long-term benefit with the chemotherapy Ara-c as a single-agent, but also demonstrate the potential clinical impact of the birinapant plus MDR1 inhibitor combination therapy.

As described in the introduction of this thesis, Smac-mimetics have been used in a diverse range of combinations in an effort to potentiate efficacy. As we have identified that birinapant, and other Smac-mimetics, are substrates for MDR1, and addition of an inhibitor of this drug-pump can potentate their efficacy, it is natural to wonder whether addition of these inhibitors could increase the potency of previously described combination therapies. Due to the toxicities previously observed with MDR1 inhibitors combined with chemotherapies, testing the potential of a triple birinapant plus MDR1 inhibitor plus etoposide or daunorubicin combination is not practicable (CALGB 9720) (Baer et al., 2002). In contrast, combination of birinapant with p38 inhibitors (Lalaoui et al., 2016), or the caspase 8 inhibitor Emricasan (IDN-6556) (Brumatti et al., 2016), have shown efficacy and tolerability in a range of AML models *in vitro* and *in vivo.* Thus, testing the ability of a MDR1 inhibitor to increase the already promising results achieved with these therapies in MDR1$_H$ leukaemias is plausible and appealing. Moreover, clinical trials are currently in progress combining Smac-mimetics with immunotherapy and radiation (**Table 2**). Investigation of the potential of MDR1 inhibitors to increase the efficacy of these treatments in MDR1$_H$ cancer, such as ovarian cancer, could have an immediate clinical impact.

6.6 LSC Killing Potential

Similar to HSPCs, it is known that LSCs have a high expression of MDR1 and targeting these cells is required to cure AML (Ho et al., 2016; Leith et al., 1999). Yet these cells are highly resistant to many currently used anti-cancer therapies and therefore are often responsible for disease relapse (Costello et al., 2000; Ishikawa et al., 2007; Shlush et al., 2017; van Rhenen et al., 2005). Our

experiments using previously generated MLL-AF9 blasts and matching LSCs (Fong et al., 2015), have established that MDR1 expression is an Achilles heel of LSCs and that birinapant is able to exploit this weakness when combined with MDR1 inhibitors. Comparison of the birinapant/tariquidar combination and the VP16/tariquidar combination indicated that, besides being a safer therapy, birinapant/tariquidar is more potent and efficacious at killing LSCs compared to VP16/tariquidar. Altogether these results show that birinapant plus MDR1 inhibitor therapy can effectively kill LSCs and thereby prolong survival and prevent disease relapse. Future experiments investigating the ability of the MDR1 inhibitor plus Smac-mimetic treatment to target LSCs includes quantifying the elimination of LSCs in murine *in vivo* treatment experiments and the efficacy of the treatment to kill primary patient LSCs *ex vivo*.

6.7 Birinapant is well Tolerated

We speculate that the specificity of birinapant towards cancerous LSCs and not healthy HSPCs may be explained by the fact that birinapant is not inherently toxic and therefore, increasing the dose of birinapant in healthy cells has no discernible effect on their viability. The results in HBV infected and uninfected mice also underlines that, despite MDR1-expressing healthy cells being able to undergo birinapant-mediated degradation of cIAPs, these cells are far less susceptible to the cytotoxic effects of birinapant. The reason why birinapant preferentially kills transformed cells while leaving normal cells intact remains unclear. One explanation put forward is that, contrary to chemotherapeutic drugs that alter multiple cellular pathways (Adams, 2004; Bywater et al., 2012; Hannan et al., 2013; Silke et al., 2008), Smac-mimetics are targeted drugs and therefore

specifically affect IAP signalling pathways. Another explanation might be that abnormal expression of IAPs and/or TNF by the tumour or stromal cells in its environment, leads to addiction to the NF-κB and/or the TNFR1 signalling pathways. Consistent with the latter idea, the findings from our *in vitro* assays with AML and ovarian cancer revealed that tumours must be able to produce TNF in response to birinapant to be killed efficiently by Smac-mimetics. This is most likely not exclusive to cancer, as mouse models of HBV highlighted the importance of TNF for the Smac-mimetic-mediated clearance of virus from infected liver cells (Ebert et al., 2015a; Ebert et al., 2015b). Collectively, these results suggest that repurposing of MDR1 inhibitors in combination with Smac-mimetics might be a safe and efficacious new approach for cancer and HBV therapy.

6.8 Combination Efficacy in HBV

The strength of the combination therapy is emphasised by its universal efficacy in multiple cancer models, both haematological and solid, as well as its potency in HBV disease. Predominately, Smac-mimetics are very safe and well tolerated drugs, however, as mentioned in the introduction, in-human clinical trials observed AEs and dose limiting toxicities when Smac-mimetics were administered at high doses. One intriguing AE was the presence of Bell's palsy with higher concentrations of birinapant (63 mg/m2) and APG-1387 (60 mg) (Amaravadi et al., 2015; Rasco et al., 2019; Xu et al., 2018). This effect is reversible upon decrease or cessation of treatment and has not significantly limited the progression of Smac-mimetics for the treatment of cancer. Not unexpectedly, similar dose limiting toxicities were observed in a clinical trial of

birinapant for HBV, prompting early termination of the trial (NCT02288208). Our results indicate that a lower dose of birinapant can be used in combination with a MDR1 inhibitor to effectively clear HBV-DNA *in vivo.* The 3rd generation specific MDR1 inhibitor zosuquidar was used predominantly in the HBV studies, in place of tariquidar, due to the polyethylene glycol (PEG) vehicle used to prepare tariquidar interfering with HBV-DNA clearance (data not shown). These studies indicate a MDR1 inhibitor can increase the amount of Smac-mimetic-mediated HBV-infected liver-cell death, resulting in higher detectable levels of ALT. However, due to inherent limitations with measuring sensitive changes in protein expression in whole organ lysates, further studies are required to investigate the molecular mechanism induced by the combination treatment. That is, an increase in cIAP degradation, and consequent activation of apoptotic machinery. Although the median clearance of HBV-DNA was the same (3.5 weeks) with high-dose birinapant (30 mg/kg) single-agent and low-dose birinapant (10 mg/kg) plus zosuquidar, analysis of side effects of these different treatment regimens would be necessary to draw conclusions about the eligibility of the combination treatment. These findings may provide a safer alternative to high-dose birinapant therapy for the treatment of chronic HBV. Furthermore, these findings are of interest due to the ongoing analysis of Smac-mimetics for the treatment of chronic HBV (NCT03585322).

6.9 Benefit of Biomarkers

Moving forward in the fight against cancer, understanding biomarkers of response that can predict sensitive patient populations is important to ensure novel therapies are successful. Upregulation of MDR1 has been identified in at

least 30% of AML patients, with the incidence increasing to 50% in relapsed and secondary AML (Leith et al., 1999). Therefore, this makes MDR1 an important consideration when developing novel AML therapies. Screening tools for MDR1 activity are readily available and inexpensive. Our findings show that MDR1 expression in AML and ovarian cancer cells can be used as a biomarker for Smac-mimetic-related therapies to improve patient stratification. Moreover, TNF is an essential aspect of Smac-mimetic mediated killing, and AML and MDS patients were selected for clinical trials with birinapant because myeloid cells, generally, produce TNF in response to Smac-mimetics (Wong et al., 2014). The importance of TNF production and signalling for birinapant-mediated combination therapies was confirmed by analysing the killing potential of LP-44 or tariquidar plus birinapant, with and without addition of TNF, in MLL-AF9 sub-groups which lack functional TNF signalling (Chapters 3 and 5). However, practically it is very difficult to measure the TNF levels in patient samples through ELISA assays. To overcome this limitation, we have established an assay where cells are treated with birinapant alone or in combination with a MDR1 inhibitor, in the presence or absence of exogenous TNF. If patient samples require the addition of TNF to be killed, it would be expected that the patient is unlikely to respond to birinapant plus MDR1 inhibitor combination treatment. This assay is quick and can give a response 48 hours after patient samples are obtained, making it attractive for patient treatment screening. From the limited primary patient samples we have tested to date, there was no correlation between a patients' cytogenetic or molecular status and their response to Smac-mimetic combination therapies. More extensive studies investigating this would be of interest. Altogether, our

findings using primary human AML samples, suggest that in the presence of adequate TNF production, MDR1 function is able to predict whether a leukaemia will respond to birinapant treatment. For example, a patient with $MDR1_L$ leukaemia will be sensitive to birinapant alone treatment, whilst a patient with $MDR1_H$ leukaemia can receive an MDR1 inhibitor to overcome Smac-mimetic resistance. This observation combined with the safety and efficacy of the birinapant plus MDR1 inhibitor drug combination in primary AML patient samples and *in vivo* models of AML, provides the rationale for conducting clinical trials with this drug combination in AML patients.

6.10 Conclusions

This thesis examined novel mechanisms by which cancer cells use to evade Smac-mimetic therapy. The experiments described within, clearly show that birinapant is a substrate for MDR1 and that combination of birinapant with 3rd generation MDR1-specific inhibitors is well tolerated, efficiently killing LSCs and prolonging survival in $MDR1_H$ leukaemia models. Thus, as MDR1 may be an Achilles heel for cancer cells, screening for MDR1 expression and activity would enable Smac-mimetic single-agent therapy to be targeted to $MDR1_L$ cancers, while combination treatment would be directed to $MDR1_H$ patients. My findings advocate the potential therapeutic benefit of MDR1 inhibitors and prompt a re-evaluation of the status of this class of drugs. Collectively, these results suggest that repurposing of MDR1 inhibitors in combination with Smac-mimetics might be a safe and efficacious new approach to treat both malignant and infectious disease.

Appendices

Appendix 1 Antibody Details for Western Blotting

Table 5 Antibodies used in Western blotting experiments

Antibody	Clone	Ab	Company	Cata #	Ref/Lot #
Full length Caspase-8	polyclonal	pAb	Cell Signaling Technology	AF1650	#JJF01
Cleaved Caspase-8	Asp387 D5B2	mAb	Cell Signaling Technology	8592	04/2019
Cleaved Caspase-3	D175	mAb	Cell Signaling Technology	9661L	06/2018
PARP	polyclonal	pAb	Cell Signaling Technology	9542S	#15
RIPK1	38/RIP	mAb	BD Transduction Labs	610459	#4073772
RIPK3	polyclonal	pAb	ProSci	2283	8337-1003
cIAP1	1E1-1-12	mAb	WEHI	n/a	n/a
cIAP2	15C8-12	mAb	WEHI	n/a	n/a
MDR1	EPR10364-57	mAb	Abcam	Ab170904	#GR217576-34
XIAP	2F1	mAb	Medical & Biological Labs	M044-3	#063
5-HT_7 R	polyclonal	pAb	Abcam	Ab61562	multiple
ERK	polyclonal	pAb	Cell Signaling Technology	9102S	#26
Phospho-ERK	T202/Y204	mAb	Cell Signaling Technology	9101S	#30
Actin	AC-15	mAb	Sigma	A-1978	multiple
Tubulin	polyclonal	pAb	Cell Signaling Technology	21485	#4

Appendix 2 Antibody Details for LSK Isolation

Table 6 Antibodies used to isolate LSK (HSPC) cells

Antibody	Clone	Signal	Company	Cata #	Lot #
CD3	14-2C11	biotin	WEHI	n/a	n/a
CD4	GK1.5	biotin	WEHI	n/a	n/a
CD4	H129	biotin	WEHI	n/a	n/a
CD8	53-6.7	biotin	WEHI	n/a	n/a
CD8	YTS.169	biotin	WEHI	n/a	n/a
TER119	TER119	biotin	WEHI	n/a	n/a
B220	RA3-6B2	biotin	WEHI	n/a	n/a
Ly6G	1A8	biotin	Biolegend	127604	B254531
CD11b	M1/7	biotin	WEHI	n/a	n/a
cKIT	2B8	BV711	BD Horizon	563160	7299976
Sca-1	E13-161.7	A594	WEHI	n/a	n/a
CD34	RAM34	APC	BD Biosciences	560230	7355686
CD16/32	2.4G2	PerCP	BD Biosciences	560540	8171841
CD150	TC15-12F12.2	BV421	Biolegend	115926	B240681
CD48	HM48-1	FITC	Invitrogen	17-0481-82	1921469
Biotinylated	n/a	A700	BD Biosciences	S32356	1504500

Appendix 3 Flow cytometry gating Strategy for LSK Isolation

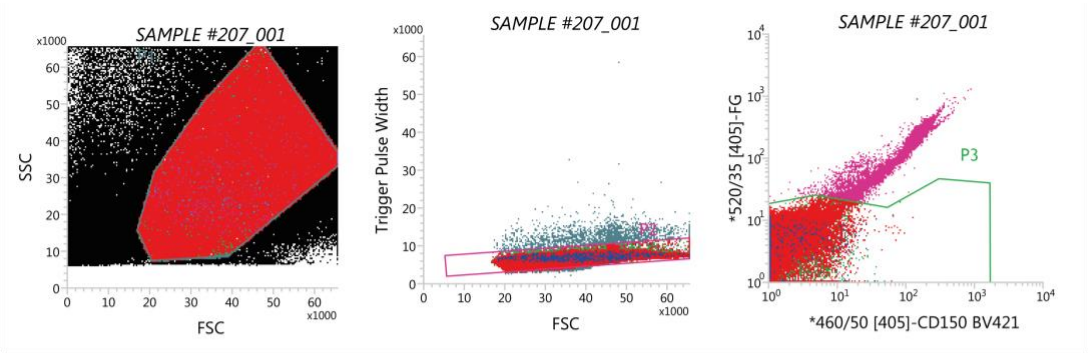

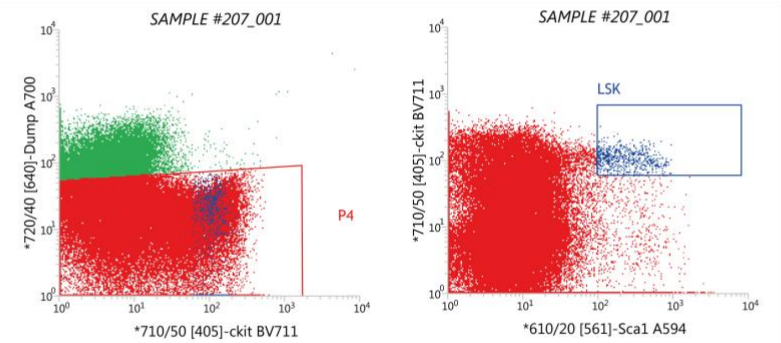

Populations: *SAMPLE #207_001*

Populations	Even...	% Total	% Parent
All Events	301,884	100.00%	####
P1	144,343	47.81%	47.81%
P2	141,863	46.99%	98.28%
P3	134,434	44.53%	94.76%
P4	100,000	33.13%	74.39%
LSK	609	0.20%	0.61%

Bibliography

Abraham, E.H., Prat, A.G., Gerweck, L., Seneveratne, T., Arceci, R.J., Kramer, R., Guidotti, G., and Cantiello, H.F. (1993). The multidrug resistance (mdr1) gene product functions as an ATP channel. Proceedings of the National Academy of Sciences *90*, 312-316.

Adams, J. (2004). The proteasome: a suitable antineoplastic target. Nature Reviews Cancer *4*, 349.

Adrain, C., Creagh, E.M., and Martin, S.J. (2001). Apoptosis-associated release of Smac/DIABLO from mitochondria requires active caspases and is blocked by Bcl-2. The EMBO journal *20*, 6627-6636.

Advani, R., Fisher, G.A., Lum, B.L., Hausdorff, J., Halsey, J., Litchman, M., and Sikic, B.I. (2001). A phase I trial of doxorubicin, paclitaxel, and valspodar (PSC 833), a modulator of multidrug resistance. Clinical Cancer Research *7*, 1221-1229.

Advani, R., Saba, H.I., Tallman, M.S., Rowe, J.M., Wiernik, P.H., Ramek, J., Dugan, K., Lum, B.*, et al.* (1999). Treatment of Refractory and Relapsed Acute Myelogenous Leukemia With Combination Chemotherapy Plus the Multidrug Resistance Modulator PSC 833 (Valspodar): Presented in part at the American Society of Hematology meeting held in San Diego, CA, December 1997. Blood *93*, 787-795.

Ahmed, M., Borsch, C.M., Neyfakh, A., and Schuldiner, S. (1993). Mutants of the Bacillus subtilis multidrug transporter Bmr with altered sensitivity to the antihypertensive alkaloid reserpine. Journal of Biological Chemistry *268*, 11086-11089.

Alessi, D.R., Cuenda, A., Cohen, P., Dudley, D.T., and Saltiel, A.R. (1995). PD 098059 is a specific inhibitor of the activation of mitogen-activated protein kinase kinase in vitro and in vivo. Journal of Biological Chemistry *270*, 27489-27494.

Allensworth, J.L., Aird, K.M., Aldrich, A.J., Batinic-Haberle, I., and Devi, G.R. (2012). XIAP Inhibition and Generation of Reactive Oxygen Species Enhances TRAIL Sensitivity in Inflammatory Breast Cancer Cells. Molecular Cancer Therapeutics *11*, 1518-1527.

Allensworth, J.L., Sauer, S.J., Lyerly, H.K., Morse, M.A., and Devi, G.R. (2013). Smac mimetic Birinapant induces apoptosis and enhances TRAIL potency in inflammatory breast cancer cells in an IAP-dependent and TNF-α-independent mechanism. Breast Cancer Research and Treatment *137*, 359-371.

Aller, S.G., Yu, J., Ward, A., Weng, Y., Chittaboina, S., Zhuo, R., Harrell, P.M., Trinh, Y.T.*, et al.* (2009). Structure of P-glycoprotein reveals a molecular basis for poly-specific drug binding. Science *323*, 1718-1722.

Allikmets, R., Schriml, L.M., Hutchinson, A., Romano-Spica, V., and Dean, M. (1998). A human placenta-specific ATP-binding cassette gene (ABCP) on chromosome 4q22 that is involved in multidrug resistance. Cancer Research *58*, 5337-5339.

Amaravadi, R.K., Schilder, R.J., Martin, L.P., Levin, M., Graham, M.A., Weng, D.E., and Adjei, A.A. (2015). A Phase I Study of the SMAC-Mimetic Birinapant in Adults with Refractory Solid Tumors or Lymphoma. Molecular Cancer Therapeutics *14*, 2569-2575.

Amaravadi, R.K., Senzer, N.N., Martin, L.P., Schilder, R.J., LoRusso, P., Papadopoulos, K.P., Weng, D.E., Graham, M.*, et al.* (2013). A phase I study of birinapant (TL32711) combined with multiple chemotherapies evaluating tolerability and clinical activity for solid tumor patients. Journal of Clinical Oncology *31,* 2504.

Anderton, H., Bandala-Sanchez, E., Simpson, D.S., Rickard, J.A., Ng, A.P., Di Rago, L., Hall, C., Vince, J.E.*, et al.* (2019). RIPK1 prevents TRADD-driven, but TNFR1 independent, apoptosis during development. Cell Death & Differentiation *26*, 877.

Anderton, H., Rickard, J.A., Varigos, G.A., Lalaoui, N., and Silke, J. (2017). Inhibitor of apoptosis proteins (IAPs) limit RIPK1-mediated skin inflammation. Journal of Investigative Dermatology *137*, 2371-2379.

Angelin, B., Arvidsson, A., Dahlqvist, R., Hedman, A., and Schenck-gustafsson, K. (1987). Quinidine reduces biliary clearance of digoxin in man. European Journal of Clinical Investigation *17*, 262-265.

Annibaldi, A., John, S.W., Berghe, T.V., Swatek, K.N., Ruan, J., Liccardi, G., Bianchi, K., Elliott, P.R.*, et al.* (2018). Ubiquitin-mediated regulation of RIPK1 kinase activity independent of IKK and MK2. Molecular cell *69*, 566-580. e565.

Appelbaum, F.R., Dahlberg, S., Thomas, E.D., Buckner, C.D., Cheever, M.A., Clift, R.A., Crowley, J., Deeg, H.J.*, et al.* (1984). Bone marrow transplantation or chemotherapy after remission induction for adults with acute nonlymphoblastic leukemia: a prospective comparison. Annals of Internal Medicine *101*, 581-588.

Arlin, Z., Case, J.D., Moore, J., Wiernik, P., Feldman, E., Saletan, S., Desai, P., Sia, L., *et al.* (1990). Randomized multicenter trial of cytosine arabinoside with mitoxantrone or daunorubicin in previously untreated adult patients with acute nonlymphocytic leukemia (ANLL). Lederle Cooperative Group. Leukemia *4*, 177-183.

Arnt, C.R., Chiorean, M.V., Heldebrant, M.P., Gores, G.J., and Kaufmann, S.H. (2002). Synthetic Smac/DIABLO peptides enhance the effects of chemotherapeutic agents by binding XIAP and cIAP1 in situ. Journal of Biological Chemistry *277*, 44236-44243.

Atanes, P., Lacivita, E., Rodriguez, J., Brea, J., Burgueno, J., Vela, J.M., Cadavid, M.I., Loza, M.I.*, et al.* (2013). The arylpiperazine derivatives N-(4-cyanophenylmethyl)-4-(2-diphenyl)-1-piperazinehexanamide and N-benzyl-4-(2-diphenyl)-1-piperazinehexanamide exert a long-lasting inhibition of human serotonin 5-HT7 receptor binding and cAMP signaling. Pharmacol Res Perspect *1*, e00013.

Bachas, C., Schuurhuis, G., Assaraf, Y., Kwidama, Z., Kelder, A., Wouters, F., Snel, A., Kaspers, G.*, et al.* (2012). The role of minor subpopulations within the leukemic blast compartment of AML patients at initial diagnosis in the development of relapse. Leukemia *26*, 1313.

Baer, M.R., George, S.L., Dodge, R.K., O'Loughlin, K.L., Minderman, H., Caligiuri, M.A., Anastasi, J., Powell, B.L.*, et al.* (2002). Phase 3 study of the multidrug resistance modulator PSC-833 in previously untreated patients 60 years of age and older with acute myeloid leukemia: Cancer and Leukemia Group B Study 9720. Blood *100*, 1224-1232.

Bagger, F.O., Kinalis, S., and Rapin, N. (2019). BloodSpot: a database of healthy and malignant haematopoiesis updated with purified and single cell mRNA sequencing profiles. Nucleic Acids Research *47*, 881-885.

Baker, E.K., Johnstone, R.W., Zalcberg, J.R., and El-Osta, A. (2005). Epigenetic changes to the MDR1 locus in response to chemotherapeutic drugs. Oncogene *24*, 8061.

Bard, J.A., Zgombick, J., Adham, N., Vaysse, P., Branchek, T.A., and Weinshank, R.L. (1993). Cloning of a novel human serotonin receptor (5-HT7) positively linked to adenylate cyclase. Journal of Biological Chemistry *268*, 23422-23426.

Bardia, A., Cameron, J., Venkatesan, K., Robinson, D., Porter, D., Kim, S., Parton, M., Kümmel, S.*, et al.* (2015). 1977 Synergy of LCL161, an antagonist of inhibitor of apoptosis proteins (IAPs), with paclitaxel in a gene expression signature-enriched cohort of triple-negative breast cancer (TNBC). European Journal of Cancer *51*, S326.

Bardia, A., Parton, M., Kummel, S., Estévez, L.G., Huang, C.-S., Cortés, J., Ruiz-Borrego, M., Telli, M.L.*, et al.* (2018). Paclitaxel with inhibitor of apoptosis antagonist, LCL161, for localized triple-negative breast cancer, prospectively stratified by gene signature in a biomarker-driven neoadjuvant trial. Journal of Clinical Oncology *36*, 3126-3133.

Barnes, N.M., and Neumaier, J.F. (2011). Neuronal 5-HT receptors and SERT. Tocris Biosci Sci Rev Ser *34*, 1-16.

Beck, J., Handgretinger, R., Klingebiel, T., Dopfer, R., Schaich, M., Ehninger, G., Niethammer, D., and Gekeler, V. (1996a). Expression of PKC isozyme and MDR-associated genes in primary and relapsed state AML. Leukemia *10*, 426-433.

Beck, J., Niethammer, D., and Gekeler, V. (1996b). MDR1, MRP, topoisomerase IIalpha/beta, and cyclin A gene expression in acute and chronic leukemias. Leukemia *10*, 39-45.

Beck, W.T., Cirtain, M.C., Glover, C.J., Felsted, R.L., and Safa, A.R. (1988). Effects of indole alkaloids on multidrug resistance and labeling of P-glycoprotein by a photoaffinity analog of vinblastine. Biochemical and Biophysical Research Communications *153*, 959-966.

Belpomme, D., Gauthier, S., Pujade-Lauraine, E., Facchini, T., Goudier, M.-J., Krakowski, I., Netter-Pinon, G., Frenay, M.*, et al.* (2000). Verapamil increases the survival of patients with anthracycline-resistant metastatic breast carcinoma. Annals of Oncology *11*, 1471-1476.

Benetatos, C.A., Mitsuuchi, Y., Burns, J.M., Neiman, E.M., Condon, S.M., Yu, G., Seipel, M.E., Kapoor, G.S.*, et al.* (2014). Birinapant (TL32711), a bivalent SMAC mimetic, targets TRAF2-associated cIAPs, abrogates TNF-induced NF-κB activation, and is active in patient-derived xenograft models. Molecular Cancer Therapeutics *13*, 867-879.

Berger, M., Gray, J.A., and Roth, B.L. (2009). The expanded biology of serotonin. Annual Review of Medicine *60*, 355-366.

Berman, E., Heller, G., Santorsa, J., McKenzie, S., Gee, T., Kempin, S., Gulati, S., Andreeff, M.*, et al.* (1991). Results of a randomized trial comparing idarubicin and cytosine arabinoside with daunorubicin and cytosine arabinoside in adult patients with newly diagnosed acute myelogenous leukemia. Blood *77*, 1666-1674.

Bertrand, M.J., Milutinovic, S., Dickson, K.M., Ho, W.C., Boudreault, A., Durkin, J., Gillard, J.W., Jaquith, J.B.*, et al.* (2008). cIAP1 and cIAP2 facilitate cancer cell survival by functioning as E3 ligases that promote RIP1 ubiquitination. Molecular Cell *30*, 689-700.

Beug, S.T., Beauregard, C.E., Healy, C., Sanda, T., St-Jean, M., Chabot, J., Walker, D.E., Mohan, A.*, et al.* (2017). Smac mimetics synergize with immune checkpoint inhibitors to promote tumour immunity against glioblastoma. Nature Communications *8*.

Beug, S.T., Pichette, S.J., St-Jean, M., Holbrook, J., Walker, D.E., LaCasse, E.C., and Korneluk, R.G. (2018). Combination of IAP Antagonists and TNF-α-Armed Oncolytic Viruses Induce Tumor Vascular Shutdown and Tumor Regression. Molecular Therapy-Oncolytics *10*, 28-39.

Beug, S.T., Tang, V.A., LaCasse, E.C., Cheung, H.H., Beauregard, C.E., Brun, J., Nuyens, J.P., Earl, N.*, et al.* (2014). Smac mimetics and innate immune stimuli synergize to promote tumor death. Nature Biotechnology *32*, 182.

Bhatnagar, U.B., Singh, D., Glazyrin, A., and Moormeier, J. (2016). Paclitaxel Induced MDS and AML: A Case Report and Literature Review. Case Reports in Oncological Medicine *2016*, 8308179.

Bishop, J.F., Matthews, J.P., Young, G.A., Szer, J., Gillett, A., Joshua, D., Bradstock, K., Enno, A.*, et al.* (1996). A randomized study of high-dose cytarabine in induction in acute myeloid leukemia. Blood *87*, 1710-1717.

Bleuler, M., and Stoll, W. (1955). Clinical use of reserpine in psychiatry: comparison with chlorpromazine. Annals of the New York Academy of Sciences *61*, 167-173.

Boess, F.G., Beroukhim, R., and Martin, I.L. (1995). Ultrastructure of the 5-Hydroxytryptamine3 Receptor. Journal of Neurochemistry *64*, 1401-1405.

Bolme, P., and Otto, U. (1977). Dose-dependence of the pharmacokinetics of quinidine. European Journal of Clinical Pharmacology *12*, 73-76.

Borst, P., and Elferink, R.O. (2002). Mammalian ABC transporters in health and disease. Annual Review of Biochemistry *71*, 537-592.

Boulton, D.W., DeVane, C.L., Liston, H.L., and Markowitz, J.S. (2002). In vitro P-glycoprotein affinity for atypical and conventional antipsychotics. Life Sciences *71*, 163-169.

Brant, S.R., Panhuysen, C.I., Nicolae, D., Reddy, D.M., Bonen, D.K., Karaliukas, R., Zhang, L., Swanson, E.*, et al.* (2003). MDR1 Ala893 polymorphism is associated with inflammatory bowel disease. The American Journal of Human Genetics *73*, 1282-1292.

Bratton, S.B., Walker, G., Srinivasula, S.M., Sun, X.-M., Butterworth, M., Alnemri, E.S., and Cohen, G.M. (2001). Recruitment, activation and retention of caspases-9 and -3 by Apaf-1 apoptosome and associated XIAP complexes. The EMBO Journal *20*, 998-1009.

Brumatti, G., Ma, C., Lalaoui, N., Nguyen, N.-Y., Navarro, M., Tanzer, M.C., Richmond, J., Ghisi, M.*, et al.* (2016). The caspase-8 inhibitor emricasan combines with the SMAC mimetic birinapant to induce necroptosis and treat acute myeloid leukemia. Science Translational Medicine *8*, 339-369

Brumatti, G., Salmanidis, M., Kok, C.H., Bilardi, R.A., Sandow, J.J., Silke, N., Mason, K., Visser, J.*, et al.* (2013). HoxA9 regulated Bcl-2 expression mediates survival of myeloid progenitors and the severity of HoxA9-dependent leukemia. Oncotarget *4*, 1933.

Brunckhorst, M.K., Lerner, D., Wang, S., and Yu, Q. (2012). AT-406, an orally active antagonist of multiple inhibitor of apoptosis proteins, inhibits progression of human ovarian cancer. Cancer Biology & Therapy *13*, 804-811.

Bunting, K.D., Galipeau, J., Topham, D., Benaim, E., and Sorrentino, B.P. (1999). Effects of Retroviral-Mediated MDR1 Expression on Hematopoietic Stem Cell Self-Renewal and Differentiation in Culture. Annals of the New York Academy of Sciences *872*, 125-141.

Burgess, D.J. (2012). Anticancer drugs: Antipsychotic to anticancer agent? Nature Reviews Drug Discovery *11*, 516-517.

Burkhart, C.A., Watt, F., Murray, J., Pajic, M., Prokvolit, A., Xue, C., Flemming, C., Smith, J.*, et al.* (2009). Small-Molecule Multidrug Resistance–Associated Protein 1 Inhibitor Reversan Increases the Therapeutic Index of Chemotherapy in Mouse Models of Neuroblastoma. Cancer Research *69*, 6573-6580.

Burnett, A., Watkins, R., Maharaj, D., McKinnon, S., Tansey, P., Alcorn, M., Singer, C., McDonald, G.*, et al.* (1984). Transplantation of unpurged autologous bone-marrow in acute myeloid leukaemia in first remission. The Lancet *324*, 1068-1070.

Burtin, C., Scheinmann, P., Salomon, J.C., Lespinats, G., and Canu, P. (1982). Decrease in tumour growth by injections of histamine or serotonin in fibrosarcoma-bearing mice: Influence of H1 and H2 histamine receptors. British Journal of Cancer *45*, 54-60.

Bywater, M.J., Poortinga, G., Sanij, E., Hein, N., Peck, A., Cullinane, C., Wall, M., Cluse, L.*, et al.* (2012). Inhibition of RNA polymerase I as a therapeutic strategy to promote cancer-specific activation of p53. Cancer Cell *22*, 51-65.

Cai, Q., Sun, H., Peng, Y., Lu, J., Nikolovska-Coleska, Z., McEachern, D., Liu, L., Qiu, S.*, et al.* (2011). A potent and orally active antagonist (SM-406/AT-406) of multiple inhibitor of apoptosis proteins (IAPs) in clinical development for cancer treatment. Journal of Medicinal Chemistry *54*, 2714-2726.

Cancer Genome Atlas Network. (2015). Comprehensive genomic characterization of head and neck squamous cell carcinomas. Nature *517*, 576.

Cannistra, S.A. (1993). Cancer of the ovary. New England Journal of Medicine *329*, 1550-1559.

Cannistra, S.A. (2004). Cancer of the ovary. New England Journal of Medicine *351*, 2519-2529.

Carter, B.Z., Milella, M., Tsao, T., McQueen, T., Schober, W., Hu, W., Dean, N., Steelman, L.*, et al.* (2003). Regulation and targeting of antiapoptotic XIAP in acute myeloid leukemia. Leukemia *17*, 2081-2089.

Cassileth, P.A., Harrington, D.P., Appelbaum, F.R., Lazarus, H.M., Rowe, J.M., Paietta, E., Willman, C., Hurd, D.D.*, et al.* (1998). Chemotherapy compared with autologous or allogeneic bone marrow transplantation in the management of acute myeloid leukemia in first remission. New England Journal of Medicine *339*, 1649-1656.

Cattaneo, M.G., Codignola, A., Vicentini, L.M., Clementi, F., and Sher, E. (1993). Nicotine Stimulates a Serotonergic Autocrine Loop in Human Small-Cell Lung Carcinoma. Cancer Research *53*, 5566-5568.

Cattaneo, M.G., Palazzi, E., Bondiolotti, G., and Vicentini, L.M. (1994). 5-HT1D receptor type is involved in stimulation of cell proliferation by serotonin in human small cell lung carcinoma. European Journal of Pharmacology: Molecular Pharmacology *268*, 425-430.

Chai, J., Du, C., Wu, J.-W., Kyin, S., Wang, X., and Shi, Y. (2000). Structural and biochemical basis of apoptotic activation by Smac/DIABLO. Nature *406*, 855-862.

Chaidos, A., Caputo, V., and Karadimitris, A. (2015). Inhibition of bromodomain and extra-terminal proteins (BET) as a potential therapeutic approach in haematological malignancies: emerging preclinical and clinical evidence. Therapeutic Advances in Hematology *6*, 128-141.

Champlin, R.E., Ho, W.G., Gale, R.P., Winston, D., Selch, M., Mitsuyasu, R., Lenarsky, C., Elashoff, R.*, et al.* (1985). Treatment of acute myelogenous leukemia: a prospective controlled trial of bone marrow transplantation versus consolidation chemotherapy. Annals of Internal Medicine *102*, 285-291.

Chan, H.S., Haddad, G., Thorner, P.S., DeBoer, G., Lin, Y.P., Ondrusek, N., Yeger, H., and Ling, V. (1991). P-glycoprotein expression as a predictor of the outcome of therapy for neuroblastoma. New England Journal of Medicine *325*, 1608-1614.

Chauncey, T.R., Rankin, C., Anderson, J.E., Chen, I.-M., Kopecky, K.J., Godwin, J.E., Kalaycio, M.E., Moore Jr, D.F.*, et al.* (2000). A phase I study of induction chemotherapy for older patients with newly diagnosed acute myeloid leukemia (AML) using mitoxantrone, etoposide, and the MDR modulator PSC 833: a southwest oncology group study 9617. Leukemia Research *24*, 567-574.

Chen, D., Yu, J., and Zhang, L. (2016). Necroptosis: an alternative cell death program defending against cancer. Biochimica et Biophysica Acta (BBA)-Reviews on Cancer *1865*, 228-236.

Chen, K.-F., Lin, J.-P., Shiau, C.-W., Tai, W.-T., Liu, C.-Y., Yu, H.-C., Chen, P.-J., and Cheng, A.-L. (2012a). Inhibition of Bcl-2 improves effect of LCL161, a SMAC mimetic, in hepatocellular carcinoma cells. Biochemical Pharmacology *84*, 268-277.

Chen, L., Li, Y., Yu, H., Zhang, L., and Hou, T. (2012b). Computational models for predicting substrates or inhibitors of P-glycoprotein. Drug Discovery Today *17*, 343-351.

Cheng, H., Liang, Y., Kuo, Y., Chuu, C., Lin, C., Lee, M., Wu, A., Yeh, C.*, et al.* (2015). Identification of thioridazine, an antipsychotic drug, as an antiglioblastoma and anticancer stem cell agent using public gene expression data. Cell Death & Disease *6*, e1753.

Chesi, M., Mirza, N.N., Garbitt, V.M., Sharik, M.E., Dueck, A.C., Asmann, Y.W., Akhmetzyanova, I., Kosiorek, H.E.*, et al.* (2016). IAP antagonists induce anti-tumor immunity in multiple myeloma. Nature Medicine *22*, 1411.

Chiorazzi, N., Rai, K.R., and Ferrarini, M. (2005). Chronic lymphocytic leukemia. New England Journal of Medicine *352*, 804-815.

Chitnis, M., Hegde, U., Chavan, S., Juvekar, A., and Advani, S. (1991). Expression of the multidrug transporter P-glycoprotein and in vitro chemosensitivity: correlation with in vivo response to chemotherapy in acute myeloid leukemia. Selective Cancer Therapeutics *7*, 165-173.

Chojnacka-Wójcik, E., and Klodzińska, A. (1992). Involvement of 5-HT 1B receptors in the anticonflict effect of m-CPP in rats. Journal of Neural Transmission/General Section *87*, 87-96.

Chonjnacka-Wójcik, E., and Przegalinski, E. (1991). Evidence for the involvement of 5-HT1A receptors in the anticonflict effect of ipsapirone in rats. Neuropharmacology *30*, 703-709.

Chou, F.H.-C., Tsai, K.-Y., Su, C.-Y., and Lee, C.-C. (2011). The incidence and relative risk factors for developing cancer among patients with schizophrenia: a nine-year follow-up study. Schizophrenia Research *129*, 97-103.

Christie, E.L., Pattnaik, S., Beach, J., Copeland, A., Rashoo, N., Fereday, S., Hendley, J., Alsop, K.*, et al.* (2019). Multiple ABCB1 transcriptional fusions in drug resistant high-grade serous ovarian and breast cancer. Nature Communications *10*, 1295.

Chu, Q., Vincent, M., Logan, D., Mackay, J.A., Evans, W.K., and Lung Cancer Disease Site Group of Cancer Care Ontario's Program in Evidence-based care (2005). Taxanes as first-line therapy for advanced non-small cell lung cancer: a systematic review and practice guideline. Lung Cancer *50*, 355-374.

Cole, S., Bhardwaj, G., Gerlach, J., Mackie, J., Grant, C., Almquist, K., Stewart, A., Kurz, E.*, et al.* (1992). Overexpression of a transporter gene in a multidrug-resistant human lung cancer cell line. Science *258*, 1650-1654.

Cole, S.P.C. (2014). Multidrug resistance protein 1 (MRP1, ABCC1), a "multitasking" ATP-binding cassette (ABC) transporter. The Journal of Biological Chemistry *289*, 30880-30888.

Collins, C., Wang, J., Miao, H., Bronstein, J., Nawer, H., Xu, T., Figueroa, M., Muntean, A.G.*, et al.* (2014). C/EBPalpha is an essential collaborator in Hoxa9/Meis1-mediated leukemogenesis. Proceedings of the National Academy of Sciences *111*, 9899-9904.

Condon, S.M. (2011). The discovery and development of Smac mimetics—small-molecule antagonists of the inhibitor of apoptosis proteins. In Annual reports in Medicinal Chemistry *46*, 211-226.

Condon, S.M., Mitsuuchi, Y., Deng, Y., LaPorte, M.G., Rippin, S.R., Haimowitz, T., Alexander, M.D., Kumar, P.T.*, et al.* (2014). Birinapant, a smac-mimetic with improved tolerability for the treatment of solid tumors and hematological malignancies. Journal of Medicinal Chemistry *57*, 3666-3677.

Costello, R.T., Mallet, F., Gaugler, B., Sainty, D., Arnoulet, C., Gastaut, J.-A., and Olive, D. (2000). Human acute myeloid leukemia CD34+/CD38− progenitor cells have decreased sensitivity to chemotherapy and Fas-induced apoptosis, reduced immunogenicity, and impaired dendritic cell transformation capacities. Cancer Research *60*, 4403-4411.

Coussens, L.M., and Werb, Z. (2002). Inflammation and cancer. Nature *420*, 860.

Cowin, P.A., George, J., Fereday, S., Loehrer, E., Van Loo, P., Cullinane, C., Etemadmoghadam, D., Ftouni, S.*, et al.* (2012). LRP1B deletion in high-grade serous ovarian cancers is associated with acquired chemotherapy resistance to liposomal doxorubicin. Cancer Research *72*, 4060-4073.

Creagh, E.M., Murphy, B.M., Duriez, P.J., Duckett, C.S., and Martin, S.J. (2004). Smac/Diablo antagonizes ubiquitin ligase activity of inhibitor of apoptosis proteins. Journal of Biological Chemistry *279*, 26906-26914.

Criscione, L., Rigollier, P., Batzl-Hartmann, C., Rüeger, H., Stricker-Krongrad, A., Wyss, P., Brunner, L., Whitebread, S.*, et al.* (1998). Food intake in free-feeding and energy-deprived lean rats is mediated by the neuropeptide Y5 receptor. The Journal of Clinical Investigation *102*, 2136-2145.

Dai, Z., Zhu, W.-G., Morrison, C.D., Brena, R.M., Smiraglia, D.J., Raval, A., Wu, Y.-Z., Rush, L.J.*, et al.* (2003). A comprehensive search for DNA amplification in lung cancer identifies inhibitors of apoptosis cIAP1 and cIAP2 as candidate oncogenes. Human Molecular Genetics *12*, 791-801.

Darding, M., Feltham, R., Tenev, T., Bianchi, K., Benetatos, C., Silke, J., and Meier, P. (2011). Molecular determinants of Smac mimetic induced degradation of cIAP1 and cIAP2. Cell Death & Differentiation *18*, 1376-1386.

De Almagro, M., and Vucic, D. (2012). The inhibitor of apoptosis (IAP) proteins are critical regulators of signaling pathways and targets for anti-cancer therapy. Experimental Oncology *34*, 200-211.

Degterev, A., Hitomi, J., Germscheid, M., Ch'en, I.L., Korkina, O., Teng, X., Abbott, D., Cuny, G.D.*, et al.* (2008). Identification of RIP1 kinase as a specific cellular target of necrostatins. Nature Chemical Biology *4*, 313-321.

Delbridge, A.R., Grabow, S., Strasser, A., and Vaux, D.L. (2016). Thirty years of BCL-2: translating cell death discoveries into novel cancer therapies. Nature Reviews Cancer *16*, 99.

Desplanques, G., Giuliani, N., Delsignore, R., Rizzoli, V., Bataille, R., and Barillé-Nion, S. (2009). Impact of XIAP protein levels on the survival of myeloma cells. Haematologica *94*, 87-93.

Di Pilato, P., Niso, M., Adriani, W., Romano, E., Travaglini, D., Berardi, F., Colabufo, N.A., Perrone, R.*, et al.* (2014). Selective agonists for serotonin 7 (5-HT7) receptor and their applications in preclinical models: an overview. Reviews in the Neurosciences *25*, 401-415.

Dickens, L.S., Boyd, R.S., Jukes-Jones, R., Hughes, M.A., Robinson, G.L., Fairall, L., Schwabe, J.W., Cain, K.*, et al.* (2012). A death effector domain chain DISC model reveals a crucial role for caspase-8 chain assembly in mediating apoptotic cell death. Molecular Cell *47*, 291-305.

Didziapetris, R., Japertas, P., Avdeef, A., and Petrauskas, A. (2003). Classification analysis of P-glycoprotein substrate specificity. Journal of Drug Targeting *11*, 391-406.

Dienstmann, R., Vidal, L., Dees, E., Chia, S., Mayer, E., Porter, D., Baney, T., Dhuria, S.*, et al.* (2012). AACR Abstract P6-11-06: A phase Ib study of LCL161, an oral inhibitor of apoptosis (IAP) antagonist, in combination with weekly paclitaxel in patients with advanced solid tumors.

Ding, L., Ley, T.J., Larson, D.E., Miller, C.A., Koboldt, D.C., Welch, J.S., Ritchey, J.K., Young, M.A.*, et al.* (2012). Clonal evolution in relapsed acute myeloid leukaemia revealed by whole-genome sequencing. Nature *481*, 506.

Dondelinger, Y., Delanghe, T., Rojas-Rivera, D., Priem, D., Delvaeye, T., Bruggeman, I., Van Herreweghe, F., Vandenabeele, P.*, et al.* (2017). MK2 phosphorylation of RIPK1 regulates TNF-mediated cell death. Nature Cell Biology *19*, 1237.

Dowling, J.P., Alsabbagh, M., Del Casale, C., Liu, Z.-G., and Zhang, J. (2019). TRADD regulates perinatal development and adulthood survival in mice lacking RIPK1 and RIPK3. Nature Communications *10*, 705.

Doyle, L.A., Yang, W., Abruzzo, L.V., Krogmann, T., Gao, Y., Rishi, A.K., and Ross, D.D. (1998). A multidrug resistance transporter from human MCF-7 breast cancer cells. Proceedings of the National Academy of Sciences *95*, 15665-15670.

Drach, J., Gsur, A., Hamilton, G., Zhao, S., Angerler, J., Fiegl, M., Zojer, N., Raderer, M.*, et al.* (1996). Involvement of P-glycoprotein in the transmembrane transport of interleukin-2 (IL-2), IL-4, and interferon-gamma in normal human T lymphocytes. Blood *88*, 1747-1754.

Dray, A. (1995). Inflammatory mediators of pain. British Journal of Anaesthesia *75*, 125-131.

Drenou, B., Fardel, O., Amiot, L., and Fauchet, R. (1993). Detection of P glycoprotein activity on normal and leukemic CD34+ cells. Leukemia Research *17*, 1031-1035.

Du, C., Fang, M., Li, Y., Li, L., and Wang, X. (2000). Smac, a mitochondrial protein that promotes cytochrome c–dependent caspase activation by eliminating IAP inhibition. Cell *102*, 33-42.

Dudley, D.T., Pang, L., Decker, S.J., Bridges, A.J., and Saltiel, A.R. (1995). A synthetic inhibitor of the mitogen-activated protein kinase cascade. Proceedings of the National Academy of Sciences *92*, 7686-7689.

Dueber, E.C., Schoeffler, A.J., Lingel, A., Elliott, J.M., Fedorova, A.V., Giannetti, A.M., Zobel, K., Maurer, B.*, et al.* (2011). Antagonists induce a conformational change in cIAP1 that promotes autoubiquitination. Science *334*, 376-380.

Dumont, Y., Cadieux, A., Doods, H., Fournier, A., and Quirion, R. (2000). Potent and selective tools to investigate neuropeptide Y receptors in the central and peripheral nervous systems: BIBO3304 (Y1) and CGP71683A (Y5). Canadian Journal of Physiology and Pharmacology *78*, 116-125.

Dürk, T., Panther, E., Müller, T., Sorichter, S., Ferrari, D., Pizzirani, C., Di Virgilio, F., Myrtek, D.*, et al.* (2005). 5-Hydroxytryptamine modulates cytokine and chemokine production in LPS-primed human monocytes via stimulation of different 5-HTR subtypes. International Immunology *17*, 599-606.

Ebert, G., Allison, C., Preston, S., Cooney, J., Toe, J.G., Stutz, M.D., Ojaimi, S., Baschuk, N.*, et al.* (2015a). Eliminating hepatitis B by antagonizing cellular inhibitors of apoptosis. Proceedings of the National Academy of Sciences *112*, 5803-5808.

Ebert, G., Preston, S., Allison, C., Cooney, J., Toe, J.G., Stutz, M.D., Ojaimi, S., Scott, H.W.*, et al.* (2015b). Cellular inhibitor of apoptosis proteins prevent clearance of hepatitis B virus. Proceedings of the National Academy of Sciences *112*, 5797-5802.

Eckhardt, S., Gallant, G., Sikic, B., Camidge, D., Burris III, H., Wakelee, H., Messersmith, W., Jones, S.*, et al.* (2010). Phase I study evaluating the safety, tolerability, and pharmacokinetics (PK) of HGS1029, a small-molecule inhibitor of apoptosis protein (IAP), in patients (pts) with advanced solid tumors. Journal of Clinical Oncology *28*, 2580-2580.

Edinger, A.L., and Thompson, C.B. (2004). Death by design: apoptosis, necrosis and autophagy. Current Opinion in Cell Biology *16*, 663-669.

Ekert, P.G., Silke, J., Hawkins, C.J., Verhagen, A.M., and Vaux, D.L. (2001). DIABLO promotes apoptosis by removing MIHA/XIAP from processed caspase 9. The Journal of Cell Biology *152*, 483-490.

Eriksson, T.M., Golkar, A., Ekström, J.C., Svenningsson, P., and Ögren, S.O. (2008). 5-HT7 receptor stimulation by 8-OH-DPAT counteracts the impairing effect of 5-HT1A receptor stimulation on contextual learning in mice. European Journal of Pharmacology *596*, 107-110.

Errico, M., Crozier, R., Plummer, M., and Cowen, D. (2001). 5-HT7 receptors activate the mitogen activated protein kinase extracellular signal related kinase in cultured rat hippocampal neurons. Neuroscience *102*, 361-367.

Esposito, I., Kleeff, J., Abiatari, I., Shi, X., Giese, N., Bergmann, F., Roth, W., Friess, H.*, et al.* (2007). Overexpression of cellular inhibitor of apoptosis protein 2 is an early event in the progression of pancreatic cancer. Journal of Clinical Pathology *60*, 885-895.

Etemadmoghadam, D., Azar, W.J., Lei, Y., Moujaber, T., Garsed, D.W., Kennedy, C.J., Fereday, S., Mitchell, C.*, et al.* (2017). EIF1AX and NRAS Mutations Co-occur and Cooperate in Low-Grade Serous Ovarian Carcinomas. Cancer Research *77*, 4268-4278.

Eytan, D.F., Snow, G.E., Carlson, S., Derakhshan, A., Saleh, A., Schiltz, S., Cheng, H., Mohan, S*., et al.* (2016). SMAC mimetic birinapant plus radiation eradicates human head and neck cancers with genomic amplifications of cell death genes FADD and BIRC2. Cancer Research *76*, 5442-5454.

Eytan, D.F., Snow, G.E., Carlson, S.G., Schiltz, S., Chen, Z., and Van Waes, C. (2015). Combination effects of SMAC mimetic birinapant with TNF α, TRAIL, and docetaxel in preclinical models of HNSCC. The Laryngoscope *125*, E118-E124.

Favata, M.F., Horiuchi, K.Y., Manos, E.J., Daulerio, A.J., Stradley, D.A., Feeser, W.S., Van Dyk, D.E., Pitts, W.J*., et al.* (1998). Identification of a novel inhibitor of mitogen-activated protein kinase kinase. Journal of Biological Chemistry *273*, 18623-18632.

Faye, M., Beug, S., Graber, T., Earl, N., Xiang, X., Wild, B., Langlois, S., Michaud, J*., et al.* (2015). IGF2BP1 controls cell death and drug resistance in rhabdomyosarcomas by regulating translation of cIAP1. Oncogene *34*, 1532.

Feltham, R., Bettjeman, B., Budhidarmo, R., Mace, P.D., Shirley, S., Condon, S.M., Chunduru, S.K., McKinlay, M.A*., et al.* (2011). Smac mimetics activate the E3 ligase activity of cIAP1 protein by promoting RING domain dimerization. Journal of Biological Chemistry *286*, 17015-17028.

Firestone, B., Conway, C., Yang, G., Gao, H., Porter, D., Slisz, J., He, D., Mosher, R*., et al.* (2009). AACR Abstract B27: Correlation between TNFα and LCL161 anti-tumor activity in patient derived xenograft models of human cancer.

Fitzgerald, M.L., Mujawar, Z., and Tamehiro, N. (2010). ABC transporters, atherosclerosis and inflammation. Atherosclerosis *211*, 361-370.

Fletcher, J.I., Haber, M., Henderson, M.J., and Norris, M.D. (2010). ABC transporters in cancer: more than just drug efflux pumps. Nature Reviews Cancer *10*, 147.

Flygare, J.A., Beresini, M., Budha, N., Chan, H., Chan, I.T., Cheeti, S., Cohen, F., Deshayes, K*., et al.* (2012). Discovery of a potent small-molecule antagonist of inhibitor of apoptosis (IAP) proteins and clinical candidate for the treatment of cancer (GDC-0152). Journal of Medicinal Chemistry *55*, 4101-4113.

Fong, C.Y., Gilan, O., Lam, E.Y., Rubin, A.F., Ftouni, S., Tyler, D., Stanley, K., Sinha, D*., et al.* (2015). BET inhibitor resistance emerges from leukaemia stem cells. Nature *525*, 538.

Ford, J.M., Prozialeck, W.C., and Hait, W. (1989). Structural features determining activity of phenothiazines and related drugs for inhibition of cell growth and reversal of multidrug resistance. Molecular Pharmacology *35*, 105-115.

Fox, E., and Bates, S.E. (2007). Tariquidar (XR9576): a P-glycoprotein drug efflux pump inhibitor. Expert Review of Anticancer Therapy *7*, 447-459.

Frey, N.V., Luger, S., Mangan, J., Zebrowski, A., Loren, A.W., Minderman, H., Baird, J., Porter, D.L*., et al.* (2014). Abstract 616. A phase I study using single agent birinapant in patients with relapsed myelodysplastic syndrome and acute myelogenous leukemia. Blood *124*, 3758.

Fulda, S. (2012). Exploiting inhibitor of apoptosis proteins as therapeutic targets in hematological malignancies. Leukemia *26*, 1155-1165.

Fulda, S., and Vucic, D. (2012). Targeting IAP proteins for therapeutic intervention in cancer. Nature Review Drug Discovery *11*, 109-124.

Fulda, S., Wick, W., Weller, M., and Debatin, K.-M. (2002). Smac agonists sensitize for Apo2L/TRAIL-or anticancer drug-induced apoptosis and induce regression of malignant glioma in vivo. Nature Medicine *8*, 808.

Füllsack, S., Rosenthal, A., Wajant, H., and Siegmund, D. (2019). Redundant and receptor-specific activities of TRADD, RIPK1 and FADD in death receptor signaling. Cell Death & Disease *10*, 122.

Furuno, T., Landi, M.-T., Ceroni, M., Caporaso, N., Bernucci, I., Nappi, G., Martignoni, E., Schaeffeler, E.*, et al.* (2002). Expression polymorphism of the blood–brain barrier component P-glycoprotein (MDR1) in relation to Parkinson's disease. Pharmacogenetics and Genomics *12*, 529-534.

Gaither, A., Porter, D., Yao, Y., Borawski, J., Yang, G., Donovan, J., Sage, D., Slisz, J.*, et al.* (2007). A Smac mimetic rescue screen reveals roles for inhibitor of apoptosis proteins in tumor necrosis factor-α signaling. Cancer Research *67*, 11493-11498.

Galbán, S., Hwang, C., Rumble, Julie M., Oetjen, Karolyn A., Wright, Casey W., Boudreault, A., Durkin, J., Gillard, John W.*, et al.* (2009). Cytoprotective effects of IAPs revealed by a small molecule antagonist. Biochemical Journal *417*, 765-771.

Ganapathi, R., Kuo, T., Teeter, L., Grabowski, D., and Ford, J. (1991). Relationship between expression of P-glycoprotein and efficacy of trifluoperazine in multidrug-resistant cells. Molecular Pharmacology *39*, 1-8.

Ganem, D., and Prince, A.M. (2004). Hepatitis B virus infection—natural history and clinical consequences. New England Journal of Medicine *350*, 1118-1129.

Gang, W., Hongjian, T., Jasheng, C., Jiemin, S., Zhong, C., Yuemin, X., Baojun, G., and Andersson, K.E. (2014). The effect of the 5-HT7 serotonin receptor agonist, LP44, on micturition in rats with chronic spinal cord injury. Neurourology and Urodynamics *33*, 1165-1170.

Garg, M., Nagata, Y., Kanojia, D., Mayakonda, A., Yoshida, K., Keloth, S.H., Zang, Z.J., Okuno, Y.*, et al.* (2015). Profiling of somatic mutations in acute myeloid leukemia with FLT3-ITD at diagnosis and relapse. Blood *126*, 2491-2501.

Gautam, J., Bae, Y.K., and Kim, J.-A. (2017). Up-regulation of cathepsin S expression by HSP90 and 5-HT 7 receptor-dependent serotonin signaling correlates with triple negativity of human breast cancer. Breast Cancer Research and Treatment *161*, 29-40.

Gautam, J., Banskota, S., Regmi, S.C., Ahn, S., Jeon, Y.H., Jeong, H., Kim, S.J., Nam, T.-g.*, et al.* (2016). Tryptophan hydroxylase 1 and 5-HT 7 receptor preferentially expressed in triple-negative breast cancer promote cancer progression through autocrine serotonin signaling. Molecular Cancer *15*, 75.

Gelenberg, A.J., Bassuk, E.L., and Schoonover, S.C. (2013). The practitioner's guide to psychoactive drugs. Springer Science & Business Media.

Gerlach, B., Cordier, S.M., Schmukle, A.C., Emmerich, C.H., Rieser, E., Haas, T.L., Webb, A.I., Rickard, J.A.*, et al.* (2011). Linear ubiquitination prevents inflammation and regulates immune signalling. Nature *471*, 591-596.

Gerrard, G., Payne, E., Baker, R.J., Jones, D.T., Potter, M., Prentice, H.G., Ethell, M., McCullough, H.*, et al.* (2004). Clinical effects and P-glycoprotein inhibition in patients with acute myeloid leukemia treated with zosuquidar trihydrochloride, daunorubicin and cytarabine. Haematologica *89*, 782-790.

Gershon, M.D., and Tack, J. (2007). The serotonin signaling system: from basic understanding to drug development for functional GI disorders. Gastroenterology *132*, 397-414.

Giacomini, K.M., Huang, S.-M., Tweedie, D.J., Benet, L.Z., Brouwer, K.L., Chu, X., Dahlin, A., Evers, R.*, et al.* (2010). Membrane transporters in drug development. Nature reviews Drug Discovery *9*, 215.

Gil-Ad, I., Shtaif, B., Levkovitz, Y., Dayag, M., Zeldich, E., and Weizman, A. (2004). Characterization of phenothiazine-induced apoptosis in neuroblastoma and glioma cell lines. Journal of Molecular Neuroscience *22*, 189-198.

Goldie, J.H., and Coldman, A.J. (1984). The genetic origin of drug resistance in neoplasms: implications for systemic therapy. Cancer Research *44*, 3643-3653.

Goodell, M.A., Brose, K., Paradis, G., Conner, A.S., and Mulligan, R.C. (1996). Isolation and functional properties of murine hematopoietic stem cells that are replicating in vivo. Journal of Experimental Medicine *183*, 1797-1806.

Gordon, J., and Barnes, N.M. (2007). Serotonin: a real blast for T cells. Blood *109*, 3130-3131.

Greenberg, P.L., Lee, S.J., Advani, R., Tallman, M.S., Sikic, B.I., Letendre, L., Dugan, K., Lum, B.*, et al.* (2004). Mitoxantrone, etoposide, and cytarabine with or without valspodar in patients with relapsed or refractory acute myeloid leukemia and high-risk myelodysplastic syndrome: a phase III trial (E2995). Journal of Clinical Oncology *22*, 1078.

Grimwade, D., Walker, H., Oliver, F., Wheatley, K., Harrison, C., Harrison, G., Rees, J., Hann, I.*, et al.* (1998). The importance of diagnostic cytogenetics on outcome in AML: analysis of 1,612 patients entered into the MRC AML 10 trial. Blood *92*, 2322-2333.

Gu, Y., Nakamura, T., Alder, H., Prasad, R., Canaani, O., Cimino, G., Croce, C., and Canaani, E. (1992). The t (4; 11) chromosome translocation of human acute leukemias fuses the ALL-1 gene, related to Drosophila trithorax, to the AF-4 gene. Cell *71*, 701-708.

Guan, Y., Gerhard, B., and Hogge, D.E. (2003). Detection, isolation, and stimulation of quiescent primitive leukemic progenitor cells from patients with acute myeloid leukemia (AML). Blood *101*, 3142-3149.

Guerci, A., Merlin, J.L., Missoum, N., Feldmann, L., Marchal, S., Witz, F., Rose, C., and Guerci, O. (1995). Predictive value for treatment outcome in acute myeloid leukemia of cellular daunorubicin accumulation and P-glycoprotein expression simultaneously determined by flow cytometry. Blood *85*, 2147-2153.

Guscott, M., Bristow, L., Hadingham, K., Rosahl, T., Beer, M., Stanton, J., Bromidge, F., Owens, A.*, et al.* (2005). Genetic knockout and pharmacological blockade studies of the 5-HT 7 receptor suggest therapeutic potential in depression. Neuropharmacology *48*, 492-502.

Guseva, D., Holst, K., Kaune, B., Meier, M., Keubler, L., Glage, S., Buettner, M., Bleich, A.*, et al.* (2014a). Serotonin 5-HT7 receptor is critically involved in acute and chronic inflammation of the gastrointestinal tract. Inflammatory Bowel Diseases *20*, 1516-1529.

Guseva, D., Wirth, A., and Ponimaskin, E. (2014b). Cellular mechanisms of the 5-HT7 receptor-mediated signaling. Frontiers in Behavioral Neuroscience *8*, 306.

Gyrd-Hansen, M., Darding, M., Miasari, M., Santoro, M.M., Zender, L., Xue, W., Tenev, T., da Fonseca, P.C.A.*, et al.* (2008). IAPs contain an evolutionarily conserved ubiquitin-binding domain that regulates NF-[kappa]B as well as cell survival and oncogenesis. Nature Cell Biology *10*, 1309-1317.

Hagan, J.J., Price, G.W., Jeffrey, P., Deeks, N.J., Stean, T., Piper, D., Smith, M.I., Upton, N.*, et al.* (2000). Characterization of SB-269970-A, a selective 5-HT7 receptor antagonist. British Journal of Pharmacology *130*, 539-548.

Hajitou, A., Rangel, R., Trepel, M., Soghomonyan, S., Gelovani, J.G., Alauddin, M.M., Pasqualini, R., and Arap, W. (2007). Design and construction of targeted AAVP vectors for mammalian cell transduction. Nature Protocols *2*, 523.

Hajitou, A., Trepel, M., Lilley, C.E., Soghomonyan, S., Alauddin, M.M., Marini, F.C., Restel, B.H., Ozawa, M.G.*, et al.* (2006). A Hybrid Vector for Ligand-Directed Tumor Targeting and Molecular Imaging. Cell *125*, 385-398.

Hallahan, D.E., Spriggs, D.R., Beckett, M.A., Kufe, D.W., and Weichselbaum, R.R. (1989). Increased tumor necrosis factor alpha mRNA after cellular exposure to ionizing radiation. Proceedings of the National Academy of Sciences *86*, 10104-10107.

Hannan, R.D., Drygin, D., and Pearson, R.B. (2013). Targeting RNA polymerase I transcription and the nucleolus for cancer therapy. Expert Opinion on Therapeutic Targets *17*, 873-878.

Heard, K.N., Bertrand, M.J., and Barker, P.A. (2015). cIAP2 supports viability of mice lacking cIAP1 and XIAP. The EMBO Journal *34*, 2393-2395.

Hedlund, P., Danielson, P., Thomas, E., Slanina, K., Carson, M., and Sutcliffe, J. (2003). No hypothermic response to serotonin in 5-HT7 receptor knockout mice. Proceedings of the National Academy of Sciences *100*, 1375-1380.

Hedlund, P.B. (2009). The 5-HT7 receptor and disorders of the nervous system: an overview. Psychopharmacology *206*, 345-354.

Hedlund, P.B., Huitron-Resendiz, S., Henriksen, S.J., and Sutcliffe, J.G. (2005). 5-HT 7 receptor inhibition and inactivation induce antidepressantlike behavior and sleep pattern. Biological Psychiatry *58*, 831-837.

Hedman, A., Angelin, B., Arvidsson, A., Dahlqvist, R., and Nilsson, B. (1990). Interactions in the renal and biliary elimination of digoxin: stereoselective difference between quinine and quinidine. Clinical Pharmacology & Therapeutics *47*, 20-26.

Hegde, R., Srinivasula, S.M., Zhang, Z., Wassell, R., Mukattash, R., Cilenti, L., DuBois, G., Lazebnik, Y.*, et al.* (2002). Identification of Omi/HtrA2 as a mitochondrial apoptotic serine protease that disrupts inhibitor of apoptosis protein-caspase interaction. Journal of Biological Chemistry *277*, 432-438.

Herbein, G., and O'brien, W.A. (2000). Tumor Necrosis Factor (TNF)–α and TNF Receptors in Viral Pathogenesis. Proceedings of the Society for Experimental Biology and Medicine: Minireviews *223*, 241-257.

Higgins, C.F. (1992). ABC transporters: from microorganisms to man. Annual review of Cell Biology *8*, 67-113.

High, J., Hassert Jr, G., Rubin, B., Piala, J., Burke, J., and Craver, B. (1960). Pharmacology of fluphenazine (Prolixin). Toxicology and Applied Pharmacology *2*, 540-552.

Hird, A.W., Aquila, B.M., Hennessy, E.J., Vasbinder, M.M., and Yang, B. (2015). Small molecule inhibitor of apoptosis proteins antagonists: a patent review. Expert Opinion on Therapeutic Patents *25*, 755-774.

Ho, T.-C., LaMere, M., Stevens, B.M., Ashton, J.M., Myers, J.R., O'Dwyer, K.M., Liesveld, J.L., Mendler, J.H.*, et al.* (2016). Evolution of acute myelogenous leukemia stem cell properties following treatment and progression. Blood, *128*, 1671-1678.

Houghton, P.J., Kang, M.H., Reynolds, C.P., Morton, C.L., Kolb, E.A., Gorlick, R., Keir, S.T., Carol, H.*, et al.* (2012). Initial testing (stage 1) of LCL161, a SMAC mimetic, by the Pediatric Preclinical Testing Program. Pediatric Blood & Cancer *58*, 636-639.

Hoyer, D., Engel, G., and Kalkman, H.O. (1985). Molecular pharmacology of 5-HT1 and 5-HT2 recognition sites in rat and pig brain membranes: radioligand binding studies with [3H] 5-HT,[3H] 8-OH-DPAT,(−)[125I] iodocyanopindolol,[3H] mesulergine and [3H] ketanserin. European Journal of Pharmacology *118*, 13-23.

Hoyer, D., Hannon, J.P., and Martin, G.R. (2002). Molecular, pharmacological and functional diversity of 5-HT receptors. Pharmacology Biochemistry and Behavior *71*, 533-554.

Hu, S., and Yang, X. (2003). Cellular inhibitor of apoptosis 1 and 2 are ubiquitin ligases for the apoptosis inducer Smac/DIABLO. Journal of Biological Chemistry *278*, 10055-10060.

Hugle, M., Czaplinski, S., Habermann, K., Vogler, M., and Fulda, S. (2019). Identification of Smac mimetics as novel substrates for p-glycoprotein. Cancer Letters *440*, 126-134.

Humphreys, R.C., Poortman, C., McCormick, K., Carrell, J., and Shepard, L. (2009). Abstract C10: A novel combination of a small molecule IAP inhibitor and a TRAIL-R1 monoclonal antibody synergize to induce apoptosis in pancreatic tumor cell lines. Molecular Cancer Therapeutics *8*, C10-C10.

Hurwitz, H.I., Smith, D.C., Pitot, H.C., Brill, J.M., Chugh, R., Rouits, E., Rubin, J., Strickler, J.*, et al.* (2015). Safety, pharmacokinetics, and pharmacodynamic properties of oral DEBIO1143 (AT-406) in patients with advanced cancer: results of a first-in-man study. Cancer Chemotherapy and Pharmacology *75*, 851-859.

Ianevski, A., He, L., Aittokallio, T., and Tang, J. (2017). SynergyFinder: a web application for analyzing drug combination dose–response matrix data. Bioinformatics *33*, 2413-2415.

Impagnatiello, M.A., Reschke, M., Reiser, U., Scharn, D., Spevak, W., Savchenko, A., Tirapu, I., Wernitznig, A.*, et al.* (2017). BI5 (BI 891065): a Novel SMAC Mimetic that Triggers Tumor Cell Death and Potentiates PD-1 Mediated Cancer Therapy. In AACR Annual Meeting 2017 (Washington D.C., USA).

Infante, J.R., Dees, E.C., Olszanski, A.J., Dhuria, S.V., Sen, S., Cameron, S., and Cohen, R.B. (2014). Phase I dose-escalation study of LCL161, an oral inhibitor of apoptosis proteins inhibitor, in patients with advanced solid tumors. Journal of Clinical Oncology *32*, 3103-3110.

Ishikawa, F., Yoshida, S., Saito, Y., Hijikata, A., Kitamura, H., Tanaka, S., Nakamura, R., Tanaka, T.*, et al.* (2007). Chemotherapy-resistant human AML stem cells home to and engraft within the bone-marrow endosteal region. Nature Biotechnology *25*, 1315.

Itil, T., Keskiner, A., Heinemann, L., Han, T., Gannon, P., and Hsu, W. (1970). Treatment of resistant schizophrenics with extreme high dosage fluphenazine hydrochloride. Psychosomatics: Journal of Consultation and Liaison Psychiatry *11*, 456-463.

Jaco, I., Annibaldi, A., Lalaoui, N., Wilson, R., Tenev, T., Laurien, L., Kim, C., Jamal, K.*, et al.* (2017). MK2 phosphorylates RIPK1 to prevent TNF-induced cell death. Molecular Cell *66*, 698-710.

Janzen, D., Tiourin, E., Salehi, J., Paik, D., Lu, J., Pellegrini, M., and Memarzadeh, S. (2015). An apoptosis-enhancing drug overcomes platinum resistance in a tumour-initiating subpopulation of ovarian cancer. Nature Communications *6*, 7956.

Jaszczyszyn, A., Gąsiorowski, K., Świątek, P., Malinka, W., Cieślik-Boczula, K., Petrus, J., and Czarnik-Matusewicz, B. (2012). Chemical structure of phenothiazines and their biological activity. Pharmacological Reports *64*, 16-23.

Ji, J., Yu, Y., Li, Z.-L., Chen, M.-Y., Deng, R., Huang, X., Wang, G.-F., Zhang, M.-X.*, et al.* (2018). XIAP Limits Autophagic Degradation of Sox2 and is a therapeutic target in nasopharyngeal carcinoma stem cells. Theranostics *8*, 1494.

Johnson-Farley, N.N., Kertesy, S.B., Dubyak, G.R., and Cowen, D.S. (2005). Enhanced activation of Akt and extracellular-regulated kinase pathways by simultaneous occupancy of Gq-coupled 5-HT2A receptors and Gs-coupled 5-HT7A receptors in PC12 cells. Journal of Neurochemistry *92*, 72-82.

Jordan, C.T., Guzman, M.L., and Noble, M. (2006). Cancer stem cells. New England Journal of Medicine *355*, 1253-1261.

Juliano, R.L., and Ling, V. (1976). A surface glycoprotein modulating drug permeability in Chinese hamster ovary cell mutants. Biochimica et Biophysica Acta (BBA)-Biomembranes *455*, 152-162.

Juliusson, G., Lazarevic, V., Hörstedt, A.-S., Hagberg, O., and Höglund, M. (2012). Acute myeloid leukemia in the real world: why population-based registries are needed. Blood *119*, 3890-3899.

Kaiser, W.J., Upton, J.W., Long, A.B., Livingston-Rosanoff, D., Daley-Bauer, L.P., Hakem, R., Caspary, T., and Mocarski, E.S. (2011). RIP3 mediates the embryonic lethality of caspase-8-deficient mice. Nature *471*, 368.

Kannan, P., Telu, S., Shukla, S., Ambudkar, S.V., Pike, V.W., Halldin, C., Gottesman, M.M., Innis, R.B.*, et al.* (2010). The "specific" P-glycoprotein inhibitor tariquidar is also a substrate and an inhibitor for breast cancer resistance protein (BCRP/ABCG2). ACS Chemical Neuroscience *2*, 82-89.

Katerinaki, E., Evans, G., Lorigan, P., and MacNeil, S. (2003). TNF-α increases human melanoma cell invasion and migration in vitro: the role of proteolytic enzymes. British Journal of Cancer *89*, 1123.

Kearney, C.J., Lalaoui, N., Freeman, A.J., Ramsbottom, K.M., Silke, J., and Oliaro, J. (2017). PD-L1 and IAPs co-operate to protect tumors from cytotoxic lymphocyte-derived TNF. Cell Death & Differentiation *24*, 1705.

Keogh, J.P., and Kunta, J.R. (2006). Development, validation and utility of an in vitro technique for assessment of potential clinical drug–drug interactions involving P-glycoprotein. European Journal of Pharmaceutical Sciences *27*, 543-554.

Kim, M., Turnquist, H., Jackson, J., Sgagias, M., Yan, Y., Gong, M., Dean, M., Sharp, J.G.*, et al.* (2002). The multidrug resistance transporter ABCG2 (breast cancer resistance protein 1) effluxes Hoechst 33342 and is overexpressed in hematopoietic stem cells. Clinical Cancer Research *8*, 22-28.

Kim, Y., and Chen, J. (2018). Molecular structure of human P-glycoprotein in the ATP-bound, outward-facing conformation. Science *359*, 915-919.

Kipp, R.A., Case, M.A., Wist, A.D., Cresson, C.M., Carrell, M., Griner, E., Wiita, A., Albiniak, P.A.*, et al.* (2002). Molecular targeting of inhibitor of apoptosis proteins based on small molecule mimics of natural binding partners. Biochemistry *41*, 7344-7349.

Kirn, R.B., Wandel, C., Leake, B., Cvetkovic, M., Fromm, M.F., Dempsey, P.J., Roden, M.M., Belas, F.*, et al.* (1999). Interrelationship between substrates and inhibitors of human CYP3A and P-glycoprotein. Pharmaceutical Research *16*, 408-414.

Kitson, J., Raven, T., Jiang, Y.-P., Goeddel, D.V., Giles, K.M., Pun, K.-T., Grinham, C.J., Brown, R.*, et al.* (1996). A death-domain-containing receptor that mediates apoptosis. Nature *384*, 372-375.

Kluck, R.M., Bossy-Wetzel, E., Green, D.R., and Newmeyer, D.D. (1997). The release of cytochrome c from mitochondria: a primary site for Bcl-2 regulation of apoptosis. Science *275*, 1132-1136.

Kobe, F., Guseva, D., Jensen, T.P., Wirth, A., Renner, U., Hess, D., Müller, M., Medrihan, L.*, et al.* (2012). 5-HT7R/G12 signaling regulates neuronal morphology and function in an age-dependent manner. Journal of Neuroscience *32*, 2915-2930.

Koh, E.H., Chung, H.C., Lee, K.B., Lim, H.Y., Kim, J.H., Roh, J.K., Min, J.S., Lee, K.S.*, et al.* (1992). The value of immunohistochemical detection of P-glycoprotein in breast cancer before and after induction chemotherapy. Yonsei Medical Journal *33*, 137-142.

Kolitz, J.E., George, S.L., Dodge, R.K., Hurd, D.D., Powell, B.L., Allen, S.L., Velez-Garcia, E., Moore, J.O.*, et al.* (2004). Dose escalation studies of cytarabine, daunorubicin, and etoposide with and without multidrug resistance modulation with PSC-833 in untreated adults with acute myeloid leukemia younger than 60 years: final induction results of Cancer and Leukemia Group B Study 9621. Journal of Clinical Oncology *22*, 4290-4301.

Kolitz, J.E., George, S.L., Marcucci, G., Vij, R., Powell, B.L., Allen, S.L., DeAngelo, D.J., Shea, T.C.*, et al.* (2010). P-glycoprotein inhibition using valspodar (PSC-833) does not improve outcomes for patients younger than age 60 years with newly diagnosed acute myeloid leukemia: Cancer and Leukemia Group B study 19808. Blood *116*, 1413-1421.

Koren, G., Woodland, C., and Ito, S. (1998). Toxic digoxin-drug interactions: the major role of renal P-glycoprotein. Veterinary and Human Toxicology *40*, 45-46.

Krepler, C., Chunduru, S.K., Halloran, M.B., He, X., Xiao, M., Vultur, A., Villanueva, J., Mitsuuchi, Y.*, et al.* (2013). The novel SMAC mimetic birinapant exhibits potent activity against human melanoma cells. Clinical Cancer Research *19*, 1784-1794.

Krivtsov, A.V., and Armstrong, S.A. (2007). MLL translocations, histone modifications and leukaemia stem-cell development. Nature Reviews Cancer *7*, 823-833.

Krönke, J., Bullinger, L., Teleanu, V., Tschürtz, F., Gaidzik, V.I., Kühn, M.W., Rücker, F.G., Holzmann, K.*, et al.* (2013). Clonal evolution in relapsed NPM1-mutated acute myeloid leukemia. Blood *122*, 100-108.

Krumlauf, R. (1994). Hox genes in vertebrate development. Cell *78*, 191-201.

Kusunoki, N., Takara, K., Tanigawara, Y., Yamauchi, A., Ueda, K., Komada, F., Ku, Y., Kuroda, Y.*, et al.* (1998). Inhibitory effects of a cyclosporin derivative, SDZ PSC 833, on transport of doxorubicin and vinblastine via human P-glycoprotein. Japanese Journal of Cancer Research *89*, 1220-1228.

Kvachnina, E., Liu, G., Dityatev, A., Renner, U., Dumuis, A., Richter, D.W., Dityateva, G., Schachner, M.*, et al.* (2005). 5-HT7 receptor is coupled to Gα subunits of heterotrimeric G12-protein to regulate gene transcription and neuronal morphology. Journal of Neuroscience *25*, 7821-7830.

Lalaoui, N., Hänggi, K., Brumatti, G., Chau, D., Nguyen, N.-Y., Vasilikos, L., Spilgies, L.M., Heckmann, D.A.*, et al.* (2016). Targeting p38 or MK2 Enhances the Anti-Leukemic Activity of Smac-Mimetics. Cancer Cell *29*, 145-158.

Laukens, B., Jennewein, C., Schenk, B., Vanlangenakker, N., Schier, A., Cristofanon, S., Zobel, K., Deshayes, K.*, et al.* (2011). Smac mimetic bypasses apoptosis resistance in FADD-or caspase-8-deficient cells by priming for tumor necrosis factor α-induced necroptosis. Neoplasia *13*, 971.

Lee, E.J., George, S.L., Caligiuri, M., Szatrowski, T.P., Powell, B.L., Lemke, S., Dodge, R.K., Smith, R.*, et al.* (1999). Parallel phase I studies of daunorubicin given with cytarabine and etoposide with or without the multidrug resistance modulator PSC-833 in previously untreated patients 60 years of age or older with acute myeloid leukemia: results of Cancer and Leukemia Group B study 9420. Journal of Clinical Oncology *17*, 2831-2831.

Legrand, O., Simonin, G., Beauchamp-Nicoud, A., Zittoun, R., and Marie, J.-P. (1999). Simultaneous activity of MRP1 and Pgp is correlated with in vitro resistance to daunorubicin and with in vivo resistance in adult acute myeloid leukemia. Blood *94*, 1046-1056.

Leith, C. (1998). Multidrug resistance in leukemia. Current Opinion in Hematology *5*, 287-291.

Leith, C.P., Kopecky, K.J., Chen, I.-M., Eijdems, L., Slovak, M.L., McConnell, T.S., Head, D.R., Weick, J.*, et al.* (1999). Frequency and clinical significance of the expression of the multidrug resistance proteins MDR1/P-glycoprotein, MRP1, and LRP in acute myeloid leukemia. A Southwest Oncology Group Study. Blood *94*, 1086-1099.

Leith, C.P., Kopecky, K.J., Godwin, J., McConnell, T., Slovak, M.L., Chen, I.-M., Head, D.R., Appelbaum, F.R.*, et al.* (1997). Acute myeloid leukemia in the elderly: assessment of multidrug resistance (MDR1) and cytogenetics distinguishes biologic subgroups with remarkably distinct responses to standard chemotherapy. A Southwest Oncology Group study. Blood *89*, 3323-3329.

Lejeune, F.J., Liénard, D., Matter, M., and Rüegg, C. (2006). Efficiency of recombinant human TNF in human cancer therapy. Cancer Immunity Archive *6*, 6.

Leon-Ponte, M., Ahern, G.P., and O'Connell, P.J. (2007). Serotonin provides an accessory signal to enhance T-cell activation by signaling through the 5-HT7 receptor. Blood *109*, 3139-3146.

Leopoldo, M., Berardi, F., Colabufo, N.A., Contino, M., Lacivita, E., Niso, M., Perrone, R., and Tortorella, V. (2004). Structure−Affinity Relationship Study on N-(1,2,3,4-Tetrahydronaphthalen-1-yl)-4-Aryl-1-Piperazinealkylamides, a New Class of 5-Hydroxytryptamine7 Receptor Agents. Journal of Medicinal Chemistry *47*, 6616-6624.

Leopoldo, M., Lacivita, E., Berardi, F., Perrone, R., and Hedlund, P.B. (2011). Serotonin 5-HT7 receptor agents: Structure-activity relationships and potential therapeutic applications in central nervous system disorders. Pharmacology & Therapeutics *129*, 120-148.

Leopoldo, M., Lacivita, E., Contino, M., Colabufo, N.A., Berardi, F., and Perrone, R. (2007). Structure− activity relationship study on N-(1, 2, 3, 4-tetrahydronaphthalen-1-yl)-4-aryl-1-piperazinehexanamides, a class of 5-HT7 receptor agents. 2. Journal of Medicinal Chemistry *50*, 4214-4221.

Leopoldo, M., Lacivita, E., De Giorgio, P., Fracasso, C., Guzzetti, S., Caccia, S., Contino, M., Colabufo, N.A.*, et al.* (2008). Structural modifications of N-(1, 2, 3, 4-tetrahydronaphthalen-1-yl)-4-aryl-1-piperazinehexanamides: influence on lipophilicity and 5-HT7 receptor activity. Part III. Journal of Medicinal Chemistry *51*, 5813-5822.

Leslie, E.M., Deeley, R.G., and Cole, S.P. (2005). Multidrug resistance proteins: role of P-glycoprotein, MRP1, MRP2, and BCRP (ABCG2) in tissue defense. Toxicology and Applied Pharmacology *204*, 216-237.

Li, B.-X., Wang, H.-B., Qiu, M.-Z., Luo, Q.-Y., Yi, H.-J., Yan, X.-L., Pan, W.-T., Yuan, L.-P.*, et al.* (2018). Novel smac mimetic APG-1387 elicits ovarian cancer cell killing through TNF-alpha, Ripoptosome and autophagy mediated cell death pathway. Journal of Experimental & Clinical Cancer Research *37*, 53.

Li, L., Thomas, R.M., Suzuki, H., De Brabander, J.K., Wang, X., and Harran, P.G. (2004). A small molecule Smac mimic potentiates TRAIL-and TNFα-mediated cell death. Science *305*, 1471-1474.

Li, N., Feng, L., Han, H.-Q., Yuan, J., Qi, X.-K., Lian, Y.-F., Kuang, B.-H., Zhang, Y.-C.*, et al.* (2016). A novel Smac mimetic APG-1387 demonstrates potent antitumor activity in nasopharyngeal carcinoma cells by inducing apoptosis. Cancer Letters *381*, 14-22.

Lin, S.L., Johnson-Farley, N.N., Lubinsky, D.R., and Cowen, D.S. (2003). Coupling of neuronal 5-HT7 receptors to activation of extracellular-regulated kinase through a protein kinase A-independent pathway that can utilize Epac. Journal of Neurochemistry *87*, 1076-1085.

List, A.F., Kopecky, K.J., Willman, C.L., Head, D.R., Persons, D.L., Slovak, M.L., Dorr, R., Karanes, C.*, et al.* (2001). Benefit of cyclosporine modulation of drug resistance in patients with poor-risk acute myeloid leukemia: a Southwest Oncology Group study. Blood *98*, 3212-3220.

Liu, H., Hou, J., and Zhang, X. (2018). Targeting cIAPs, a New Option for Functional Cure of Chronic Hepatitis B Infection? Virologica Sinica *33*, 459-461.

Liu, N., Tao, Z., Le Blanc, J.M., Zaorsky, N.G., Sun, Y., Vuagniaux, G., Dicker, A.P., and Lu, B. (2014). Debio 1143, an antagonist of multiple inhibitor-of-apoptosis proteins, activates apoptosis and enhances radiosensitization of non-small cell lung cancer cells in vitro. American Journal of Cancer Research *4*, 943.

Lovenberg, T.W., Baron, B.M., de Lecea, L., Miller, J.D., Prosser, R.A., Rea, M.A., Foye, P.E., Racke, M.*, et al.* (1993). A novel adenylyl cyclase-activating serotonin receptor (5-HT7) implicated in the regulation of mammalian circadian rhythms. Neuron *11*, 449-458.

Löwenberg, B., Abels, J., van Bekkum, D.W., Dzoljic, G., Hagenbeek, A., Hendriks, W.D., van de Poel, J., Sizoo, W.*, et al.* (1984). Transplantation of non-purified autologous bone marrow in patients with AML in first remission. Cancer *54*, 2840-2843.

Lowenberg , B., Downing , J.R., and Burnett , A. (1999). Acute Myeloid Leukemia. New England Journal of Medicine *341*, 1051-1062.

Löwenberg, B., Verdonck, L.J., Dekker, A.W., Willemze, R., Zwaan, F.E., de Planque, M., Abels, J., Sonneveld, P.*, et al.* (1990). Autologous bone marrow transplantation in

acute myeloid leukemia in first remission: results of a Dutch prospective study. Journal of Clinical Oncology *8*, 287-294.

Mace, P.D., Smits, C., Vaux, D.L., Silke, J., and Day, C.L. (2010). Asymmetric recruitment of cIAPs by TRAF2. Journal of Molecular Biology *400*, 8-15.

MacLean, B., Tomazela, D.M., Shulman, N., Chambers, M., Finney, G.L., Frewen, B., Kern, R., Tabb, D.L.*, et al.* (2010). Skyline: an open source document editor for creating and analyzing targeted proteomics experiments. Bioinformatics *26*, 966-968.

Mahadevan, D., and List, A.F. (2004). Targeting the multidrug resistance-1 transporter in AML: molecular regulation and therapeutic strategies. Blood *104*, 1940-1951.

Mahoney, D., Cheung, H., Mrad, R.L., Plenchette, S., Simard, C., Enwere, E., Arora, V., Mak, T.*, et al.* (2008). Both cIAP1 and cIAP2 regulate TNFα-mediated NF-κB activation. Proceedings of the National Academy of Sciences *105*, 11778-11783.

Marcelletti, J.F., Multani, P.S., Lancet, J.E., Baer, M.R., and Sikic, B.I. (2009). Leukemic blast and natural killer cell P-glycoprotein function and inhibition in a clinical trial of zosuquidar infusion in acute myeloid leukemia. Leukemia Research *33*, 769-774.

Martin, C., Berridge, G., Higgins, C.F., Mistry, P., Charlton, P., and Callaghan, R. (2000). Communication between multiple drug binding sites on P-glycoprotein. Molecular Pharmacology *58*, 624-632.

Matsuzawa, A., Tseng, P.-H., Vallabhapurapu, S., Luo, J.-L., Zhang, W., Wang, H., Vignali, D.A., Gallagher, E.*, et al.* (2008). Essential cytoplasmic translocation of a cytokine receptor–assembled signaling complex. Science *321*, 663-668.

Matzinger, O., Viertl, D., Tsoutsou, P., Kadi, L., Rigotti, S., Zanna, C., Wiedemann, N., Vozenin, M.-C.*, et al.* (2015). The radiosensitizing activity of the SMAC-mimetic, Debio 1143, is TNFα-mediated in head and neck squamous cell carcinoma. Radiotherapy and Oncology *116*, 495-503.

Mayer, R.J., Davis, R.B., Schiffer, C.A., Berg, D.T., Powell, B.L., Schulman, P., Omura, G.A., Moore, J.O.*, et al.* (1994). Intensive postremission chemotherapy in adults with acute myeloid leukemia. New England Journal of Medicine *331*, 896-903.

McComb, S., Aguadé-Gorgorió, J., Harder, L., Marovca, B., Cario, G., Eckert, C., Schrappe, M., Stanulla, M.*, et al.* (2016). Activation of concurrent apoptosis and necroptosis by SMAC mimetics for the treatment of refractory and relapsed ALL. Science Translational Medicine *8*, 339-370.

McGlynn, K.A., Petrick, J.L., and London, W.T. (2015). Global epidemiology of hepatocellular carcinoma: an emphasis on demographic and regional variability. Clinical Liver Disease *19*, 223-238.

Menon, M.B., Gropengießer, J., Fischer, J., Novikova, L., Deuretzbacher, A., Lafera, J., Schimmeck, H., Czymmeck, N.*, et al.* (2017). p38MAPK/MK2-dependent phosphorylation controls cytotoxic RIPK1 signalling in inflammation and infection. Nature Cell Biology *19*, 1248.

Merino, D., Kelly, G.L., Lessene, G., Wei, A.H., Roberts, A.W., and Strasser, A. (2018). BH3-mimetic drugs: blazing the trail for new cancer medicines. Cancer Cell *34*, 879-891.

Meyer, C., Burmeister, T., Gröger, D., Tsaur, G., Fechina, L., Renneville, A., Sutton, R., Venn, N.*, et al.* (2018). The MLL recombinome of acute leukemias in 2017. Leukemia *32*, 273.

Meyer, C., Hofmann, J., Burmeister, T., Groger, D., Park, T.S., Emerenciano, M., Pombo de Oliveira, M., Renneville, A.*, et al.* (2013). The MLL recombinome of acute leukemias in 2013. Leukemia *27*, 2165-2176.

Micheau, O., and Tschopp, J. (2003). Induction of TNF receptor I-mediated apoptosis via two sequential signaling complexes. Cell *114*, 181-190.

Michie, J., Beavis, P.A., Freeman, A.J., Vervoort, S.J., Ramsbottom, K.M., Narasimhan, V., Lelliott, E.J., Lalaoui, N.*, et al.* (2019). Antagonism of IAPs enhances CAR T-cell efficacy. Cancer Immunology Research *7*, 183-192.

Mistry, P., Stewart, A.J., Dangerfield, W., Okiji, S., Liddle, C., Bootle, D., Plumb, J.A., Templeton, D.*, et al.* (2001). In vitro and in vivo reversal of P-glycoprotein-mediated multidrug resistance by a novel potent modulator, XR9576. Cancer Research *61*, 749-758.

Miyake, K., Mickley, L., Litman, T., Zhan, Z., Robey, R., Cristensen, B., Brangi, M., Greenberger, L.*, et al.* (1999). Molecular cloning of cDNAs which are highly overexpressed in mitoxantrone-resistant cells: demonstration of homology to ABC transport genes. Cancer Research *59*, 8-13.

Miyamoto, S., Duncan, G.E., Marx, C.E., and Lieberman, J.A. (2004). Treatments for schizophrenia: a critical review of pharmacology and mechanisms of action of antipsychotic drugs. Molecular Psychiatry *10*, 79-104.

Molderings, G., Werner, K., Likungu, J., and Göthert, M. (1990). Inhibition of noradrenaline release from the sympathetic nerves of the human saphenous vein via presynaptic 5-HT receptors similar to the 5-HT 1D subtype. Naunyn-Schmiedeberg's Archives of Pharmacology *342*, 371-377.

Mommeja-Marin, H., Mondou, E., Blum, M.R., and Rousseau, F. (2003). Serum HBV DNA as a marker of efficacy during therapy for chronic HBV infection: analysis and review of the literature. Hepatology *37*, 1309-1319.

Monti, J.M., and Jantos, H. (2014). The role of serotonin 5-HT7 receptor in regulating sleep and wakefulness. Reviews in the Neurosciences *25*, 429-437.

Moons, T., De Roo, M., Claes, S., and Dom, G. (2011). Relationship between P-glycoprotein and second-generation antipsychotics. Pharmacogenomics *12*, 1193-1211.

Morrison, S.J., Uchida, N., and Weissman, I.L. (1995). The biology of hematopoietic stem cells. Annual Review of Cell and Developmental Biology *11*, 35-71.

Mortensen, P.B. (1989). The incidence of cancer in schizophrenic patients. Journal of Epidemiology & Community Health *43*, 43-47.

Mortensen, P.B. (1994). The occurence of cancer in first admitted schizophrenic patients. Schizophrenia Research *12*, 185-194.

Moulin, M., Anderton, H., Voss, A.K., Thomas, T., Wong, W.W.L., Bankovacki, A., Feltham, R., Chau, D.*, et al.* (2012). IAPs limit activation of RIP kinases by TNF receptor 1 during development. The EMBO Journal *31*, 1679-1691.

Mrózek, K., Heinonen, K., and Bloomfield, C. (1997). Clinical significance of cytogenetics in acute myeloid leukemia. Seminars in Oncology *24*,17-31.

Mullins, U.L., Gianutsos, G., and Eison, A.S. (1999). Effects of Antidepressants on 5-HT7 Receptor Regulation in the Rat Hypothalamus. Neuropsychopharmacology *21*, 352-367.

Murphy, J.M., Czabotar, P.E., Hildebrand, J.M., Lucet, I.S., Zhang, J.-G., Alvarez-Diaz, S., Lewis, R., Lalaoui, N.*, et al.* (2013). The pseudokinase MLKL mediates necroptosis via a molecular switch mechanism. Immunity *39*, 443-453.

Murphy, J.M., and Silke, J. (2014). Ars Moriendi; the art of dying well–new insights into the molecular pathways of necroptotic cell death. EMBO reports *15*, 155-164.

Nakagawa, Y., Abe, S., Kurata, M., Hasegawa, M., Yamamoto, K., Inoue, M., Takemura, T., Suzuki, K.*, et al.* (2006). IAP family protein expression correlates with poor outcome of multiple myeloma patients in association with chemotherapy-induced overexpression of multidrug resistance genes. American Journal of Hematology *81*, 824-831.

National Cancer Institute (2016). Stat Fact Sheets: Acute Myeloid Leukemia (AML). Surveillance, Epidemiology, and End Results Program (SEER). Available at: https://seer.cancer.gov/statfacts/html/amyl.html. Accessed 17/11/2019.

Naumenko, V.S., Kondaurova, E.M., and Popova, N.K. (2011). On the role of brain 5-HT7 receptor in the mechanism of hypothermia: Comparison with hypothermia mediated via 5-HT1A and 5-HT3 receptor. Neuropharmacology *61*, 1360-1365.

NCI Thesaurus. (2019). Fluphenazine Hydrochloride (C47995). Available from: https://ncit.nci.nih.gov/ncitbrowser/ConceptReport.jsp?dictionary=NCI%20Thesaurus&code=C47995. Accessed 10/01/2020.

Ndubaku, C., Varfolomeev, E., Wang, L., Zobel, K., Lau, K., Elliott, L.O., Maurer, B., Fedorova, A.V.*, et al.* (2009). Antagonism of c-IAP and XIAP proteins is required for efficient induction of cell death by small-molecule IAP antagonists. ACS Chemical Biology *4*, 557-566.

Neale, G., Su, X., Morton, C.L., Phelps, D., Gorlick, R., Lock, R.B., Reynolds, C.P., Maris, J.M.*, et al.* (2008). Molecular characterization of the pediatric preclinical testing panel. Clinical Cancer Research *14*, 4572-4583.

Neyfakh, A.A. (1988). Use of fluorescent dyes as molecular probes for the study of multidrug resistance. Experimental Cell Research *174*, 168-176.

Noonan, A.M., Bunch, K.P., Chen, J.Q., Herrmann, M.A., Lee, J.M., Kohn, E.C., O'sullivan, C.C., Jordan, E.*, et al.* (2016). Pharmacodynamic markers and clinical results

from the phase 2 study of the SMAC mimetic birinapant in women with relapsed platinum-resistant or-refractory epithelial ovarian cancer. Cancer *122*, 588-597.

Nordenberg, J., Fenig, E., Landau, M., Weizman, R., and Weizman, A. (1999). Effects of psychotropic drugs on cell proliferation and differentiation. Biochemical Pharmacology *58*, 1229-1236.

NØrgaard, J.M., Bukh, A., Tyge Langkjer, S., Clausen, N., Palshof, T., and Hokland, P. (1998). MDR1 gene expression and drug resistance of AML cells. British Journal of Haematology *100*, 534-540.

Novus Biologicals. (2017). What are the major differences between Apoptosis, Necroptosis and Autophagy? Available at: https://www.novusbio.com/antibody-news/antibodies/what-are-the-major-differences-between-apoptosis-necroptosis-and-autophagy. Accessed 10/12/2019.

Obexer, P., and Ausserlechner, M.J. (2014). X-linked inhibitor of apoptosis protein–a critical death resistance regulator and therapeutic target for personalized cancer therapy. Frontiers in Oncology *4*, 197.

Ofengeim, D., and Yuan, J. (2013). Regulation of RIP1 kinase signalling at the crossroads of inflammation and cell death. Nature Reviews Molecular Cell Biology *14*, 727-736.

Ofran, Y., and Rowe, J.M. (2013). Genetic profiling in acute myeloid leukaemia ─ where are we and what is its role in patient management. British Journal of Haematology *160*, 303-320.

Oguro, H., Ding, L., and Morrison, S.J. (2013). SLAM family markers resolve functionally distinct subpopulations of hematopoietic stem cells and multipotent progenitors. Cell Stem Cell *13*, 102-116.

Oost, T.K., Sun, C., Armstrong, R.C., Al-Assaad, A.-S., Betz, S.F., Deckwerth, T.L., Ding, H., Elmore, S.W.*, et al.* (2004). Discovery of potent antagonists of the antiapoptotic protein XIAP for the treatment of cancer. Journal of Medicinal Chemistry *47*, 4417-4426.

Ossenkoppele, G., and Löwenberg, B. (2015). How I treat the older patient with acute myeloid leukemia. Blood *125*, 767-774.

Ozols, R.F., Cunnion, R.E., Klecker Jr, R.W., Hamilton, T.C., Ostchega, Y., Parrillo, J.E., and Young, R.C. (1987). Verapamil and adriamycin in the treatment of drug-resistant ovarian cancer patients. Journal of Clinical Oncology *5*, 641-647.

Pan, W., Luo, Q., Yan, X., Yuan, L., Yi, H., Zhang, L., Li, B., Zhang, Y.*, et al.* (2018). A novel SMAC mimetic APG-1387 exhibits dual antitumor effect on HBV-positive hepatocellular carcinoma with high expression of cIAP2 by inducing apoptosis and enhancing innate anti-tumor immunity. Biochemical Pharmacology *154*, 127-135.

Parkin, B., Ouillette, P., Li, Y., Keller, J., Lam, C., Roulston, D., Li, C., Shedden, K.*, et al.* (2013). Clonal evolution and devolution after chemotherapy in adult acute myelogenous leukemia. Blood *121*, 369-377.

Patch, A.-M., Christie, E.L., Etemadmoghadam, D., Garsed, D.W., George, J., Fereday, S., Nones, K., Cowin, P., *et al.* (2015). Whole–genome characterization of chemoresistant ovarian cancer. Nature *521*, 489.

PDQ® Adult Treatment Editorial Board. PDQ Adult Acute Myeloid Leukemia Treatment. Bethesda, MD: National Cancer Institute. Available at: https://www.cancer.gov/types/leukemia/patient/adult-aml-treatment-pdq. Accessed 15/11/2019 [PMID: 26389377].

Pedersen, K., Christiansen, B., Klitgaard, N., and Nielsen-Kudsk, F. (1983a). Effect of quinidine on digoxin bioavailability. European Journal of Clinical Pharmacology *24*, 41-47.

Pedersen, K.E., Christiansen, B.D., Kjaer, K., Klitgaard, N.A., and Nielsen-Kudsk, F. (1983b). Verapamil-induced changes in digoxin kinetics and intraerythrocytic sodium concentration. Clinical Pharmacology & Therapeutics *34*, 8-13.

Pedersen, K.E., Madsen, J.L., Klitgaard, N., Kjaer, K., and Hvidt, S. (1985). Effect of quinine on plasma digoxin concentration and renal digoxin clearance. Acta Medica Scandinavica *218*, 229-232.

Pedersen-Bjergaard, J., Andersen, M.K., Christiansen, D.H., and Nerlov, C. (2002). Genetic pathways in therapy-related myelodysplasia and acute myeloid leukemia. Blood *99*, 1909-1912.

Perimenis, P., Galaris, A., Voulgari, A., Prassa, M., and Pintzas, A. (2016). IAP antagonists Birinapant and AT-406 efficiently synergise with either TRAIL, BRAF, or BCL-2 inhibitors to sensitise BRAFV600E colorectal tumour cells to apoptosis. BMC Cancer *16*, 624.

Petersen, S.L., Wang, L., Yalcin-Chin, A., Li, L., Peyton, M., Minna, J., Harran, P., and Wang, X. (2007). Autocrine TNFalpha signaling renders human cancer cells susceptible to Smac-mimetic-induced apoptosis. Cancer Cell *12*, 445-456.

Pettersson, M., Jernberg-Wiklund, H., Larsson, L., Sundstrom, C., Givol, I., Tsujimoto, Y., and Nilsson, K. (1992). Expression of the bcl-2 gene in human multiple myeloma cell lines and normal plasma cells. Blood *79*, 495-502.

Porsolt, R.D., Anton, G., Blavet, N., and Jalfre, M. (1978). Behavioural despair in rats: a new model sensitive to antidepressant treatments. European Journal of Pharmacology *47*, 379-391.

Porsolt, R.D., Le Pichon, M., and Jalfre, M. (1977). Depression: a new animal model sensitive to antidepressant treatments. Nature *266*, 730.

Poulain, S., Lepelley, P., Cambier, N., Cosson, A., Fenaux, P., and Wattel, E. (1999). Assessment of P-glycoprotein expression by immunocytochemistry and flow cytometry using two different monoclonal antibodies coupled with functional efflux analysis in 34 patients with acute myeloid leukemia. Drug Resistance in Leukemia and Lymphoma III. Advances in Experimental Medicine and Biology, vol 457. Springer, Boston, MA

Prasad R., Shah A.H., Rawal M.K. (2016) Antifungals: Mechanism of Action and Drug Resistance. In: Ramos J., Sychrová H., Kschischo M. (eds) Yeast Membrane Transport. Advances in Experimental Medicine and Biology, vol 892. Springer, Cham

Pratt, D.S., and Kaplan, M.M. (2000). Evaluation of abnormal liver-enzyme results in asymptomatic patients. New England Journal of Medicine *342*, 1266-1271.

Pui, C.-H., Relling, M.V., and Downing, J.R. (2004). Acute lymphoblastic leukemia. New England Journal of Medicine *350*, 1535-1548.

Pusztai, L., Wagner, P., Ibrahim, N., Rivera, E., Theriault, R., Booser, D., Symmans, F.W., Wong, F.*, et al.* (2005). Phase II study of tariquidar, a selective P-glycoprotein inhibitor, in patients with chemotherapy-resistant, advanced breast carcinoma. Cancer *104*, 682-691.

Qian, F., Wei, D., Zhang, Q., and Yang, S. (2005). Modulation of P-glycoprotein function and reversal of multidrug resistance by (–)-epigallocatechin gallate in human cancer cells. Biomedicine & Pharmacotherapy *59*, 64-69.

Qin, Q., Zuo, Y., Yang, X., Lu, J., Zhan, L., Xu, L., Zhang, C., Zhu, H.*, et al.* (2014). Smac mimetic compound LCL161 sensitizes esophageal carcinoma cells to radiotherapy by inhibiting the expression of inhibitor of apoptosis protein. Tumor Biology *35*, 2565-2574.

Quitkin, F., Rifkin, A., and Klein, D.F. (1975). Very high dosage vs standard dosage fluphenazine in schizophrenia. Archives of General Psychiatry *32*, 1276-1281.

Rabindran, S.K., Ross, D.D., Doyle, L.A., Yang, W., and Greenberger, L.M. (2000). Fumitremorgin C reverses multidrug resistance in cells transfected with the breast cancer resistance protein. Cancer Research *60*, 47-50.

Ramakrishnan, V., Gomez, M., Prasad, V., Kimlinger, T., Painuly, U., Mukhopadhyay, B., Haug, J., Bi, L.*, et al.* (2016). Smac mimetic LCL161 overcomes protective ER stress induced by obatoclax, synergistically causing cell death in multiple myeloma. Oncotarget *7*, 56253.

Ramakrishnan, V., Painuly, U., Kimlinger, T., Haug, J., Rajkumar, S.V., and Kumar, S. (2014). Inhibitor of apoptosis proteins as therapeutic targets in multiple myeloma. Leukemia *28*, 1519.

Randolph, G.J., Beaulieu, S., Pope, M., Sugawara, I., Hoffman, L., Steinman, R.M., and Muller, W.A. (1998). A physiologic function for p-glycoprotein (MDR-1) during the migration of dendritic cells from skin via afferent lymphatic vessels. Proceedings of the National Academy of Sciences *95*, 6924-6929.

Rasco, D.W., Li, Y., Tang, Y., Men, L., Wang, H., Ji, J., Liang, Z., Sun, J.*, et al.* (2019). Abstract 3125. A phase I study of a novel IAP inhibitor APG-1387 as a monotherapy or in combination with pembrolizumab in treatments of patients with advanced solid tumors. American Society of Clinical Oncology *37*, 3125.

Ravindranath, Y., Yeager, A.M., Chang, M.N., Steuber, C.P., Krischer, J., Graham-Pole, J., Carroll, A., Inoue, S.*, et al.* (1996). Autologous bone marrow transplantation versus intensive consolidation chemotherapy for acute myeloid leukemia in childhood. New England Journal of Medicine *334*, 1428-1434.

Reese, N.D., and Schiller, G.J. (2013). High-dose cytarabine (HD araC) in the treatment of leukemias: a review. Current Hematologic Malignancy Reports *8*, 141-148.

Reichmann, F., and Holzer, P. (2016). Neuropeptide Y: a stressful review. Neuropeptides *55*, 99-109.

Relling, M.V. (1996). Are the major effects of P-glycoprotein modulators due to altered pharmacokinetics of anticancer drugs? Therapeutic Drug Monitoring *18*, 350-356.

Rex, A., Voigt, J., Wicke, K., and Fink, H. (2008). In vivo/ex vivo and behavioural study on central effects of 5-HT1B/1D and 5-HT1A antagonists in guinea pigs. Pharmacology Biochemistry and Behavior *88*, 196-204.

Roberts, N.J., Zhou, S., Diaz Jr, L.A., and Holdhoff, M. (2011). Systemic use of tumor necrosis factor alpha as an anticancer agent. Oncotarget *2*, 739.

Rodriguez-Proteau, R., Mata, J., Miranda, C., Fan, Y., Brown, J., and Buhler, D. (2006). Plant polyphenols and multidrug resistance: Effects of dietary flavonoids on drug transporters in Caco-2 and MDCKII-MDR1 cell transport models. Xenobiotica *36*, 41-58.

Rogan, A.M., Hamilton, T.C., Young, R.C., Klecker, R.W., and Ozols, R.F. (1984). Reversal of adriamycin resistance by verapamil in human ovarian cancer. Science *224*, 994-996.

Rosetti, M., Frasnelli, M., Tesei, A., Zoli, W., and Conti, M. (2006). Cytotoxicity of different selective serotonin reuptake inhibitors (SSRIs) against cancer cells. Journal of Experimental Therapeutics & Oncology *6*, 23-29.

Ruat, M., Traiffort, E., Leurs, R., Tardivel-Lacombe, J., Diaz, J., Arrang, J.M., and Schwartz, J.C. (1993). Molecular cloning, characterization, and localization of a high-affinity serotonin receptor (5-HT7) activating cAMP formation. Proceedings of the National Academy of Sciences *90*, 8547-8551.

Sachlos, E., Risueño, Ruth M., Laronde, S., Shapovalova, Z., Lee, J.-H., Russell, J., Malig, M., McNicol, Jamie D.*, et al.* (2012). Identification of Drugs Including a Dopamine Receptor Antagonist that Selectively Target Cancer Stem Cells. Cell *149*, 1284-1297.

Salvesen, G.S., and Duckett, C.S. (2002). Apoptosis: IAP proteins: blocking the road to death's door. Nature Reviews Molecular Cell Biology *3*, 401.

Samdani, A., Vijapurkar, U., Grimm, M.A., Spier, C.S., Grogan, T.M., Glinsmann-Gibson, B.J., and List, A.F. (1996). Cytogenetics and P-glycoprotein (PGP) are independent predictors of treatment outcome in acute myeloid leukemia (AML). Leukemia Research *20*, 175-180.

Sawyers, C.L. (1999). Chronic myeloid leukemia. New England Journal of Medicine *340*, 1330-1340.

Schaich, M., Soucek, S., Thiede, C., Ehninger, G., Illmer, T., and group, S.A.s. (2005). MDR1 and MRP1 gene expression are independent predictors for treatment outcome in adult acute myeloid leukaemia. British Journal of Haematology *128*, 324-332.

Scharenberg, C.W., Harkey, M.A., and Torok-Storb, B. (2002). The ABCG2 transporter is an efficient Hoechst 33342 efflux pump and is preferentially expressed by immature human hematopoietic progenitors. Blood *99*, 507-512.

Schenk, B., and Fulda, S. (2015). Reactive oxygen species regulate Smac mimetic/TNFα-induced necroptotic signaling and cell death. Oncogene *34*, 5796.

Schilder, R.J., Albertella, M., Strauss, J., Sydvander, M., Nair, S.M., Urakpo, K., Norin, S., and Öhd, J. (2018). Abstract TPS3131. A phase 1/2 study with birinapant in combination with pembrolizumab. Journal of Clinical Oncology *36*.

Schiller, G.J. (1998). Treatment of resistant disease. Leukemia *12*, 20-24.

Schimmer, A.D., Welsh, K., Pinilla, C., Wang, Z., Krajewska, M., Bonneau, M.-J., Pedersen, I.M., Kitada, S.*, et al.* (2004). Small-molecule antagonists of apoptosis suppressor XIAP exhibit broad antitumor activity. Cancer Cell *5*, 25-35.

Schinkel, A., Smit, J., van Tellingen, m., Beijnen, J., Wagenaar, E., Van Deemter, L., Mol, C., Van der Valk, M.*, et al.* (1994). Disruption of the mouse mdr1a P-glycoprotein gene leads to a deficiency in the blood-brain barrier and to increased sensitivity to drugs. Cell *77*, 491-502.

Schinkel, A.H., Mayer, U., Wagenaar, E., Mol, C.A., Van Deemter, L., Smit, J.J., Van Der Valk, M.A., Voordouw, A.C.*, et al.* (1997). Normal viability and altered pharmacokinetics in mice lacking mdr1-type (drug-transporting) P-glycoproteins. Proceedings of the National Academy of Sciences *94*, 4028-4033.

Schleuning, M., Brumme, V., and Wilmanns, W. (1993). Growth inhibition of human leukemic cell lines by the phenothiazine derivative fluphenazine. Anticancer Research *13*, 599-602.

Seelig, A. (1998). A general pattern for substrate recognition by P-glycoprotein. European Journal of Biochemistry *251*, 252-261.

Seeman, P., and Lee, T. (1975). Antipsychotic drugs: direct correlation between clinical potency and presynaptic action on dopamine neurons. Science *188*, 1217-1219.

Segawa, Y., Ohnoshi, T., Hiraki, S., Ueoka, H., Kiura, K., Kamei, H., Tabata, M., Shibayama, T.*, et al.* (1993). Immunohistochemical detection of P-glycoprotein and carcinoembryonic antigen in small cell lung cancer: with reference to predictability of response to chemotherapy. Acta Medica Okayama *47*, 181-189.

Senzer, N.N., LoRusso, P., Martin, L.P., Schilder, R.J., Amaravadi, R.K., Papadopoulos, K.P., Segota, Z.E., Weng, D.E.*, et al.* (2013). Abstract 3621. Phase II clinical activity and tolerability of the SMAC-mimetic birinapant (TL32711) plus irinotecan in irinotecan-relapsed/refractory metastatic colorectal cancer. Journal of Clinical Oncology *31*, 3621.

Shaffer, B.C., Gillet, J.-P., Patel, C., Baer, M.R., Bates, S.E., and Gottesman, M.M. (2012). Drug resistance: still a daunting challenge to the successful treatment of AML. Drug Resistance Updates *15*, 62-69.

Shapiro, A.B., Fox, K., Lam, P., and Ling, V. (1999). Stimulation of P-glycoprotein-mediated drug transport by prazosin and progesterone: Evidence for a third drug-binding site. European Journal of Biochemistry *259*, 841-850.

Shapiro, A.B., and Ling, V. (1997). Positively cooperative sites for drug transport by P-glycoprotein with distinct drug specificities. European Journal of Biochemistry *250*, 130-137.

Shen, Y., Monsma, F.J., Metcalf, M.A., Jose, P.A., Hamblin, M.W., and Sibley, D.R. (1993). Molecular cloning and expression of a 5-hydroxytryptamine7 serotonin receptor subtype. Journal of Biological Chemistry *268*, 18200-18204.

Shlush, L.I., Mitchell, A., Heisler, L., Abelson, S., Ng, S.W., Trotman-Grant, A., Medeiros, J.J., Rao-Bhatia, A.*, et al.* (2017). Tracing the origins of relapse in acute myeloid leukaemia to stem cells. Nature *547*, 104.

Sibley, D.R., and Monsma Jr, F.J. (1992). Molecular biology of dopamine receptors. Trends in Pharmacological Sciences *13*, 61-69.

Sikic, B., Eckhardt, S., Gallant, G., Burris, H., Camidge, D., Colevas, A., Jones, S., Messersmith, W.*, et al.* (2011). Safety, pharmacokinetics (PK), and pharmacodynamics (PD) of HGS1029, an inhibitor of apoptosis protein (IAP) inhibitor, in patients (Pts) with advanced solid tumors: Results of a phase I study. Journal of Clinical Oncology *29*, 3008-3008.

Silke, J., Ekert, P.G., Day, C.L., Hawkins, C.J., Baca, M., Chew, J., Pakusch, M., Verhagen, A.M.*, et al.* (2001). Direct inhibition of caspase 3 is dispensable for the anti-apoptotic activity of XIAP. The EMBO Journal *20*, 3114-3123.

Silke, J., Hawkins, C.J., Ekert, P.G., Chew, J., Day, C.L., Pakusch, M., Verhagen, A.M., and Vaux, D.L. (2002). The anti-apoptotic activity of XIAP is retained upon mutation of both the caspase 3–and caspase 9–interacting sites. The Journal of Cell Biology *157*, 115-124.

Silke, J., Miasari, M., and Puthalakath, H. (2008). Ubiquitylation and Cancer Development. Current Cancer Drug Targets *8*, 118-123.

Silke, J., Rickard, J.A., and Gerlic, M. (2015). The diverse role of RIP kinases in necroptosis and inflammation. Nature Immunology *16*, 689.

Silke, J., Verhagen, A.M., Ekert, P.G., and Vaux, D.L. (2000). Sequence as well as functional similarity for DIABLO/Smac and Grim, Reaper and Hid? Cell Death & Differentiation *7*, 1275-1275.

Skingle, M., Beattie, D., Scopes, D., Starkey, S., Connor, H., Feniuk, W., and Tyers, M. (1995). GR127935: a potent and selective 5-HT1D receptor antagonist. Behavioural Brain Research *73*, 157-161.

Slater, L., Sweet, P., Stupecky, M., Wetzel, M., and Gupta, S. (1986a). Cyclosporin A corrects daunorubicin resistance in Ehrlich ascites carcinoma. British Journal of Cancer *54*, 235.

Slater, L.M., Sweet, P., Stupecky, M., and Gupta, S. (1986b). Cyclosporin A reverses vincristine and daunorubicin resistance in acute lymphatic leukemia in vitro. The Journal of Clinical Investigation *77*, 1405-1408.

Sleight, A.J., Carolo, C., Petit, N., Zwingelstein, C., and Bourson, A. (1995). Identification of 5-hydroxytryptamine7 receptor binding sites in rat hypothalamus: sensitivity to chronic antidepressant treatment. Molecular Pharmacology *47*, 99-103.

Smit, J., Schinkel, A.H., Elferink, R.O., Groen, A., Wagenaar, E., Van Deemter, L., Mol, C., Ottenhoff, R.*, et al.* (1993). Homozygous disruption of the murine mdr2 P-glycoprotein gene leads to a complete absence of phospholipid from bile and to liver disease. Cell *75*, 451-462.

Souers, A.J., Leverson, J.D., Boghaert, E.R., Ackler, S.L., Catron, N.D., Chen, J., Dayton, B.D., Ding, H.*, et al.* (2013). ABT-199, a potent and selective BCL-2 inhibitor, achieves antitumor activity while sparing platelets. Nature Medicine *19*, 202-208.

Spiller, R. (2007). Serotonin, inflammation, and IBS: fitting the jigsaw together? Journal of Pediatric Gastroenterology and Nutrition *45*, 115-119.

Starling, J.J., Shepard, R.L., Cao, J., Law, K.L., Norman, B.H., Kroin, J.S., Ehlhardt, W.J., Baughman, T.M.*, et al.* (1997). Pharmacological characterization of LY335979: a potent cyclopropyldibenzosuberane modulator of P-glycoprotein. Advances in Enzyme Regulation *37*, 335-347.

Steinhart, L., Belz, K., and Fulda, S. (2013). Smac mimetic and demethylating agents synergistically trigger cell death in acute myeloid leukemia cells and overcome apoptosis resistance by inducing necroptosis. Cell Death & Disease *4*, e802.

Steinwascher, S., Nugues, A.-L., Schoeneberger, H., and Fulda, S. (2015). Identification of a novel synergistic induction of cell death by Smac mimetic and HDAC inhibitors in acute myeloid leukemia cells. Cancer Letters *366*, 32-43.

Stitzel, R.E. (1976). The biological fate of reserpine. Pharmacological Reviews *28*, 179-208.

Takara, K., Sakaeda, T., and Okumura, K. (2006). An update on overcoming MDR1-mediated multidrug resistance in cancer chemotherapy. Current Pharmaceutical Design *12*, 273-286.

Takara, K., Sakaeda, T., Tanigawara, Y., Nishiguchi, K., Ohmoto, N., Horinouchi, M., Komada, F., Ohnishi, N.*, et al.* (2002). Effects of 12 Ca2+ antagonists on multidrug resistance, MDR1-mediated transport and MDR1 mRNA expression. European Journal of Pharmaceutical Sciences *16*, 159-165.

Talbott, R.L., Borzilleri, R.M., Chaudhry, C., Fargnoli, J., Shen, H., Fairchild, C., Barnhart, B., Ortega, M.*, et al.* (2015). Pharmacology of smac mimetics; chemotype differentiation based on physical association with caspase regulators and cellular transport. Experimental Cell Research *338*, 251-260.

Tanimoto, T., Tsuda, H., Imazeki, N., Ohno, Y., Imoto, I., Inazawa, J., and Matsubara, O. (2005). Nuclear expression of cIAP-1, an apoptosis inhibiting protein, predicts lymph

node metastasis and poor patient prognosis in head and neck squamous cell carcinomas. Cancer Letters *224*, 141-151.

Tchoghandjian, A., Soubéran, A., Tabouret, E., Colin, C., Denicolaï, E., Jiguet-Jiglaire, C., El-Battari, A., Villard, C.*, et al.* (2016). Inhibitor of apoptosis protein expression in glioblastomas and their in vitro and in vivo targeting by SMAC mimetic GDC-0152. Cell Death & Disease *7*, e2325.

Te Boekhorst, P., de Leeuw, K., Schoester, M., Wittebol, S., Nooter, K., Hagemeijer, A., Lowenberg, B., and Sonneveld, P. (1993). Predominance of functional multidrug resistance (MDR-1) phenotype in CD34+ acute myeloid leukemia cells. Blood *82*, 3157-3162.

Thibault, B., Genre, L., Le Naour, A., Broca, C., Mery, E., Vuagniaux, G., Delord, J.P., Wiedemann, N.*, et al.* (2018). DEBIO 1143, an IAP inhibitor, reverses carboplatin resistance in ovarian cancer cells and triggers apoptotic or necroptotic cell death. Scientific Reports *8*, 17862.

Thomas, E.D., Buckner, C.D., Clift, R.A., Fefer, A., Johnson, F.L., Neiman, P.E., Sale, G.E., Sanders, J.E.*, et al.* (1979). Marrow transplantation for acute nonlymphoblastic leukemia in first remission. New England Journal of Medicine *301*, 597-599.

Thornberry, N.A., and Lazebnik, Y. (1998). Caspases: enemies within. Science *281*, 1312-1316.

Thorsteinsdottir, U., Kroon, E., Jerome, L., Blasi, F., and Sauvageau, G. (2001). Defining roles for HOX and MEIS1 genes in induction of acute myeloid leukemia. Molecular Cell Biology *21*, 224-234.

Tkachuk, D.C., Kohler, S., and Cleary, M.L. (1992). Involvement of a homolog of Drosophila trithorax by 11q23 chromosomal translocations in acute leukemias. Cell *71*, 691-700.

Tolcher, A.W., Bendell, J.C., Papadopoulos, K.P., Burris, H.A., Patnaik, A., Fairbrother, W.J., Wong, H., Budha, N.*, et al.* (2016). A phase I dose-escalation study evaluating the safety tolerability and pharmacokinetics of CUDC-427, a potent, oral, monovalent IAP antagonist, in patients with refractory solid tumors. Clinical Cancer Research *22*, 4567-4573.

Tsuruo, T., Iida, H., Tsukagoshi, S., and Sakurai, Y. (1981). Overcoming of vincristine resistance in P388 leukemia in vivo and in vitro through enhanced cytotoxicity of vincristine and vinblastine by verapamil. Cancer Research *41*, 1967-1972.

Tsuruo, T., Iida, H., Tsukagoshi, S., and Sakurai, Y. (1982). Increased accumulation of vincristine and adriamycin in drug-resistant P388 tumor cells following incubation with calcium antagonists and calmodulin inhibitors. Cancer Research *42*, 4730-4733.

Twentyman, P.R., and Bleehen, N.M. (1991). Resistance modification by PSC-833, a novel non-immunosuppressive cyclosporin A. European Journal of Cancer and Clinical Oncology *27*, 1639-1642.

Ucci, G., Petrini, M., Riccardi, A., Invernizzi, R., Carulli, G., Luoni, R., Giordano, M., and Danova, M. (1992). Expression of p170 protein in multiple myeloma: a clinical study. Hematological Oncology *10*, 213-220.

Vallabhapurapu, S., Matsuzawa, A., Zhang, W., Tseng, P.-H., Keats, J.J., Wang, H., Vignali, D.A.A., Bergsagel, P.L.*, et al.* (2008). Nonredundant and complementary functions of TRAF2 and TRAF3 in a ubiquitination cascade that activates NIK-dependent alternative NF-κB signaling. Nature Immunology *9*, 1364.

van Helvoort, A., Smith, A.J., Sprong, H., Fritzsche, I., Schinkel, A.H., Borst, P., and van Meer, G. (1996). MDR1 P-glycoprotein is a lipid translocase of broad specificity, while MDR3 P-glycoprotein specifically translocates phosphatidylcholine. Cell *87*, 507-517.

van Rhenen, A., Feller, N., Kelder, A., Westra, A.H., Rombouts, E., Zweegman, S., van der Pol, M.A., Waisfisz, Q.*, et al.* (2005). High stem cell frequency in acute myeloid leukemia at diagnosis predicts high minimal residual disease and poor survival. Clinical Cancer Research *11*, 6520-6527.

Van Tellingen, O., Buckle, T., Jonker, J., Van der Valk, M., and Beijnen, J. (2003). P-glycoprotein and Mrp1 collectively protect the bone marrow from vincristine-induced toxicity in vivo. British Journal of Cancer *89*, 1776.

Vanden Berghe, T., Kaiser, W.J., Bertrand, M.J.M., and Vandenabeele, P. (2015). Molecular crosstalk between apoptosis, necroptosis, and survival signaling. Molecular & Cellular Oncology *2*, e975093.

Vandenabeele, P., Galluzzi, L., Vanden Berghe, T., and Kroemer, G. (2010). Molecular mechanisms of necroptosis: an ordered cellular explosion. Nature Reviews Molecular Cellular Biology *11*, 700-714.

Varfolomeev, E., Blankenship, J.W., Wayson, S.M., Fedorova, A.V., Kayagaki, N., Garg, P., Zobel, K., Dynek, J.N.*, et al.* (2007). IAP antagonists induce autoubiquitination of c-IAPs, NF-κB activation, and TNFα-dependent apoptosis. Cell *131*, 669-681.

Varfolomeev, E.E., Schuchmann, M., Luria, V., Chiannilkulchai, N., Beckmann, J.S., Mett, I.L., Rebrikov, D., Brodianski, V.M.*, et al.* (1998). Targeted Disruption of the Mouse Caspase 8 Gene Ablates Cell Death Induction by the TNF Receptors, Fas/Apo1, and DR3 and Is Lethal Prenatally. Immunity *9*, 267-276.

Vaux, D.L., and Silke, J. (2005). IAPs, RINGs and ubiquitylation. Nature Reviews Molecular Cell Biology *6*, 287.

Velamakanni, S., Wei, S.L., Janvilisri, T., and van Veen, H.W. (2007). ABCG transporters: structure, substrate specificities and physiological roles. Journal of Bioenergetics and bBiomembranes *39*, 465-471.

Verhagen, A.M., Ekert, P.G., Pakusch, M., Silke, J., Connolly, L.M., Reid, G.E., Moritz, R.L., Simpson, R.J.*, et al.* (2000). Identification of DIABLO, a mammalian protein that promotes apoptosis by binding to and antagonizing IAP proteins. Cell *102*, 43-53.

Verweij, J., Herweijer, H., Oosterom, R., Van Der Burg, M., Planting, A., Seynaeve, C., Stoter, G., and Nooter, K. (1991). A phase II study of epidoxorubicin in colorectal cancer

and the use of cyclosporin-A in an attempt to reverse multidrug resistance. British Journal of Cancer *64*, 361.

Vicaut, E., Laemmel, E., and Stücker, O. (2000). Impact of serotonin on tumour growth. Annals of Medicine *32*, 187-194.

Vijayan, N.N., Mathew, A., Balan, S., Natarajan, C., Nair, C.M., Allencherry, P.M., and Banerjee, M. (2012). Antipsychotic drug dosage and therapeutic response in schizophrenia is influenced by ABCB1 genotypes: a study from a south Indian perspective. Pharmacogenomics *13*, 1119-1127.

Villalobos-Ortiz, M., Ryan, J., Mashaka, T.N., Opferman, J.T., and Letai, A. (2019). BH3 profiling discriminates on-target small molecule BH3 mimetics from putative mimetics. Cell Death & Differentiation, 1-9.

Vince, J.E., Wong, W.W., Khan, N., Feltham, R., Chau, D., Ahmed, A.U., Benetatos, C.A., Chunduru, S.K.*, et al.* (2007). IAP antagonists target cIAP1 to induce TNFalpha-dependent apoptosis. Cell *131*, 682-693.

Vince, J.E., Wong, W.W.-L., Gentle, I., Lawlor, K.E., Allam, R., O'Reilly, L., Mason, K., Gross, O.*, et al.* (2012). Inhibitor of apoptosis proteins limit RIP3 kinase-dependent interleukin-1 activation. Immunity *36*, 215-227.

Vogler, M., Weber, K., Dinsdale, D., Schmitz, I., Schulze-Osthoff, K., Dyer, M., and Cohen, G. (2009). Different forms of cell death induced by putative BCL2 inhibitors. Cell Death and Differentiation *16*, 1030.

Vogler, W.R., Velez-Garcia, E., Weiner, R.S., Flaum, M.A., Bartolucci, A.A., Omura, G.A., Gerber, M.C., and Banks, P. (1992). A phase III trial comparing idarubicin and daunorubicin in combination with cytarabine in acute myelogenous leukemia: a Southeastern Cancer Study Group Study. Journal of Clinical Oncology *10*, 1103-1111.

Wacher, V.J., Wu, C.Y., and Benet, L.Z. (1995). Overlapping substrate specificities and tissue distribution of cytochrome P450 3A and P-glycoprotein: implications for drug delivery and activity in cancer chemotherapy. Molecular Carcinogenesis *13*, 129-134.

Waghray, D., and Zhang, Q. (2017). Inhibit or Evade Multidrug Resistance P-Glycoprotein in Cancer Treatment: Miniperspective. Journal of Medicinal Chemistry *61*, 5108-5121.

Wang, H., Sun, L., Su, L., Rizo, J., Liu, L., Wang, L.-F., Wang, F.-S., and Wang, X. (2014). Mixed lineage kinase domain-like protein MLKL causes necrotic membrane disruption upon phosphorylation by RIP3. Molecular Cell *54*, 133-146.

Wang, J.-S., Zhu, H.-J., Markowitz, J.S., Donovan, J.L., and DeVane, C.L. (2006). Evaluation of antipsychotic drugs as inhibitors of multidrug resistance transporter P-glycoprotein. Psychopharmacology *187*, 415-423.

Wang, Z., Chen, Y., Liang, H., Bender, A., Glen, R.C., and Yan, A. (2011). P-glycoprotein substrate models using support vector machines based on a comprehensive data set. Journal of Chemical Information and Modeling *51*, 1447-1456.

Weick, J.K., Kopecky, K.J., Appelbaum, F.R., Head, D.R., Kingsbury, L.L., Balcerzak, S.P., Bickers, J.N., Hynes, H.*, et al.* (1996). A randomized investigation of high-dose versus standard-dose cytosine arabinoside with daunorubicin in patients with previously untreated acute myeloid leukemia: a Southwest Oncology Group study. Blood *88*, 2841-2851.

Weisberg, E., Kung, A.L., Wright, R.D., Moreno, D., Catley, L., Ray, A., Zawel, L., Tran, M.*, et al.* (2007). Potentiation of antileukemic therapies by Smac mimetic, LBW242: effects on mutant FLT3-expressing cells. Molecular Cancer Therapeutics *6*, 1951-1961.

Weisberg, E., Ray, A., Barrett, R., Nelson, E., Christie, A., Porter, D., Straub, C., Zawel, L.*, et al.* (2010). Smac mimetics: implications for enhancement of targeted therapies in leukemia. Leukemia *24*, 2100.

Westover, D., and Li, F. (2015). New trends for overcoming ABCG2/BCRP-mediated resistance to cancer therapies. Journal of Experimental & Clinical Cancer Research *34*, 159.

Wiernik, P.H., Banks, P., Case, D.J., Arlin, Z.A., Periman, P.O., Todd, M.B., Ritch, P.S., Enck, R.E.*, et al.* (1992). Cytarabine plus idarubicin or daunorubicin as induction and consolidation therapy for previously untreated adult patients with acute myeloid leukemia. Blood *79*, 313-319.

Wong, H., Gould, S.E., Budha, N., Darbonne, W.C., Kadel, E.E., La, H., Alicke, B., Halladay, J.S.*, et al.* (2013). Learning and confirming with preclinical studies: modeling and simulation in the discovery of GDC-0917, an inhibitor of apoptosis proteins antagonist. Drug Metabolism and Disposition *41*, 2104-2113.

Wong, W.W.-L., Vince, J.E., Lalaoui, N., Lawlor, K.E., Chau, D., Bankovacki, A., Anderton, H., Metcalf, D.*, et al.* (2014). cIAPs and XIAP regulate myelopoiesis through cytokine production in an RIPK1-and RIPK3-dependent manner. Blood *123*, 2562-2572.

World Health Organization. (2017). Hepatitis B vaccines: WHO position paper - July 2017. Weekly Epidemiological Record *92*, 369-392.

Wu, G., Chai, J., Suber, T.L., Wu, J.-W., Du, C., Wang, X., and Shi, Y. (2000). Structural basis of IAP recognition by Smac/DIABLO. Nature *408*, 1008-1012.

Wuilleme-Toumi, S., Robillard, N., Gomez, P., Moreau, P., Le Gouill, S., Avet-Loiseau, H., Harousseau, J., Amiot, M.*, et al.* (2005). Mcl-1 is overexpressed in multiple myeloma and associated with relapse and shorter survival. Leukemia *19*, 1248.

Xia, Z., Depierre, J.W., and Nässberger, L. (1996). The Tricyclic Antidepressants Clomipramine and Citalopram Induce Apoptosis in Cultured Human Lymphocytes. Journal of Pharmacy and Pharmacology *48*, 115-116.

Xia, Z., DePierre, J.W., and Nässberger, L. (1998). Modulation of Apoptosis Induced by Tricyclic Antidepressants in Human Peripheral Lymphocytes. Journal of Biochemical and Molecular Toxicology *12*, 115-123.

Xu, R., Li, Y., Ji, J., Qiu, M., Zhang, Y., Liu, W., Tian, X., Li, S.*, et al.* (2018). Abstract 2593. A phase I study of a novel IAP inhibitor APG-1387 in patients with advanced solid tumors. American Society of Clinical Oncology *36*, 2593.

Yang, C., Wang, H., Zhang, B., Chen, Y., Zhang, Y., Sun, X., Xiao, G., Nan, K.*, et al.* (2016). LCL161 increases paclitaxel-induced apoptosis by degrading cIAP1 and cIAP2 in NSCLC. Journal of Experimental & Clinical Cancer Research *35*, 158.

Yang, J., Liu, X., Bhalla, K., Kim, C.N., Ibrado, A.M., Cai, J., Peng, T.-I., Jones, D.P.*, et al.* (1997). Prevention of apoptosis by Bcl-2: release of cytochrome c from mitochondria blocked. Science *275*, 1129-1132.

Yang, Q.-H., and Du, C. (2004). Smac/DIABLO Selectively Reduces the Levels of c-IAP1 and c-IAP2 but Not That of XIAP and Livin in HeLa Cells. Journal of Biological Chemistry *279*, 16963-16970.

Yasuda, K., Lan, L.-b., Sanglard, D., Furuya, K., Schuetz, J.D., and Schuetz, E.G. (2002). Interaction of cytochrome P450 3A inhibitors with P-glycoprotein. Journal of Pharmacology and Experimental Therapeutics *303*, 323-332.

Yuan, Z., Syrkin, G., Adem, A., Geha, R., Pastoriza, J., Vrikshajanani, C., Smith, T., Quinn, T.*, et al.* (2013). Blockade of inhibitors of apoptosis (IAPs) in combination with tumor-targeted delivery of tumor necrosis factor-α leads to synergistic antitumor activity. Cancer Gene Therapy *20*, 46.

Zeisig, B.B., Kulasekararaj, A.G., Mufti, G.J., and So, C.W. (2012). SnapShot: Acute myeloid leukemia. Cancer Cell *22*, 698-698 e691.

Zender, L., Spector, M.S., Xue, W., Flemming, P., Cordon-Cardo, C., Silke, J., Fan, S.-T., Luk, J.M.*, et al.* (2006). Identification and Validation of Oncogenes in Liver Cancer Using an Integrative Oncogenomic Approach. Cell *125*, 1253-1267.

Zhang, T., Li, Y., Zou, P., Yu, J.y., McEachern, D., Wang, S., and Sun, D. (2013). Physiologically based pharmacokinetic and pharmacodynamic modeling of an antagonist (SM-406/AT-406) of multiple inhibitor of apoptosis proteins (IAPs) in a mouse xenograft model of human breast cancer. Biopharmaceutics & Drug Disposition *34*, 348-359.

Zhelev, Z., Ohba, H., Bakalova, R., Hadjimitova, V., Ishikawa, M., Shinohara, Y., and Baba, Y. (2004). Phenothiazines suppress proliferation and induce apoptosis in cultured leukemic cells without any influence on the viability of normal lymphocytes. Cancer Chemotherapy and Pharmacology *53*, 267-275.

Zheng, C., Kabaleeswaran, V., Wang, Y., Cheng, G., and Wu, H. (2010). Crystal structures of the TRAF2: cIAP2 and the TRAF1: TRAF2: cIAP2 complexes: affinity, specificity, and regulation. Molecular Cell *38*, 101-113.

Zhou, D., Zittoun, R., and Marie, J. (1995). Expression of multidrug resistance-associated protein (MRP) and multidrug resistance (MDR1) genes in acute myeloid leukemia. Leukemia *9*, 1661-1666.

Zhou, S., Schuetz, J.D., Bunting, K.D., Colapietro, A.-M., Sampath, J., Morris, J.J., Lagutina, I., Grosveld, G.C.*, et al.* (2001). The ABC transporter Bcrp1/ABCG2 is expressed in a wide variety of stem cells and is a molecular determinant of the side-population phenotype. Nature Medicine *7*, 1028.

Zobel, K., Wang, L., Varfolomeev, E., Franklin, M.C., Elliott, L.O., Wallweber, H.J., Okawa, D.C., Flygare, J.A.*, et al.* (2006). Design, synthesis, and biological activity of a potent Smac mimetic that sensitizes cancer cells to apoptosis by antagonizing IAPs. ACS Chemical Biology *1*, 525-533.

Zuber, J., Radtke, I., Pardee, T.S., Zhao, Z., Rappaport, A.R., Luo, W., McCurrach, M.E., Yang, M.-M.*, et al.* (2009). Mouse models of human AML accurately predict chemotherapy response. Genes & Development *23*, 877-889.

Zuber, J., Shi, J., Wang, E., Rappaport, A.R., Herrmann, H., Sison, E.A., Magoon, D., Qi, J.*, et al.* (2011). RNAi screen identifies Brd4 as a therapeutic target in acute myeloid leukaemia. Nature *478*, 524.